Structure-activity studies of ligands for brain nicotinic acetylcholine receptors

Thomas, Philip

Award date:
1995

Awarding institution:
University of Bath

Structure-activity studies of ligands for brain nicotinic acetylcholine receptors

Submitted by Philip Thomas

for the degree of PhD
of the University of Bath

1995

Copyright

Signed: 

ProQuest LLC
789 East Eisenhower Parkway
P.O. Box 1346
Ann Arbor, MI 48106-1346

Abstract

The pharmacological complexity of the now numerous subtypes of neuronal nicotinic acetylcholine receptors (nAChRs) has been increasingly refined through the appearance of greater numbers of pharmacological agents, derived from both natural and synthetic sources. This large structural data base of agonist and antagonist molecules harbours information required to refine the present model of the nicotinic pharmacophore - a unifying structural model for ligands active at the nicotinic receptor. Exploration of the relationships between structure and biological activity of such ligands is essential to the resolution of such a model, and consequently to the design of future ligands that may prove useful tools in subsequent receptor characterisation, or even have therapeutic use.

Biological descriptors of agonist molecules taken from structurally diverse families were generated through both a biochemical and physiological route. The former avenue, employing competition binding assays, established relative potencies of ligands at two subtypes of neuronal nAChR, and monitored the initial effects of structural modification. The latter method determined the functional activity of molecules at a reconstituted receptor expressed in the *Xenopus* oocyte system. Allied to these investigations was an exploration of feasible molecular geometries of ligands, examined using theoretical computational chemistry techniques. Through studying the biological effects of various molecules and their analogues, and the molecular features and geometries of these small ligands, the structural requirements of the nicotinic pharmacophore have further evolved.

Much attention in the project has focused on (+)anatoxin-a, a natural ligand found to be the most potent agonist at neuronal nicotinic acetylcholine receptors. The rigidity of this molecule and chemically modifiable nature, made it an attractive structure from which to explore structure-activity relationships of the neuronal nicotinic receptor. Rational design and synthesis of novel analogues of anatoxin-a to determine the bioactive configuration, revealed that extension of the sidechain retained, or possibly improved, activity yet had little influence on preferred geometry. These synthetic analogues provide an insight into the constraints imposed on the pharmacophore and those imposed by the receptor binding pocket, and represent important structures from which to further investigate the bioactive conformation of this ligand. The extended sidechain of the active analogues bestows potential for their use as affinity ligands for the nicotinic receptor.

Acknowledgements

I am much indebted to two people in particular, Dr Sue Wonnacott and Prof George Lunt, whose generous support, guidance, sterling patience and provision of red hot poker throughout the course of this project never waned. I also have to say a huge thankyou to one small but non-the-less very generous electrophysiologist, Dr Muriel Amar, whose timely arrival at Bath provided much inspiration, a refreshing practical technique as well as all manner of anglo-french hybrid expletives. The men behind the synthesis of the anatoxin analogues used in this study were Drs Tim Gallagher and Paul Brough without whom much of the progress made would not have been possible. Thanks must also go to Jim Knight and the amphibian house entourage who kept the toads coming and saw to their every, though meagre, needs.

Of course money makes the world go round and the providers of the cranking handle for the project were the RJR Tobacco company, without whose help the radioligands would have been cold, as would the landlord's reception.

Final thanks must go to the generations of the laboratory for providing many forms of advice, amusement and entertainment, and of course to all the technical staff at Bath for keeping the wheels turning and providing invaluable assistance at various junctures.

Contents

1.Introduction

Acetylcholine (ACh) functions as a neurotransmitter in many regions of the mammalian peripheral and central nervous systems by activating two structurally distinct classes of cell surface receptors: those activated by the mushroom alkaloid muscarine - the muscarinic receptors (mAChRs), and those by the tobacco alkaloid nicotine - the nicotinic receptors (nAChRs). Binding of ACh to mAChRs elicits responses mediated by GTP-binding proteins which modulate various effector molecules such as enzymes and ion channels. nAChRs are Ligand-Gated Ion Channels (LGICs) prevalent in the membrane of nerve and muscle which facilitate cation flux in response to the binding of effector molecules (e.g. ACh and nicotine), resulting in depolarisation of the excitable cell membrane. Such effects are made possible by transient conformational changes in the complex architecture of the receptor induced by the binding of effector molecules (agonists) many thousands of times smaller in size. This structural perturbation creates a temporary channel through the protein which provides an aqueous pathway for the passage of ions across the membrane (Figure 1.1).

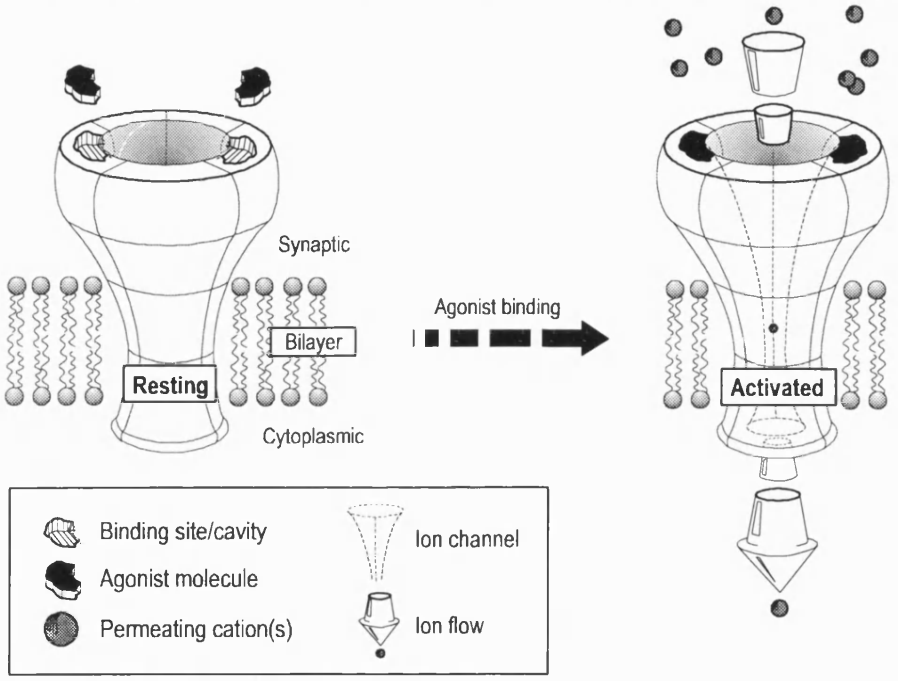

Figure 1.1: The Ligand-gated Ion Channel (LGIC). Stylised representation of the receptor which traverses the membrane of excitable cells and is responsible for the creation of an ion conducting pathway in response to the binding of small agonist molecules. The protein possesses all the elements required for agonist recognition through to the complex structural features responsible for channel opening and desensitisation.

nAChRs are prevalent at the neuromuscular junction where they mediate contraction of muscle fibres. This contraction event serves as a convenient means of directly measuring receptor function and it is this, coincident with the abundance of the receptor in the electric organs of certain fish, and the availability of certain highly selective probes for the receptor, which has made the nAChR the most extensively studied of membrane receptors to date. Much more recently attention has focused on the physiological role of this receptor in the brain and its relevance to the addictive and behavioural effects associated with the use of tobacco-derived nicotine. Such motivations have catalysed extensive advances in the biochemical, molecular biological, ultrastructural and

physiological approaches to the understanding of the complex structure-function relationships associated with this receptor.

1.1 The neurotransmitter-gated receptor family

The nAChR is currently regarded as the prototypical Ligand-Gated Ion Channel (LGIC) receptor. This growing family of neurotransmitter-gated channels includes those found at excitatory synapses (nAChR, serotonin- ($5HT_3$) and glutamate-sensitive receptors) which gate the passage of cations, and those found at inhibitory synapses ($GABA_A$- and Glycine-sensitive channels) which are anion selective. All these proteins share the common function of regulated opening and closing of an integral ion channel.

Two subfamilies exist within this LGIC classification based on amino acid sequence identity. The subunits of nACh, $5HT_3$, $GABA_A$ and Glycine channels are homologous, particularly in their membrane-spanning segments (see below), whereas this family shares no overall homology with the glutamate-gated family which consists of AMPA- (α-amino-3-hydroxy-5-methyl-4-isoxazole proprionic acid), NMDA- (N-methyl-D-aspartate) and kainate-sensitive receptors - these channels, like certain members of the nAChR family, are cation selective. Homology between the subunits of different members of these two families is between 20% and 40%, whereas in the different subunits which create the individual channels of each family homology is generally at least 40%.

Despite the lack of overall homology among ACh- and glutamate-gated channel families, many conserved features are evident, among them the presence of four significant hydrophobic segments (Figure 1.2) which, although not yet unambiguously determined, are presumed to correspond to

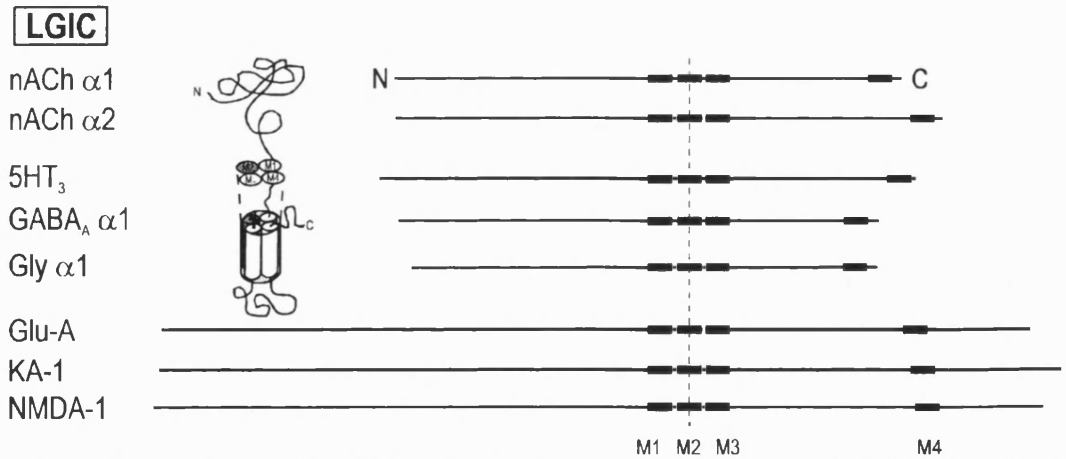

Figure 1.2: Subunits of the LGIC family members. Represented are the ACh family (first 5 subunits) and the glutamate family (remainder) aligned at the pore forming M2 region - lengths correspond directly to amino acid numbers. Membrane-spanning regions common to all subunits are shown (M1-M4). N-terminal domains are longest, noticeably so in the glutamate family (~450 cf. ~200 for ACh). A possible folding arrangement for the subunit is shown (inset) - an expanded representation is given in section 1.4.3.

membrane-spanning regions (M1-M4) which create the conduction pathway (see section 1.4.3). Among other conserved features are an extracellular N-terminal signal sequence, a long hydrophilic

N-terminal domain harbouring the agonist and competitive antagonist binding sites, conserved residues in the proposed pore-lining M2 region where non-competitive antagonists interact, and a large intracellular loop (located between M3 and M4) accommodating phosphorylation sites. This conserved topology and evident sequence similarity are sufficient to suggest that the LGIC channels may be based on similar 3-dimensional motifs.

Although these proteins are relatives in the same gene superfamily, they differ significantly in pharmacology, ion selectivity and response to allosteric modulators. The features that underlie these differences are beginning to emerge principally through the application of molecular biological techniques. Genes corresponding to the subunits of these receptors are being discovered and cloned with great rapidity, and are providing the foundations for the rigorous biochemical and pharmacological characterisation required to gain insight into the actual constitution of the different receptors found *in situ.* As will be demonstrated in section 1.3, the neuronal nAChRs are no exception, there now being at least ten different subunit genes, some of which contribute to the subtypes observed in neuronal tissue.

1.2 *Torpedo* electric organ nAChR - a LGIC prototype

Release of ACh into the synaptic cleft at the neuromuscular junction results in the rapid contraction of muscle fibres. Initial work on the characterisation of the nAChR mediating these events was performed on the electric organs of the electric eel, *Electrophorus*, and electric ray, *Torpedo.* These tissues are extremely rich in cells called electrocytes (or electroplax) which develop from muscle cells in the embryonic fish and are innervated by cholinergic neurons and therefore are an abundant source of nAChR - it is the summation of ACh-induced depolarisation of these cells which gives rise to the large electrical discharges associated with electric organs. Considered, therefore, to be an amenable model of the neuromuscular junction, the muscle-type nAChR of electric organ has been an invaluable tool for purification and characterisation studies on the nAChR protein. An additional factor which facilitated these studies is the occurrence of polypeptide toxins in certain snake venoms. Of these so-called α-toxins, α-bungarotoxin (αBgt) from the venom of *Bungarus multicinctus*, (the Taiwan banded krait), proved to be an almost irreversible antagonist of the muscle-type receptor, and can be radiolabelled to a high specific activity. These attributes make this toxin an extremely useful affinity ligand and have proved instrumental in the localisation, and isolation of the nACh receptor, and as such has established this protein complex as the LGIC benchmark.

1.3 Heterogeneity of the nACh receptor family

Before introducing the pharmacological subtypes of native nAChRs and functional array of cloned putative cholinergic receptors found in neuronal tissue, it is perhaps pertinent to briefly mention some of the more homologous attributes of the muscle-type and neuronal receptors - a detailed structural picture of the receptor will be presented in section 1.4.

Subunit composition

Highly purified detergent extracts of *Electrophorus* and *Torpedo* electric organ reveal a strong α-toxin binding component. When reconstituted in lipid bilayers, this 290kDa glycoprotein mimics the ligand binding, ion channel function and ligand-induced desensitisation phenomena associated with functional nAChR *in situ* (Galzi *et al* 1991). Electrophoretic studies using protein from all vertebrate species analysed to date, reveal this molecule to be composed of four distinct polypeptide subunits assembled into a heterooligomeric pentamer (Figure 1.3). The subunits, α, β, γ and δ, are all glycosylated with apparent molecular weights of 39, 48, 58 and 64kDa respectively (Schmidt & Raftery 1973), and form into a complex with $\alpha_2\beta\gamma\delta$ stoichiometry. Reconstitution of the protein in frog oocytes following injection of subunit mRNAs shows that the $\alpha_2\beta\gamma\delta$ oligomer contains all the structural elements required for the physiological response. In contrast to the muscle-type receptor, there are just two types of neuronal receptor subunits designated α and non-α (alias β), of which multiple subtypes have been described: α2-α9 and β2-β4 (see section 1.3.1). In the case of both the muscle-type and neuronal receptor the α subunits are characterised by the presence of two disulphide bridged cysteine residues located at positions 192 and 193 (*Torpedo* numbering), and form part of the principal ACh binding surface of the nAChR (see section 1.4.3.1). Non-α subunits are primarily structural though some amino acid residues are implicated in the formation of effector binding site(s) (see section 1.4.3.3).

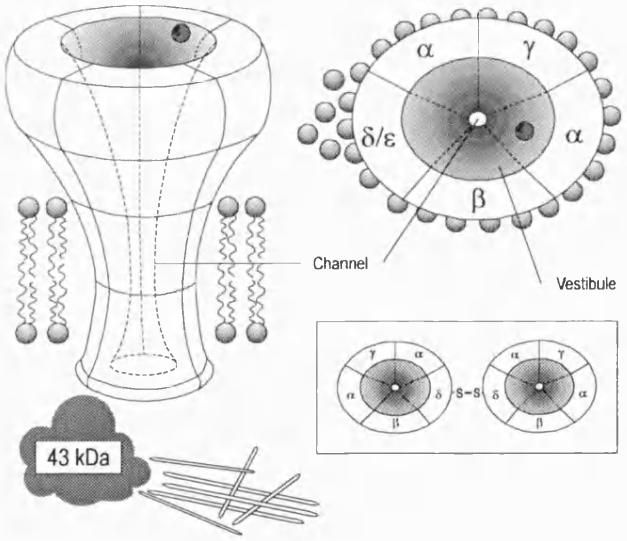

Figure 1.3: Associations of the muscle-type nAChR complex in its membrane environment. The heterooligomeric protein and ion channel results from the union of five subunits - α, β, γ and δ in muscle, but only α and β in neuronal tissue - at least two α subunits are required. In the native membrane environment the receptor is anchored via contact with a 43kDa protein and cytoskeletal elements. Unique to muscle nAChR is the formation of dimers via disulphide bridging of adjacent δ subunits (inset).

Variations in subunit composition of the receptor affect its physiological function. In adult muscle the ε subunit replaces γ, modifying both conductance and kinetic characteristics (Camacho *et al* 1993). In order to be functionally effective, muscle-type receptors require α and either just two (Sine & Claudio 1991) or even one (Golino & Hamill 1992) other subunit type. However, the pentameric complex is essential to maintain function: for example, omission of γ creates receptors of $\alpha_2\beta\delta_2$ stoichiometry (Charnet *et al* 1992b). The capacity for heterogeneity is accentuated among the neuronal proteins as combinations of α2, α3 or α4 subunits with either β2 or β4, manifest functional protein complexes which have unique sensitivities to cholinergic ligands (see sections 1.3.1.4 and

1.3.1.5). Neuronal receptors also form pentamers (see section 1.3.1.5) but may contain more than one type of α subunit, with, or without a β subunit. For instance the α7 subtype, a feature of this project, readily forms functional homomeric channels (Couturier *et al* 1990a) of a pentameric stoichiometry (Anand *et al* 1993).

Homology among the nAChR subunit sequences

The four polypeptide subunits of *Torpedo* share 54% homology overall (Noda *et al* 1983) and are therefore likely to have arisen from gene duplication.. Human muscle and electric fish α subunits show 80% sequence homology (Numa *et al* 1983) emphasising the strong evolutionary conservation of this receptor subunit. Mammalian and avian neuronal nAChR subunit sequences are equally homologous: comparisons of all α and β subunits from rat, chicken and human (see table1 of Sargent 1993) reveals amino acid sequence homologies of 40-60%, and corresponding sequences from rat and chicken are highly homologous (>70%). Even the subunit genes isolated from insects (Housefly and cockroach) and goldfish share significant homology with their more evolved counterparts. It should be pointed out that although neuronal non-α subunits are named β, this does not imply they are homologous to muscle-type β subunits, for they are not. In fact they are as similar to each other as they are to some of the neuronal α subunits.

Putative membrane spanning regions are indicated by strong conservation of stretches of hydrophobic amino acids (see section 1.4.1). Although overall amino acid sequence homology between gene products from neuronal and muscle sources from the same species is 40-55%, this may increase to nearly 100% in the transmembrane regions (especially M1-M2), and in certain regions of the ligand binding N-terminal domain.

1.3.1 Neuronal nAChR subtypes present *in situ*

Although the muscle nAChR is now relatively well defined much less is known about nAChR in the nervous system. Extensive genetic characterisation of the neuronal nicotinic receptor has recently been possible using the knowledge gained from work on the muscle subtype, primarily through the use of monoclonal antibody (MAb) and complementary DNA (cDNA) probes. Hampered by a lack of suitable ligand probes, a paucity of the receptor in neuronal tissue and the paradox of non-functional αBgt binding proteins (see section 1.3.1.2) in brain, the genetic makeup of neuronal nAChR did not become apparent until the mid to late 1980's (rev. Clarke 1992). As mentioned above, ten genes have since been identified in rat and chicken neuronal tissue that are homologous to the muscle nAChR genes - eight putative agonist binding subunits (α2-α9) and 3 structural subunits (β2-β4) (see Deneris *et al* 1991: Elgoyhen *et al* 1995). Before the functional implications of these subunits is considered the pharmacologically distinct native nAChR subtypes found *in situ* will be reviewed.

Three classes of pharmacological agents are recognised as affecting the behaviour of the nAChR as defined by pharmacological studies and radioligand binding experiments. Agonists (e.g. ACh, (-)nicotine, (-)cytisine, (-)lobeline, (+)anatoxin-a) initiate the mechanism(s) which open the

receptor channel. Antagonists, which prevent signal transduction events, are classified as either competitive (e.g. snake venom αtoxins, dihydroβerythroidine (DHβE) or methyllycaconitine (MLA)) which block the receptor response by binding to a site(s) overlapping with the agonist site, or non-competitive (e.g. d-tubocurarine (d-TC) and local anaesthetics such as hexamethonium and mecamylamine). The latter group operate by binding directly in the channel pore thus sterically hindering ion flow (hence the term 'channel blocker'), but alternatively may bind to distinct regulatory sites (see section 1.4.4.1 & 1.4.4.2). Comparative analysis of the interaction of these ligands with muscle and neuronal nAChR reveals the presence of pharmacologically distinct receptor populations.

1.3.1.1 Native neuronal nAChR subtypes identified by [^{3}H]-(-)-nicotine

[^{3}H]-(-)-nicotine binding to mammalian brain preparations were first carried out some 20 years ago (Schleiffer & Eldefrawi 1974). The advent of commercially available [^{3}H]-(-)-nicotine of high specific activity initiated a series of studies describing its binding to brain sites (rev. Wonnacott 1987a). Most extensively studied has been the rodent brain (see Romano & Goldstein 1980: Marks & Collins 1982: Yamada *et al* 1985: Lipiello *et al* 1987: Martino-Barrows & Kellar 1987) which demonstrates saturable, high affinity binding (K_d 2-60nM) of [^{3}H]-(-)-nicotine to what is now recognised to be a single receptor site - reported disparities in binding affinities have been attributed to the differences between protocols used for membrane preparation and binding assays. Although all nAChR recognise nicotine by definition, only those that bind nicotine with nanomolar affinity are labelled with the radiolabelled agonist. [^{3}H]-(-)-nicotine binding to brain is strongly stereospecific; (-) nicotine is some 10-60 times more effective than its isomer. Pharmacologically, the [^{3}H]-(-)-nicotine labelled sites show high affinities for cholinergic agonists and competitive antagonists, but lower affinities for non-competitive antagonists - see Wonnacott 1990. αBungarotoxin (see section 1.3.1.2) is unable to inhibit high affinity [^{3}H]-(-)-nicotine up to high micromolar concentrations.

The less stable, though no less effective, [^{3}H]ACh has also been used in the study of nAChRs. Irrefutable evidence from pharmacological studies (Schwartz *et al* 1982: Martino-Barrows & Kellar 1987), autoradiographic and biochemical studies reveal that the site recognised by [^{3}H]-(-)-nicotine and [^{3}H]ACh in the brain are the same - see section 1.3.1.3. Similarly, [^{3}H]cytisine and [^{3}H]methylcarbamylcholine label the same receptor population as [^{3}H]-(-)-nicotine (Wonnacott 1990).

1.3.1.2 Native neuronal nAChR labelled by snake αtoxins

[^{125}I]α Bungarotoxin (α Bgt)

There exist many functional nACh proteins in mammalian, avian, amphibian and insect neuronal tissue which exhibit a binding site for αbungarotoxin (αBgt). These sites, referred to as α bungarotoxin binding proteins (αBgtBPs), were for some time thought to be distinct from functional neuronal nAChRs (rev. Clarke 1992), despite exhibiting a nicotinic pharmacology, and being coincident on the same neurons as functional [^{3}H]-(-)-nicotine labelled nAChR (Jacob & Berg 1983: Smith *et al* 1986). Many features of neuronal αBgtBPs paralleled those of the muscle homologue: α Bgt binding could be blocked by the affinity reagents 4-(N-maleimido)-benzyltrimethylammonium

(MBTA) and bromoacetylcholine (Lukas & Bennett 1980), and sulphydral reduction (Marks *et al* 1986), whilst preincubation with non-competitive nicotinic antagonists enhanced the inhibition of [^{125}I] αBgt binding by ACh (Lukas & Bennett 1979). Although a successful probe for the muscle-type receptor, the usefulness of αBgt in identifying nAChRs of mammalian brain and ganglia was considered to be limited, given its failure to antagonise most nicotinic responses (Schmidt *et al* 1980). This was all the more confusing given the very good evidence for αBgt binding to a physiologically functional nAChR of the insect nervous system, and the isolation of a locust protein, (of comparable weight to that found in *Torpedo*), using a monoclonal antibody raised against nAChR from electric organ (Breer *et al* 1985). Despite these conflicting reports, work with this stable αtoxin, amenable to iodination, has continued (see Clarke 1992) and the persistence has been rewarded by the now conclusive evidence that mammalian neuronal αBgtBPs do represent functional nAChR (see section 1.3.1.7).

[^{125}I] neuronal bungarotoxin (nBgt)

A minor component of *Bungarus multicinctus* venom, and variously referred to as κ-Bgt, toxin 3.1 or toxin F, neuronal bungarotoxin (nBgt) specifically blocks the functional cholinergic responses associated with nAChRs of autonomic ganglia at concentrations of 5-100nM (Ravdin & Berg 1979: Chiappinelli 1983: Loring *et al* 1984). For instance [^{125}I]nBgt demonstrates high affinity for chick ciliary ganglia nAChR (K_d=5-6nM) being displaced by micromolar concentrations of ACh and nicotine, but not by αBgt (Halvorsen & Berg 1986) - ganglionic nAChRs, with the exception of α7- and α8-containing proteins, have greater affinity for nBgt (K_d=300nM for α3) than αBgt, which generally fails to block most ganglionic receptors up to 1μM concentrations.

[^{125}I]nBgt identifies two high affinity sites in the chick ciliary ganglion (Halvorsen & Berg 1986), one shared by αBgt (which binds extrasynaptically in ganglia) and another, synaptic site that is not. At the latter site, [^{125}I]nBgt binding is inhibited by nicotinic antagonists such as tubocurarine and DHβE, and nicotinic agonists such as DMPP. However, the affinities of these cholinergic agents (micromolar) contrasts with the nM affinities displayed by [^{3}H]-(-)-nicotine sites, an observation consistent with the absence of high affinity [^{3}H]agonist binding to ganglionic neurons. Distributions of [^{125}I]nBgt- and [^{125}I]αBgt-labelled sites on ciliary ganglia differ considerably - αBgt receptors are uniformly distributed whereas the nBgt site not recognised by αBgt is concentrated at synaptic membranes (see Loring & Zigmond 1988). This coincides with the localisation of α3, α5 and β2 subunits immunopurified from the same tissue (Conroy *et al* 1992) using mAb35, a monoclonal antibody raised against *Torpedo* nAChR and confirmed to identify functional receptors (rev. Loring & Zigmond 1988). Therefore in ganglia at least nBgt labels a distinct cholinergic receptor, whose distribution and number is essentially mirrored by mAb35.

It is unfortunate that the difficulty of obtaining isolated, pure toxin from snake venom has raised questions about the validity of the receptors identified using nBgt as specific probes for the nAChR, as with many other LGICs, are few and far between.

1.3.1.3 Distribution of high affinity [^{3}H]-(-)-nicotine and [^{125}I]αBgt receptor sites

Autoradiographic analysis of rat brain sections labelled with [^{3}H]-(-)-nicotine and [^{3}H]ACh reveal an identical pattern of distribution of binding of these ligands (Clarke *et al* 1985). The strongest presence is revealed in the interpeduncular nucleus, superior colliculus, medial hebenular and thalamus. This distribution is very different from that observed for [^{125}I]αBgt (Clarke *et al* 1985) which is high in the cerebral cortex, hypothalamus, hippocampus, inferior colliculus and some regions of the brain stem. A more refined picture is revealed by Swanson and co-workers (1987) through immunohistochemical studies of avian and mammalian CNS. If the pharmacological profiles of these two distinct sites are also compared, little correlation is evident (Figure 1.4).

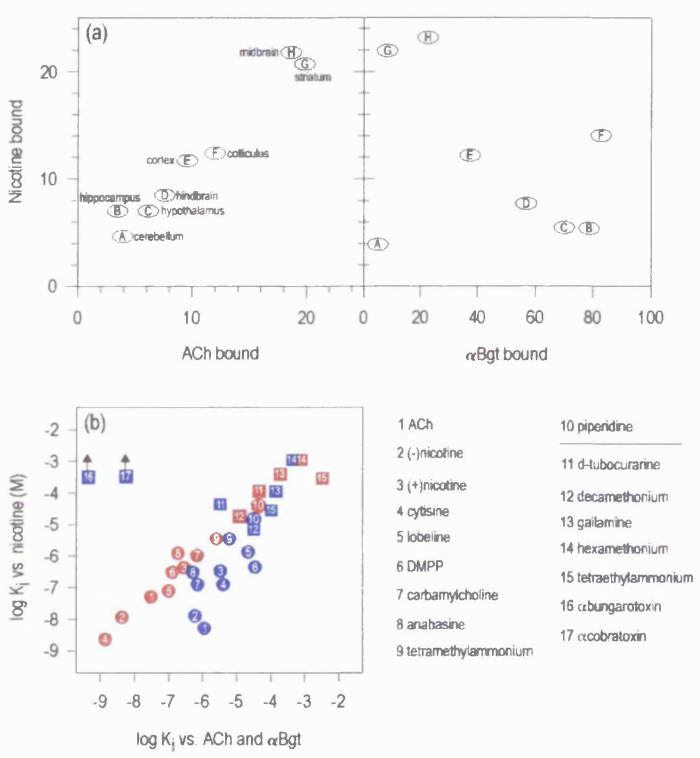

Figure 1.4: Regional distribution (a) and pharmacological specificity (b) of nicotinic cholinergic binding sites in rat brain. (a) binding site numbers (fmol/mg protein) in different brain regions relate to radiolabelled ligands - data is taken from Marks *et al* (1986). Sites labelled by nicotine and ACh are highly correlated (r=0.99), the same cannot be said of nicotine and αBgt (r=0.33). This pattern is mirrored in the pharmacological correlations of these sites (b): nicotine/ACh (red), r=0.98: nicotine/αBgt (blue), r=0.14. Agonists (❍) are more potent than antagonists (□). Figure redrawn from Wonnacott (1990).

Consideration of immunocytochemical studies using monoclonal antibodies specific for particular subunits corroborates the distinctness of [^{3}H]-(-)-nicotine and [^{125}I]αBgt labelled brain nAChRs and in general confirms the α4 subunit to associate mainly with [^{3}H]-(-)-nicotine/[^{3}H]ACh binding and α7 and α8 with αBgt (rev. Lindstrom *et al* 1987: Sargent 1993).

The pattern of gene expression for the subunits has refined speculation as to the putative subunit composition of the nAChRs identified by radioligands. *In situ* hybridisation assays show that at least one nAChR gene is expressed in numerous areas within rat brain and that each gene is expressed in a distinct pattern (Wada *et al* 1989: Seguela *et al* 1992). The anatomical distribution of rat brain regions expressing nAChR genes correlates fairly well with the distribution of high affinity [^{3}H]-(-)-nicotine and [^{3}H]ACh sites (Clarke *et al* 1985) and with anti-AChR antibody binding (Swanson *et al* 1987). As such these observations, and those resulting from heterologous expression of subunit

genes in various cell lines (see section 1.3.1.4), have confirmed the heterogeneity of the nAChR and the probable subunit composition of principle receptors identified by radioligands.

1.3.1.4 Heterologous expression of cloned neuronal nAChR subunits

Many lines of evidence support the notion that the genes identified, cloned and sequenced from mammalian and avian nervous tissue could be those that encode nAChR subunits. As discussed above, the pattern of expression of these genes in autonomic neurons and brain nuclei closely resembles that of high affinity [^{3}H]-(-)-nicotine/ACh and [^{125}I]αBgt sites, and is consistent with nicotinic responses in the same regions. Perhaps the most solid support for these genes representing nAChR subunit sequences is apparent when they are transfected, or the corresponding cDNAs/mRNAs injected, into non-neuronal cells and are able to form fully functional receptors responsive to cholinergic ligands.

Following injection of mRNAs of the rat α2, α3 or α4 subunits in combination with either the β2 or β4 gene into *Xenopus* oocytes (Boulter *et al* 1987: Wada *et al* 1988: Deneris *et al* 1989) functional nAChRs are expressed and appear in the membrane (Figure 1.5). Only the α4 subunit, of these clones, is able to form, albeit unstable, homomeric channels. This picture is repeated for the equivalent chicken subunits following cDNA injection into the oocyte nucleus (Ballivet *et al* 1988: Couturier *et al* 1990b). This suggests that these genes do indeed encode valid nAChR subunits and that specific combinations of α and β coassemble to form individual functional nAChRs, complementing the immunocytochemical and autoradiographic findings (see Sargent 1993).

The rat α5 and α6 cDNAs are unable to form functional channels in oocytes even when injected with several other α and β clones (Boulter *et al* 1990). Similarly, rat β3 does not form channels when coinjected as mRNA with α2, α3 and α4 clones (Deneris *et al* 1989). These subunits may be required to coassemble with as yet undiscovered subunits in the formation of the channel or, as with α5, which has been found to be assembled with α4 and β2 in the same complex (Conroy *et al* 1992), require more than one different subunit type. Of course there is always the possibility that the 'non-functional' subunits are members of another family of LGICs or are incorrectly, or insufficiently, modified following their translation in the amphibian oocyte. It is evident that the stably expressed nAChRs in mouse fibroblasts (M10) transfected with chicken α4 and β2 cDNAs (Whiting *et al* 1991), are pharmacologically very similar to those in chicken brain where both α4 and β2 predominate (Morris *et al* 1990).

Agonists and antagonists distinguish proteins with distinct cholinergic pharmacologies

Pairwise injection of α2, α3 or α4 with either β2 or β4 yields six pharmacologically distinct nAChRs as demonstrated by their unique rank order of potency to the agonists nicotine, ACh, cytisine and DMPP (Luetje & Patrick 1991). Both α and β subunits contribute significantly to the observed potencies. Notably cytisine sensitivity is radically affected depending on the nature of the β subunit: β4-containing nAChRs are more sensitive to cytisine than other agonists, while β2-containing receptors are almost completely insensitive to cytisine. Properties of these putative

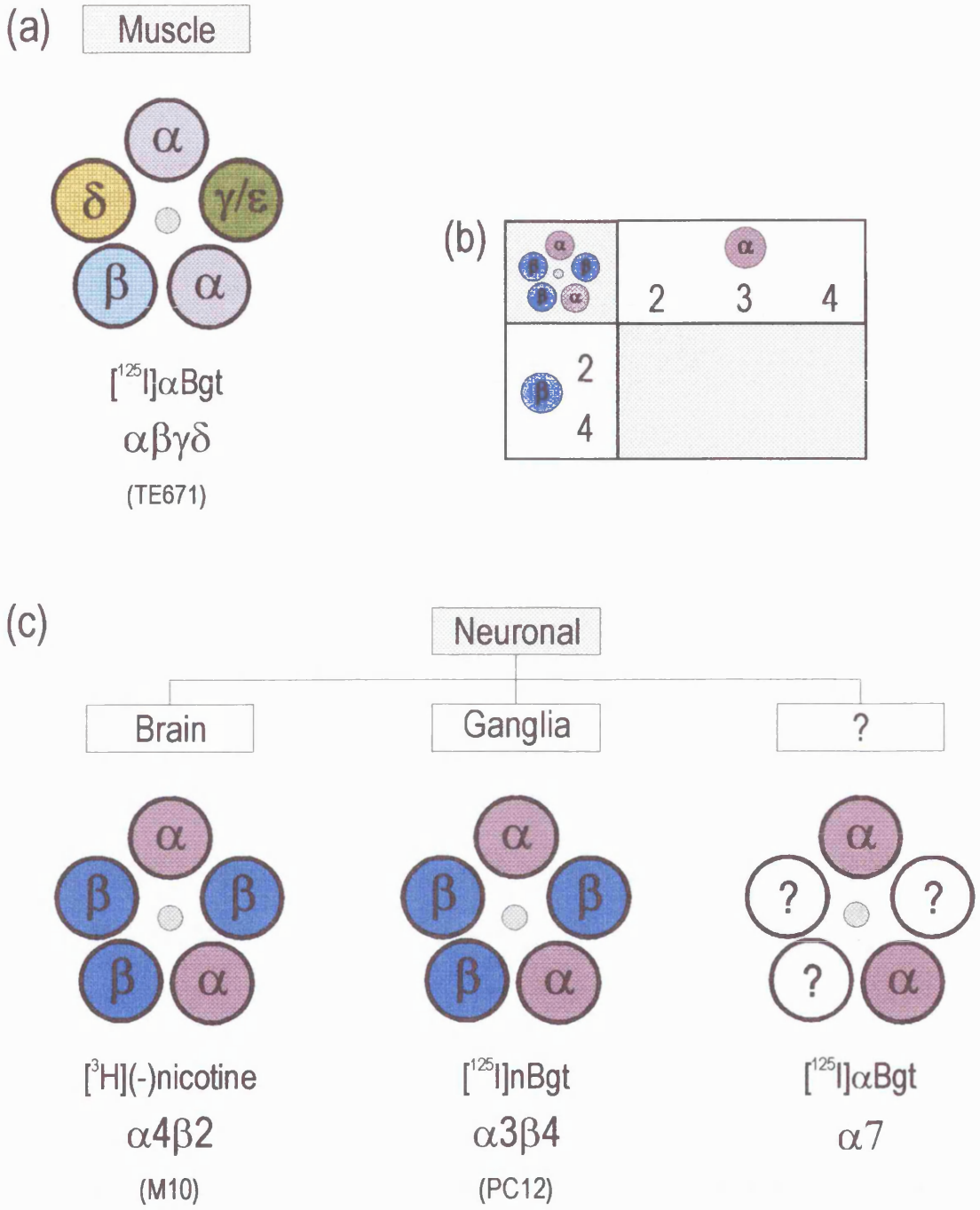

Figure 1.5: Subunits represented in muscle and principle brain nAChRs following injection into non-neuronal cells. Both muscle and neuronal nAChR form as pentameric complexes as represented. [^{125}I]αBgt binds with high affinity to receptors in muscle and electric organ, complexes that comprise αβγ/ε and δ subunits (a). Injection of cloned neuronal subunit mRNA or cDNA into *Xenopus* oocytes in various combinations (b) reveals that pharmacologically equivalent receptors to those labelled *in situ* by [^{3}H]-(-)-nicotine, [^{125}I]nBgt and [^{125}I]αBgt are expressed (c): the principle brain receptor (labelled by [^{3}H]-(-)-nicotine) comprises α4β2 subunits, the nAChR of autonomic ganglia (that labelled by [^{125}I]nBgt), constitutes α3β4, and receptors identified by [^{125}I]αBgt comprise α7 (and/or α8) subunits which are functional as homomeric channels, though this may not necessarily represent their native form. Cell line models of these various receptors are given in parenthesis.

nAChR are equally affected by the nature of the α subunit. α4β2 heterooligomers have higher affinity for ACh and desensitise to a lesser extent than do α3β2 nAChRs (Gross *et al* 1991). Species differences are also apparent between equivalent nAChR subunits because the differences observed for the chicken α4β2 and α3β2 receptors are not apparent for the equivalent heterooligomers of rat (Luetje & Patrick 1991). The α7 homomeric receptor is very different again from chicken α4β2 and rat α4β2 demonstrating a higher affinity for nicotine than ACh and more extensive desensitisation (Couturier *et al* 1990b).

Oocyte expression of heterologous subunits has confirmed the existence of the nAChR subtype sensitive to nBgt and has identified the α3 subunit as responsible for conferring this specificity. nBgt (100nM) completely abolishes ACh-induced currents of receptors formed on injection of α3 and β2 mRNAs in oocytes (Luetje *et al* 1990). The α4β2 nAChR is less sensitive and α2β2 are completely insensitive to this toxin. As with the agonist sensitivities, antagonists are also differentially influenced by the nature of the β subunit and α3β4 nAChRs are completely insensitive to nBgt (Duvoisin *et al* 1989). The αBgt binding protein component α7 is the only subunit whose ACh-induced currents are functionally blocked by αBgt (IC_{50}=0.9nM), and it does so as a homomeric receptor (Couturier *et al* 1990a).

1.3.1.5 Electrophysiological diversity of reconstituted receptors

Combinations of α2, α3 or α4 mRNA with β2 generate cell surface proteins in the oocyte which have unique single channel properties, and in the case of α2β2 and α3β2 two conductance states are observed (Papke *et al* 1989) - Charnet and co-workers (1992a) report three electrophysiologically distinct channels following α4 and β2 injection. This latter phenomenon raises the question of how more than one distinct nAChR population appears in the oocyte following injection of a single α and single β subunit? There may be two explanations for this:

- subunit coassembly is a promiscuous event: for instance subunit stoichiometry may vary (e.g. $\alpha_2\beta_2$, $\alpha_3\beta_2$, $\alpha_2\beta_3$, $\alpha_3\beta_3$), as might the subunit order around the pore (e.g. αβαββ, ααββββ etc.). Present opinion favours an α:β stoichiometry of 2:3 for the neuronal nAChRs. Besides activation characterised by Hill coefficients greater than unity and a size (~300kDa) indicative of a pentameric structure, α4β2 nAChRs have also been ^{35}S-methionine labelled (Anand *et al* 1991) and indeed the ratio of α:β subunits was 1:1.46 implying a $\alpha_2\beta_3$ stoichiometry. The α4β2 nAChR stably transfected into M10 mouse fibroblast corroborates this (Whiting *et al* 1991), as do the channel conductance studies of Cooper and co-workers (1991).
- channels of the same subunit arrangement may undergo different post-translational modifications in the oocyte.

Whatever the reason, these multiple conductance states are also apparent in β4-containing receptors (Papke & Heinemann 1991), though mean conductances are again distinct from β2-containing proteins.

1.3.1.6 Correlations of native and expressed receptors

One goal of expression studies is to be able to interpret experimental observations in terms of native receptors. However caution must be emphasised. For example heterologously expressed α3 β2 and α3β4 nAChRs have higher affinities for ACh (Bertrand *et al* 1991: Gross *et al* 1991) than the native chick ciliary ganglion receptors of the same constitution (Margiotta *et al* 1987). Likewise the channel conductance of reconstituted α4β4 nAChRs does not match that of the native channels in the interpeduncular nucleus (IPN). This brain region also shows the presence of α2, α3, α4, α5, β2 and β4 subunit genes (although not necessarily on the same neuron) - the nicotinic receptors of IPN neurons have a channel conductance of 35pS (Mulle *et al* 1991), a value very close to that exhibited by the predominant nAChR, α2β2, found in these neurons (34pS: Papke *et al* 1989). This correlation may indicate that α2 and β2 subunits form the principal nAChR of IPN neurons.

This latter case currently represents the only situation where there is direct correlation between the native nAChR and that observed upon expression of subunit genes in the oocyte. If more physiological attributes are considered then the number of variables defined for the match markedly reduces the hit rate. Even considering simply agonist rank order of potency and conductance characteristics can reduce the coincidence. For example in the rat medial hebenular and the autonomic ganglion cell model (PC12 cell), conductance states (26pS) indicate the presence of α3β4 channels (22pS), yet the agonist rank order of potency of these same channels resembles that of no other heterologously expressed nAChR subtype (Luetje & Patrick 1991: Mulle *et al* 1991). As mentioned previously, these anomalies may be a consequence of factors alluded to earlier: poor processing by the oocyte or a requirement for different subunits, which may as yet be unidentified.

1.3.1.7 Functional role of αbungarotoxin Binding Proteins

αBgtBPs of chick optic lobe (Wong & Schmidt 1976) and retina (Betz 1981), and goldfish brain (Henley & Oswald 1987), exhibit high (nM) affinity for [^{125}I]αBgt and demonstrate a nicotinic pharmacology (i.e. low micromolar affinity for agonists, ACh and nicotine). The isolated protein complexes are similar in size (with sedimentation coefficients ~11S) to those of electric organ, muscle and brain, though antigenic complementarity is limited (see Lindstrom *et al* 1987). That these αBgtBPs are members of the same nAChR gene family is apparent when it is realised that the lighter (48kDa) of the 4 to 5 polypeptides that constitute the αBgtBP complex, shows considerable homology with the N-terminal sequence of electric organ and muscle derived nAChR subunits (Conti-Tronconi *et al* 1985), and furthermore by the presence of homologous cysteines 192 and 193 (Norman *et al* 1982). Unequivocal support for the function of αBgtBPs as Ligand-Gated Ion Channels has since been demonstrated in the chick ciliary ganglion (Zhang *et al* 1994), where these proteins appear responsible for increasing levels of intracellular calcium.

Rodent brain αBgtBPs have also been extensively investigated (Marks & Collins 1982: Lukas 1986: Marks *et al* 1986), and as with their insect, fish and avian counterparts have a distinctly nicotinic pharmacology. As mentioned earlier, these proteins are distinct from those neuronal nAChR which bind nicotine and ACh with high affinity, exhibiting a quite different distribution pattern in brain

(see section 1.3.1.3). Limited antigenic and structural homology is evident between electric organ and muscle nAChRs, and neuronal αBgtBPs (Morley *et al* 1983: Mills & Wonnacott 1984). Affinity chromatography purification of a rat brain αBgtBP (Whiting & Lindstrom 1987) identifies a complex of four polypeptides (MW: 45, 52, 56 and 65 kDa). [^{3}H]MBTA and [^{3}H]-bromoacetylcholine (BAC) alkylate a 55kDa component which is presumed to be an α subunit for the αBgtBP (Norman *et al* 1982: Kemp *et al* 1985). As many as four additional components have been reported to copurify with this subunit (Conti-Tronconi *et al* 1985) but it is unclear whether these may be artefactual or represent other subunits that form an αBgtBP heterooligomer.

Two groups (Couturier *et al* 1990*a*: Schoepfer *et al* 1990) have since unequivocally demonstrated the presence of two subunits (α7 and α8) in chick brain able to bind αBgt with high affinity. Furthermore α7 appears as a 57kDa protein in denaturing gels, concurrent with the size of the subunit affinity alkylated by [^{3}H]MBTA and [^{3}H]-BAC. The α7 subunit is predominant among the [^{125}I] αBgt binding sites - an α7-specific MAb immunoprecipitates >90% of the αBgt sensitive nAChRs. Rat (Seguela *et al* 1992) and human (Peng *et al* 1994) brain α7 subunit genes have also been identified. Use of an antisense probe to supress the expression of the α3 subunit in chick sympathetic neurons provides strong evidence that this subunit may be associated in the same complex with α7 (Listerud *et al* 1991). The rat α9 subunit also exhibits high affinity for αBgt and, as with α7 and α8 subunits, is able to form functional homomeric proteins gated by nicotinic, but also muscarinic, ligands (Elgoyhen *et al* 1995).

1.4 Structural features of the nicotinic receptor complex

Section 1.3 briefly outlined the themes that underlie the 3-dimensional structure of the muscle-like and neuronal nicotinic receptors. These features (Figure 1.6) stem from a series of conserved motifs among the constituent subunits and will be reviewed in more detail in the ensuing sections with a view to mapping the locations of the various effector sites and understanding how the associations impart the functional character of the receptor. Emphasis will be placed on the residues implicated in, and nature of, the ligand binding site(s) as it is this region which is most crucial to receptor activation events via interaction with ligands which dictate the nature of the nAChR pharmacophore.

1.4.1 Motifs of subunit primary structure

The following observations have been widely reviewed (see Galzi *et al* 1991a: Sargent 1993). Four distinct regions of hydrophobic amino acids are obvious on alignment of *Torpedo*, muscle and neuronal derived subunit sequences (Figure 1.6c & d). These putative membrane-spanning regions (M1-M4), some 20-30 amino acids in length, are presumed to fold into mainly α helix (Noda *et al* 1983) as they span the ~32Å hydrophobic portion of the bilayer (Figure 1.4e). M2 lines and gates the channel and carries the binding site for non-competitive channel blockers (see section 1.4.4.2).

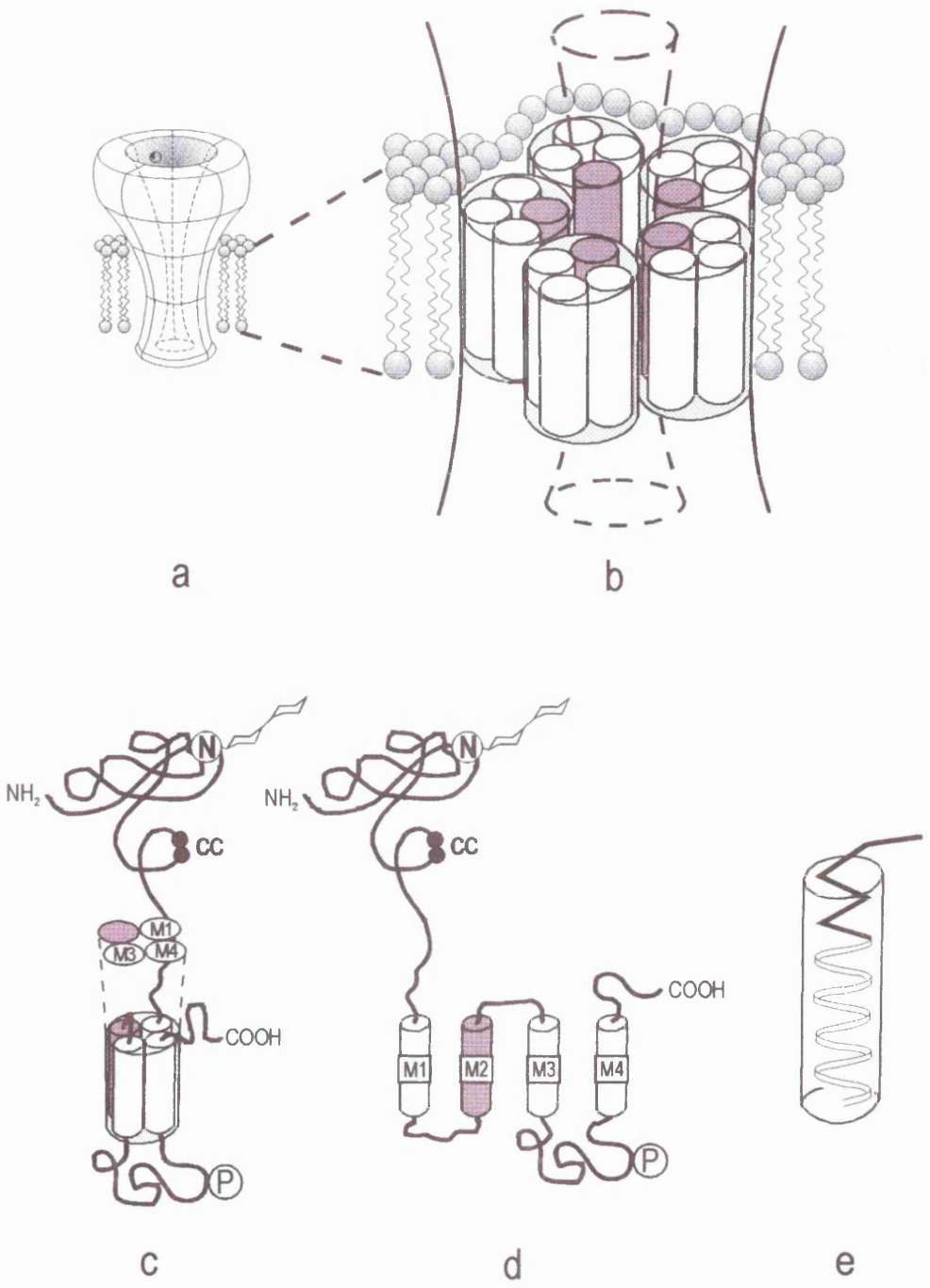

Figure 1.6: Model of transmembrane topology and organisation of the nAChR subunits. Possible arrangement of the five subunits about the axis of pseudosymmetry of the receptor (a) in the creation of the ion pore (b). Models of the subunit topology, largely based on hydrophobicity profiles of the amino acid sequence and antibody studies, reveal the presence of four transmembrane regions (M1-M4) per subunit which associate non-covalently as they cross the membrane with the M2 portion (purple) facing the channel lumen (b). Each subunit (c) & (d) is characterised by a large extracelluiary located N-terminal domain bearing glycosylation sites and, in α subunits, a pair of conserved cysteines (CC). Between M3 and M4 is an intracellular loop containing potential phosphorylation sites through which receptor function can be modulated. Channel lining residues of M2 have periodicity indicative of α helical structure while the remainder may be β-barrel (e) (Unwin 1993) - this may be reflected in the other transmembrane sequences.

All nAChR subunit sequences have a large hydrophilic N-terminal domain oriented toward the synaptic cleft which bears an N-glycosylation site (N141 - *Torpedo* labelling). Hydrophobic M1, M2 and M3 regions separate this domain from a smaller but similarly hydrophilic variable cytoplasmic loop which carries consensus sites for phosphorylation. Modulation of the receptor through phosphorylation of these sites by protein kinases influences the desensitisation characteristics of the receptor. M4 connects this loop to the short C-terminal region, creating a model whereby both N- and C-terminus are extracellularly located (DiPaola *et al* 1989). The agonist binding site is confined to the N-terminal domain (see section 1.4.3) with the ion channel in the axis of pseudosymmetry of the protein complex, as revealed by electron microscopy (see section 1.4.2). It is apparent from the remoteness of effector site and channel that indirect or 'allosteric' interactions must occur in order for effective signal transduction to take place.

A stretch of ~40 amino acids is also rigorously conserved in all muscle and neuronal nAChR subunits. Characteristically amphipathic and with the periodicity of an α helix (Finer-Moore & Stroud 1984: Guy 1984), this sequence does not appear in subunits of other LGIC family members. Its original designation as a transmembrane segment lining the channel has now been discounted but its role is still an enigma.

1.4.2 Electron microscopic structure of the receptor

The subunits of the nAChR protein complex are intimately associated by non-covalent interactions and in *Torpedo* the receptor predominately occurs as a dimer of oligomers (Figure 1.3). This association, unique among LGICs, occurs through disulphide cross-linking of cysteine residues at the carboxy terminus of the adjacent δ subunits (Dunn *et al* 1986). The quaternary structure of the nAChR is unknown, but a rudimentary picture is emerging through studies on tubular crystals of *Torpedo* membranes densely packed with nAChR using electron microscopy (Unwin 1993). A consensus representation of the membrane-bound configuration is as drawn in Figure 1.1. At 9Å resolution the receptor appears perpendicular to the membrane being some 120Å in length with subunits arranged rosette-like in a left-handed twist around a central axis. The conduction pathway consists of a narrow pore across the bilayer some 30Å long, with the narrowest diameter, around 7Å, representing the gating site and ion selectivity filter . Much of the receptor is extracellular with protein extending some 55Å above the membrane. These extracellular domains of each of the five subunits form a cylindrical vestibule which accounts for ~20% of the solvent accessible surface area of the extracellular region. A protein wall some 25Å thick insulates this entrance cavity from changes in the membrane potential field, having dimensions indicative of β-barrel structure. Analysis of aligned sequences predicts a net charge of -50mV for this extracellular domain (residues 1-228) at pH7 (Stroud *et al* 1990). If evenly distributed the vestibule could contain at least 10 negative charges thus concentrating cations at the mouth of the channel (Dani & Eisenmann 1987). Notably, anion conducting $GABA_A$ and glycine receptors have excess positive charge in this same region.

Disposition of agonist and non-competitive antagonist sites.

The distance between the agonist and channel sites is estimated to be 20-40Å according to studies using the fluorescent agonist dansyl choline (Waksman *et al* 1980), and the competitive antagonist bis(choline)-N-(4-nitrobenzo-2-oxa-1,3-diazol-7-yl)-iminodipropionate (BCNI: Bolger *et al* 1984). More recent fluorescence lifetime and energy transfer experiments (Herz *et al* 1989) place the acetylcholine binding site 20-30Å from the membrane, a finding consistent with electron microscopy results of the whole receptor (Unwin 1993) - the reconstituted image of the receptor reveals distinct bulges at this point and even at quite low resolution (Toyoshima & Unwin 1990) a cleft and internal cavity are evident suggesting that this binding pocket is as close to the membrane as to the top of the protein. Therefore, the allosteric interaction between ACh binding sites and channel occurs over considerable distances, suggesting an intricate model of the binding site required to bring about such long-range interactions.

The 43kDa receptor-associated entity

Another prominent feature of the membrane bound muscle receptor which is revealed through electron microscopy is the presence of a large cytoplasmic element which intimately associates with the receptor (Figure 1.3). Various cytoskeletal and regulatory molecules, including protein kinases (Huganir & Greengard 1990) converge here, in particular a so-called '43kDa protein' which may represent the receptor associated entity revealed by EM images. Several indirect lines of evidence suggest that this protein may be involved in the establishment and/or maintenance of nAChR clusters at synaptic junctions.

1.4.3 Structure of the acetylcholine binding site

Three classes of pharmacological agents are recognised as affecting the nAChR as defined by pharmacological studies and radioligand binding experiments (see section 1.3.1). Agonists initiate the mechanism(s) which open the receptor channel. Competitive antagonists prevent signal transduction events by occluding the agonist site. Non-competitive antagonists operate by binding directly in the channel pore thus sterically hindering ion flow (hence the term 'channel blocker'), but alternatively may bind to distinct regulatory sites (see section 1.4.4.1). The pharmacologically distinct nAChR populations of muscle and neuronal tissue are united by the fact that the agonists and competitive antagonists impinging on them exert their effects by binding to overlapping site(s) carried principally by the α subunits (rev. Lindstrom *et al* 1987). The residues implicated in the recognition and binding phenomena leading up to activation (and desensitisation), or inhibition are described below.

1.4.3.1 Residues labelled using cholinergic affinity probes

The agonist molecules that bind to and activate the nicotinic receptor complex are very small in comparison to the protein. This suggests that the binding site itself need only be a small region of the protein, the remainder of the complex providing the architecture required for the channel and for transducing the long-range conformational changes between the topographically remote agonist and channel sites. The changes leading up to channel opening may be initiated through a local

disturbance on agonist binding which could be envisaged through a complex 3-dimensional architecture around the agonist molecule. Indeed acetylcholinesterase hydrolyses ACh through a spatially complex site consisting of a narrow gorge lined by some 14 aromatic residues (Sussman *et al* 1991), though conformational changes are not prerequisite for this latter case.

Although there is evidence that the nAChR binding site may lie, at least partially, between the interface of the α subunit and its neighbour (see section 1.4.3.3), many residues of the α subunit contribute to the ACh binding region. The disulphide-linked adjacent cysteines at positions α192 and α193 of native nAChR from all species and tissues, when reduced, are the site of incorporation of the affinity label MBTA (4-(N-maleimido)-benzyltrimethylammonium) (Kao *et al* 1984). A variety of studies based on snake αtoxin binding to regions including these residues, and mutagenesis experiments, have confirmed that the region containing cysteines 192 and 193 contributes to the binding site for nicotinic ligands (see Galzi *et al* 1991a).

The intimate molecular organisation of the ACh-binding site has been probed most extensively and successfully using the photoaffinity probe DDF (N,N-(dimethylamine) benzenediazonium flouroborate). This molecule acts as a reversible competitive antagonist of the nAChR of *Electrophorus* and the C2 mouse cell line (Langenbuch-Cachet *et al* 1988) under light-excluding conditions. Photoactivation of this ligand via an excited tryptophan residue in the binding site, improves the labelling specificity with no need for prior reduction, and reveals that DDF strongly labels the agonist/competitive antagonist binding site with one molecule being incorporated per αBgt binding site (Langenbach-Cachet *et al* 1988). Residues labelled by [^{3}H]DDF, in a carbamylcholine-sensitive manner, are identified in three distinct regions of the α subunit (Dennis *et al* 1986).

Five residues are strongly labelled by DDF: Tyrosine 93, Tryptophan 149, Tyrosine 190 and the two cysteines 192 and 193 (*Torpedo* numbering). Additionally, some weak affinity is also demonstrated for Tryptophan 86, Tyrosine 151 and Tyrosine 198 of the α subunit (Dennis *et al* 1988: Galzi *et al* 1990). DDF labelling of these regions is competitive with both αtoxin and carbamylcholine. Thus it seems that the architecture of the binding site on the α subunit is indeed complex involving a cavity created by at least three loops of amino acids in the N-terminal hydrophilic domain (Figure 1.7). Complexity is extended by the confirmation that as yet unidentified residue(s) of the γ subunit are also labelled by [^{3}H]DDF (Langenbuch-Cachet *et al* 1988), providing direct support for the involvement of non-α subunit residues in the building of the site (see section 1.4.3.3).

Any preconceptions that these DDF labelled residues may be artefactual or coincidental can be discounted for a number of reasons:

- Cysteines 192 and 193 are labelled both by DDF and MBTA.
- Tyrosine 190 reacts covalently with the competitive antagonist lophotoxin from marine coral (Abramson *et al* 1989).
- All the residues labelled by DDF are conserved at homologous positions in all α subunits from muscle and neuronal sources from all species examined to date, including humans. The only

exception being the neuronal α5 subunit, which lacks Tyr93 and Tyr190, but this subunit is unable to form functional nAChR with any non-α subunits when expressed in the *Xenopus* oocyte system (Boulter *et al* 1990).

- Muscle-type non-α subunits (i.e. β1, γ and δ) lack the principal five amino acids labelled by DDF.

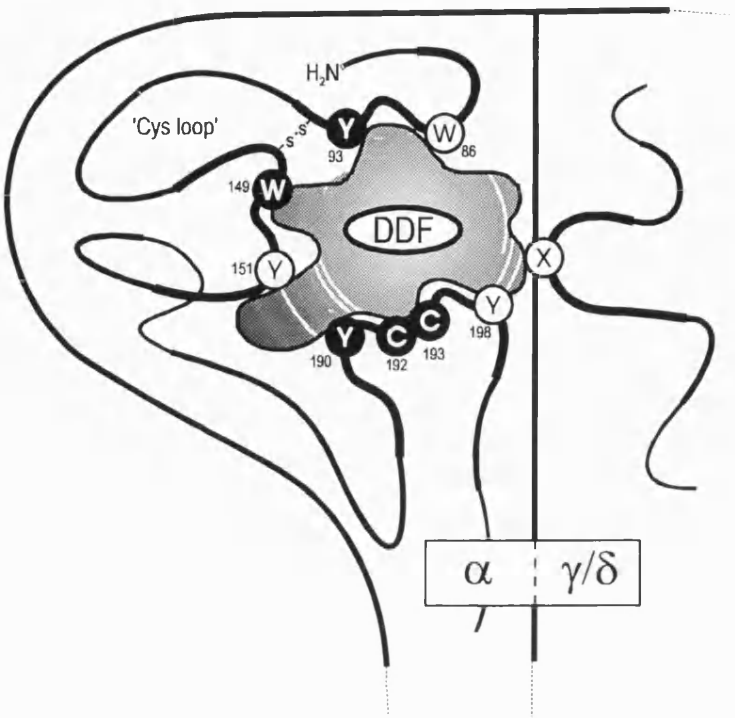

Figure 1.7: Model of the agonist/competitive antagonist binding site. Represented are the key residues in the α subunit of the nAChR identified by the photoactivatable competitive antagonist DDF. Black balls represent amino acids most strongly labelled and include those labelled by lophotoxin (Y190) and MBTA (C192/193) - *Torpedo* numbering. The site appears to consist of three loops of amino acids which are mainly hydrophobic in character. The conserved 'Cys-loop' (see section 1.4.3.2) is also shown containing potential interaction sites yet no residues of this sequence are identified by the photolabel. Unidentified residues (X) in the γ and δ subunits of muscle nAChR are also identified by DDF and may be a negative subsite.

Neuronal nAChR non-α subunits have however conserved two of the DDF residues, namely: Tyr93 and Trp149 (Deneris *et al* 1988: Nef *et al* 1988: Duvoisin *et al* 1989: Isenberg & Meyer 1989). This conservation of some α-like features implies that these subunits may have a function in neuronal tissue. This is not altogether surprising given that γ and δ subunit equivalents appear to be absent in neuronal receptors and that the α subunit seems only to provide part of the binding site (see section 1.4.3.3).

The evidence is therefore very clear. Residues labelled by DDF, MBTA and lophotoxin, all molecules which demonstrate a clear nicotinic cholinergic pharmacology, are highly conserved through evolution and must therefore be strong candidates in the formation of the ACh binding site of the α subunits. More recently, a further region encompassing Trp54 of the α subunit has been implicated in the binding of cholinergic ligands to the α7 homomeric receptor (Corringer *et al* 1995), a position which is analogous to Trp residues labelled by d-TC in the γ and δ subunits of the *Torpedo* receptor, supporting a role for non-α subunits in the formation of the site (see section 1.4.3.3).

1.4.3.2 Contribution of other sequences on the α subunit to the site - the 'Cys-loop'

Two additional cysteine residues, 128 and 142, are conserved in the subunits of all nAChR subunits, as well as $GABA_A$ and Glycine receptors. These residues have been proposed to form a

disulphide bridge *in vivo* generating a highly conserved 15-residue loop, termed the 'Cys-loop' (Kao & Karlin 1986). A synthetic peptide of this region interacts with ACh and αBgt (McCormick & Atassi 1984) and sequential mutation of all the residues to serine totally abolishes ACh-induced responses in the native receptor (Mishina *et al* 1985). As regards the brain receptor, high affinity nicotine binding is specifically inhibited by antibodies raised to a peptide encompassing positions 3-12 of the neuronal α subunit loop.

It has long been a widely held belief that carboxylate anions (side chains of aspartic and glutamic acids) are the principal species which interact with the cationic headgroup of nicotinic ligands. Good candidates for this anionic site exist in the δ subunit of the muscle-type receptor (see section 1.4.3.3 and 1.4.3.5) and also at position 11 of the 'Cys loop' (Figure 1.8), an invariant aspartate, one of only two invariant acidic residues in the whole of the N-terminal hydrophilic domain of LGIC subunits. Theoretically modelled as forming a rigid β-hairpin (Cockcroft *et al* 1990), the loop has inherited a number of additional features which are proposed to account for neurotransmitter specificities of the various ligand-gated channels and provision of binding surface residues. More specifically, conserved hydrophobic and hydrophilic residues are positioned such that the structure assumes an amphipathic character, the hydrophilic face containing four invariant or strongly conserved residues which includes the anionic and specificity residues. Although the theoretical picture being painted is a very neat one, unfortunately none of the residues in this loop are labelled by photoaffinity reagents, though this may reflect orientation and/or reactivity restrictions of these chemicals in this region.

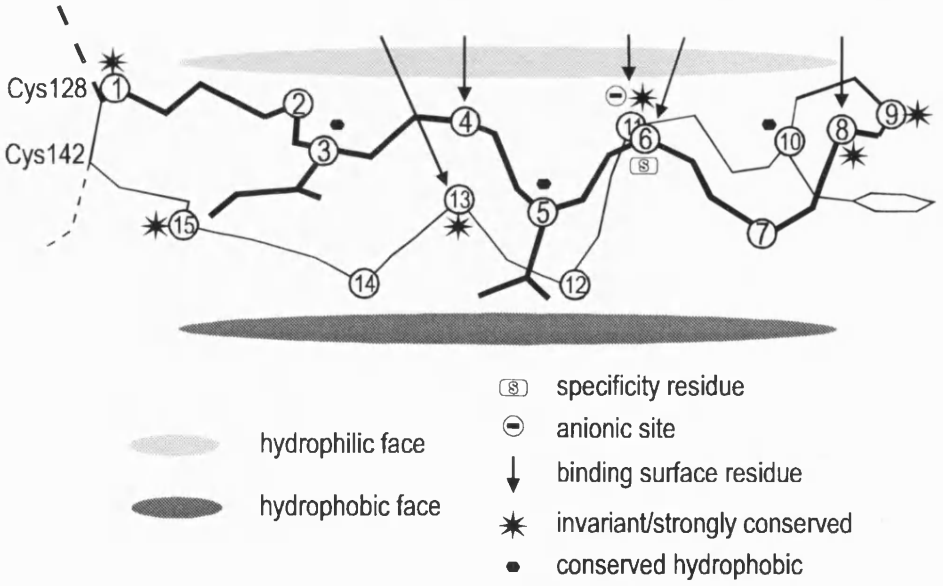

Figure 1.8: Energy minimised model of the 'Cys-loop' structure of the chick α2 subunit. Containing many attractive features of a potential binding surface this conserved 15 residue sequence has been modelled (Cockcroft *et al* 1990) as a proline turn-induced (position 9) amphipathic β-hairloop structure which is stabilised by a disulphide bridge. A conserved anionic residue at position 11 creates a natural charge interaction site for all LGIC effectors, with a specificity residue at position 6 which varies to accommodate ligands of the particular LGIC. Although highly conserved among LGICs there is little experimental evidence which supports this region as a major contributor to the formation of the ligand binding site

Thus this conserved motif may play a subsidiary role in the creation of the binding pocket or may serve an as-yet unknown purpose.

1.4.3.3 Contribution of non-α subunits to the ACh binding site

α *Subunit binding sites are non-equivalent*

As described, the α subunit of the nAChR contains principle elements of the ligand binding site. Each receptor contains two copies of this subunit and hence has two binding sites (Reynolds & Karlin 1978). Both sites are required to be occupied for effective activation and interact in a positive, co-operative manner (rev. Changeux 1990). However, although α1 subunits are encoded by a single gene in *Torpedo* (Klarsfeld *et al* 1984) and mouse (Merlie *et al* 1983), the two agonist binding sites are not equivalent. The most probable cause of this non-equivalence is due to the contribution of additional subunits to the binding surface for agonist and competitive antagonist molecules. Evidence for this is apparent in the association and dissociation kinetics of αtoxin binding, which occurs in two steps (Ratnam *et al* 1986) indicating the presence of two sites with different affinities for the same ligand. Furthermore, dissociation of bound toxin occurs at different rates in the presence of competing cholinergic ligand. Many other lines of evidence support this view including equilibrium binding experiments with the antagonists [^{3}H]d-tubocurarine and lophotoxin, and affinity reagents MBTA or bromoacetylcholine, all of which bind to both sites with different affinities (see Galzi *et al* 1991a).

Both the γ and δ subunits contribute to the ligand binding surface of the muscle receptor. Irradiation of the [^{3}H]αtoxin-receptor complex results in the covalent incorporation of radioactivity in γ and δ subunits in addition to α (Oswald & Changeux 1982). Also DDF, demonstrated to covalently label specific residues of the α subunit, is also incorporated in a carbamyl-sensitive manner into the γ subunit (Langenbach-Cachet *et al* 1988). Likewise, α and γ subunits, and α and δ subunits, are photoaffinity labelled by [^{3}H]-(-)d-tubocurarine when bound to its low- and high-affinity site respectively (Pederson & Cohen 1990). Binding sites consistent with αγ and αδ association are also observed when these subunit combinations from mouse muscle are expressed in fibroblast cells revealing different high-affinity binding sites for d-tubocurarine (Blount & Merlie 1989) - omission of γ or δ generates receptors which have poor affinity and cooperativity for nicotinic ligands (Karlin 1991).

Notably, affinity labelling, (using MBTA and BAC), of neuronal αBgtBPs produces a monophasic concentration curve indicating either labelling at a single site, or at more than one site with the same affinity (Ratnam *et al* 1986). Thus it could be that the ACh binding subunits of certain neuronal nAChRs create a more symmetrical environment than muscle-type which is unsurprising given that only α and β subunits constitute the protein complex.

Order of subunits around the channel

The β1 subunit of muscle nAChR has failed to be identified as contributing to the binding site(s) and is consequently regarded to have a purely structural role - this contradicts previous observations

(Kubalek *et al* 1987) that placed the β subunit adjacent to α subunits. The evidence for the involvement of the γ and δ subunits in the formation of the effector site(s) concurs with the current model which supports a αγαβδ arrangement for the muscle-type receptor. Neuronal receptors are possibly simplified by the presence of only the α and β subunits.

1.4.3.4 An aromatic preference

As discussed in section 1.4.3.1, the conserved residues that are labelled by photoaffinity labels are aromatic in character. This is consistent with a model where either the lone pair of electrons of the phenolic oxygen of tyrosine and/or the π electron system associated with the hydrophobic ring provide the principal electronegative character required for association with the cationic head, the prerequisite of all cholinergic ligands. Indeed synthetic analogues of the receptor binding pocket in the guise of hydrophobic macrocycles and macrocyclic polyphenoxides, demonstrate micromolar affinity for methyl-substituted ammonium groups (see Dougherty & Stauffer 1990), observations consistent with the need for electrostatic and hydrophobic interactions in the binding pocket.

More recently NMR techniques have pin-pointed Trp184 in the *Torpedo* sequence α184-200 as interacting through its aromatic protons with the $N(CH_3)_3^+$ and CH_3 groups of ACh (Fraenkel *et al* 1991). Cross-peaks indicated that the interaction occurred over a distance of less than 5Å.

1.4.3.5 Negative subsite of the binding pocket

It would be fool-hardy to discount the presence of a negatively charged subsite, created by anion residues, which may provide the opportunity for significant charge-charge interactions to occur between the nicotinic receptor and its ligand(s). Although aromatics seem to be prevalent and the Cys-loop aspartate seems not to react with affinity reagents, more recent evidence lends credence to a binding site model that incorporates a negative subsite.

Aspartates and glutamates are present in much larger numbers in the δ subunit of muscle-type receptor. It is known that a subsite binding the quaternary ammonium of ACh exists some 10Å from Cys192/193 (Karlin 1991). Carboxyl groups within the *Torpedo* δ subunit specifically react with a 9Å crosslinker designed to interact with carboxyl groups at one end and sulphydryls at the other (Czajkowski & Karlin 1991). Greatest reactivity is observed for the δ164-224 fragment which in mouse contains four aspartates and eight glutamates. Mutation of these residues to asparagine or glutamine (Czajkowski *et al* 1992) reveals that residues δAsp180 and δGlu189 reduce the affinity of the receptor for ACh by 100- and 10-fold respectively. Asp and Glu residues in analogous positions are present in δ, γ and ε subunits. This conservation is consistent with the location of these residues within the agonist binding sites formed by αδ, αγ and αε subunit interfaces (see section 1.4.3.3). In the β1 subunit, which is not implicated in contributing to a binding site, the equivalent residues at these positions are histidine, or asparagine, and glutamine respectively (see Karlin 1993). The α1 subunit lacks these two residues (Blount & Merlie 1989) but paradoxically so does neuronal α7 which forms a functional homomeric channel (Couturier *et al* 1990a).

1.4.3.6 Holistic model of ACh binding to the whole receptor

All the key residues so far identified to interact closely with cholinomimetic ligands are represented in possible binding site model in figure 1.9. DDF predominantly labels residues exclusive to the α subunit. The unknown residues that are also labelled by DDF on the γ and δ subunits may correspond to the anionic residues at positions δ180 and δ189 - however it should be born in mind that the affinity label acetylcholine mustard, which is capable of reacting with carboxylates, labels only αTyr93 (Cohen *et al* 1991). Given that the muscle subunits probably have similar folding arrangements, and the fivefold symmetry of the complex, an equivalent negative subsite may be formed by Asp174 and Glu183 of the γ subunit (which align with δAsp180 and δ Glu189) on the αγ interface of the second α subunit. Thus, although the two ACh binding sites associated with the receptor are non-equivalent, experimental evidence implicates the same key residues as possibly participating in the creation of the site (Figure 1.9). Perhaps then the orientation and reactivity of these residues is quite different in their individual local environment associated with each site, manifesting the non-equivalence.

1.4.4 The competitive antagonist binding site - αbungarotoxin

Curarimimetic snake toxins, such as αBgt, also bind in the vicinity of αCys192/193. αBgt has been used extensively to distinguish different nAChR subtypes (Deneris *et al* 1991), being a potent inhibitor of nAChRs containing the α1 subunit (see section 1.3.1.2) and neuronal α7 and α8 subunits (Schoepfer *et al* 1990: Couturier *et al* 1990a). Isolated *Torpedo* α1 subunit is able to bind α Bgt, even after denaturation, indicating that many of the determinants for toxin binding are contained on the α subunit (Haggerty & Froehner 1981). Some overlap of the binding site for this large toxin must occur with that for ACh. However, because αBgt is specific only for functional neuronal receptors which contain the α7 or α8 subunit, additional regions must also be involved in the formation of the αBgt site. Indeed high affinity toxin binding diminishes considerably when key fragments of the α subunit are considered individually, suggesting the involvement of multiple domains in the organisation of the toxin binding area.

Regions of the α subunit implicated in the formation of the α toxin binding site

Many techniques have been used in attempts to clarify which part(s) of the receptor sequence react with αBgt. Among the most successful have been those which have assessed toxin binding to proteolytic fragments, bacterially expressed fusion proteins and synthetic peptides of specific regions of the α subunit. Assimilation of results from peptide mapping studies defines the region α 174-204 of *Torpedo* as forming the main αBgt binding 'prototope' (see McLane *et al* 1991a, b & c), & 1994). A homologous region is also found in the vertebrate muscle α1 subunit of several species, and the avian brain α7 and α8 subunits (McLane *et al* 1991a & b), suggesting this region as a potential universal αBgt binding site (Figure 1.10).

Other regions of the *Torpedo* α1 subunit are also recognised to interact with αBgt, among them positions 55-74 (Conti-Tronconi *et al* 1990), and additionally regions between 1-16, 23-49 and 122-138 of *Torpedo* and Human α1 subunit (Ruan *et al* 1991). This sensitivity to αBgt of more than one

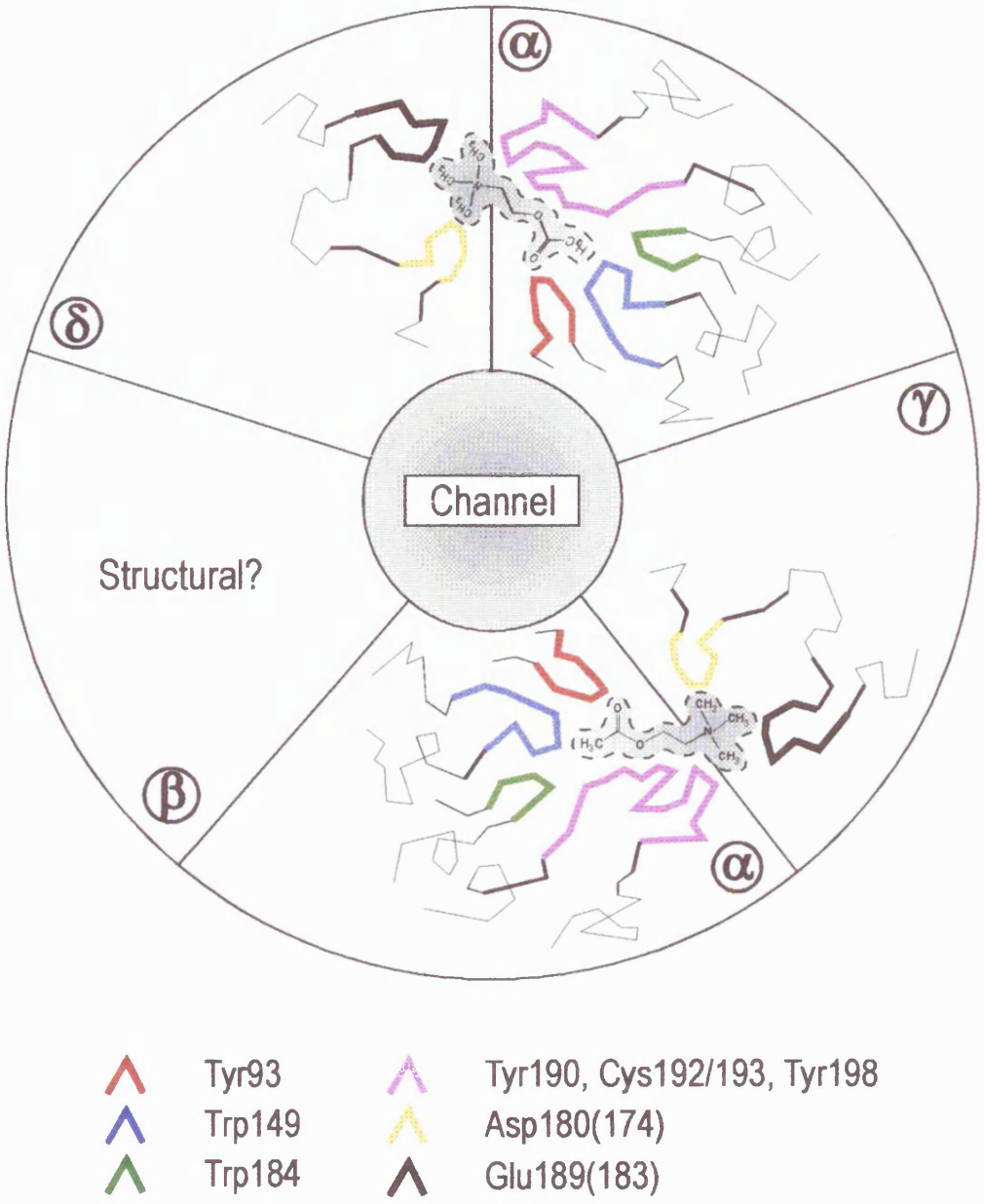

Figure 1.9: Holistic model of the muscle nAChR binding site. Viewed from the top, agonist binding sites are represented at the interface between αγ and αδ subunits of the muscle receptor with the channel in the centre. Main contributions to the site (represented by the ACh molecule) in the α subunit are from multiple loops of hydrophobic residues. A possible anionic site, which may interact with the cationic headgroup of all nAChR ligands, might originate from aspartate and/or glutamate residues in the γ (180 & 189) and δ (174 & 183) subunits. Due to the local environments associated with the formation of the sites at subunit interfaces the ligand sites are not equivalent though they do interact in a positive co-operative manner.

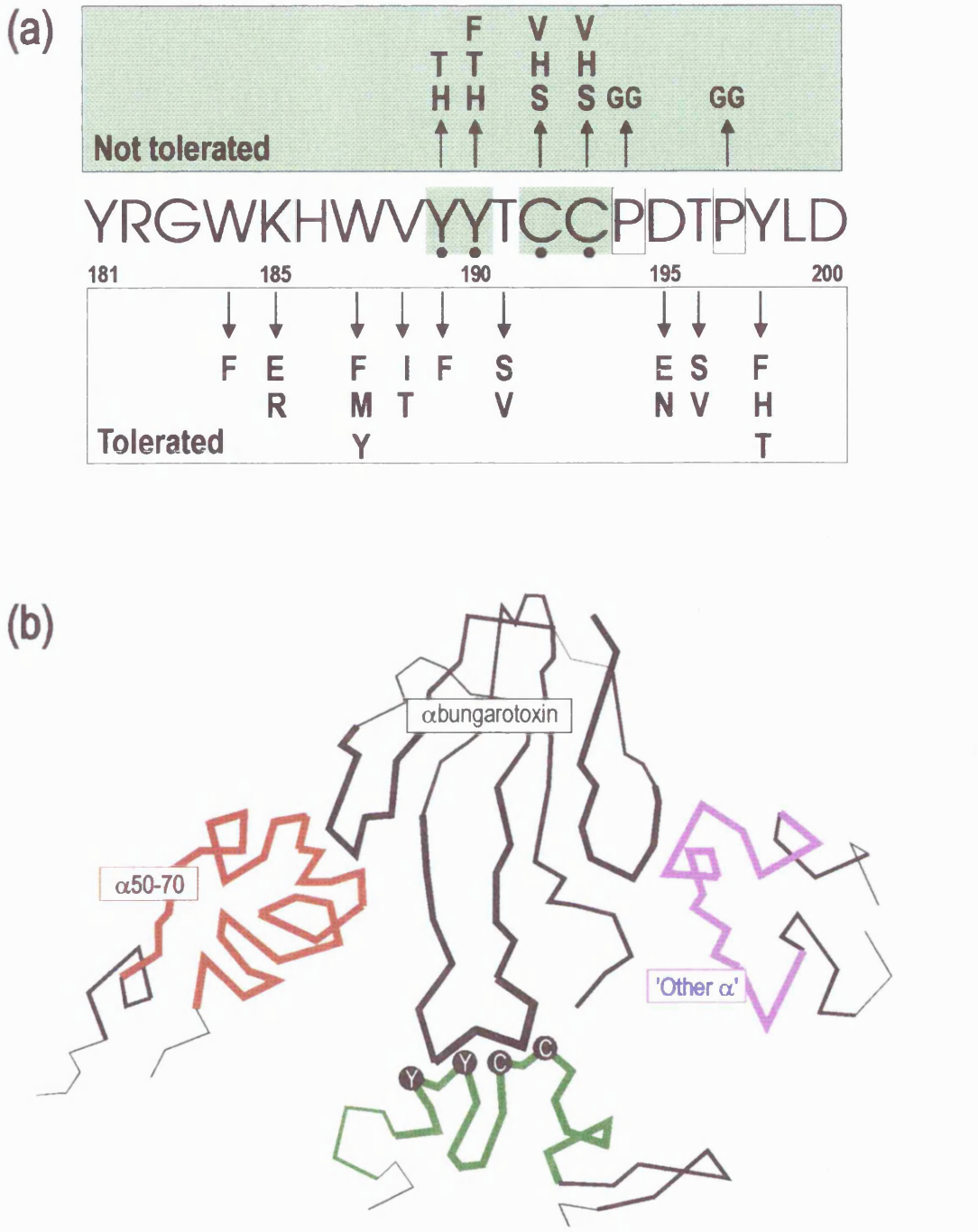

Figure 1.10: The residues of the αbungarotoxin binding surface. Summary of the effect of conservative amino acid substitutions on the binding of αBgt to the α181-200 sequence of *Torpedo* nAChR (a) - modified from McLane *et al* 1994. Indicated are the mutations of the original peptide sequence (centre) which are tolerated (↓), i.e. αBgt binding activity is the same or slightly reduced, and those which are not (↑). The '3-fingered' structure of αBgt derived from x-ray crystallographic measurements (b) is shown interacting via its variable loop extremities with the residues indicated in (a) and an α50-70 sequence which seems to be common to both long and short αneurotoxins. Although not as strongly implicated as residues in the α181-200 peptide, additional regions of the α subunit also interact with this long snake toxin. (The receptor peptide structures are entirely notional whereas the structure of αBgt is derived from x-ray data.)

region in the same subunit sequence conveys a picture, concurrent with that for the agonist binding site, of a complex 3-dimensional contact region. The β subunits of neuronal receptors may also be important. Neuronal bungarotoxin (nBgt), a toxin closely related to αBgt, is proposed to be a selective competitive antagonist for α3β2 nAChR of brain and sympathetic ganglia (see Lindstrom *et al* 1987). However, an α3β4 complex is not inhibited by nBgt (Duvoisin *et al* 1989: Luetje *et al* 1990) suggesting, as with the agonist site, that other non-α subunits may help generate the binding site for snake toxins.

The αneurotoxins isolated from the *Elapidae* family of snakes (e.g. krait, cobra, mamba) are distinguished on the basis of a 'short' (≤60 residues) or a 'long' (≤70 residues) polypeptide chain. Despite there being numerous sequence differences between the αtoxins (mainly deletions and mutations) their 3-demensional structures are similar (see Dufton & Harvey 1989). X-ray crystallographic maps of long (αBgt and αcobratoxin) and short (erabutoxin b) toxins, and a cytotoxin, reveal a common '3-fingered' folding motif throughout (Figure 1.10b). Major residue differences occur in the surface regions, especially the loop extremities. Conversely, the pharmacological action of these toxins are quite different (Loring & Zigmond 1988). The conserved shape and extent of rearrangement of loop residues would imply that probably at least three contact zones interact with the receptor which could account for the specificity and pseudo-irreversible nature of the binding. Possibly, one loop remains relatively conserved in some αtoxins, which is why although erabutoxin b does not bind α181-200 of *Torpedo* it will bind with high affinity to α56-71, and α100-115 (Ruan *et al* 1991). These partially conserved residues of a particular loop may provide the initial recognition event between toxin and receptor. The other more variable loops may confer the specificity by interacting with residues that overlap the agonist binding site. Another common binding site (α122-138) is also evident for some short and long neurotoxins in both human (Ruan *et al* 1990) and *Torpedo* (Mulac-Jericevic & Atassi 1987) α1 subunit sequences.

Experimental evidence

The full complement of conserved residues in all α subunits from muscle and neuronal sources labelled by MBTA and DDF are not essential for conferring αBgt affinity as, until recently, all cloned neuronal nAChRs expressed in *Xenopus* oocytes were insensitive to αBgt (Boulter *et al* 1987: Deneris *et al* 1988: Wada *et al* 1988). These same affinity labelled residues are present in the two αBgt-sensitive neuronal receptor subunits α7 and α8 (see section 1.4.3.1), an observation consistent with a model where αBgt interacts with many more amino acid residues than those strictly involved in agonist binding. Despite this, certain residues in and adjacent to the ACh site seem crucial to the αBgt sensitivity of the receptor.

Conserved or conservatively substituted residues in the 181-200 fragment of αBgt-sensitive neuronal α subunits are Lys185, Tyr189, Tyr190, Pro194, Asp195, Pro197 and Tyr198 (McLane *et al* 1991c). These residues are almost entirely conserved among nAChR α1 subunit sequences from different species (>75% amino acid identity). In attempts to identify the crucial residues of the αBgt binding interface, Conti-Tronconi and co-workers (1991) have employed synthetic single substitution

peptide analogues of the α181-200 *Torpedo* sequence. Non-conservative glycine substitution found residues at positions Val188, Tyr189, Tyr190, Cys192/193 and Pro194 were critical to αBgt binding. Other residues were less strongly implicated (Trp184, Lys185, Trp187, Asp195, Tyr196, Pro197 and Tyr198). A later, more refined conservative substitution approach on the same sequence aimed to identify some of the more physicochemical and structural attributes important in binding (McLane *et al* 1994). In summary, crucial residues in the formation of the αBgt interaction site appear to be Tyr189, Tyr190 and Cys192/193 as replacement of these amino acids by physicochemically equivalent residues dramatically reduced affinities (Figure 1.10a). Also, although experiments were performed using only the 20 residue peptides, when proline residues at α194 and α197 were removed toxin affinity decreased, indicating a structural role for these residues.

Attempts to construct a 3-dimensional model of human nAChR toxin binding site using information gleaned from peptide binding, predict a conical cavity ~30Å in depth, with most favourable energetic interactions occurring in the α125-136 region, which are not coincident with any of the residues of the ACh binding site (McCormick & Atassi 1984). This provision of a deep cavity fits with a model involving few electrostatic and primarily hydrophobic and possibly hydrogen bonding interactions.

1.4.4.1 Ion conducting pathway of the nicotinic receptor

The permeability response associated with the activation of muscle and neuronal nAChR agonists can be inhibited by non-competitive blockers. As their name suggests their action is via a site remote from the agonist site (rev. Heidman *et al* 1983 (muscle-like): Rapier *et al* 1987: Ramoa *et al* 1990 (neuronal)). Structurally diverse, this group of pharmacological agents includes hydrophobic local anaesthetics, the anticonvulsant MK801, the hallucinogen phencyclidine and the tree frog toxin histrionicotoxin (HTX) (see Galzi *et al* 1991a). Functional responses in other LGICs (Albuquerque *et al* 1988) are also blocked by some of these compounds.

Two main categories of sites exist: a single high affinity site, sensitive to HTX, and low affinity sites, insensitive to HTX, which considering their number (10-30 per complex) and lipid-dependent location, may be resident at the receptor-membrane interface. The former site is located in the ion channel, an environment concordant with the voltage sensitivity of the block such as occurs with QX222 (Neher & Steinbach 1978: Cohen *et al* 1992).

1.4.4.2 A structural view of the channel

Affinity labelling agents were, as in the case with the ACh site, pivotal in the identification of key channel residues. Four of the subunits of *Torpedo* nAChR are specifically labelled by [^{3}H]chlorpromazine (Heidman & Changeux 1984). The only place where this is feasible is the narrowest part along the axis of pseudosymmetry of the receptor, namely the channel. Indeed all the interactions are common to the transmembrane M2 segment of each subunit (Giraudat *et al* 1986, 1987 & 1989: Revah *et al* 1990). A series of experiments using different affinity labels and recombinant DNA technology (rev. Deviellers-Thiery *et al* 1993) refined the channel model to its current status (see Figure 1.6) whereby:

- M2 segments are arranged symmetrically about the channel
- labelling appears, in part at least, to be consistent with an α helical organisation (see Akabas *et al* 1992).
- homologous residues from each subunit line the channel lumen forming five important rings: the Threonine, Serine, equatorial Leucine, Valine and outer Leucine rings. Additional rings of negatively charged residues flank the luminal rings.

The functional roles of the residues forming the rings have been explicitly demonstrated through mutagenesis experiments and the effects are comprehensively reviewed (see Deviellers-Theiry *et al* 1993). In simple summary it seems that the NCI site is formed mainly by the Serine ring and that the channel gate is carried by the hydrophobic Leucine and Valine, and polar Serine rings. Ion selectivity filters appear to be provided by the Threonine ring and can be switched from cationic to anionic in α 7 by mutation of the residues Glu237 and Val251. The negatively charged rings at the extremes and outer Leucine ring have significant roles in the permeability of the receptor to Ca^{++}.

1.5 Pharmacophore of the nicotinic acetylcholine receptor.

Central to the rationalisation of the wealth of pharmacological data for the many ligands which have now been characterised at the nAChR, is the notion of the pharmacophore - the specific 3-dimensional configuration of essential chemical groups common to active molecules that is recognised by a single receptor inducing a pharmacological effect. Although potential nAChR binding site-forming residues have been identified, the dynamic nature of the large transmembrane nAChR protein has precluded detailed analysis of the molecular organisation of the ligand site at an atomic level. As such the current description of the site gleaned through affinity labelling and mutagenesis studies can be married with observations of structural and physicochemical features of ligands interacting at the receptor. Inactive ligands should be equally informative as active and delineating the features which confer activity, or inactivity, for a range of structurally diverse molecules should, at least in part, reflect the structural nature of the complementary receptor binding pocket. However, because the events of receptor activation are complex there will probably exist pharmacophore modes for recognition, binding and subsequent activation and desensitisation phases. Alternatively, different elements of the pharmacophore may be required for each step. Therefore, in attempting to correlate observed pharmacology with a set of interacting groups, it must be understood that the actual number of effective pharmacophore modes may not be trivial. This said, the initial barrier is the recognition event between ligand and receptor so this mode will be, initially at least, the most pertinent.

A pharmacophore model applies to a single receptor type. The heterogeneity of neuronal nAChR (see section 1.3) makes the task of finding a single model for each subtype very large. The approach has been to consider structure-activity relationships of ligands at many nAChR and thus to generate a unifying pharmacophore model which both identifies common features of active ligands

at all nAChR types, and identifies aspects of this model which may be flexible and thus generate some receptor subtype specificity.

1.5.1 Principle features of the nicotinic pharmacophore

The tetramethylammonium ion is the minimum essential structure that activates the nAChR complex. Potency is enhanced by the presence of an aliphatic hydrocarbon chain (e.g. decamethonium) or an atom with unshared electrons (e.g. ACh and nicotine). The atom bearing the unshared electrons (a carbonyl oxygen in most agonists) is proposed to form a hydrogen bond with the receptor.

'Beers-Reich' model

The first cogent model of the pharmacophore for ligands active at the nAChR was introduced by Beers & Reich (1970) who compared semi-rigid agonists (mainly cytisine and nicotine) and some competitive antagonists. Briefly, they concluded that in order for ligands to have cholinergic activity they must possess a centre of positive charge (a cationic head) and a hydrogen bond acceptor group (usually a carbonyl oxygen) which are disposed in a particular geometrical relationship characterised by a separating distance of 4.8Å (±0.3Å) - the 'Beers-Reich' distance - and the angle between the cationic centre and the C=O bond (Figure 1.11a).

The Sheridan 'triangle'

This model generally corroborates observations by previous authors (Wasserman *et al* 1979), each recognising the two hydrophilic centres required for effective receptor-agonist interaction. A somewhat different approach was applied to the problem by Sheridan *et al* (1986) who treated the four structurally diverse agonists (-)-nicotine, (-)-cytisine, (-)-ferruginine methiodide and (-)-muscarone, collectively as an ensemble, identifying a pharmacophore triangle (Figure 1.11b). This comprised a cationic centre (**A**), an electronegative atom (**B**) and an atom (**C**) which forms a dipole with (**B**). The model agrees well with that of Beers & Reich, including an exact 4.8Å distance, but differs in its selection of template molecules opting for a conformational search approach of semi-rigid agonists and using rigid antagonists such as strychnine and dihydro-β-erythroidine (DHβE) to confirm the model. Additionally, the angle between the cationic head, the centre of the hydrogen bond acceptor, and the line through the carbonyl bond (or its equivalent) directed toward the donor, is around 137°, a little larger than that associated with the Beers-Reich model (120°). Studies with stereospecific molecules revealed that active isomers have the bulk of their volumes on one specific side of the plane defined by the cationic head and the carbonyl oxygen and its associated carbon, or in the case of nicotine and analogues, the cationic head and centre point of the pyridine ring.

'Flexibility' model

As the structure set has become larger through the products of synthetic chemistry, so the pharmacophore model has been progressively modified. Consequently, an alternative pharmacophore model proposed by Barlow & Johnson (1989) has suggested that rather than

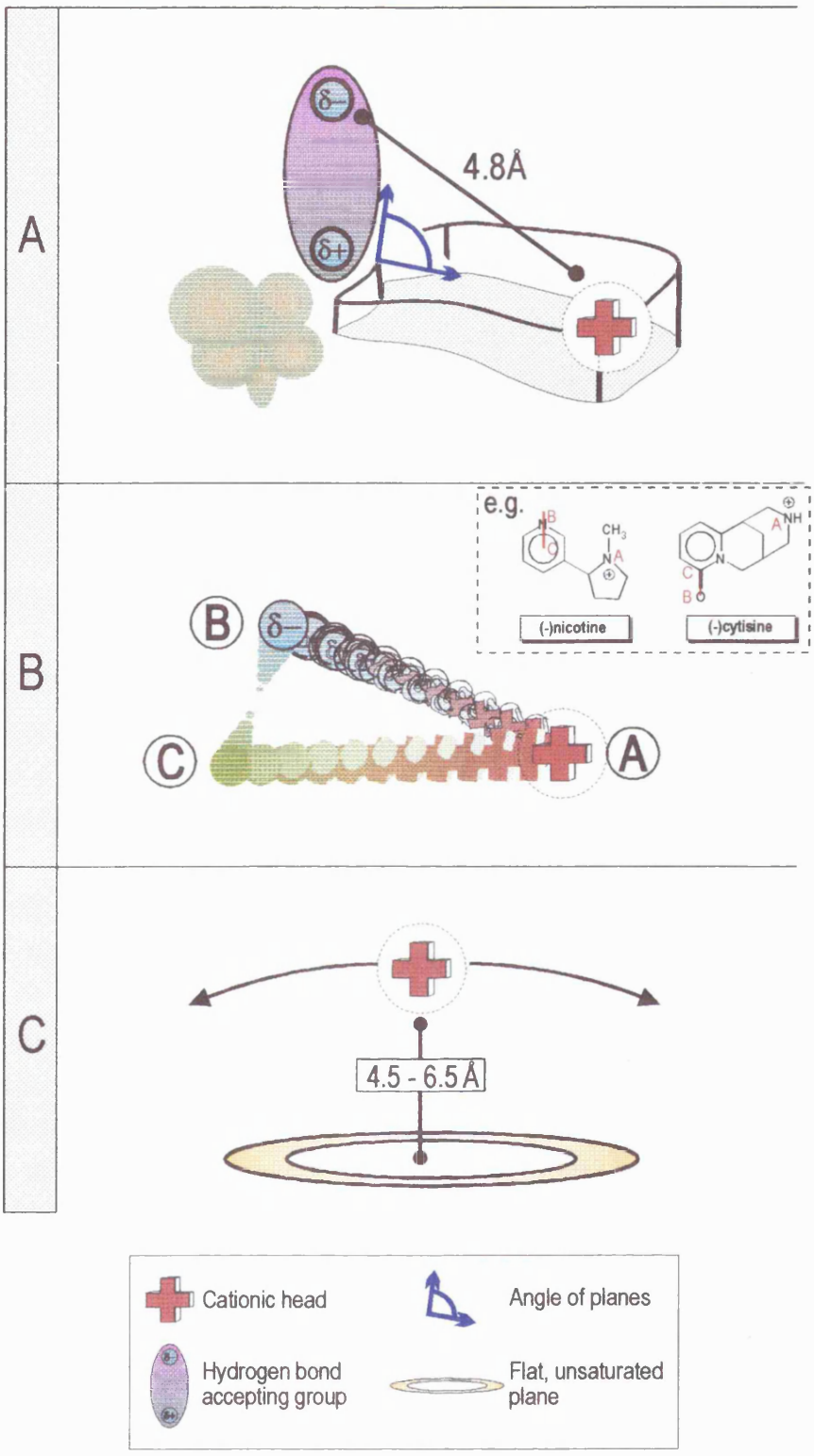

Figure 1.11: Unified nAChR pharmacophore models. Salient features common to molecules active at the nicotinic receptor are schematically represented. The omnipresent cationic headgroup is a prerequisite for all active ligands and appears as an amine function. Models are as follows: (A) 'Beers-Reich' model, (Beers & Reich 1970), (B) 'pharmacophore triangle' (examples of how the triangle points apply to active ligands are shown (inset)) (Sheridan *et al* 1986), (C) 'Flexibility' model which better explains the large potency differences observed for active ligands (Barlow & Johnson 1989). Descriptions of each model are given in the text.

specific groups in the active molecules being involved, activity at the receptor depends on a more generalised theme, that being the possession of a flat area containing double bonds, or double bond systems, and a cationic binding group some 4.5-6.5Å from the flat area (Figure 1.11c). This model although skeletal, at least goes some way to explaining the activity of pharmacologically important molecules possessing unsaturated systems such as nicotine, cytisine, 1,1-dimethyl-4-phenylpiperazinium (DMPP).

1.5.2 Additional factors to consider in the pharmacophore model

These models, while independently derived and complementary, are insufficient to explain the pharmacological profiles of all the ligands and their analogues assayed against the nAChR to date. Additional factors must be considered to explain disparities, such as

- small deviations from optimal conformation
- deviations in electrostatic potentials about the cationic head and carbonyl group
- presence of bulky groups α to the carbonyl carbon.

Quantitation of how the introduction of a single, isolated discrete change to the structure of a ligand effects the physicochemical character of that ligand is complex. For example modification intended to demonstrate the influence of inductive effects will concomitantly shuffle the ground state, steric effects, solvation and have other subtle effects.

1.5.3 3-Dimensional structure of active nicotinic agonists

The spatial arrangement of atoms about the crucial pharmacophore points is important in dictating potency of a particular ligand, as demonstrated by the stereoselectivity of the [^{3}H]-(-)-nicotine and [^{125}I]αBgt labelled neuronal receptors in favour of (-)nicotine (10-60-fold) and (+)anatoxin-a (>200-fold) (see Wonnacott 1987a) for example. Therefore, although the pharmacophore model may be a useful template, it is insufficient to predict potency, thus a 3-dimensional view of ligands is necessary to attempt to explain these differences. However, determination of bioactive conformation is not trivial. For example, ACh is very conformationally labile and the number of conformations varies depending on the environment - the receptor bound conformation of ACh is very different from that in solution (Behling *et al* 1988), as are conformations determined *in vacuo* and from crystal scattering data. Once possible stable bioactive conformations are found not all of the pharmacophore features are necessarily fulfilled: e.g. anatoxin-a and the closely related ferruginines in the *cis* conformation fit the Beers-Reich distance but not the associated angle. The same can be said of arecolone methiodide.

Synthetic chemistry has provided the means to investigate the structure of the nicotinic cholinergic pharmacophore, most notably through modifications to active, semi-rigid molecules such as piperazines (Spivak *et al* 1986 & 1989) and anatoxins (see Swanson *et al* 1991: Wonnacott *et al* 1991), which are reviewed in chapter 2.

2. Radioligand binding

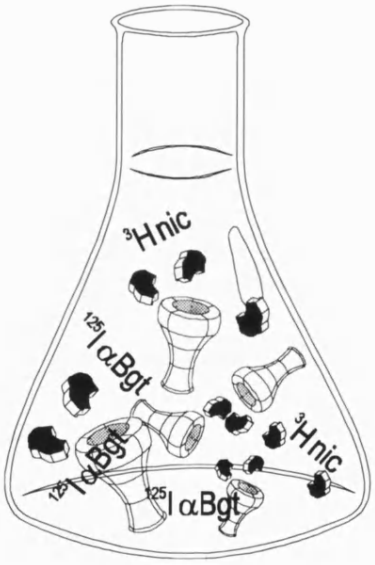

2.1 Introduction

In order that a biological macromolecule, such as a receptor protein, may be characterised and understood, there must exist a means by which the specific protein, or class of proteins, can be targeted and identified among the tissue milieu in which it exists. In 1905, when Langley observed that nicotine excited the contraction of skeletal muscle, he proposed that the interaction of the exogenous agent with 'receptive substances' was responsible for the observed physiological reaction. The concept of a receptor for nicotine was thus born and set into motion experiments to identify, isolate and characterise this physiologically important protein.

It has already been described how the densely packed muscle-like receptors of the electric organs of certain fish were invaluable in laying the foundations for the understanding of the nicotinic receptor (see section 1.2). Of equal importance, especially since the investigative field was broadened to include neuronal tissue where the same protein is less abundant, has been the concurrent use of receptor specific ligands. These molecules (which are mainly natural toxins) have, through their high affinity and specificity for certain subtypes of the nAChR, been used to target native nAChR proteins *in situ*, thus facilitating extensive pharmacological characterisation. The now familiar αbungarotoxin (αBgt) is one such ligand which specifically binds with high affinity to the muscle-like receptor, and certain neuronal subtypes - nicotine itself binds to the predominant neuronal nAChR (see section 1.3.1.1). Unfortunately only one other ligand, neuronal bungarotoxin (nBgt), has so far been able to identify a different nAChR subtype.

This shortfall emphasises the current restriction imposed on neuronal nAChR classification, namely a paucity of suitable, specific molecular probes. Given the extensive number of subunits that have now been cloned from neuronal cholinergic proteins, and the potential for heterogeneity, there exists a need for more ligands able to distinguish pharmacologically distinct nicotinic receptor subtypes in the anatomically complex wiring system that is the brain. The primary focus of this study has been to attempt to underpin some of the structural attributes of cholinergic agonist molecules which confer activity at two receptor populations. This has involved making novel chemical modifications in certain instances, modifications which may concurrently introduce selectivity features into these molecules. If successful this would go some way towards redressing the imbalance of selective neuronal nicotinic ligands.

Focus of the radioligand binding assay experiments

In summary, the strategy has involved the establishment of pharmacological profiles for the [^{3}H]-(-)-nicotine and [^{125}I]αBgt labelled brain acetylcholine receptors to compare with profiles in the literature. The potencies of many classical and novel agonists have been assessed in competition binding experiments. Much attention has focused on the potent anatoxin ligand whose structure we have synthetically modified (Paul Brough and Timothy Gallagher, Univ. Bristol). The initial line of attack has been through competition binding assays, used to monitor the effects of structural modifications on the affinity or selectivity demonstrated by these ligands for the receptors - this is delt with in this chapter. We speculate that perhaps certain features of agonist molecules bestow

functional potency, (as distinct from those that bestow binding affinity), and so have reinforced the pharmacological properties of some of the agonists used by concurrently assessing potency profiles at the functional α7 homomeric receptor expressed in *Xenopus* oocytes - this is the subject of chapter 3. A theoretical modelling approach has also been applied to agonist molecules as an aid to predicting spatial orientation of atoms with a view to understanding the pharmacophore model, which in its present form is insufficient to explain the diversity of pharmacological activity of agonists at neuronal nicotinic receptors - this theoretical aspect is presented in chapter 4.

Before going any further it is perhaps pertinent to introduce the diverse array of ligands active at the nAChR. Attention, like that of the project, is drawn largely to the small agonist molecules which bind to and activate the receptor, though it also seems useful to mention some of the antagonist molecules which have such profound inhibitory affects.

2.1.1 Common cholinergic agonists

Examples and features

The tetramethylammonium (TMA) ion is the simplest nicotinic agonist and serves to demonstrate the fundamental role of the cationic head (see below) in the nicotinic pharmacophore. More complex structures generally enhance potency, though this is not always the case: for example, the relative potencies of nornicotine and ferruginine, as assayed by contracture of frog muscle, are lower than that for TMA (see table 1 of Gund & Spivak 1991). The structure of TMA and some of the more complex, widely studied agonists are represented in figure 2.1. The neuronal nAChRs are stereoselective for certain molecules, e.g. (-)nicotine and (+)anatoxin (see section 2.3.5). The geometrical displacement of supporting atoms around the basic pharmacophore points is crucial for activity in these ligands.

All agonists are small in size, (generally around 30 atoms), when compared to competitive antagonists, which are presumed to overlap the agonist site on the receptor. This size and volume limitation imposed on these agonist molecules is very strict. For instance, although competitive antagonists share the pharmacophore features of agonists (see section 2.1.2), their inability to activate the receptor is most likely dictated by their larger structure. This would imply that the basic pharmacophore features of agonists are primarily for recognition, whereas activation may only be initiated through further interactions with other aspects of the molecule, which can only occur through tighter association in a pocket or cavity designed for small ligands. This may also explain the partial agonist properties of slightly smaller molecules like phenyltrimethylammonium (PTMA), though the reasons for some agonists being only partially active are difficult to ascertain.

A cationic head, be it ammonium, sulphonium or phosphonium, is essential for activity. Quaternary amines are most common (e.g. ACh, DMPP), but secondary (e.g. AnTx, cytisine) and tertiary (e.g. nicotine, lobeline) amines have activity in cyclic compounds. The active non-quaternary amines are expected to be overwhelmingly protonated at physiological pH, e.g. anatoxin-a is >99% protonated at pH7 (Koshkinen & Rapoport 1985). Increasing bulk around the cationic head through N-

methylation diminishes activity among simple alklyammonium compounds (R-N(CH_3)$_3$). The same trend is not apparent among the semi-rigid bi- and tri-cyclic agonists. For instance the secondary

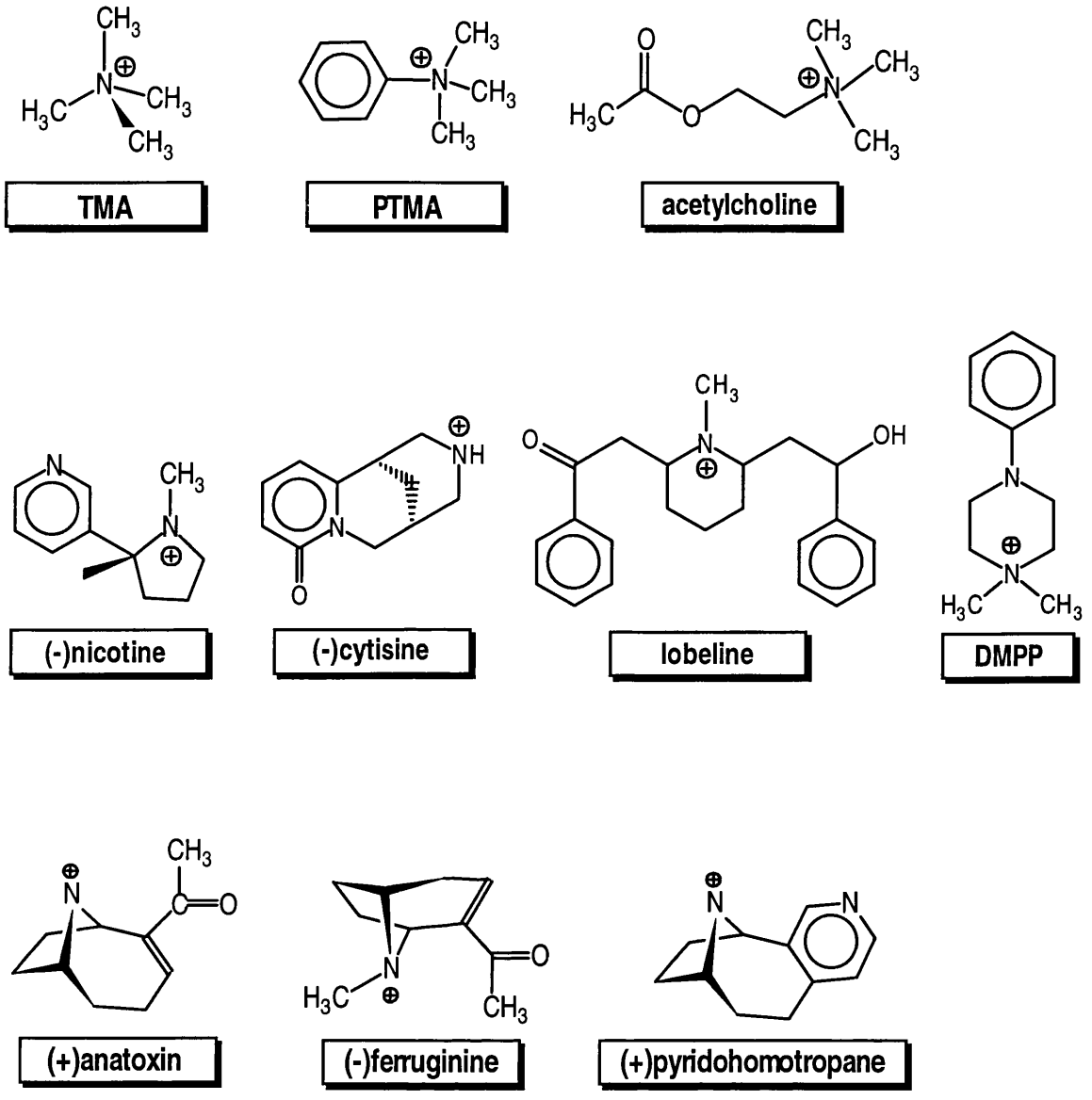

Figure 2.1: Structural representations of some common agonists active at the nicotinic receptor. Abbreviations: TMA (tetramethylammonium), PTMA (phenyl tetramethylammonium), DMPP (1,1-dimethyl-4-phenylpiperazinium).

amine cytisine becomes progressively less active when one, then two extra methyls are added (Barlow & Mcloed 1969), while there is no significant conformational perturbation. Conversely, as we will see in section 2.3.5.2, nicotine increases in potency following methylation of nornicotine to nicotine. The N-methylated ferruginines behave disparately (Spivak *et al* 1983).

The group which may function as a hydrogen bond acceptor appears in many guises, yet predominantly it is a carbonyl oxygen (ACh and AnTx). In nicotine and pyrido[3,4-*b*]homotropane

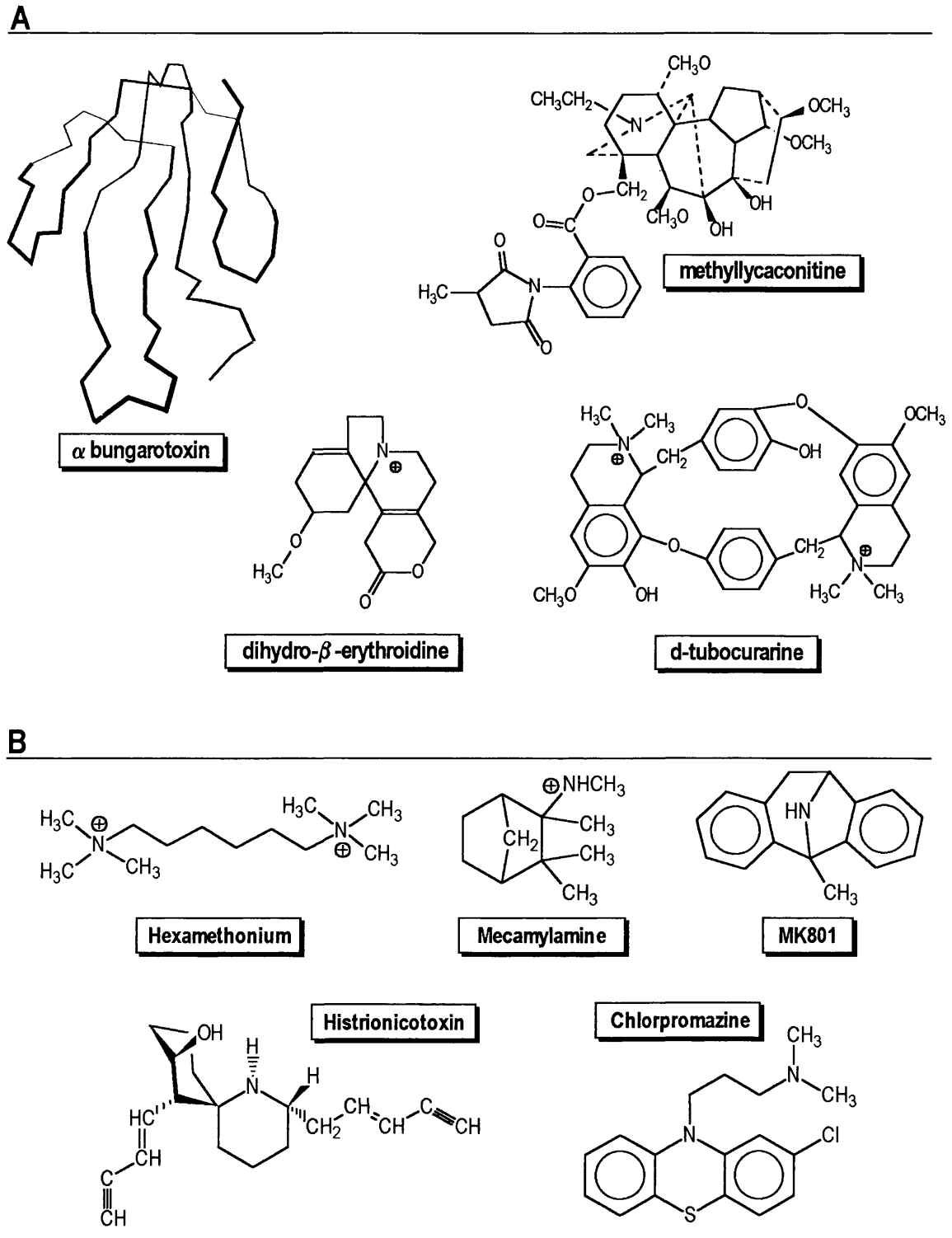

Figure 2.2: Structural representations of nicotinic cholinergic antagonists. In the top panel (a) are drawn the complex structures recognised as competitive antagonists as mentioned in the text. The large polypeptide chain conformation of αBgt derived from crystal data, is represented in ribbon form. The lower panel (b) shows some non-competitive antagonists thought to bind mainly in the channel.

(PHT) it becomes an amine, but in a few cases it appears as either a phenolic or alcoholic OH. The existence of these latter auxiliary groups in active compounds indicates that a permanent dipole is not critical.

Pharmacological specificity

The pharmacological profiles of the two neuronal nAChR populations of concern to this project are the subject of many reviews, for instance, Wonnacott 1987a: Wonnacott 1990: Clarke 1993. The agonists ACh, (-)nicotine, (-)cytisine, lobeline, DMPP and carbamylcholine are particularly potent at inhibiting [^{3}H]-(-)-nicotine binding being active at nanomolar concentrations with the rank order: cytisine> (-)nicotine> ACh> DMPP= lobeline> carbamylcholine (see table 7.2 of Wonnacott 1990). (+)Anatoxin-a is the most potent agonist at this protein. All of these molecules discriminate between the sites labelled by [^{3}H]-(-)-nicotine and [^{125}I]αBgt, having greatest affinity for the former. However the pharmacological specificity exhibited by the [^{3}H]-(-)-nicotine labelled receptor is not common to all agonists as (+)nicotine, DMPP, anabasine and carbamylcholine are almost equipotent at both sites. Nicotinic agonists are only physiologically active when at micromolar concentrations, a discrepancy which results from the prolonged incubation periods associated with the binding assay converting the binding site into a high affinity, desensitised configuration (Schwartz *et al* 1982). That [^{3}H]-(-)-nicotine identifies a distinct population of neuronal nAChR is evidenced by the failure of αBgt to inhibit [^{3}H]-(-)-nicotine binding. [^{3}H]cytisine binds to nicotinic sites in rat brain membrane homogenates with a K_D<1nM (Pabreza *et al* 1991) which, along with its slow dissociation rate, low non-specific binding and high stability, make it a very useful alternative probe to [^{3}H]-(-)-nicotine. Similarly, other radiolabelled agonists, [^{3}H]acetylcholine (Schwartz *et al* 1982) and N-[^{3}H]methylcarbamylcholine, have the same binding characteristics with affinities for the same neuronal nAChR of 3-12nM.

2.1.2 Cholinergic antagonists

Examples and features

While compounds that lack the full complement of structural characteristics of agonists behave as partial agonists, so the addition of larger groups confers antagonist properties to these molecules. Retention of certain agonist features without the associated agonist activity is a property of the competitive antagonists such as methyllycaconitine (MLA), dihydro-β-erythroidine (DHβE) and d-tubocurarine (d-TC) - figure 2.2a. All these molecules possess a cationic headgroup and a number of candidate sites for the formation of hydrogen bonds with the receptor. The larger bulk of the antagonists distinguishes them from agonists, a feature most probably responsible for the activity deficit. αBgt, being a polypeptide, is exceptional in terms of size though this bulk does not preclude it binding with high affinity to the receptor with which it interacts via possibly hydrophobic residues (see section 1.4.4). Being larger structures the nicotinic competitive antagonists are most probably more conformationally labile than the small, semi-rigid agonists, a feature which may also discourage receptor activation.

Non-competitive inhibitors (NCIs) are structurally more closely related to the agonists and are comprised largely of ring systems which lend rigidity to many of the molecules (Figure 2.2b). They too possess a centre of positive charge which comes in various guises but most commonly as an amine function. This positive charge is presumed to be the main interaction site with polar amino acid residues in the narrowest part of the ion channel (see section 1.4.4.1 & 1.4.4.2), a site which poses obvious size restrictions. There is generally a notable lack of any hydrogen bond accepting moiety.

Pharmacological specificity

Romano and Goldstein (1980) were the first to report the inability of most classical nicotinic antagonists to effectively inhibit ligand binding to neuronal proteins labelled by [^{3}H]-(-)-nicotine. This has since also proved to be the case for the [^{125}I]αBgt labelled site (see table 7.2 of Wonnacott 1990). The few notable exceptions to this are DHβE (see Reavill *et al* 1988), d-TC (Marks *et al* 1986), MLA (MacAllen *et al* 1988) and neosurugatoxin (see Rapier *et al* 1985).

DHβE is an effective neuromuscular blocking agent, but is equally potent in autonomic ganglia and CNS (Wonnacott 1987b). Tritiated DHβE shows saturable, specific binding to two sites in rat brain (K_D=4 and 21nM). The high affinity site resembles the [^{3}H]-(-)-nicotine labelled receptor in its pharmacology, the other being the [^{125}I]αBgt site. d-TC, a curare alkaloid used in poison arrow tips, used as a tritiated derivative also labels two brain sites showing some correlation with [^{3}H]-(-)-nicotine and [^{125}I]αBgt sites - however it is a relatively weak antagonist in brain (Larson & Nordberg 1985). d-TC unusually shows a preference for [^{125}I]αBgt labelled sites (Marks *et al* 1986). This selectivity is also demonstrated, though more extremely, with MLA. Isolated from delphinium seeds, MLA is thus an important, highly selective competitive antagonist of neuronal [^{125}I]αBgt labelled sites, and as such is presently the subject of intensive structure-activity studies in this laboratory. Neosurugatoxin, an extract of the Japanese ivory shell, is a highly selective ganglionic blocker (see Wonnacott 1987b), which in the CNS competes for [^{3}H]-(-)-nicotine binding sites, but does not inhibit binding to [^{125}I]αBgt or [^{3}H]QNB sites.

It is increasingly recognised that many of these drugs block nicotinic transmission by interacting with the ion channel of the nicotinic receptor, and there is much evidence from electrophysiological, pharmacological and molecular biological sources to indicate this (see Sargent 1993).

The ten carbon atom containing (C10) antagonist decamethonium and its shorter analogue hexamethonium (C6) were used in early classification of nicotinic receptors as they distinguished the muscle receptor (termed the 'C10 receptor') from that found in neurons (the 'C6 receptor'). These classical antagonists although able to block functional receptors which demonstrate a clear nicotinic profile are, like mecamylamine, MK801 and others, ineffective competitors of [^{3}H]-(-)-nicotine and [^{125}I]αBgt binding. This observation is attributed to their non-competitive mechanism of action at a site remote from that of the competitive antagonists described above.

2.2 Experimental procedures

2.2.1 Tissue preparation

Preparation of rat P_2 membrane fraction

Male Wistar rats, (200-250g, maintained in a 12h:12h light:dark cycle, with free access to food and water), were killed by cervical dislocation. Whole brains were removed following decapitation, and were either used immediately or rapidly frozen at -70°C before use. This latter treatment has no significant effect on the number of detectable high affinity nicotine binding sites (Benwell & Balfour 1985).

The method essentially follows the protocol devised in this laboratory (MacAllen *et al* 1988). Whole brains (minus the cerebellum) were homogenised in a glass homogeniser (10%(w/v)) in 0.32M sucrose (4°C, pH 7.4), containing protease inhibitors (1mM EDTA, 0.1mM PMSF and 0.01%(w/v) NaN_3), by repeated (x10) up and down strokes at approximately 300 rpm. The resulting homogenate was centrifuged at 1000xg for 10min (Sorval RC-5B) at 4°C. Supernatant (S_1) was decanted and retained on ice, and the pellet (P_1) was resuspended in 0.32M sucrose, (5ml/g original wet weight), and recentrifuged as above.

Supernatants were combined and centrifuged at 12000xg for 30min at 4°C. The pellet (P_2) was washed twice by resuspension in 50mM potassium phosphate buffer (40mM K_2HPO_4, 10mM KH_2PO_4 and anti-proteases: 5mM EDTA, 0.1mM PMSF and 0.02%(w/v) NaN_3, pH 7.4), giving a final volume of 2.5ml/g original wet weight, and centrifugation as before (12,000xg, 30min, 4°C), before final resuspension in 50mM phosphate buffer. TRIS-HEPES buffer, (118mM NaCl, 4.8mM KCl, 2.5mM $CaCl_2$, 20mM HEPES, 200mM Tris, and protease inhibitors: 0.1mM PMSF, 0.01%(w/v) NaN_3, pH 7.4), was used for resuspension for [^{3}H]-(-)-nicotine assays, as this buffer reduces the level of non-specific binding (Romm *et al* 1990). Samples (5ml) were stored at -20°C until required. Figure 2.3 describes the procedure.

Preparation of rat muscle extract (RME).

Male Wistar rats, (200-250g, kept as described in section 2.2.1), were killed by cervical dislocation. Their hind limbs were skinned, muscle tissue stripped from the bone and the tissue used immediately or rapidly frozen for storage.

Extract was prepared according to the method described by Rozental and co-workers (1989) for frog muscle. Muscle tissue from six rats (approximately 100g) was pooled and homogenised (40%(w/v)) in 2.5mM sodium phosphate buffer (90mM NaCl, 3mM KCl including protease inhibitors (1mM EDTA, 2mM benzamide, 0.1mM benzethonium chloride, 0.1mM PMSF, 0.01%(w/v) NaN_3, pH 7.2)), using a Waring blender for 60s at high speed. This and subsequent procedures were carried out at 4°C.

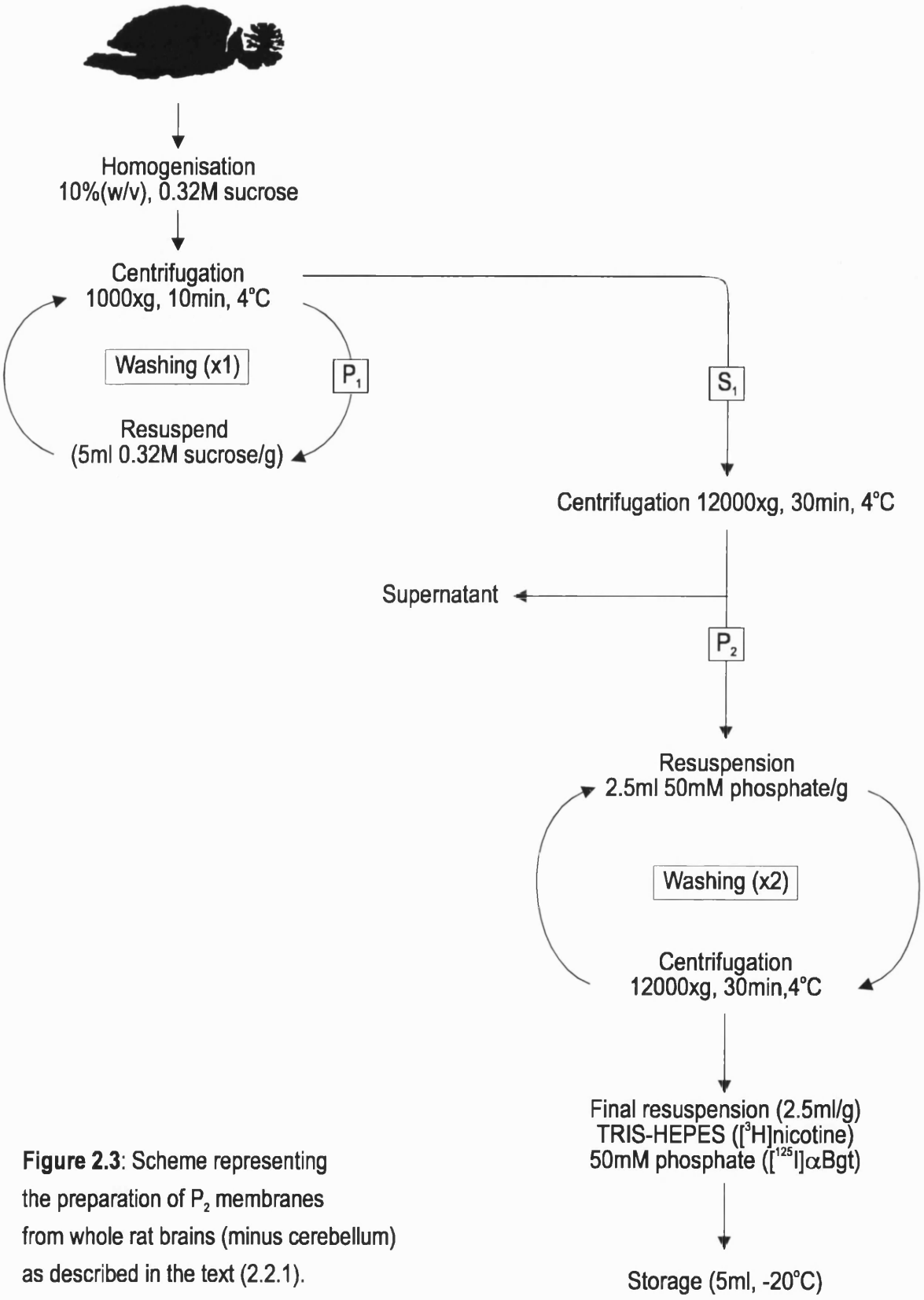

Figure 2.3: Scheme representing the preparation of P_2 membranes from whole rat brains (minus cerebellum) as described in the text (2.2.1).

Homogenate was centrifuged at 20,000xg for 60min, supernatant decanted and the pellet resuspended in the same buffer (1.5 ml/g wet weight), by re-homogenising in the Waring blender as before. Triton X100 was added (final concentration 2%(v/v)) before stirring for 3h at 4°C. Centrifugation at 100,000xg for 60min yielded the rat muscle extract (RME) as supernatant, which was decanted and stored at 4°C. The procedure is summarised in figure 2.4.

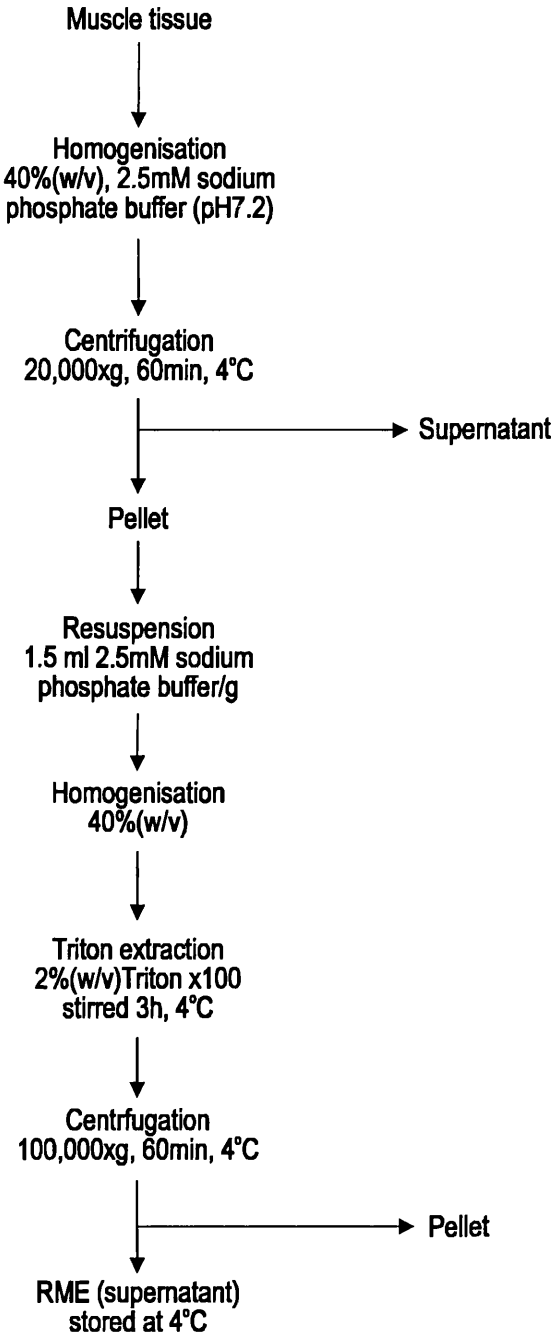

Figure 2.4: Flow diagram demonstrating the preparation of rat muscle extract (RME) as described in the text (2.2.1).

2.2.2 Protein determination

Protein content of samples was measured essentially according to the method of Lowry and co-workers (1951). Standard curves were constructed using bovine serum albumen (BSA) in a concentration range of 50-500 μg/ml.

Sample duplicates (200µl) of BSA standards, P_2 membranes or rat muscle extract, were diluted with distilled water between the range 1:40 to 1:1000. Equal volumes of 1%(w/v) $CuSO_4.5H_2O$ and 2%(w/v) sodium tartrate were diluted 1:100 with 0.1M NaOH containing 2%(w/v) Na_2CO_3 to make alkaline cupric tartrate, 1ml of which was added to each sample. Following incubation at 20°C for 10min, 0.1ml Folins-Ciocalteaus reagent (100µl; freshly diluted 1:1 with distilled water), was added with immediate mixing, and the colour left to develop for 40min. Water controls were treated similarly. Absorbancies at 690 nm were measured on a Titertek Multiscan Spectrophotometer using 96 well plates and relative protein concentrations determined from standard curves.

Triton X100 and TRIS-HEPES buffer perturb the colour reaction, therefore samples with these constituents were modified to maintain constant Triton X100 and buffer concentrations relative to each sample.

2.2.3 Iodination of αbungarotoxin (αBgt)

αBgt was labelled to high specific activity with [^{125}I]Na. All procedures were carried out at room temperature. [^{125}I]Na (20µl; 100mCi/ml, stored at ambient temperature), and αBgt (20µl; 0.5mg/ml), were mixed with reaction buffer (10µl, 0.05M potassium phosphate, pH 7.5). The reaction was initiated by the addition of Chloramine T (10µl, 0.5%(w/v)), and allowed to continue for 1min with continuous stirring, after which time sodium metabisulphite (750µl, 0.016%(w/v)), and potassium iodide (200 µl, 1%(w/v)), were added to terminate the reaction.

The reaction mixture was immediately chromatographed on a Sephadex G25 column (25x1 cm), equilibrated in 0.01M potassium phosphate (pH 7.5) containing 1%(w/v) BSA, and eluted with the same buffer. Fractions (1ml) were collected and samples (5µl) counted using an LKB 1280 Ultragamma counter (efficiency 70%) for 10s. Peak fractions of the radio-iodinated protein were pooled, and the specific activity of the [^{125}I]αBgt calculated assuming 100% recovery of protein and radiolabel. The protein was stored at 4°C and used for up to 21 days following iodination. Typical values for the specific activity of the radiolabelled toxin were >700Ci/mmol.

2.2.4 Generic binding protocol

Procedures for determining levels of radioligand bound to rat brain P_2 membranes and rat muscle extract were determined for three independent types of assay and involved the application of constant conditions. These conditions are outlined below for the three radioligands used and were applied in protein dependence (section 2.2.5), saturation binding (section 2.2.6) and competition binding (section 2.2.7) assays, except [^{3}H]QNB with which only competition assays were performed. Physostigmine (10µM) was included in assays involving acetylcholine (ACh).

2.2.4.1 [^{3}H]-(-)-nicotine

Binding of [^{3}H]-(-)-nicotine was based on the methods of Romano and Goldstein (1980) and Marks and Collins (1982), using ligand stored in mercaptoacetic acid (Romano & Goldstein 1980). All assays were carried out as triplicate determinations at 20°C using TRIS-HEPES buffer (Romm *et*

al 1990) and 250µl P_2 samples (diluted to 2mg protein/ml). Levels of specific binding were determined by measuring the difference between total binding (i.e. 10µl [^{3}H]-(-)-nicotine at a final concentration of 10nM in the assay) and non-specific binding (i.e. 10µl [^{3}H]-(-)-nicotine (10nM) in the presence of 1mM (10µl) unlabelled (-)nicotine). Reactants were thoroughly mixed and incubated for 60min.

Separation of bound from free ligand was carried out at 4°C. Initially, samples were chilled to 4°C (60min), before addition of 2ml ice-cold phosphate buffered saline (PBS: 10mM potassium phosphate, 0.15mM NaCl and 0.01%(w/v) NaN_3, pH7.4), and rapid filtration, under vacuum, through double thickness Gelmann A/E glass fibre filters, (pre-soaked in 0.3% polyethyleneimine (diluted in PBS) for at least 3h), using a Brandell cell harvester. Sample tubes were rinsed with 2x3ml PBS - filtration and washing was achieved within 20s. Filters were counted in 5ml Optiphase scintillant using a Packard scintillation spectrophotometer (counting efficiency 30%).

2.2.4.2 [^{125}I]αbungarotoxin (αBgt)

P_2 membranes **-** A similar protocol was employed to that described above (section 2.2.4.1) involving triplicate determinations. Assay reactants were mixed at 20°C using 50mM potassium phosphate buffer and 500µl P_2 samples (1mg protein/ml). Total binding (20µl; [^{125}I]αBgt at a final concentration of 1nM) and non-specific binding ([^{125}I]αBgt (1nM) in the presence of excess (20µl; 1µM) unlabelled αBgt) levels were assessed to determine specific effects. Following thorough mixing, reactants were incubated at 37°C for 2h.

Ligand bound to P_2 membranes was precipitated from unbound at 20°C by centrifugation (MSE microfuge, 2min @10,000xg). Supernatant was disgarded and membrane pellets washed two times by resuspension in PBS (1ml, 4°C) and recentrifugation. P_2 pellets were counted directly on a LKB ultragamma counter.

Rat muscle extract **-** Assays to determine total and non-specific binding were setup as for the P_2 preparation using homogenisation buffer. Protein separation of free ligand from that bound to muscle extract (RME) was achieved by rapid filtration through Whatman GFC filters (pre-soaked in 0.3% polyethyleneimine overnight at 4°C), using a benchtop millipore vacuum manifold. Samples were rapidly washed with 3x3ml PBS (4°C) containing 0.1%(w/v) BSA. Filters were counted using an LKB ultragamma counter.

2.2.4.3 [^{3}H]Quinuclidinylbenzilate

In this study [^{3}H]QNB binding was occasionally performed to ascertain whether novel synthetic ligands displayed any muscarinic activity. [^{3}H]QNB, a potent muscarinic cholinergic antagonist, has been extensively used as an effective probe in CNS AChR characterisation using various brain preparations. In whole brain [^{3}H]QNB exhibits a K_D of 0.04nM and reveals the number of muscarinic sites labelled by this ligand as 20- and 4-fold larger than [^{3}H]-(-)-nicotine and [^{125}I]αBgt sites, respectively, on the same tissue (Marks & Collins 1982). The distribution of central muscarinic

receptors is distinct from that of both [^{3}H]-(-)-nicotine and [^{125}I]αBgt. [^{3}H]QNB binding to rat brain exhibits a characteristically cholinergic pharmacology with the most effective competitor being atropine (K_i=2.8nM).

Triplicates were setup to determine total (10μl; 0.2nM [^{3}H]QNB) and non-specific (0.2nM [^{3}H]QNB in the presence of 10nM atropine) binding to P_2 membranes (250μl; 2mg/ml in PBS). Reactants were mixed and incubated at 20°C for 60min. Separation of bound and free ligand was performed by filtration at 4°C, as described for [^{3}H]-(-)-nicotine (section 2.2.4.1). Filters were counted for tritium using a Packard scintillation spectrophotometer.

2.2.5 Protein dependence of binding

The linearity of [^{3}H]-(-)-nicotine and [^{125}I]αBgt binding with increasing tissue concentrations was investigated in rat brain P_2 preparations and rat muscle extracts (RME). Protein content was varied by dilution of stock P_2 in TRIS-HEPES buffer ([^{3}H]-(-)-nicotine) or phosphate buffer ([^{125}I]α Bgt). RME was diluted in homogenisation buffer. Specific binding, defined as the difference between total and non-specific binding, was determined for [^{3}H]-(-)-nicotine and [^{125}I]αBgt as described in sections 2.2.4.1 and 2.2.4.2 respectively.

Possible effects due to the presence of Triton X100 on the binding of [^{125}I]αBgt to RME were investigated by maintaining a constant protein concentration (1mg/ml) while varying Triton levels between 0% and 2%(v/v).

2.2.6 Saturation binding

The saturability of [^{3}H]-(-)-nicotine binding to P_2 membranes, and [^{125}I]αBgt binding to P_2 and RME, was established over a concentration range of 1-40nM for [^{3}H]-(-)-nicotine, 1-20nM for [^{125}I]α Bgt binding at P_2, and 1-10nM for [^{125}I]αBgt at RME. Total binding and non-specific binding, determined in the presence of the respective unlabelled ligand (see sections 2.2.4.1 and 2.2.4.2), established specific binding levels which were used to calculate K_D and B_{max} values - see section 2.2.8.

2.2.7 Competition binding

[^{3}H]-(-)-nicotine - All drugs were assayed up to mM concentration using, in most cases, 10-fold serial dilutions prepared from frozen stocks on the day of assay. Drug (10μl), was pre-incubated with P_2 membranes (2mg /ml TRIS-HEPES) for 10 min at 20°C prior to addition of [^{3}H]-(-)-nicotine (10nM) - total and non-specific levels of binding were determined as described in section 2.2.4.1.

[^{125}I] αBgt - Drug (20 μl), prepared as described for [^{3}H]-(-)-nicotine binding above, was pre-incubated with P_2 membranes (1mg/ml 50mM phosphate buffer), or RME (1mg/ml in homogenisation buffer) for 10min at 20°C prior to addition of [^{125}I]αBgt (1nM) and subsequent incubation at 37°C - full details of this assay are described in section 2.2.4.2.

[^{3}H]QNB - Each of the ligands (10µl - prepared as described for [^{3}H]-(-)-nicotine) was preincubated with P_2 (2mg /ml 50mM phosphate buffer) for 10min. Following the addition of [^{3}H]QNB (0.2nM) the mixture was incubated at room temperature for 1h and samples processed as detailed in section 2.2.4.3.

2.2.8 Data analysis

First order linear regression of Scatchard plots (i.e. bound/free radiolabel verses bound label) was used to determine values for K_D (dissociation constant for the equilibrium binding of the radiolabel) and B_{max} (the maximum number of binding sites). Hill plots (log (bound/B_{max}-bound) verses log free ligand) of the same data were used to derive Hill numbers (η_H) also by linear regression. Data from radiolabel protein dependence and saturation assays were fitted to a rectangular hyperbola ($y=(B_{max}\cdot x)/(K_D+x)$) using B_{max} and K_D estimates from Scatchard analysis - where x=protein concentration or radioligand concentration.

Semilogarithmic plots of dose-response curves for competition assays were used to derive IC_{50} values (the concentration of drug that inhibits specific binding by 50%) by linear transformation. These values were used to determine K_i values by the method of Cheng and Prusoff (1973) - $K_i=IC_{50}/(1+([\text{radiolabel}]/K_D))$, assuming K_D values of 10nM (for the [^{3}H]-(-)-nicotine labelled rat brain site), 1nM (for the [^{125}I]αBgt labelled site of both rat brain and muscle) and 0.2nM (for the [^{3}H]QNB labelled muscarinic receptor of rat brain). All assays were performed using radiolabel at its calculated K_D. Means (±SEM) of the experimental data were plotted. The mean K_D values from at least three experiments were used to curve fit the data according to the sigmoid function $y=a-((a-b)\cdot(1/1+(K_D/x)^{\eta_H}$ - where a=value of minimum inhibition(%), b=value of maximum inhibition(%) and x=[radiolabel].

2.2.9 Materials

(-)-[N-methyl-^{3}H]Nicotine (80 Ci/mmol: stored at 4°C in 4-fold molar excess of mercaptoacetic acid), [^{125}I]Na and [*benzylic*-4,4'-^{3}H]Quinuclidinyl benzilate (40 Ci/mmol: stored at 4°C) were purchased from NEN Dupont (Stevenage, Herts). αBungarotoxin, (-)nicotine base, ACh.HCl, (-)lobeline, cytisine, physostigmine and atropine sulphate were supplied by the Sigma Chemical Co. (Poole, Dorset). (+)Nicotine hydrogen tartrate came from BDH (Poole, Dorset). DMPP.I was obtained from Aldrich (Gillingham, Dorset), and AMP.HCl (dissolved in 70% ethanol) and AMP.MeI (prepared as a 50mM solution in DMSO) were gifts from Dr I. Stolerman. (+)Anatoxin-a.HCl was initially provided by Dr E.X. Albuquerque, as was N,1'-dimethylanatoxinol (Me-AnTx-mol). Subsequent preparations of anatoxin.HCl, (as the (+) enantiomer and the racemate (±)), were supplied by Drs P.A. Brough & T. Gallagher, who also supplied homoanatoxin (HomoAnTx), propylanatoxin (PropylAnTx), isopropylanatoxin (IsopropylAnTx), HeteroAnTx, EpoxyAnTx and HydroxyAnTx. The hydrochloride salts of the AnTx analogues were dissolved in aqueous ethanol (AnTx, 19%; HomoAnTx 50%; PropylAnTx, 95%; IsopropylAnTx, 50%; Hetero-, Epoxy- and Hydroxy-AnTx, 100%). Methyllycaconitine (citrate salt) was a gift from Prof. M. Benn. Unless otherwise stated, all drugs used in binding assays (and electrophysiological studies - see section

3.2.3.2.2) were made as 10mM stock solutions in distilled water, adjusted to pH7.4, and stored in aliquots at -20°C. Serial dilutions of drugs for competition assays were made in assay buffer. Control samples of aqueous ethanol and DMSO were used to confirm that these solvents had no effect on binding.

2.3 Results

2.3.1 Protein content of tissue preparations

Total protein levels in P_2 preparations and rat muscle extract were determined using the Lowry reaction (see section 2.2.2) with BSA standards. The linearity of the colour reaction with increasing concentrations of tissue was examined from which protein concentrations were derived as summarised in table 2.1. Approximately 40% of the total protein in the rat muscle P_2 pellet was recovered by solubilisation with Triton X100.

Table 2.1: Protein contents of various tissues. Data are for at least 3 independent determinations.

	[Protein] mg/g wet wt. (± SEM)
P_2 (brain)	0.35 ± 0.05
Muscle homogenate	0.73 ± 0.09
RME	0.28 ± 0.03

2.3.2 [^{3}H]-(-)-nicotine binding to P_2 membranes

The effect of altering the protein level of the P_2 membrane preparation in the reaction medium on [^{3}H]-(-)-nicotine binding is demonstrated in figure 2.5. Total binding initially increased linearly, but saturated at P_2 concentrations above 3mg/ml - data were best described by a rectangular hyperbola. Non-specific binding levels showed a shallow linear increase with protein concentration. Specific [^{3}H]-(-)-nicotine binding, (the difference between total and non-specific levels), essentially mirrored the total binding profile, being linear to ~3mg/ml before saturating at around 3000cpm in the example shown. A protein concentration of 2mg/ml accounted for between 50-70% of the specific binding, depending on individual P_2 preparations, and consequently was selected as the working protein concentration in all subsequent [^{3}H]-(-)-nicotine binding assays.

Saturation assays, performed to assess the effect of increasing [^{3}H]-(-)-nicotine concentration on specific binding to P_2 membranes at a protein concentration of 2mg/ml, are demonstrated in figure 2.5b. Specific binding was almost completely saturable at 20nM, and Scatchard analysis (inset) gave a straight line indicative of a single binding site. Linear transformation of Scatchard data from three independent P_2 membrane preparations gave a K_D of 13nM and a B_{max} of 65fmol/mg (Table 2.2).

A Hill plot (Figure 2.5c) of the specific binding data from figure 2.5b, produced a Hill coefficient (η_H) of 1.1. Mean data from four independent rat brain P_2 preparations are summarised in table 2.2.

2.3.3 Iodination of αbungarotoxin (αBgt)

Commercially purified αBgt was labelled with ^{125}I to a specific activity of 740±28 Ci/mmol with >90% incorporation of the total ^{125}I used in the reaction. Values (±SEM) represent 3 independent iodinations, an example of which is given in figure 2.6.

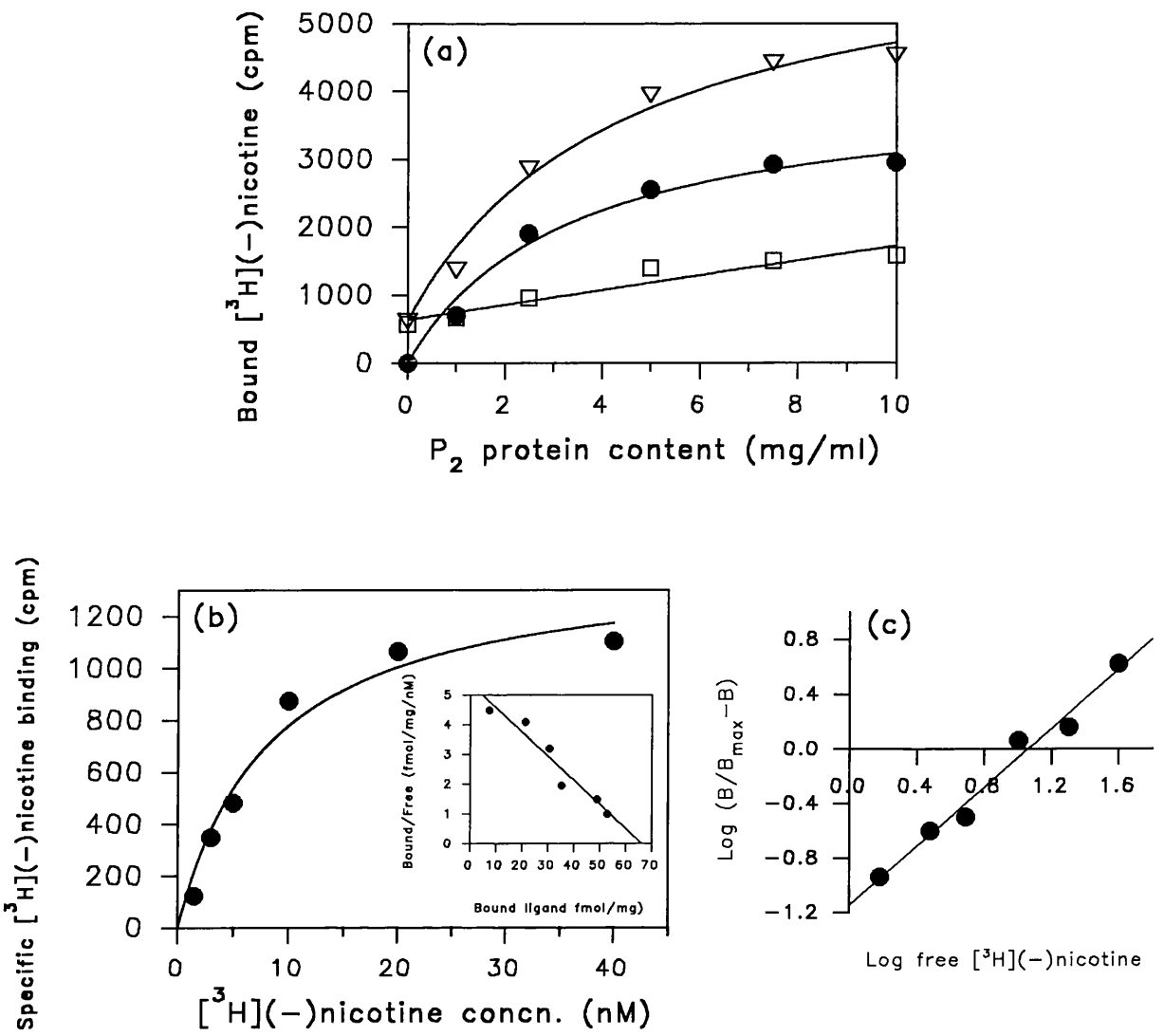

Figure 2.5. Protein dependence and saturability of [^{3}H]-(-)-nicotine binding to rat brain P_2 membranes. [^{3}H]-(-)-nicotine (10nM) was incubated for 1h with increasing levels of P_2 protein in the presence and absence of 1mM unlabelled (-)nicotine, as described in 2.2.5. Bound radiolabel was recovered by rapid filtration at 4°C. Data from a representative experiment (a) show levels of total [^{3}H]-(-)-nicotine bound (∇) and non-specific binding (□) which were used to determine the levels of specific [^{3}H]-(-)-nicotine binding (●). Points represent the means of triplicate determinations. The same tissue preparation (at 2mg protein/ml) was incubated with various concentrations of [^{3}H]-(-)-nicotine (1-40nM), and the degree of specific binding (●) determined (b) - see section 2.2.6. Scatchard analysis (inset) revealed an apparent K_D=9.6nM and B_{max}=66fmol [^{3}H]-(-)-nicotine/mg protein (r^2=0.94). A Hill plot (c) of the specific binding levels from the saturation assay, using the B_{max} from (b), gave a Hill coefficient n_H=1.10. Mean data are represented in table 2.2.

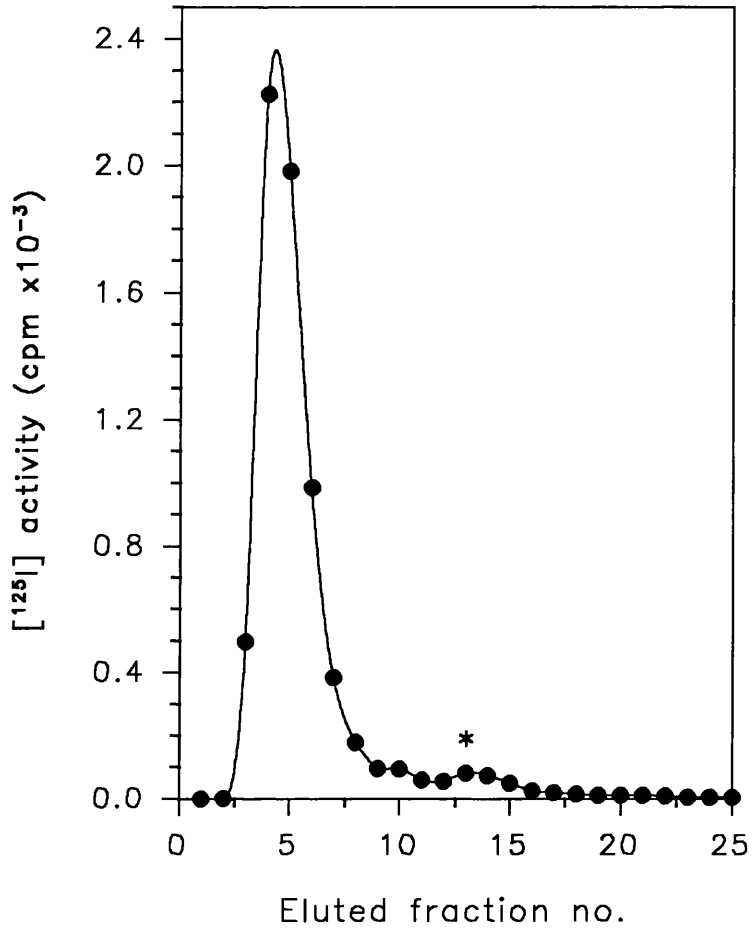

Figure 2.6. Iodination of αbungarotoxin. Commercially purified αbungarotoxin (αBgt) was radio labelled to high specific activity with ^{125}Iodine as described in section 2.2.3. Activated αBgt was mixed with ^{125}Iodine for 1min and following termination of the reaction the products were chromatographed on a Sephadex G25 column (25 x 1 cm). Fractions (25 in total) were collected and their activity counted: activity associated with the large [^{125}I]αBgt peptide was eluted first (large peak), and unbound label was eluted @ fraction 13 (*). The example here achieved 96% incorporation of the radiolabel resulting in [^{125}I]αBgt with a specific activity of 765Ci/mmol.

	K_D (nM)	B_{max} (fmol/mg)	η_H
P_2 ([^{3}H]-(-)-nicotine)	13.2 ± 3.7	65 ± 12	1.08 ± 0.13
P_2 ([^{125}I] αBgt)	1.3 ± 0.7	84 ± 24	1.05 ± 0.15
RME ([^{125}I] αBgt)	0.9 ± 0.3	11 ± 3	0.98 ± 0.08

Table 2.2. Parameters for [^{3}H]-(-)-nicotine and [^{125}I]αBgt binding to rat brain and muscle nAChR. P_2 membranes of whole rat brain, and rat skeletal muscle extracts (RME), were prepared as described in section 2.2.1. The saturability of [^{3}H]-(-)-nicotine and [^{125}I]αBgt binding to P_2 membranes, and [^{125}I]αBgt binding to RME, was assessed and parameters determined from Scatchard analysis of at least three independent tissue preparations. Experiments were performed in triplicate. Values for the apparent K_D(nM) and B_{max}(fmol/mg), ±SEM, were derived by linear transformation of the data for the radioligands at their respective binding sites. Hill coefficients (η_H) were determined by linear regression of Hill plots. The B_{max} for [^{125}I]αBgt binding sites in whole brain was higher than expected (20 fmol/mg: Schmidt *et al* 1980), though values between 100-500 fmol/mg are obtained for 'low-affinity' nicotine sites (Wonnacott 1986).

2.3.4 [^{125}I]αBgt binding to rat brain P_2 membranes and muscle extract (RME)

Whole rat brain P_2 membranes

Radiolabelled αBgt binding to increasing protein levels of P_2 membranes was assessed using a centrifugation method for separating bound and unbound radiolabel (see section 2.2.4.2). Equilibrium binding data was generally less reproducible compared with [^{3}H]-(-)-nicotine, though a similar hyperbolic saturation binding profile was observed with increasing levels of P_2 membranes (Figure 2.7a). Non-specific binding levels remained relatively constant and equilibrium was achieved with a protein concentration of about 3mg/ml - around 70% of the total radiolabel signal was detected at a protein concentration of 1mg/ml and this became the concentration used in subsequent saturation and competition assays. Equilibrium binding of [^{125}I]αBgt to P_2 preparations (1mg/ml) was assessed up to a toxin concentration of 20nM (Figure 2.7b). Specific binding approached saturation at 5nM [^{125}I]αBgt, and generated a linear Scatchard plot (inset) with a mean K_D of 1.3nM and B_{max} of 84fmol/mg (Table 2.2). An average Hill coefficient (η_H) of 1.05 was derived from Hill plots (Figure 2.7c) for 3 independent tissue preparations. There appeared to be roughly equal numbers of [^{3}H]-(-)-nicotine and [^{125}I]αBgt binding sites in the whole rat brain preparations studied.

Rat skeletal muscle extract (RME)

Protein in rat muscle was extracted with Triton X100 due to heavy contamination of the preparation with connective tissue. Quantitative detergent extraction has been documented as inactivating a significant proportion of [^{3}H]-(-)-ACh binding sites (Schneider *et al* 1985), so steps were taken to assess whether muscle αBgtBPs were similarly affected using a filtration method. The variance in binding levels as protein, and consequently Triton X100, levels were increased to 17mg/ml and 2%(v/v) respectively, are shown in figure 2.8a. Non-specific binding levels were

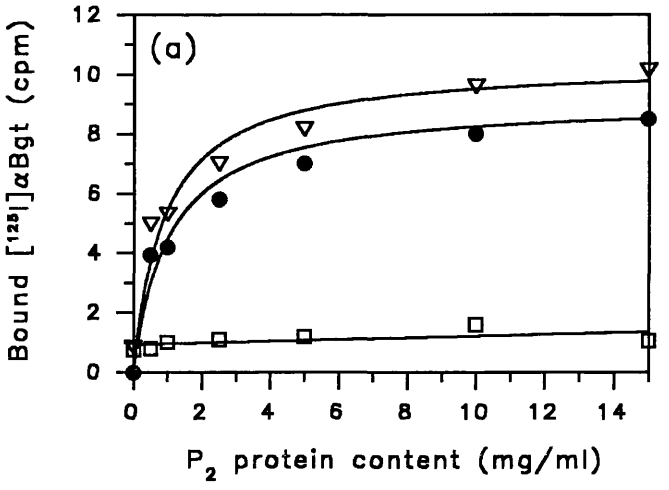

Figure 2.7. Protein dependence and saturability of [^{125}I]αbungarotoxin binding to rat brain P_2 membranes. [^{125}I]αBgt (1nM) was incubated for 2h with increasing levels of P_2 protein in the presence and absence of 1μM unlabelled αBgt, as described in section 2.2.5. Bound radiolabel was recovered by centrifugation. Data from a representative experiment (a) show levels of total [^{125}I]αBgt bound (∇) and non-specific binding (□) which were used to determine the levels of specific [^{125}I]α Bgt binding (●). Points represent the means of triplicate determinations. The same tissue preparation (at 1mg protein/ml) was incubated with various concentrations of [^{125}I]αBgt (1-20nM), and the degree of specific binding (●) determined (b) - see section 2.2.6. Scatchard analysis (inset) revealed an apparent K_D=0.76nM and B_{max}=77fmol [^{125}I]αBgt/mg protein (r^2=0.96). A Hill plot (c) of the specific binding levels from the saturation assay, using the B_{max} from (b), gave a Hill coefficient n_H=1.06. Mean data are represented in table 2.2.

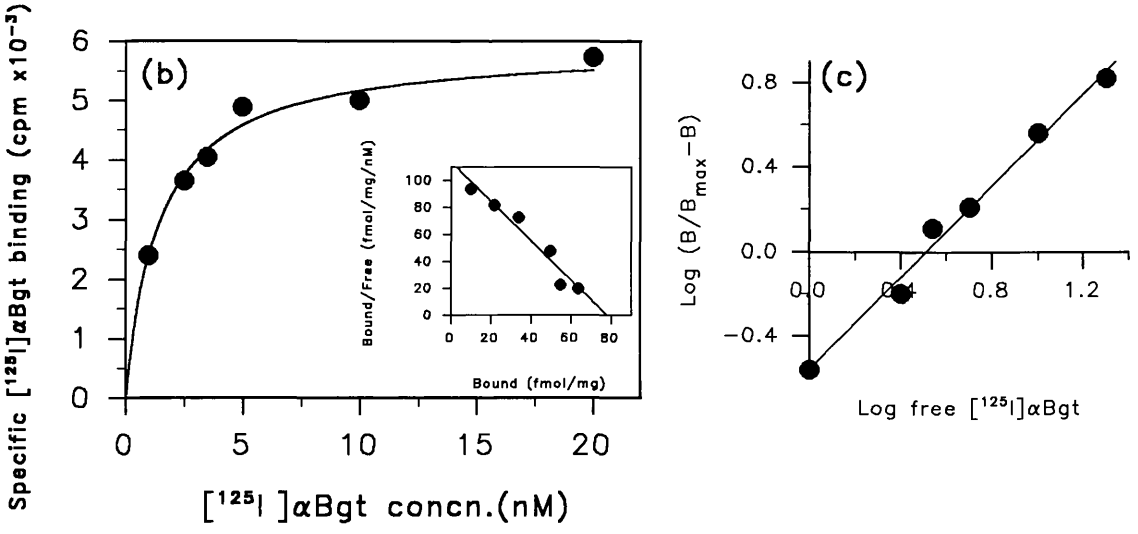

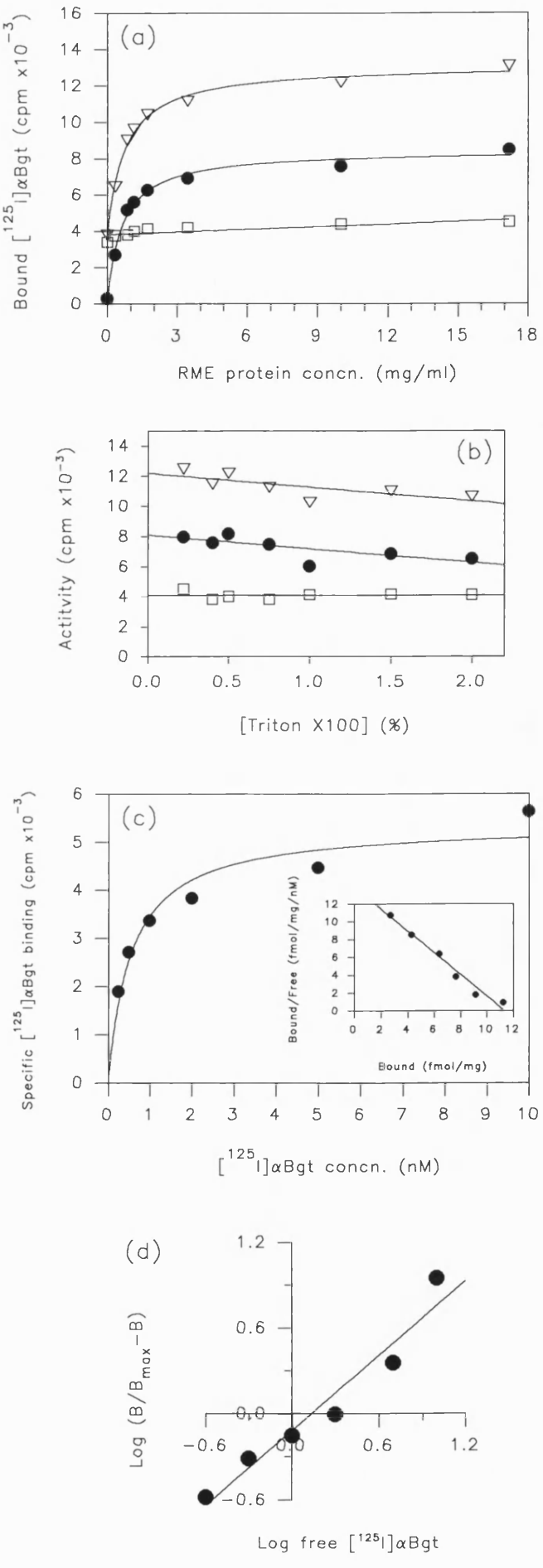

Figure 2.8. Protein dependence and saturability of [^{125}I]αbungarotoxin binding to rat muscle extract (RME), and the effect of detergent. [^{125}I]αBgt (1nM) was incubated for 2h with increasing levels of RME protein in the presence and absence of 1μM unlabelled αBgt, as described in section 2.2.5. Bound radiolabel was recovered by rapid filtration. Data from a representative experiment (a) show levels of total [^{125}I]α Bgt bound (∇) and non-specific binding (□) which were used to determine the levels of specific [^{125}I]αBgt binding (●). Points represent the means of triplicate determinations. A similar experiment to (a) in which [^{125}I]αBgt (1nM) was incubated with RME protein (1mg/ml), in the presence and absence of 1μM αBgt, included increasing levels of Triton X100 (0-2.0%(v/v)) (b) - see section 2.2.2. Total(∇), non-specific(□) and specific(●) binding levels were established, as above, from triplicate determinations.

The same tissue preparation (at 1mg protein/ml) as that used in (a), was incubated with various concentrations of [^{125}I]αBgt (1-10nM), and the degree of specific binding (●) determined (c) - see section 2.2.6. Scatchard analysis (inset) revealed an apparent K_D=0.55nM and B_{max}=11.2fmol [^{125}I]αBgt/mg protein (r^2=0.95). A Hill plot (d) of the specific binding levels from the saturation assay, using the B_{max} from (c), gave a Hill coefficient n_H=0.99. Mean data are represented in table 2.2.

generally higher than in brain preparations, with specific binding saturating above 3mg/ml. When protein levels were maintained at 1mg/ml, specific binding levels appeared to be relatively unaffected up to 2%(v/v) Triton X100 (Figure 2.8b). Consequently a working protein concentration of 1mg/ml (0.1%(v/v) Triton X100) was used for all subsequent assays.

The saturability of [^{125}I]αBgt binding to RME at 1mg protein/ml, is represented in figure 2.8c. Results were very reproducible, with specific binding saturating almost fully at levels greater than 3nM of radiolabelled toxin. Linear regression of the Scatchard plots revealed a receptor site with a very similar apparent K_D (0.9nM) to that found in whole brain P_2 membranes, though 8 times fewer sites were present (Table 2.2). A Hill plot (Figure 2.8d) of specific binding data produced an average coefficient of 0.98. Mean data for all parameters from 3 independent tissue preparations are summarised in table 2.2.

2.3.5 Competition binding - agonists

A series of agonists were assessed for their biological potency at two distinct nicotinic cholinergic receptor sites, as measured by their ability to inhibit the binding of [^{3}H]-(-)-nicotine and [^{125}I]αBgt to receptor proteins in whole rat brain, and in certain instances [^{125}I]αBgt labelled rat muscle sites. The agonists, and putative agonists, have been rationalised into structurally related groups to facilitate more direct correlations between affinity and structure. The group termed 'classical agonists' (section 2.3.5.1) share little structural homology but have served to gauge the correlation between the sites identified in this project and similar sites reported in the literature.

2.3.5.1 Classical agonists

Effects due to the direct competition of the classical ganglionic agonists; (-)cytisine, (-)lobeline and (-)nicotine, at brain [^{3}H]-(-)-nicotine and [^{125}I]αBgt labelled sites were examined in preincubation assays for comparison with the published pharmacological characteristics of these sites. Inhibition binding curves (Figure 2.9) were used to calculate the IC_{50} values represented in table 2.3. The endogenous ligand (ACh) was least potent of the agonists assayed at the [^{3}H]-(-)-nicotine site with a K_i of 0.17μM, being well within the values cited in the literature (Wonnacott 1987a) - this ligand is some 60-fold less potent an inhibitor of [^{125}I]αBgt binding with a K_i of 11μM. Physostigmine was impotent at both neuronal receptor types up to concentrations of 100μM (data not shown). The (-) enantiomer of nicotine was 8 times more potent than ACh at the [^{3}H]-(-)-nicotine site, (K_i=22nM). Greatest potency among this group was displayed by (-)cytisine (K_i=14nM) but was only marginally more effective than (-)nicotine, whereas lobeline was less potent with a K_i of 81nM. The potency rank order demonstrated by these ligands at the [^{3}H]-(-)-nicotine site of cytisine>(-) nicotine>lobeline>ACh upholds the trend observed in the literature, which has a consensus ranking of: cytisine>(-)nicotine>lobeline=ACh. At the [^{125}I]αBgt site the potency order of (-) nicotine>cytisine>lobeline>ACh was observed with K_i values of 1.0, 2.6, 6.4 and 11μM respectively. However, there was a decrease in potency of between 50-200-fold for these ligands, with greatest discrimination between the receptor sites displayed by cytisine. Such a

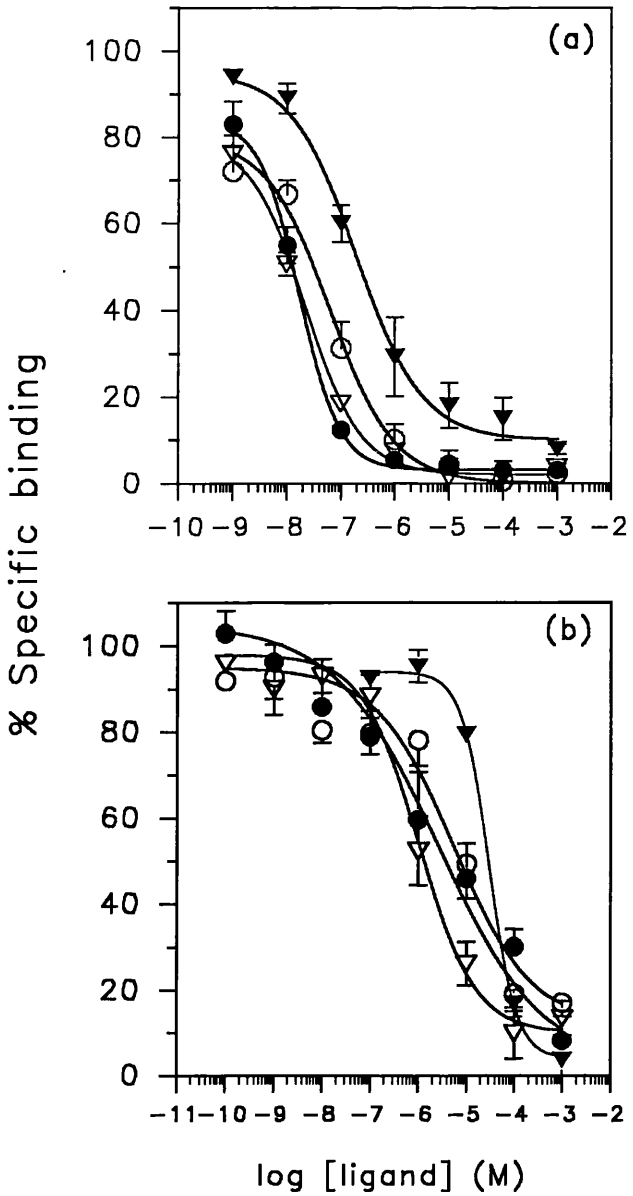

Figure 2.9. Competition binding assays of cholinergic agonists at (a) [^{3}H]-(-)-nicotine and (b) [^{125}I]α bungarotoxin binding sites in rat brain membranes. Serial dilutions of (-) cytisine(●), (-)lobeline(○), (-)nicotine(▽) and acetylcholine(▼) were assessed in preincubation assays for their ability to inhibit the binding of radiolabel, as described in section 2.2.7. Points represent the mean from at least three independent experiments, with bars indicating SEM. Linear transformation of the data determined values for 50% inhibition of radiolabel binding (IC_{50}), which were used to calculate an inhibition constant, K_i, (Table 2.3) according to the method of Cheng and Prusoff - radiolabel was used at its calculated K_D (Table 2.2). Mean data were fitted to a sigmoid function (see section 2.2.8).

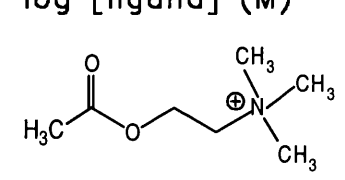

acetylcholine

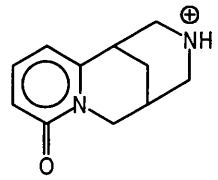

cytisine

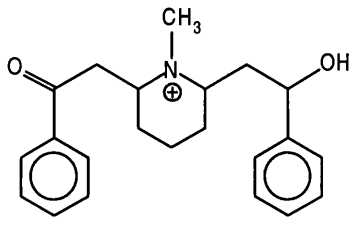

lobeline

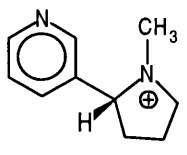

(-)nicotine

	K_i (M)			
Ligand	**[^{3}H]-(-)-nicotine sites**	η_H	**[^{125}I]α Bgt**	η_H
Acetylcholine	$1.7 \pm 2.9 \times 10^{-7}$	0.91 ± 0.19	$1.1 \pm 0.4 \times 10^{-5}$	1.4 ± 0.03
(-)Nicotine	$2.2 \pm 1.8 \times 10^{-8}$	1.04 ± 0.13	$1.0 \pm 2.7 \times 10^{-6}$	0.84 ± 0.14
Cytisine	$1.4 \pm 2.0 \times 10^{-8}$	1.16 ± 0.17	$2.6 \pm 2.5 \times 10^{-6}$	0.67 ± 0.12
Lobeline	$8.1 \pm 1.2 \times 10^{-8}$	0.93 ± 0.11	$6.4 \pm 1.2 \times 10^{-6}$	0.79 ± 0.09

Table 2.3. Inhibition of [^{3}H]-(-)-nicotine and [^{125}I]αBgt binding to rat brain by cholinergic agonists. The ability of various agonists to inhibit the binding of [^{3}H]-(-)-nicotine and [^{125}I]αBgt to preparations of P_2 membranes was determined in competition assays (Figure 2.9). [^{3}H]-(-)-nicotine and [^{125}I]αBgt were used at their K_D values (10nM and 1nM respectively) in all assays, which were performed in triplicate. Concentrations of agonist required to inhibit radioligand binding by 50% (IC_{50}) were estimated by linear transformations of dose-response curves. Inhibition constants (K_i), calculated from IC_{50} values using the method of Cheng and Prusoff, and Hill coefficients (η_H), are the means (±SEM) of at least three independent determinations.

preference for the tritiated agonist site is typical of nicotinic agonists (Wonnacott 1990: Wonnacott *et al* 1991).

Inhibition curves for ligands binding to [^{3}H]-(-)-nicotine and [^{125}I]αBgt labelled sites generated Hill coefficients of near unity, an observation that is consistent with literature reports. The quantitative significance of these values is unclear.

2.3.5.2 Nicotine

The active form of nicotine appears to be the univalent nicotinium ion, as methylation of the pyrrolidine nitrogen, in nicotine monomethiodide, retains a significant degree of activity in competition assays at sites identified by [^{3}H]-(-)-nicotine (Figure 2.10). The 40-fold shift in activity on methylation (Table 2.4) is largely attributable to the increased bulk at the cationic head (see section 2.1.1), which may reflect the volume of the binding cavity around this crucial pharmacophore point.

Nicotine was found to be nearly 2 orders of magnitude less effective in the (+) stereoisomer at the [^{3}H]-(-)-nicotine brain site (Table 2.4), exemplifying the obvious stereospecificity of this nAChR population for this ligand. Indeed the (+) isomer may bind exclusively to the low affinity site for nicotine (see section 2.4). Previous studies have found (+)nicotine to be generally 20-70 times weaker in inhibiting binding than (-)nicotine (Wonnacott 1987a). This nicotine stereoselectivity is exclusive to the [^{3}H]-(-)-nicotine labelled brain sites. Hill numbers were close to one for all the nicotine analogues.

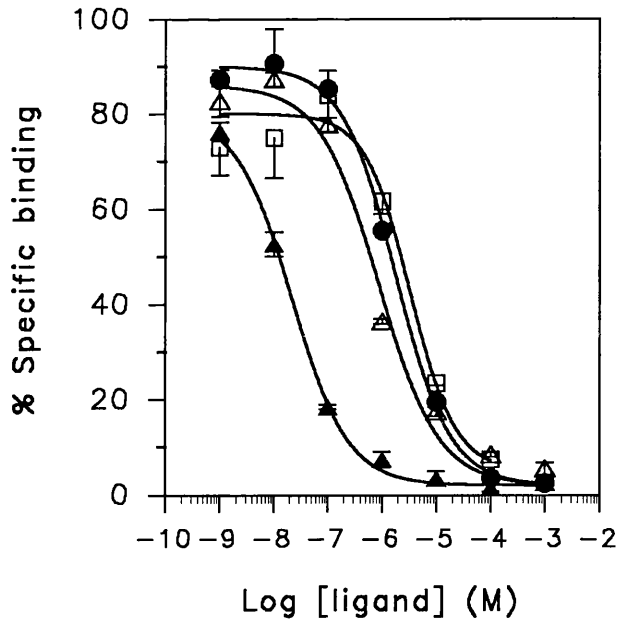

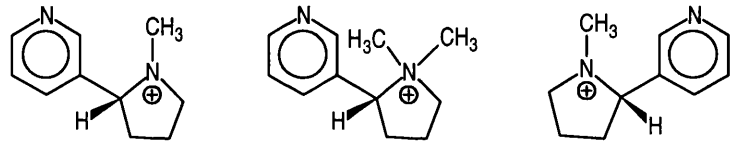

Figure 2.10. Competition binding assays of nicotine analogues at [^{3}H]-(-)-nicotine binding sites in rat brain membranes. Serial dilutions of (-)nicotine(▲), (-)nicotine monomethiodide(Δ), (+)nicotine tartrate(□) and (+)nicotine toluoyltartrate(●) were assessed in preincubation assays for their ability to inhibit the binding of radiolabel, as described in section 2.2.7. Points represent the means from at least three independent experiments, with bars indicating SEM. Linear transformation of the data determined values for 50% inhibition of radiolabel binding (IC_{50}), which were used to calculate K_i values (Table 2.4) according to the method of Cheng and Prusoff - radiolabel was used at its calculated K_D (Table 2.2). Mean data were fitted to a sigmoid function (see section 2.2.8).

	K_i (M)		
Ligand	[^{3}H]-(-)-nicotine	η_H	Relative potency
(-)Nicotine (1)	$2.2 \pm 1.8 \times 10^{-8}$	1.04 ± 0.13	1
(-)Nicotine monomethiodide (2)	$8.7 \pm 0.9 \times 10^{-7}$	0.89 ± 0.09	40
(+)Nicotine (3)	$3.3 \pm 1.1 \times 10^{-6}$	1.14 ± 0.10	150
(+)Nicotine-di-toluoyltartrate	$1.8 \pm 2.5 \times 10^{-6}$	0.97 ± 0.09	82

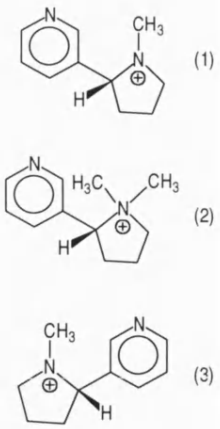

Table 2.4. Inhibition of [^{3}H]-(-)-nicotine binding to rat brain by nicotine and analogues. The ability of the stereoisomers and an N-methylated analogue of nicotine to inhibit the binding of [^{3}H]-(-)-nicotine to preparations of P_2 membranes was determined in competition assays (Figure 2.10). [^{3}H]-(-)-nicotine was used at 10nM (K_D) in all assays, which were performed in triplicate. Concentrations of agonist required to inhibit radioligand binding by 50% (IC_{50}) were estimated by linear transformations of dose-response curves. Inhibition constants (K_i), calculated from IC_{50} values using the method of Cheng and Prusoff (see section 2.2.8), and Hill coefficients (η_H), are the means (±SEM) of at least three independent determinations.

2.3.5.3 Piperazine based compounds

As their names suggest, this group of ligands all have a piperazine ring as the structural core - see figure 2.11 for structures. In this study the affinities of these 'piperazines' were assessed at the rat brain sites labelled by [^{3}H]-(-)-nicotine (Figure 2.11a) and [^{125}I]αBgt (Figure 2.11b), and additionally, for comparison with *Torpedo* data, against [^{125}I]αBgt receptors of rat muscle (Figure 2.11c) - see also Garcha *et al* 1993. Binding affinity data are summarised in table 2.5.

	K_i brain sites (M)				K_i RME site (M)	
Ligand	[^{3}H]-(-)-nicotine	η_H	[^{125}I] α Bgt	η_H	[^{125}I] α Bgt	η_H
DMPP	$1.1 \pm 0.5 \times 10^{-7}$	0.92 ± 0.05	$3.8 \pm 1.4 \times 10^{-6}$	0.75 ± 0.11	$2.9 \pm 1.4 \times 10^{-6}$	1.07 ± 0.12
AMP.MeI	$2.5 \pm 0.7 \times 10^{-7}$	0.85 ± 0.08	$1.9 \pm 1.1 \times 10^{-5}$	0.94 ± 0.1	$7.0 \pm 5.0 \times 10^{-6}$	0.98 ± 0.09
AMP.HCl	$3.0 \pm 0.3 \times 10^{-5}$	1.14 ± 0.09	$>10^{-3}$	-	$1.2 \pm 0.1 \times 10^{-3}$	0.82 ± 0.05

Table 2.5. Inhibition of [^{3}H]-(-)-nicotine and [^{125}I]αBgt binding to rat brain, and [^{125}I]αBgt binding to rat muscle extract, by compounds based on the piperazine ring structure. The ability of piperazines to inhibit the binding of [^{3}H]-(-)-nicotine and [^{125}I]αBgt to preparations of P_2 membranes, and [^{125}I]αBgt to rat muscle extract (RME), was determined in competition assays (Figure 2.11). [^{3}H]-(-)-nicotine and [^{125}I]αBgt were used at their K_D values (10nM and 1nM respectively) in both brain and muscle assays, which were performed in triplicate. Concentrations of ligands required to inhibit radioligand binding by 50% (IC_{50}) were calculated by linear transformation of dose-response curves. Inhibition constants (K_i), calculated from IC_{50} values using the method of Cheng and Prusoff (see section 2.2.8), and Hill coefficients (η_H), are the means (±SEM) of at least three independent determinations.

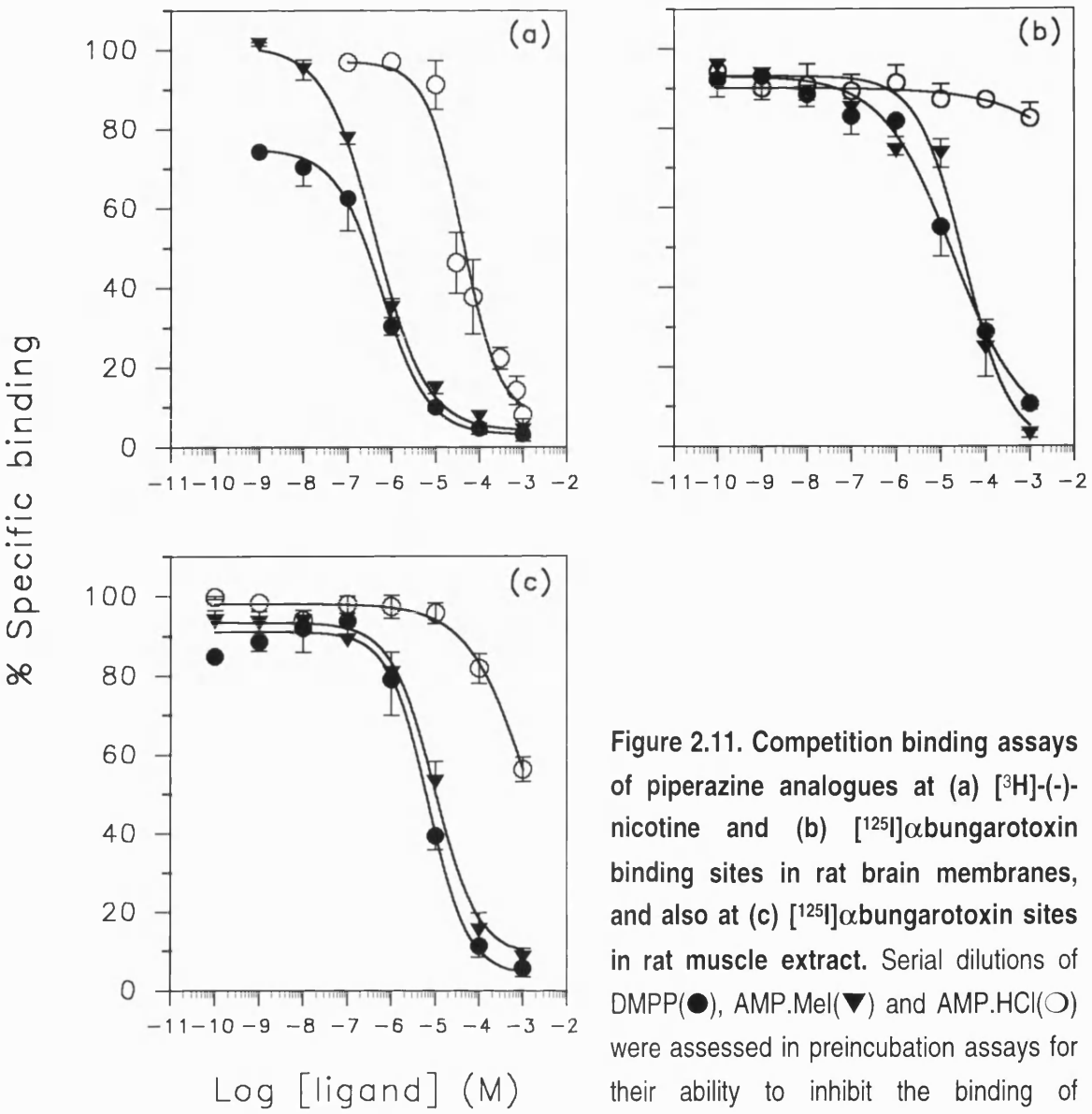

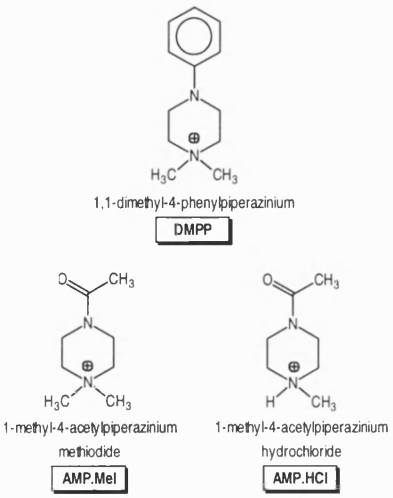

Figure 2.11. Competition binding assays of piperazine analogues at (a) [^{3}H]-(-)-nicotine and (b) [^{125}I]αbungarotoxin binding sites in rat brain membranes, and also at (c) [^{125}I]αbungarotoxin sites in rat muscle extract. Serial dilutions of DMPP(●), AMP.MeI(▼) and AMP.HCl(❍) were assessed in preincubation assays for their ability to inhibit the binding of radiolabel, as described in section 2.2.7. Points represent the means from at least three independent experiments, with bars indicating SEM. Linear transformation of the data determined values for 50% inhibition of radiolabel (IC_{50}), which were used to calculate an inhibition constant, K_i, (Table 2.5) according to the method of Cheng and Prusoff - radiolabel was used at its calculated K_D (Table 2.2). Mean data were fitted to a sigmoid function (see section 2.2.8).

1,1-dimethyl-4-phenylpiperazinium (DMPP) was able to inhibit 50% of [^{3}H]-(-)-nicotine binding to rat brain sites at a concentration of 0.2μM (K_i=0.1μM), making it the least potent of the classical nicotinic agonists (cytisine>(-)nicotine>lobeline>ACh≥DMPP), 10-fold less effective than cytisine and almost equipotent with ACh. DMPP is almost invariably the least potent of these five agonists at rat brain P_2 receptor sites (Wonnacott 1987a). Affinity for the neuronal [^{125}I]αBgt site is 40-fold lower than for [^{3}H]-(-)-nicotine, though in some studies there is little discrimination (Marks *et al* 1986). At the homologous rat muscle nAChR labelled by [^{125}I]αBgt, DMPP potency was comparable to that observed at the brain protein (K_i=2.9μM (muscle) cf. 3.8μM (brain)).

The DMPP analogue, 1-methyl-4-acetylpiperazinium methiodide (AMP.MeI) displays agonist potency at the frog neuromuscular junction (Spivak *et al* 1986). In this study, AMP.MeI inhibited [^{125}I] αBgt binding to the rat muscle site with a K_i of 7μM, nearly 3 times more effective than at the equivalent brain site (K_i=19μM). AMP.MeI is nearly two orders of magnitude more potent at inhibiting [^{3}H]-(-)-nicotine binding to the same brain tissue preparation. The methiodide was between 2 and 5 times less potent than DMPP at each of the sites assayed.

The hydrochloride salt of AMP proved to be considerably less potent, being in excess of two orders of magnitude less so relative to the methiodide, at both the brain and muscle nAChR populations. K_i values were greater than 1mM at [^{125}I]αBgt binding sites in brain and muscle, with a value of 30μM at [^{3}H]-(-)-nicotine sites (Table 2.5). Hill coefficients were near unity for all the compounds.

2.3.5.4 Anatoxins

This family of ligands is structurally based on the semi-rigid azabicyclononene skeleton of anatoxin-a (AnTx: see figure 2.12 for structures). Figure 2.12 represents inhibition binding curves for the parent compound, (+)anatoxin-a, and a series of rationally designed alkyl modified sidechain analogues, synthesised to probe configurations relevant to the nAChR pharmacophore (Thomas *et al* 1994). All were very effective inhibitors of brain receptors (Figure 2.12a and b), but fail to have any significant effect at muscarinic sites (Figure 2.12c). Figure 2.13 comprises more conformationally constrained analogues, which were considerably less potent. These potential ligands were synthesised by Paul Brough (Brough *et al* 1992: Thomas *et al* 1994), with the exception of the tertiary alcohol (N-methyl anatoxin-10-methyl alcohol (Me-AnTx-mol)), which was synthesised previously (Sardina *et al* 1989: Howard *et al* 1990), and was used for comparative purposes in this study. All analogues were assayed as racemic mixtures with the exception of (+)Me-AnTx-mol.

(+)Anatoxin-a ((+)AnTx) inhibited the binding of [^{3}H]-(-)-nicotine to rat brain membranes with a K_i of 8.2nM (Figure 2.12a: Table 2.6), a value which corroborates previous findings with this toxin (MacAllen *et al* 1988: Wonnacott *et al* 1991), making (+)AnTx the most potent agonist at neuronal nAChRs. (+)AnTx was approximately 60-fold less potent at [^{125}I]αBgt labelled binding sites. Inhibition by (±)AnTx at the same sites generated K_i values of 19nM and 0.9μM respectively. The roughly two-fold difference in potency between (+) and (-) forms are in line with those observed at peripheral receptors (Spivak *et al* 1983), though 50- and 150-fold potency differences are apparent

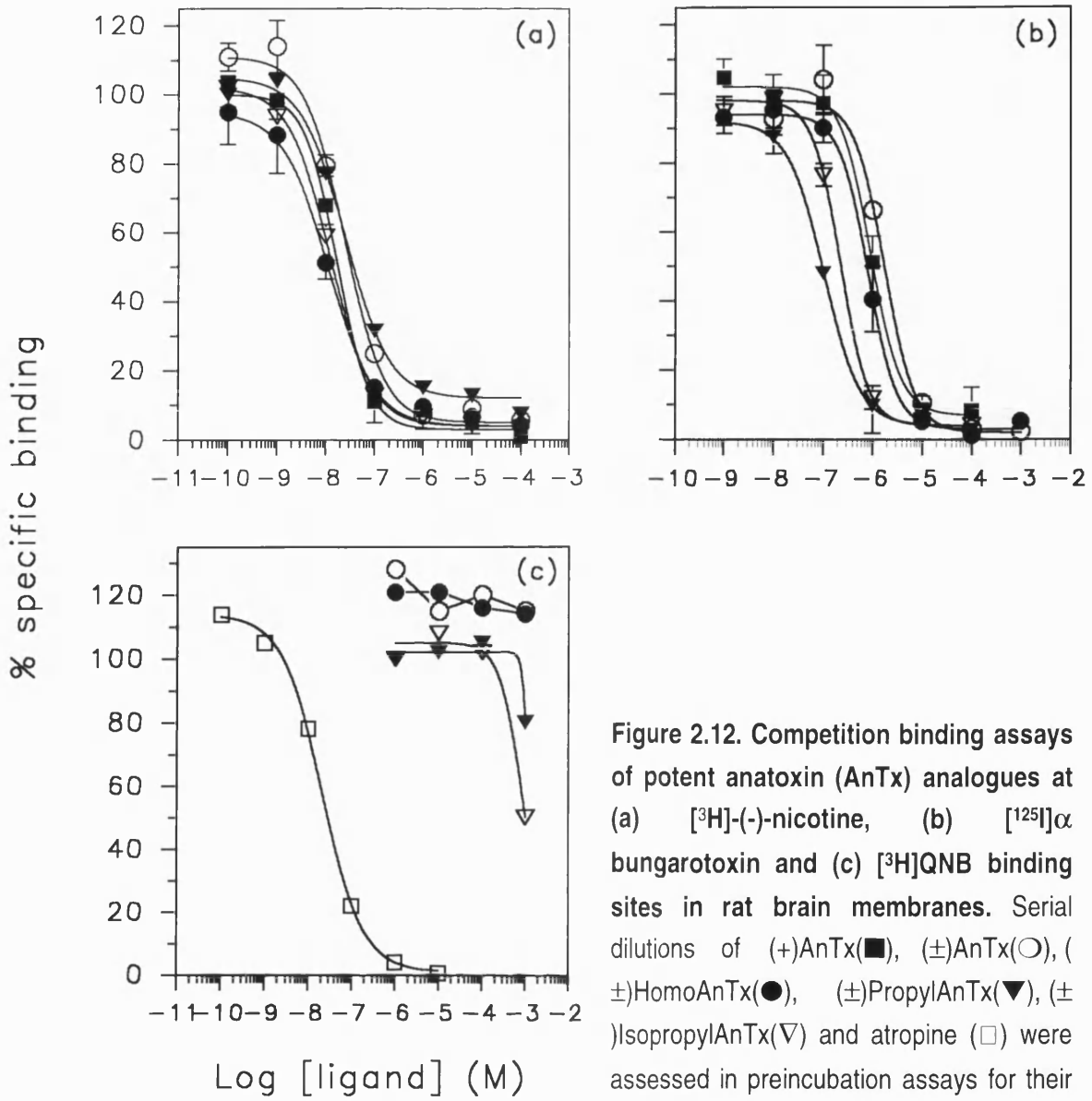

Figure 2.12. Competition binding assays of potent anatoxin (AnTx) analogues at (a) [^{3}H]-(-)-nicotine, (b) [^{125}I]α bungarotoxin and (c) [^{3}H]QNB binding sites in rat brain membranes. Serial dilutions of (+)AnTx(■), (±)AnTx(❍), (±)HomoAnTx(●), (±)PropylAnTx(▼), (±)IsopropylAnTx(∇) and atropine (□) were assessed in preincubation assays for their ability to inhibit the binding of radiolabel, as described in section 2.2.7. Points represent the means from at least three independent experiments, with bars indicating SEM. Linear transformation of the data determined values for 50% inhibition of radiolabel (IC_{50}), which were used to calculate K_i values (Table 2.6), according to the method of Cheng and Prusoff - radiolabel was used at its calculated K_D (Table 2.2). Mean data were fitted to a sigmoid function (see section 2.2.8).

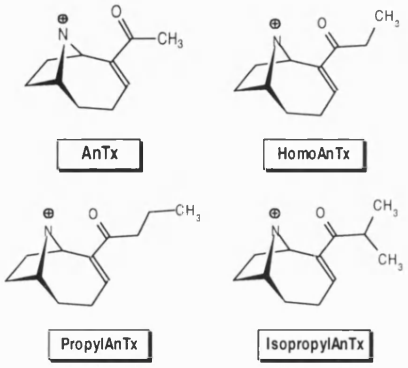

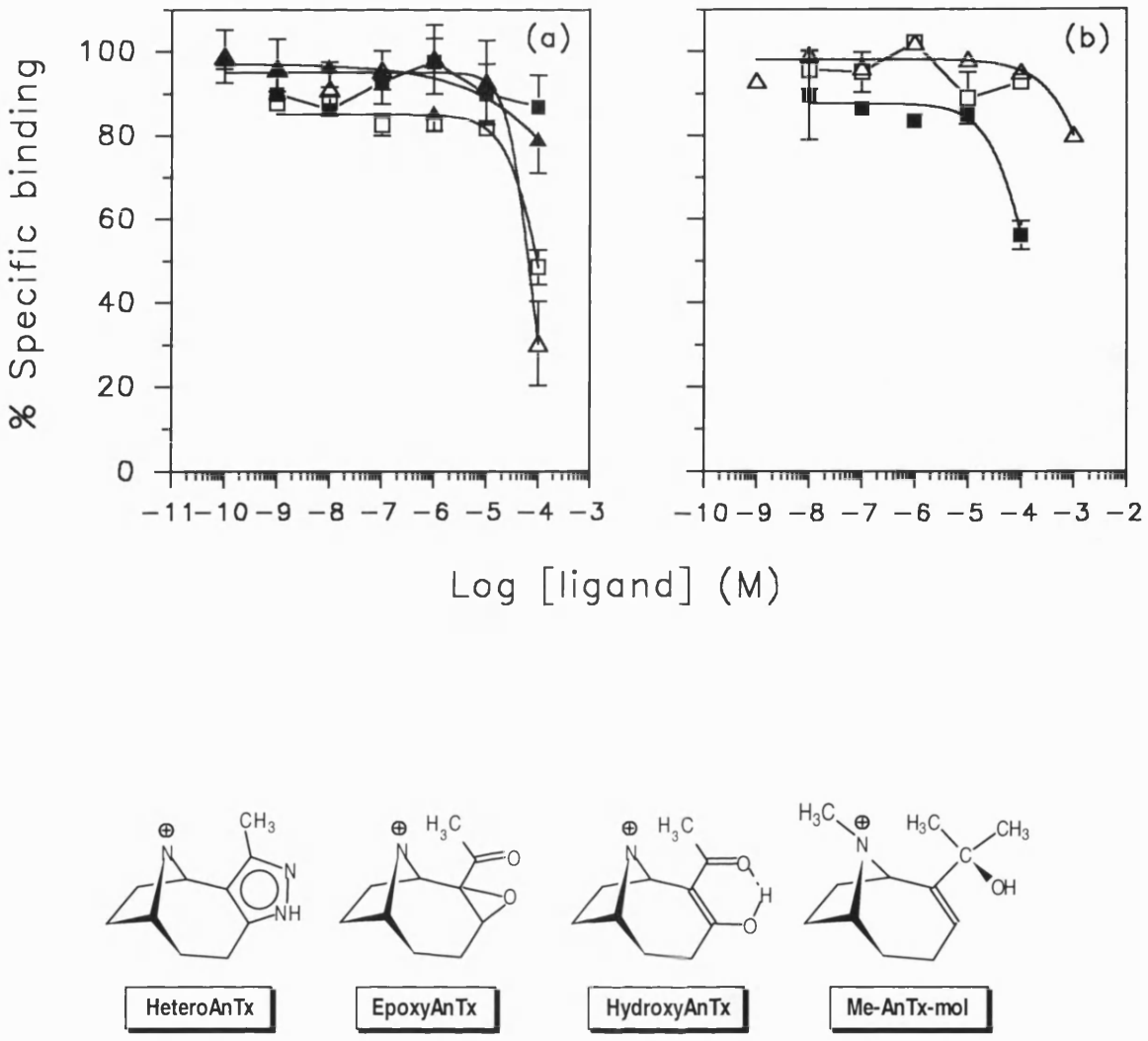

Figure 2.13. Competition binding assays of conformationally constrained anatoxin (AnTx) analogues at (a) [^{3}H]-(-)-nicotine and (b) [^{125}I]αbungarotoxin binding sites in rat brain membranes. Serial dilutions of (±)HeteroAnTx(□), (±)EpoxyAnTx(■), (±)HydroxyAnTx(Δ) and (+)Me-AnTx-mol(▲) were assessed in preincubation assays for their ability to inhibit the binding of radiolabel, as described in section 2.2.7. Points represent the means from at least three independent experiments, with bars indicating SEM. Linear transformation of the data determined values for 50% inhibition of radiolabel binding (IC_{50}), which were used to calculate K_i values (see Table 2.6) according to the method of Cheng and Prusoff - radiolabel was used at its calculated K_D (Table 2.2). Mean data were fitted to a sigmoid function (see section 2.2.8).

between (+) and (-) racemates at hippocampal and cerebellar [^{3}H]-(-)-nicotine labelled sites respectively (Zhang & Nordberg 1993).

Addition of methine or methylene units to the acetyl side chain of the AnTx skeleton to produce the compounds homoanatoxin (HomoAnTx), propylanatoxin (PropylAnTx) and isopropylanatoxin (IsopropylAnTx), did not appear to diminish binding potency at either radiolabelled brain site (Figure 2.12: Table 2.6).

	K_i (M)			
Ligand	**[^{3}H]-(-)-nicotine**	η_H	**[^{125}I]α Bgt**	η_H
(+)Anatoxin-a (AnTx) (1)	$8.2 \pm 2.3 \times 10^{-9}$	1.32 ± 0.15	$5.3 \pm 2.6 \times 10^{-7}$	1.41 ± 0.15
(±)AnTx	$1.9 \pm 0.3 \times 10^{-8}$	1.07 ± 0.03	$9.0 \pm 0.5 \times 10^{-7}$	1.43 ± 0.11
(±)HomoAnTx (2)	$5.5 \pm 0.5 \times 10^{-9}$	0.93 ± 0.05	$3.4 \pm 0.8 \times 10^{-7}$	1.51 ± 0.09
(±)PropylAnTx (3)	$2.4 \pm 1.1 \times 10^{-8}$	0.97 ± 0.06	$4.4 \pm 0.7 \times 10^{-8}$	1.19 ± 0.08
(±)IsopropylAnTx (4)	$7.5 \pm 3.0 \times 10^{-9}$	1.03 ± 0.07	$1.2 \pm 0.3 \times 10^{-7}$	1.56 ± 0.12
(±)HeteroAnTx (5)	$5.0 \pm 1.2 \times 10^{-5}$	1.26 ± 0.13	$>10^{-4}$	-
(±)EpoxyAnTx (6)	$>10^{-4}$	-	$>10^{-4}$	-
(±)HydroxyAnTx (7)	$6.8 \pm 1.5 \times 10^{-5}$	1.95 ± 0.2	$>10^{-3}$	-
(±)Me-AnTx-mol (8)	$>10^{-4}$	-	nd	-

Table 2.6. Inhibition of [^{3}H]-(-)-nicotine and [^{125}I]αBgt binding to rat brain by anatoxin and a series of analogues. The ability of anatoxins to inhibit the binding of [^{3}H]-(-)-nicotine and [^{125}I]αBgt to preparations of P_2 membranes was determined in competition assays (Figures 2.12 & 2.13). [^{3}H]-(-)-nicotine and [^{125}I]αBgt were used at their K_D values (10nM and 1nM respectively) in all assays, which were performed in triplicate. Concentrations of toxins required to inhibit radioligand binding by 50% (IC_{50}) were calculated by linear transformation of dose-response curves. Inhibition constants (K_i), calculated from IC_{50} values using the method of Cheng and Prusoff (see section 2.2.8), and Hill coefficients (η_H), are the means (±SEM) of at least three independent determinations.

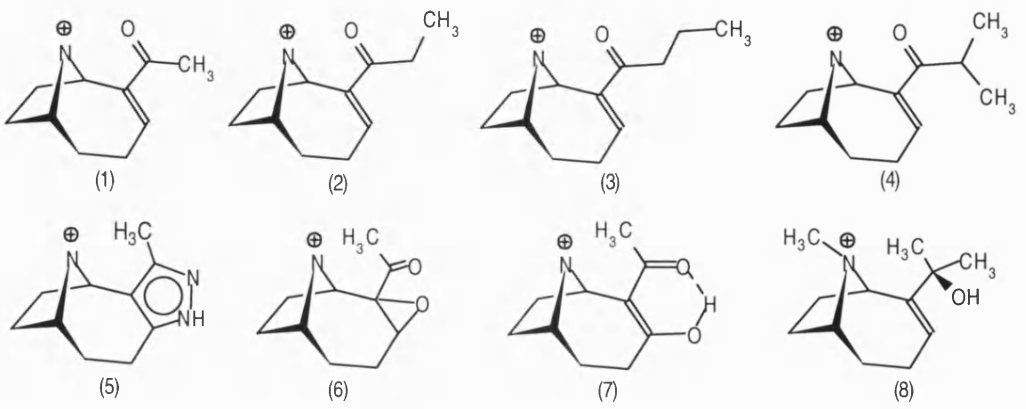

HomoAnTx, PropylAnTx and IsopropylAnTx competed for [^{3}H]-(-)-nicotine binding sites with K_i values of 5.5, 24 and 7.5 nM respectively. Corresponding values at [^{125}I]αBgt sites were 0.3, 0.04 and 0.1 μM respectively. Estimates for HomoAnTx mirror those of previous determinations (Wonnacott *et al* 1992), and PropylAnTx appears to be more selective for the [^{125}I]αBgt labelled receptor protein, the difference in affinity being less than two-fold between the two sites. No affinity for these compounds was displayed by muscarinic AChRs (Figure 2.12c).

Of the more conformationally constrained analogues poor affinity was observed at both of the neuronal nAChR sites (Figure 2.13: Table 2.6). N-methylation of the alcohol derivative abolished activity, as reported by Wonnacott and co-workers (1991). A lack of material precluded investigation above 100μM concentrations of some ligands.

2.3.6 Summary

Competition binding potencies (relative to acetylcholine) of all agonists assayed in this study are summarised in figures 2.14 and 2.15, representing [^{3}H]-(-)-nicotine- and [^{125}I]αBgt-labelled rat brain sites respectively - potencies were calculated using the K_i values from data tables in this chapter. The relative potencies of certain competitive antagonists are also included although the data has not been formally presented in this section - (IC_{50} values (M) for [^{3}H]-(-)-nicotine-labelled brain site: MLA (2.2×10^{-6}), DHβE (1.7×10^{-6}) and d-TC (4.9×10^{-5}), and the [^{125}I]αBgt-labelled brain site: (MLA 3.9×10^{-9}).

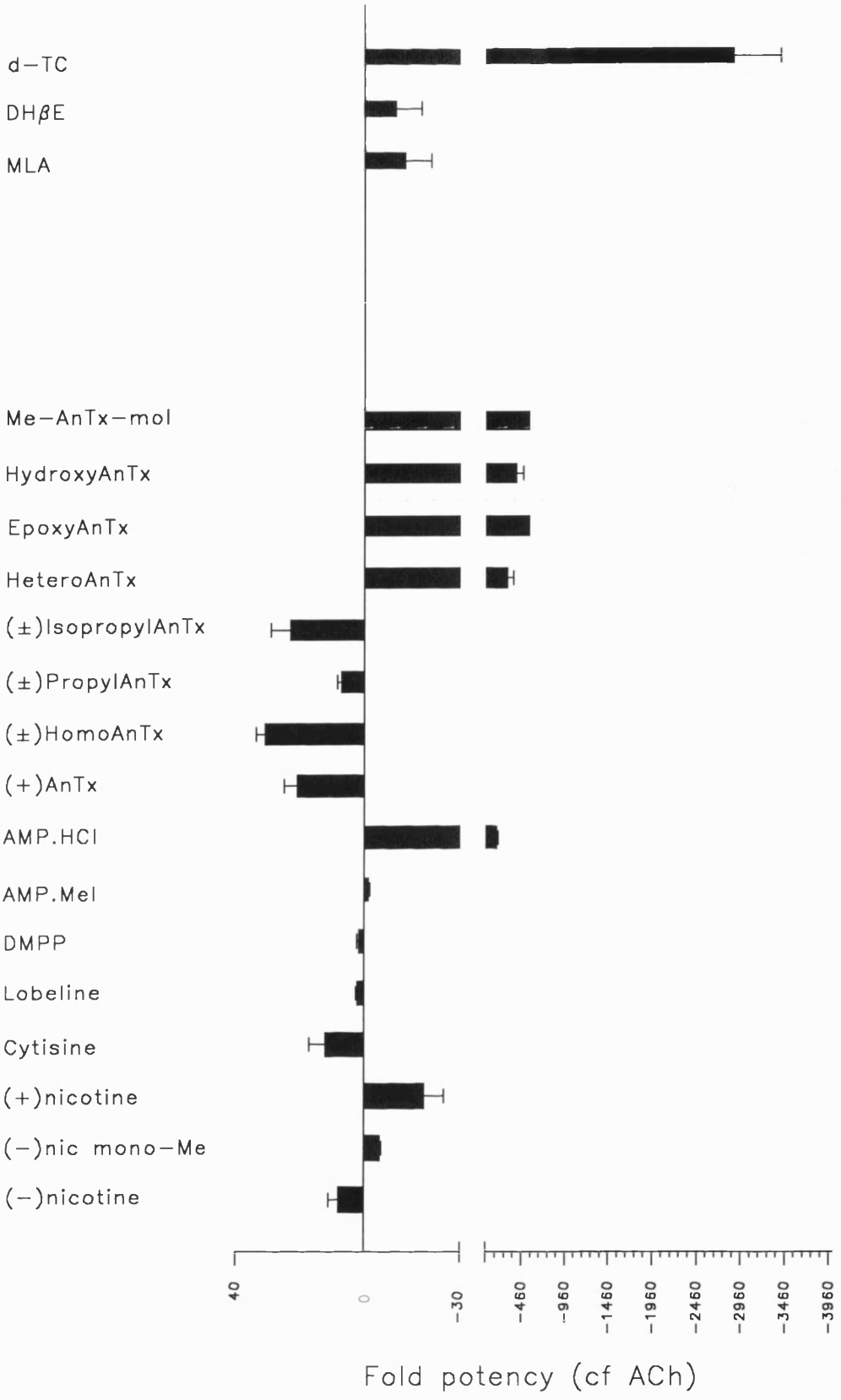

Figure 2.14. Relative potencies of all compounds assayed in competition studies at the [^{3}H]-(-)-nicotine binding site. Potencies of all drugs (agonists and antagonists) inhibiting [^{3}H]-(-)-nicotine binding to rat brain P_2 membranes are represented relative to the endogenous ligand acetylcholine (ACh, K_i=0.17μM). Potency values were determined from K_i values (±SEM) calculated from data in section 2.3.5. Bars deflecting to the right indicate lower potency, whereas those to the left are more potent than ACh.

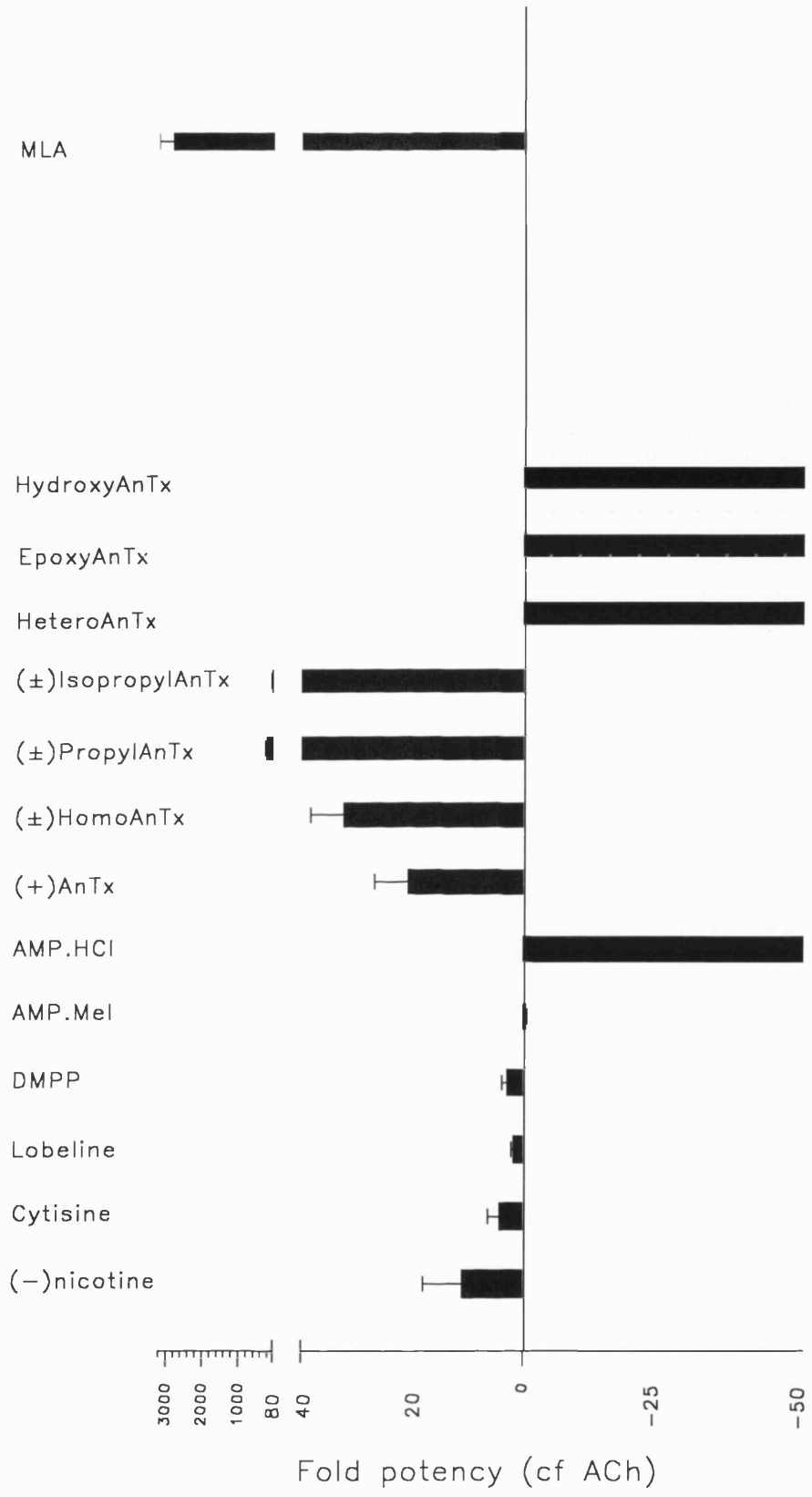

Figure 2.15. Relative potencies of all compounds assayed in competition studies at the [^{125}I] αBgt binding site. Potencies of all drugs inhibiting [^{125}I]αBgt binding to rat brain P_2 membranes are represented relative to the endogenous ligand acetylcholine (ACh, K_i=11μM). Potency values were determined from K_i values (±SEM) calculated from data in sections 2.3.5. Bars deflecting to the right indicate lower potency, whereas those to the left are more potent than ACh.

2.4 Discussion

Two principal radioligands selective for distinct neuronal nACh receptor subtypes were used in this study. Although all nAChR recognise nicotine by definition, only those that bind nicotine with nanomolar affinity are labelled by the radiolabelled agonist. The single site labelled by [^{3}H]-(-)-nicotine in brain appears to represent the presence of α4 and β2 subunits (Flores *et al* 1992). [^{125}I]α Bgt also binds with high affinity to another class of receptor(s) which are believed to contain α7 and/or α8 subunits. In certain cases in this study, comparisons have been made between the [^{125}I]α Bgt-sensitive sites of rodent central and peripheral nervous system in order to gage the effects due to the presence of α7/α8- or α1-containing receptors, alongside the effects due to α4-containing receptors.

[^{3}H]nicotine displays saturable high affinity binding to brain tissue (Figure 2.5) exhibiting a dissociation constant (K_D) of 13nM (Table 2.2) - in mammalian brain in general the range is between 1 and 10nM (Wonnacott *et al* 1990), reported disparities being attributable to many factors such as assay method, tissue preparation and ligand purity. The rodent brain sites identified by [^{125}I]αBgt also showed high affinity for this iodinated toxin ($K_D \approx$1nM: Table 2.2), though again the literature reports some variation among K_D values, though all exhibit nanomolar affinity (Schmidt *et al* 1980). In contrast to the affinity for αBgt in muscle and electric organ ($K_D \approx$1nM), neuronal receptors bind α Bgt in a reversible fashion. Scatchard analysis and Hill plots of the saturation binding data (Figures 2.5, 2.7 and 2.8) indicate binding to a single class of receptor for both ligands. However, although α7-containing αBgtBPs predominate in brain (Schoepfer *et al* 1990: Anand *et al* 1993), other minor components are also present and may represent α7α8- or α8-containing receptors.

Pharmacological specificity

Binding of well established classical nicotinic agonists to the nAChR sites labelled in this study was initially undertaken in order to provide a standard against which to compare results obtained for novel ligands not previously assessed for their activity at the nicotinic receptor. Acetylcholine, (-)nicotine, cytisine and lobeline are particularly potent at inhibiting [^{3}H]-(-)-nicotine binding to rat brain P_2 membranes (Table 2.3). The potency rank order of cytisine>(-)nicotine>lobeline>ACh closely agrees with previous studies (see Wonnacott 1987a). All of these agonists discriminate the [^{125}I]αBgt brain binding site, showing markedly reduced affinity (roughly 100-fold) relative to the [^{3}H]-(-)-nicotine labelled receptor site. (+)Nicotine exhibits greater than 100-fold lower potency than the (-) enantiomer at [^{3}H]-(-)-nicotine sites (Table 2.4), demonstrating the extreme stereoselectivity of the receptor for this ligand (Romano & Goldstein 1980), a trait not common to the [^{125}I]αBgt binding site (Marks *et al* 1986: Wonnacott *et al* 1986).

A general feature of the binding of these ligands to the two populations of brain receptor is their higher affinity relative to the concentrations that are required to activate the functional physiological equivalents. This deficit is reconciled by the understanding that in the equilibrium binding assay, prolonged incubation with ligand converts the binding site into a high affinity, desensitised state (Schwartz *et al* 1982). Although desensitisation is also seen with the functional receptor, whereby

the channel becomes unresponsive in the continued presence of the agonist following its initial confrontation with the receptor, the pharmacological response is more a measure of the affinity of the initial resting state of the receptor for the ligand. The desensitised state represented in the binding assays is therefore quite different, its induction and conversion to alternative modes most probably being via a complex series of intermediate states (Hucho 1986). Support for this conversion of the agonist binding site is apparent from kinetic analysis of binding (Lippiello *et al* 1987) and functional desensitisation (Higgins & Berg 1988) by nicotine. Now discounted theories suggested that desensitisation occurred via a site remote from the ligand binding site (Conti-Tronconi & Raftery 1982). The desensitised state predominant in the radioligand binding assays may be a consequence of induced fit of the ligand in the agonist site, a phenomenon which would be influenced by structural properties of the ligand beyond those essential to the pharmacophore which is recognised by and causes activation of the receptor. Evidence from an investigation undertaken as a part of this project, though not presented, exploring the hydrophobicity of ligands revealed that in general the more hydrophobic a ligand the greater was its potency, and furthermore that active ligands at the [^{125}I]αBgt labelled neuronal receptor were roughly 20% more hydrophobic than those active at the [^{3}H]-(-)-nicotine site. The data set for this study was derived from in excess of 120 ligands comprising the basic pharmacophore features and ranging widely in size and electrostatic character. Each had been assessed for activity at both the [^{3}H]-(-)-nicotine and [^{125}I]α Bgt labelled neuronal site in radioligand binding assays. Hydrophobicity indicators, generated using the CLOGP program, were representative of whole molecules thus were unable to distinguish specific effects due to, for example, the introduction of hydrophobic moieties around sensitive aspects of the pharmacophore model. This evidence may indicate that beyond the recognition event between receptor and ligand, increased hydrophobic character may be important in promoting transition of the receptor to a desensitised state, consistent with an induced fit model of a hydrophobic molecule in a hydrophobic binding pocket. Many hydrophobic aromatic amino acid residues have been implicated to participate in the formation of the binding site (see section 1.4). Thus it may be that the stability of the desensitised state presented in the binding assay is dictated by the extent of the hydrophobic interaction between ligand and these receptor residues, more hydrophobic molecules inducing a tighter fit and thus demonstrating higher affinity for the receptor. This situation would demonstrate how the features of the pharmacophore which are required for initial recognition events may be less relevant in the desensitised mode of the nicotinic receptor. It might then be a useful exercise to quantitate the hydrophobic parameters of individual functional groups of nicotinic ligands to ascertain around which area of the pharmacophore hydrophobicity plays the most important role.

Thus, although both [^{3}H]-(-)-nicotine and [^{125}I]αBgt binding sites in brain demonstrate a nicotinic pharmacology the inhibition of the binding of these radioligands by nicotinic agents is dissimilar. Furthermore, αBgt is unable to inhibit [^{3}H]-(-)-nicotine binding (data not shown), findings consistent with the distinctness of the nAChR proteins labelled by these ligands, and which correlate with the variation in relative densities and non-overlapping distributions of these two sites (Romano & Goldstein 1980: Schwartz *et al* 1982: Clarke *et al* 1985).

Classical ganglionic antagonists hexamethonium and mecamylamine, and MK801, were totally ineffective competitors of [^{3}H]-(-)-nicotine and [^{125}I]αBgt binding (data not shown). However, other ganglionic antagonists, DHβE and d-TC exhibited antagonistic effects at the [^{3}H]-(-)-nicotine site (with K_i values of 2μM and 50μM respectively), and are reported to be equally effective at the [^{125}I]α Bgt site (see Wonnacott 1990). These results are in line with those of previous studies (Marks *et al* 1986: McAllen *et al* 1988), and exemplify the non-competitive nature of small antagonists, which act by blocking the channel site (see section 1.4.4.1 & 1.4.4.2.), and the competitive properties common to larger antagonists which share features of the nicotinic pharmacophore (see section 2.1.2) and bind directly to a site shared by agonists. The only other antagonist used in this study to verify the fidelity of these two distinct receptor sites was MLA which showed quite significant selectivity (more than 3 orders of magnitude greater affinity) for the [^{125}I]αBgt-sensitive site ($K_i \approx 4$nM). This specificity goes beyond that of [^{125}I]αBgtBPs in general (having lower affinity for muscle sites), as reconstitution of neuronal nAChR subunits in *Xenopus* oocytes reveals possible α7 specificity for this complex molecule (see section 3.3.3.1).

The univalent nicotinium ion is the active form of nicotine. Quaternisation of the pyrrolidine nitrogen in nicotine monomethiodide demonstrates this as potency is largely retained (Table 2.4), the 40-fold decrease in affinity more probably a consequence of the increased steric bulk. Notably, the secondary amine derivative of nicotine, nornicotine, is also weaker (9-fold) than (-)nicotine but the stereoisomers, unlike nicotine, are equipotent when displacing [^{3}H]-(-)-nicotine (Copeland *et al* 1991). This effect is not a consequence of changing the physical properties of the cationic site, as the basicity of the pyrrolidine nitrogen in nicotine and nornicotine is similar so should have little effect on the proportions of mono-cation for each ligand. However, lipophilicity is altered by the presence or absence of methyls around this nitrogen. Since the binding affinity of (+)nicotine is considerably less than (-), and since nicotine monomethiodide and nornicotine stereoisomers are slightly less potent, although the latter are equipotent with each other, it is evident that the N-methyl group exerts a profound effect on binding to the nAChR. This effect is reflected in the affinities exhibited by many other nicotinic ligands. For instance N-methylation of piperazine derivatives (see section 2.3.5.3) and cytisine increases potency, yet the same modification to anatoxin-a and its derivatives (see section 2.3.5.4) and ferruginines serves to reduce the potency of these ligands at the nicotinic receptor. Thus, simple extrapolations regarding the effects of N-methylation are not possible.

In the case of nicotine it would appear that the addition or removal of an N-methyl group destabilises the conformation and that consequent effects on hydrophilicity and basicity are of less importance. For instance the proton attached to the pyrrolidine nitrogen of the protonated form of nicotine may be directed towards the complementary cationic binding site (i.e. the bulky methyl is out of the way). In (-)nicotine this structure may be represented where N-methyl and pyridine ring are in the *trans* configuration (see section 4.3.2). Binding of (+)nicotine would require that in order for the proton to assume the same directionality, the pyridine ring would be forced into an energetically less favourable *cis* configuration relative to the N-methyl. The stereoselectivity of nicotine may therefore

be a consequence of steric repulsion between pyridine ring and N-methyl decreasing stability of the ligand-receptor complex. Alternatively, if the *trans* configuration were retained in (+)nicotine then the methyl would be oriented towards the cationic site which may not be favourable. In nornicotine these steric interactions due to the N-methyl group would not apply, hence the observed lack of stereoselectivity. If this is the case, then (+)nicotine monomethiodide should also demonstrate equipotency with the (-) stereoisomer.

DMPP was roughly equipotent with ACh at the [^{3}H]-(-)-nicotine labelled site yet did not appear to favour this site over that labelled by αBgt to the same extent as that of other nicotinic agonists (Table 2.5). This reflects the observations of Marks and co-workers (1986), who found DMPP to be almost equipotent at these two rodent brain sites. Remarkably, DMPP showed similar affinity for the α1-containing skeletal muscle receptor of the rat as for the brain site. Given the limited sequence homology that exists between α1 and α7/α8 genes, and the presence of β, γ, δ subunits in the muscle protein homologue, and presence of only non-α subunits in the neuronal receptors, the conservation of potency between αBgtBP subtypes is perhaps significant. This may reflect either a well conserved feature in the αBgt-sensitive α subunit which forms the binding site, or a minimal contribution to the binding site from neighbouring subunits, suggesting a less subunit interface oriented binding site in the αBgtBPs.

The novel nicotinic ligand AMP.MeI inhibited the binding of nicotinic radioligands to sites in rodent muscle and brain. Previously this salt was examined in preparations of *Torpedo* electric organ (Spivak *et al* 1989a) and at frog neuromuscular junction (Spivak *et al* 1986). The present study extends this profile (Garcha *et al* 1993). Replacement of the benzene ring of DMPP with an acetyl group in AMP.MeI produces a ligand of comparable potency (Table 2.5). Whereas AMP.MeI exhibited potencies at [^{125}I]αBgt sites similar to those of *Torpedo* (Spivak *et al* 1989a), removal of an N-methyl group in the hydrochloride salt (AMP.HCl) reduced potency by some two orders of magnitude at each of the brain and muscle binding sites examined (Table 2.5). Similarly, the hydrochloride salt of the structurally related isoarecolone has been shown to be 25-fold less potent than the corresponding methiodide at [^{3}H]-(-)-nicotine binding sites of rat brain (Reavill *et al* 1987), contrary to the effects of N-methylation of cytisine and anatoxin-a. It has been proposed that simple tertiary amines are weak agonists because the requirement for steric bulk perpendicular to the plane defined by the carbonyl carbon and its substituents is not fulfilled (Spivak *et al* 1989a). The N,N-dimethylpiperazinium structure is common to both DMPP and AMP.MeI and these two ligands are almost equipotent at each site. However, the hydrochloride salt of AMP does not share the potency of the methiodide despite existing as a monovalent ion. Thus it seems that although the univalent piperazinium ion is common to potent ligands, the presence of a methyl around this cationic head is also important, perhaps due to increased lipophilicity or stability differences. The hydrogen bond accepting moiety is substitutable and therefore is of secondary importance, represented by delocalised pi electrons. The benzene ring associated with DMPP may occupy a hydrophobic pocket in the receptor, residues for the provision of this there is certainly no shortage of. Many of the more potent nicotinic agonists are semi-rigid and the bulk of their volume is asymmetrically displaced.

Piperazines are essentially substituted cyclohexanes with a rotatable bond between the tertiary nitrogen and substituent carbon, and thus are relatively flexible in their number of conformations and are, perhaps crucially, fairly planar (see section 4.3.3). The quaternary nitrogen is evidently crucial in bestowing potency via the introduction of the out of plane bulk, and possible alterations to the lipophilic character. Notably, the carbamyl analogue of AMP.MeI is 17-fold less potent in evoking twitch responses in the frog muscle (Spivak *et al* 1989a), a factor ascribed mainly to the greater hydrophilicity of the carbamyl, which disfavours the partitioning of this agonist from the aqueous phase to the receptor phase. This may be a general rule for ligands with groups which can donate hydrogen bonds to water.

Although AnTx has a rigid azabicyclononene ring system, the rotatable bond of the acetyl sidechain means the enone moiety can adopt two important low energy conformations where the carbonyl bond is either *cis* or *trans* (see section 4.3.4). Which of these two conformations represents the bioactive form is controversial (see section 4.1.2). According to the Beers-Reich model of the nicotinic pharmacophore the *cis* conformation of AnTx best complies with the distance between cationic group and carbonyl oxygen, but the angle by which these two groups are disposed is best fulfilled by *trans* AnTx. Given the universally potent nature of (+)AnTx at neuronal nAChR (Thomas *et al* 1993), determining the bioactive conformation may have significant implications for an extended model of the nicotinic pharmacophore.

Previous studies with AnTx and a series of 18 rationally designed analogues (see table 4.7 and Swanson *et al* 1991: Wonnacott *et al* 1991) re-evaluated the nicotinic pharmacophore and chemical hypotheses concerning agonist interaction with nAChRs. The analogues comprised rational changes to the acetyl moiety and secondary amine function, and mainly evaluated the importance of hydrogen bonding strength, planarity, steric bulk and side chain configuration - structural modifications of these analogues and respective K_i values at [^{3}H]-(-)-nicotine and [^{125}I]αBgt sites are given in table 4.7. In this previous study, (+)AnTx was the most potent competitor of binding to [^{3}H]-(-)-nicotine and [^{125}I]αBgt labelled neuronal sites, a feature repeated in this current study. Modification of the AnTx structure reduced potency. N-methylation reduced potency by at least two orders of magnitude (Table 4.7) consistent with the same effect among piperazine based compounds, but contrary to effects on ferruginine and cytisine (Swanson & Albuquerque 1992). The potential of AnTx as a starting point for structure-activity relationships was clearly illustrated among the amido analogues, two of which (AnTxNOMe and AnTxisox) demonstrated a 1000-fold preference for the [^{3}H]-(-)-nicotine site, and another (AnTxMe_2N) was relatively more potent at αBgt sites (Table 4.7).

With some of the lessons from this previous study in mind a series of constrained analogues were synthesised (Paul Brough & Timothy Gallagher, Univ. Bristol). The objective behind these rational modifications was to determine the bioactive configuration of the carbonyl of the acetyl sidechain by restricting its conformational freedom - the racemic compounds synthesised are shown with table 2.6. In the so-called HeteroAnTx and HydroxyAnTx the hydrogen bond accepting group was locked

in the *cis* configuration, in the former through the addition of a pyrazole ring system and in the latter by a hydrogen bond with an adjacent hydroxyl (Brough *et al* 1992). EpoxyAnTx was designed to effectively distort the carbonyl group away from *cis* via charge repulsion due to the introduction of an epoxide - it is unlikely that this structure exists as either *cis* or *trans* as a result. Additionally, the N-methylated tertiary alcohol, Me-AnTx-mol (structure 8 in table 2.6), a synthetic analogue from the previous AnTx study mentioned above (Swanson *et al* 1991), was also included. Unfortunately, these constrained analogues were largely ineffective at both nicotinic (Table 2.6) and muscarinic (data not shown) sites. The *cis* constrained analogues (HeteroAnTx and HydroxyAnTx) were possibly slightly more effective than the epoxide, but given the extent to which the AnTx structure has been modified in volume and charge this observation cannot be ascribed to configuration of the hydrogen bond accepting moiety alone. Therefore, although not a positive result, these observations could be informative in that they reflect effects due to changes in charge distribution, loss of flexibility and steric restraints about the hydrogen bond accepting group, as well as conformation alterations. It should be noted that for this initial characterisation racemic compounds were employed yet the nicotinic potency of AnTx resides predominantly in the (+) enantiomer (Table 2.6: Spivak *et al* 1983): thus the assays may underestimate nicotinic potency by a factor of two.

Having taken on board the message that significant structural changes around and to the hydrogen bond accepting group are detrimental to activity, alternative alkyl-modified sidechain analogues of AnTx were deemed to be a less disruptive and less complicated approach. Previously extension of the acetyl sidechain, in HomoAnTx, has been shown not to affect potency (Wonnacott *et al* 1992). Further extension of this sidechain was undertaken by addition of one or more methine of methylene units producing PropylAnTx and IsopropylAnTx (see structures with table 2.6). It was assumed these alterations would be tolerated to a certain extent by the receptor binding site and perhaps that the extra hydrocarbon bulk, especially of IsopropylAnTx, would influence the configuration of the carbonyl group.

In competition binding assays AnTx and the three alkyl modified sidechain analogues inhibited [^{3}H]-(-)-nicotine binding with K_i values between 5nM and 24nM as racemic mixtures (Table 2.6): the rank order of potency at this site was HomoAnTx>IsopropylAnTx>AnTx>PropylAnTx. K_i values for these analogues at the [^{125}I]αBgt binding site were between 40nM and 900nM with the rank order PropyAnTx>IsopropylAnTx>HomoAnTx>AnTx. Thus the parent compound was not the most potent of the series, and there appeared to be some evidence of subtype specificity with PropylAnTx in favour of the [^{125}I]αBgt labelled neuronal site. HomoAnTx retained its potency relative to a previous study investigating the same sites (Wonnacott *et al* 1992); K_i=7.5nM ([^{3}H]-(-)-nicotine) and 1.1μM ([^{125}I]αBgt). In contrast, none of these novel AnTx analogues was effective at the muscarinic acetylcholine receptor, as defined by [^{3}H]-quinuclidinyl benzilate competition binding (Figure 2.12).

HomoAnTx and IsopropylAnTx gave comparable K_i values (0.34μM and 0.12μM respectively) at the [^{125}I]αBgt sensitive brain site. Activation of the α7 nAChR in *Xenopus* oocytes by these two analogues (see section 3.3.3.4) was also comparable, taking into account the different receptor

states, with EC_{50} values of 0.72μM and 0.66μM, giving EC_{50}/K_i ratios of 2 and 5 respectively. These potencies compare well with our published data for enantiomerically pure (+)AnTx at the α7 nAChR (Amar *et al* 1993) which yielded an EC_{50} value of 0.58μM and an EC_{50}/K_i ratio of 1.5. In the same study (Amar *et al* 1993) we obtained EC_{50}/K_i ratios between 0.8 and 8.4 for six other agonists, so these novel AnTx analogues seem to fall within the same range.

Interestingly, PropylAnTx appears to be more selective for the [^{125}I]αBgt site, having a K_i value (44nM) less than twice that at the nicotine site - AnTx, HomoAnTx and IsopropylAnTx exhibit ratios for the two sites of 46, 62 and 16 respectively, as is more common for nicotinic ligands. A previous series of AnTx analogues (Wonnacott *et al* 1991), typically gave K_i ratios for [^{3}H]-(-)-nicotine:[^{125}I]α Bgt sites of between 30 and 100. The apparent selectivity of PropylAnTx for the [^{125}I]αBgt site is an interesting feature. Unfortunately a shortage of material precluded investigations with this ligand at the functional α7 nAChR.

These structure-activity studies based on the potent naturally occurring agonist AnTx have defined two new potent nicotinic ligands at neuronal nAChR that retain or exceed the potency of the parent compound. The agonist properties of AnTx are also retained by HomoAnTx, PropylAnTx and IsopropylAnTx at the α7 receptor (see section 3.3.3.4). Comparison of results from competition binding assays acknowledge that the ligand binding site of the receptor is able to accommodate the increasing hydrophobic bulk of the extended side chain of these analogues. Indeed, PropylAnTx may show some α7 subtype selectivity requiring a very exact hydrophobic subsite for the sidechain to interact with, a subsite which is too remote to be reached even by either the IsopropylAnTx or HomoAnTx sidechain. The existence of this hydrophobic subsite could be probed using even longer extensions of the side chain, or its toleration of charged groups be examined by substitution at the extremity of the sidechain. The apparent specificity shown by PropylAnTx argues against the orientation of the sidechain away from the binding surface and into an aqueous environment for the αBgt-sensitive receptor, for if this were the case then there would probably be little if any difference in [^{3}H]-(-)-nicotine:[^{125}I]αBgt potency ratios for this ligand. If this is so then there could exist important differences in the local environment of the binding site of the two receptor subtypes studied in this project. The many hydrophobic aromatic residues identified in this region could be candidates for this as mentioned previously. Receptor mutants in which these hydrophobic residues are substituted would be useful in exploring whether PropylAnTx in particular suffers any decrease in potency as a result.

It has been shown that the acetyl sidechain of AnTx can be extended considerably with little loss of potency (Huby *et al* 1991: Thomas *et al* 1994:). As such these novel analogues represent potential affinity ligand candidates which could be coupled to CNBr-activated sepharose and used to affinity purify nAChR of rat brain, cultured cell lines (e.g. M10, BC3H1, PC12), *Xenopus* oocytes etc. At present there is a paucity of affinity ligands for nAChR. These small analogues have the added advantage that elution using other nicotinic ligands would not denature the receptors, as happens with immunoisolated proteins (Whiting & Lindstrom 1987). Considering that the subunit composition

of neuronal nAChR is largely unknown, these ligands could prove to be excellent starting structures, especially PropylAnTx if it is confirmed to be α7 selective. Conroy and co-workers (1992) have reported association of the α5 subunit with α4 and β2 subunits which were considered to comprise the high affinity agonist binding sites (Whiting *et al* 1987a: Flores *et al* 1992). This sort of complication, as well as the unresolved issue of the subunit composition of neuronal αBgtBPs, could be investigated using an AnTx analogue purification procedure.

At present these synthetic AnTx analogues probably have greater potential as tritiated radioligands. Their high affinity may enable the detection of α3-containing nAChR that are not detectable using the currently available tritiated nicotinic agonists. Also, being secondary amines, passage across the blood brain barrier is possible and would facilitate examination of the pharmacokinetics of CNS delivery following systemic injection. Centrally acting nicotinic agents could have an important therapeutic future in the symptomatic treatment of Alzheimer's disease (Kellar & Wonnacott 1990). Distribution patterns of a tritiated AnTx analogue could also be compared to those of other tritiated nicotinic ligands.

A hybrid of anatoxin-a and nornicotine, known as pyridohomotropane (PHT), is comparable in potency to anatoxin-a in its ability to compete with [^{3}H]-(-)-nicotine at rat brain nicotinic receptor sites (Kane & Abood 1988). Methylation of the pyrrolidine ring nitrogen of PHT to generate a structure equivalent to nicotine reduced potency considerably. This structure is potentially a more precise tool with which to extend the pharmacophore model and map of the receptor binding cavity, since the position and orientation of its hydrogen bond acceptor and pyrrolidine nitrogen are more strictly defined.

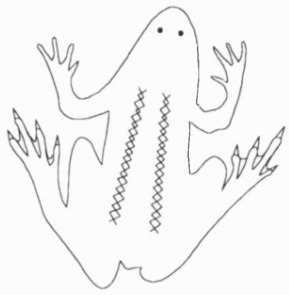

3. Whole cell voltage clamp electrophysiology

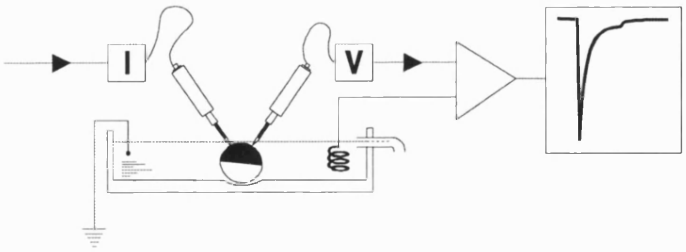

3.1 Introduction

3.1.1 Oocytes as tools to probe receptor function

Since the early 1970s a powerful tool has been exploited and developed which has made easier the assessment of the products of molecular biology. The technique essentially involves the injection of exogenous nucleic acid into the oocyte of the African clawed toad, *Xenopus laevis,* whose biosynthetic machinery provides the surrogate translation system for the production of the related protein.

The oocyte's suitability for this role stemmed from its extensive use in elucidating gene expression mechanisms and the mechanism by which cell division is regulated. *Xenopus laevis* is unique among other laboratory anurans in that a new reproductive cycle can be initiated through the administration of certain hormones and, moreover, oogenesis in this *Xenopinae* subfamily is a continuous, asynchronous process with ovaries containing oocytes at all stages of development throughout the adult life.

The first demonstration of this system's ability to manufacture exogenous protein involved the synthesis of rabbit haemoglobin after microinjection of reticulocyte 9s mRNA (Gurdon *et al* 1971). Although the cell-free system of reticulate lysate had been successfully used to this point, it was estimated that the efficiency of the oocyte system was about 30 times that of the lysate over the same incubation period. Furthermore, the culture of oocytes over long periods of time increased this efficiency to over 1000-fold. The advantages of the oocyte were quickly realised, though for more routine assays the cell-free extracts remain the simplest and most economical translation systems available. Advantages of the oocyte lie in their ability to carry out post-translational modifications of the foreign protein, such as precursor processing, glycosylation and phosphorylation. These cells are also able to direct proteins to the correct cell membrane and export secretory proteins. Additionally, synthesised macromolecules acquire their native activity even if this requires co-assembly of many subunits, as has now very convincingly been demonstrated for the proteins which represent neuronal receptor subunits.

It is only relatively recently that there has been increased interest in the routine use of oocytes in assessing the viability of cloned proteins. The reasons for this result largely from the huge advances achieved in the micromanipulation and analysis of genetic material, coupled with the urgent need for a robust gene expression system in which to assess these products. Particularly attractive as a tool for the investigation of structure-function relationships of membrane proteins, the oocyte was the obvious choice for the cloned voltage and ligand-gated ion channels, and neurotransmitter receptors that began to appear in the early 1980s. *Xenopus* oocytes were used in the expression of AChRs for the first time by Sumikawa and co-workers (1981) who injected heterologous mRNA isolated from *Torpedo* electric organ. The subsequent synthesis and assembly of the multisubunit nAChR was detected immunologically and by [^{125}I]αBgt binding, which identified four polypeptides with molecular weights very similar to those found in the native *Torpedo* receptor (Lindstrom *et al* 1979). Notably, the cell-free system was incapable of faithfully synthesising intact receptor molecules. Later studies

implementing the same technique confirmed this receptor to be membrane-bound, and when challenged with ACh, the voltage-clamped oocytes were observed to gate ions with a permeability which resembled that of nicotinic cholinergic receptors in other cells (Barnard *et al* 1982). These currents were also blocked by d-tubocurarine and αBgt.

Fully grown, mature oocytes at stage VI of their anatomical development, consist of two halves referred to as animal and vegetal hemispheres. The whole cell is contained within the plasma membrane which, in the follicular form, is surrounded by four layers (Figure 3.1): the fibrous vitelline membrane; a monolayer of follicle cells (which form many membranal contacts with the oocyte); a connective tissue layer (theca) containing capillaries, nerve fibres and fibroblasts; and a layer of ovarian epithelial cells, a continuation of the ovary wall (Dascal 1987). The follicle cell layer contains endogenous receptors for catecholamines, gonadotrophins and purinergic agonists, as well as GTP-binding proteins (Kusano *et al* 1982: Dascal *et al* 1985: Snutch 1988). Follicular oocytes (those dissected from the ovarian envelope) also possess an endogenous response to ACh, of a muscarinic nature (Kusano *et al* 1977), which can be blocked by atropine (see section 3.3.1) or lost through collagenase treatment. Denuded oocytes, (those stripped of everything but vitelline and plasma membranes using collagenases and other proteolytic enzymes), retain the ability to generate endogenous voltage gated Na^+, K^+ and Ca^{++} currents (Dascal 1987) but these are small relative to the larger (10-100 fold) currents resulting from exogenous nucleic acid microinjection.

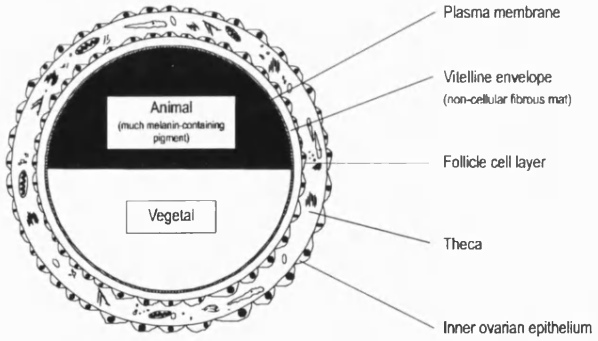

Figure 3.1: Anatomy of the follicular oocyte. Schematic diagram of the *Xenopus* oocyte and surrounding tissues as dissected from the ovarian envelope of the toad. In this follicular form the oocyte is enveloped by several cellular and non-cellular layers which must be removed as they harbour endogenous receptors which may complicate interpretation of electrophysiological recordings following the injection of exogenous nucleic acid.

Because oocytes are actually germ line cells in the meiotic prophase of cell division, they contain considerable quantities of various enzymes and storage yolk protein and are very active in RNA and protein synthesis, though not in DNA synthesis (Gurdon & Wickens 1983). However, although mature *Xenopus* oocytes contain much maternal cytoplasmic mRNA (~70ng), the presence of inhibitory binding proteins largely prevents their translation. It is this inablility to process native mRNA, coupled with the high translational capacity of this self-sustaining cell, which have led to its exploitation as an effective message-dependent translation system for exogenous mRNA and cDNA. Additional attributes such as their robust nature and large size (≤1.3mm diameter) also make them amenable to a series of electrophysiological manipulations.

3.1.2 Dual electrode voltage clamp electrophysiology

Most electrophysiological methods are applicable to oocytes. In the simplest arrangement, the membrane can be penetrated with a single microelectrode and the membrane potential measured. Impalement with two microelectrodes (Figure 3.2) permits current- or voltage-clamp recording

methods, the latter being the most popular. Patch-clamp methods are applied to oocytes in the study of single channels. The whole cell voltage-clamp technique was employed in this study, a procedure which measures the ion flux across the whole of the lipid membrane as electric current, whilst the potential difference (voltage) across the membrane is held under experimental control (Figure 3.2). In the case of LGIC currents, once leakage has been accounted for, the ion flux is only observed on application of agonist molecules to the oocyte which is maintained in physiological buffer. The principles of this technique were first described by Cole in 1949, and extended through studies on squid giant axon (Hodgkin & Huxley 1952).

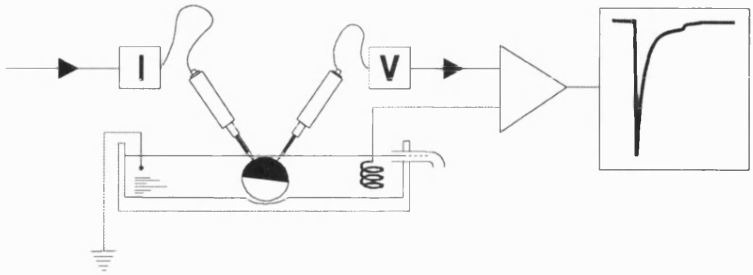

Figure 3.2: Dual electrode voltage-clamp electrophysiology. Recording of the electrical current across the oocyte membrane induced by the bath application of agonists to cells expressing exogenous nACh receptors. A voltage recording electrode (V) inserted in the membrane is used to 'clamp' the membrane potential to the desired value while a second electrode (I) injects the required current into the cell in order to maintain this potential difference. Current injected as a result of the opening of ion channels in the presence of agonist molecules can be recorded - a downward deflection of the activity spike represents the movement of ions into the cell.

3.1.3 The resting oocyte membrane

Microelectrode impalement reveals that the membrane of a healthy oocyte is electrically negative inside relative to the outside by some tens of millivolts. This resting potential (RP) can vary widely among oocytes of different frogs and among frogs from different batches and sources. However, this does not mean that a healthy oocyte may have a RP anywhere between -20 to -90mV (see table 2 of Colman 1986). Several factors may contribute to this discrepancy such as maturity of the cell, the method of its dissection, and others. The membrane of the oocyte possesses an active Na-K pump which is largely responsible for the unequal distributions of ions either side of the semi-permeable membrane. Thus, treatments which affect this pump affect the RP - immediately following manual or chemical defolliculation cells tend to hyperpolarise, but 'repolarise' to less negative values 2h to 48h later (typically -45 to -65mV). These phenomena may be explained by the 'uncovering' of pump sites or their activation due to the increase in $[Na]_{in}$ that accompanies defolliculation. Thus, the observed RP value (E) is maintained largely by the Na-K pump which creates a chemical imbalance either side of the membrane as described by the Nernst equation:

$$E = \frac{RT}{zF.\ln([ion]_o/[ion]_i)} \qquad (1)$$

Many different ionic populations contribute to the potential difference (principally Na^+, Ca^{++}, K^+ and Cl^-) and include those associated with proteins and other organic anions which are trapped inside the cell due to the selective permeability of the membrane.

The appearance of active nicotinic receptors in the membrane permits the inward flow of ions (Na^+, K^+ and Ca^{++}) perturbing the equilibrium. The electric charge that results from the opening of thousands of such channels, driven by the P.D. across the membrane, is detected using electrophysiological methods - Ohm's law states that the current is proportional to the P.D.:

$$I = V / R \qquad (2)$$

When inactive the closed receptors behave as electrical resistors (R). Therefore, the agonist-induced current is proportional to the receptor conductance, G(=1/R), so when the P.D. is held constant (clamped) the current observed results directly from the properties of the predominant receptor population, i.e. ion selectivity, activation and desensitisation properties, gating mechanisms etc. In the whole cell clamp setup, especially with cells as large as oocytes, the membrane capacitance (C, due to ionic charge stored therein) is so large that electronic effects due to it are negligible.

3.1.4 Exploitation of oocytes in the project

In the present study oocytes have been employed as a functional index for the α7 homomeric receptor derived from nAChR of avian brain. Given that there is now a well established background for the use of oocytes in the study of functional neuronal nAChR formed upon injection of certain combinations of cloned subunits from native receptors (rev. Sargent 1993) this system seemed an obvious choice for our first steps into electrophysiological recording. The paucity of αBgt-sensitive functional cholinergic responses in other, biochemical preparations, has required that some confirmation and pharmacological characterisation of a functional homomeric receptor sensitive to α Bgt be undertaken. Additionally, the acquisition of α7 has permitted the study of structure-function relationships with agonist molecules in attempts to identify features of the functional pharmacophore of the neuronal nicotinic receptor.

3.2 Experimental procedures

3.2.1 *Xenopus* oocyte preparation

Animals

Mature *Xenopus laevis* females were kept in groups of up to six animals for at least 3 months in a 12h light:dark cycle at 18°C with access to diced heart or liver on alternate days. On the day of use, animals were killed by decapitation following submersion in iced water for 1h. All ovarian sacs were removed following abdominal incisions. Ovaries were washed in Isolation medium (NaCl 108mM, KCl 2mM, EDTA 0.1mM, HEPES 1mM, pH7.9) where individual lobes were cut away and opened out to expose the oocytes. All procedures were carried out at room temperature under sterile conditions.

Oocyte isolation

Oocytes were washed thoroughly in Isolation medium to remove contaminating proteases from ruptured eggs. Dissection was performed under a binocular microscope in Isolation medium. Individual oocytes were removed from their ovarian envelope using fine watchmakers forceps (Dumont no.5), and transferred to Modified Barth's Solution (MBS; NaCl 88mM, KCl 1mM, HEPES 10mM, $MgSO_4$ 0.82mM, $Ca(NO_3)_2.4H_2O$ 0.33mM, $CaCl_2$ 0.91mM, $NaHCO_3$ 2.4mM, pH7.5). Oocytes used were at stage V or VI of development, characterised by a distinctive boundary between animal and vegetal poles, and were the largest at ~1mm in diameter. Oocytes dissected in this way were generally washed at least twice in MBS and left overnight at 20°C to identify damaged eggs which were apparent as ruptured cells by the following morning. Roughly three times the number of cells to be injected were routinely isolated in order to compensate for such loses and to provide sufficient controls.

3.2.2 Nucleic acid injection

A subclone of α7 cDNA, from which 700 base pairs of 3' untranslated sequence had been deleted, was spliced into the *Xenopus* oocyte expression plasmid bluescript (Bertrand *et al* 1990) to yield the plasmid flip α7Δ. The plasmid was generously donated by Marc Ballivet. The subcloning procedure of this plasmid is explained in section 3.2.5: each generation of clones was equally effective in the *Xenopus* oocyte expression system when compared to the original flip α7Δ plasmid. The Simian Virus 40 (SV40) early promoter controls expression of the α7 gene. Samples of the α7 cDNA were stored at -20°C and thawed on the day of use before dilution in sterile water to a concentration of 250 ng/μl.

Injection needles were pulled on a 763 programmable micropipette puller (Campden Instruments, Loughborough) using 10μl borosilicate capillaries. Tip diameters were typically <10μm. Needles were sealed with mineral oil and cDNA (total volume ~2μl) was drawn slowly into the needle using a Drummond syringe (10μl) secured to a micromanipulator. Approximately 10nl (c. 10^8 copies of DNA) were injected into the oocyte nucleus under binocular magnification.

Incubation

Injected oocytes were transferred to 24 well titre plates, 2-3 oocytes per well containing 2.5ml Incubation medium (containing penicillin-streptomycin 50mgs/ml, gentomycin sulphate 30mgs/ml, and pyruvic acid 2.5mM, in MBS), and incubated at 20°C under sterile conditions - expression levels are very temperature sensitive. Functional receptors (as judged by ACh-induced responses) appeared in the oocyte membrane about two days after injection of cDNA. Incubation medium was replaced every 2-3 days.

3.2.3 Whole cell electrophysiology of injected oocytes

3.2.3.1 Perfusion chamber

Two types of chamber were used for the application of cholinergic drugs during electrophysiological recording of α7 responses, the essential difference being in the volume of perfusion medium in the bath surrounding the oocyte. The initial perfusion chamber (demonstrated in figure 3.3a) comprised a solid perspex block with a conical chamber which was fed with medium from above and evacuated through a capillary at the bottom. The egg rested on a perforated plastic mesh in the bath (volume ~300μl), through which medium freely flowed (enlargement of figure 3.3a) at a rate of approximately 5ml/min - this flow rate maintained mechanical stability of the oocytes and recording electrodes. Whole cell recordings of α7 responses to nicotine for this chamber are represented in figure 3.7. The importance of a smaller volume bath was realised in a second chamber suggested and constructed by Daniel Bertrand. In this setup, bath volume was reduced to 50μl by using a plastic trough in which the oocyte was partially secured in a small recess (Figure 3.3b). Rapid solution exchange was achieved through the close proximity of perfusion inlet and outlet to the oocyte. A desensitisation plateau, not discernible with the previous chamber, was apparent in the α7 response (Figure 3.7). This improved setup was employed for subsequent recordings.

In both of the above cases superfusion was based on gravity flow. Perfusion medium, (degassed MBS containing 0.5μM atropine to block the endogenous muscarinic AChR of the oocyte), was placed above the recording chamber and, as with drug reservoirs, was connected to the chamber via a continuous siliconised rubber tube (1.8mm diameter). Switching between reservoirs of the various drug and perfusion solutions was achieved using a manually operated pinch-valve system. The dead space between reservoir and chamber was kept to a minimum and no mixing between solutions was possible. The outlet from the chamber was a polyethylene tube leading to a trap.

3.2.3.2 Dual electrode voltage-clamp electrophysiology

Current, Voltage and Reference electrodes were pulled on a 763 programmable micropipette puller (Campden Instruments) using GC150TF-10 borosilicate glass capillaries (Clark Electromedical Instruments) and filled with 3M KCl. Electrical connection to the recording equipment was established through silver chloride wire insulated with Teflon. Typical tip resistances were 1-5M Ω, i.e. small enough to inject current effectively and minimise damage to the oocyte.

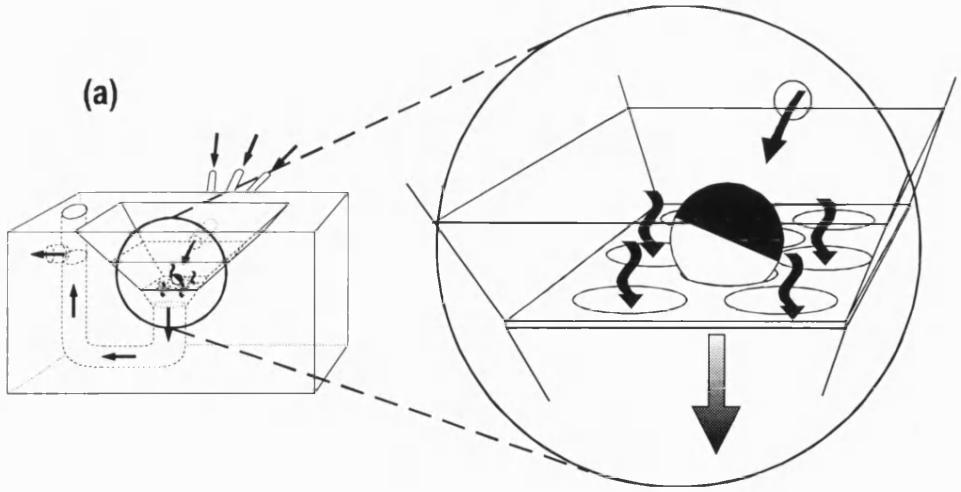

Figure 3.3: Oocyte perfusion chambers used in the application of cholinergic drugs during electrophysiological recording of α7 responses. Initially, experiments were performed using a relatively large volume chamber (300µl) in which the oocyte was supported on a perforated plastic mesh (a). Several such perforations allowed free flow of perfusion medium around the cell at a rate of ~5mls/min. In this configuration the response profile of the α7 homomeric receptor to cholinergic ligands was as demonstrated in figure 3.7a. Later experiments employed a chamber of 1/6th the volume of (a) consisting of a plastic trough mounted in a petri dish (b). In this arrangement the oocyte rested in a small recess in the plastic with medium perfusing horizontally rather than vertically as in (a).

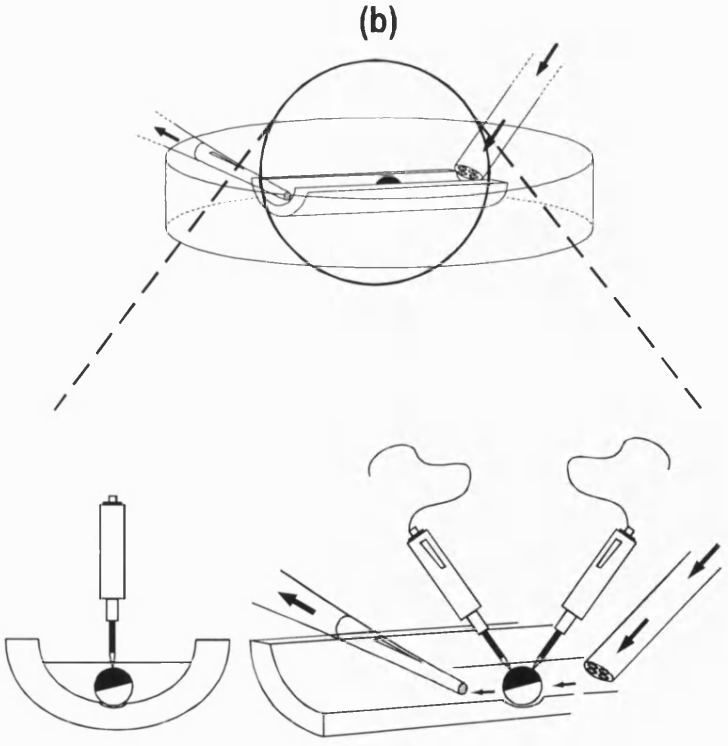

The smaller volume chamber (suggested by Daniel Bertrand) was required to disclose the desensitisation plateau of the α7 response (Figure 3.7b). In both chambers, buffer (MBS containing atropine) and all drugs were applied through a gravity fed perfusion system and removal was aided by a peristaltic pump (a) and tap vacuum (b). Perfusion medium was connected to earth through an agar bridge. (Arrows indicate the direction of flow of the bath applied drugs). Refer also to section 3.2.3.1.

Ligand induced currents were measured using conventional two electrode voltage-clamp. The resting potential of the cell was measured using a recording (Voltage) electrode connected to the input of a VF120 amplifier (Biologic, Herts.). A second (Reference) electrode was connected to a subtractor amplifier where the value of the Reference was subtracted from that of the Voltage. This value was fed into a CA100 clamping amplifier which was used to set the desired clamping potential. The output of this amplifier became the input to a VF180 microelectrode amplifier which was used to inject the required current into the cell to attain the desired clamping potential through a third (Current) electrode. The output of the CA100 clamping amplifier was passed through a filter, a second amplifier and an attenuator, before being displayed using a pen recorder and oscilloscope. The same output was also captured and stored on a DTR1200 analogue-to-digital DAT recorder (Biologic).

For data acquisition, recordings were selected from the DAT tape and fed to an IBM AT compatible computer. Here they were digitised using a data translation (DT2801A) A/D converter activated through the program AQ (Amar *et al* 1991), before being directly stored on the hard disc. The resulting 12-bit binary files were then analysed using the program PAT2L (Amar *et al* 1991) and manipulated using the graphics package SIGMAPLOT version 4.1.

3.2.3.2.1 Current-voltage (I/V) relationships

The I/V characteristics of a ligand induced current were determined by holding the membrane potential at a constant voltage and perfusing ligand to evoke a current response. The holding voltage was then stepped to new values and the drug applied at each step. A minimum wash period of 5min was allowed between each 3s drug pulse (see section 3.2.3.2.2). The I/V curve was obtained by plotting the amplitude of the ligand-evoked currents as a function of the holding voltage.

3.2.3.2.2 Drugs and their application

Stocks solutions (made up as described in section 2.2.9) were stored in aliquots at -20°C and thawed immediately prior to use when they were diluted as required in MBS containing 0.5μM atropine. All solutions were retained on ice prior to use in the perfusion system. Control samples of aqueous ethanol and DMSO were used to confirm that these solvents had no direct effect.

Generally drug was perfused through the chamber in which the egg was being monitored for 3s. At lower concentrations of agonist, perfusion times were sometimes extended to 5s in order that slower onset responses might be observed. The α7 receptor is fully activatable approximately 3min after a 3s desensitising concentration of drug so to ensure complete recovery the test oocyte was washed with MBS for a minimum period of 5min under such conditions.

Inhibition studies with αcobratoxin (αCbt - a close analogue of αBgt) and Methyllycaconitine (MLA) required that the antagonist be incubated with the egg in the chamber for a period of up to 45min for αBgt or 15min for MLA, before perfusion of the activating ligand. In order that antagonist would not be washed off during agonist perfusion, the same concentration of the antagonist was included in

the agonist solution. Again, stimulations were of 3s duration, immediately after which the time for full or partial recovery of the α7 response was recorded following application of the same agonist.

3.2.4 Data analysis

α7 dose response curves were constructed for the various ligands by normalising currents to the largest induced current for a particular ligand on a specific oocyte. The peak heights of all the activation spikes for a particular ligand were measured directly from the program PAT2L (Amar *et al* 1991) and converted into nA currents, the values of which were used to generate the response curves at the various ligand concentrations. Curves were iteratively fitted to, and values for the EC_{50} (half maximal activation of the receptor) and Hill coefficient (η_H) were calculated, according to the non-linear Hill equation:

$$Y=1/(1+(EC_{50}/X)^{\eta_H}) \qquad (3)$$

where X= agonist concentration and Y=% of maximum response. Current responses to 25μM (-)-nicotine were used to standardise oocyte responses.

3.2.5 Molecular biology

3.2.5.1 Transformation of bacterial cells

Escherichia coli bacterial cells (stored in glycerol at -20°C) were cultured overnight at 37°C in Luria Broth (LB: NaCl 10g, yeast extract 5g and tryptone 10g in 1l sterile water, pH7.5). Enriched LB was inoculated with this culture and cells grown with vigorous shaking for 3h before being chilled on ice (10min). Cells were harvested by centrifugation (4000g, 5min, 4°C) - surplus bacterial cells were stored in a 15% glycerol solution at -20°C - and permeabilised by resuspension in an ice-cold, sterile solution (pH8) of 50mM $CaCl_2$ (0.5vol of original culture, 30min, 4°C). This procedure was repeated and the suspension retained on ice for at least 1h.

The bluescript plasmid incorporating the α7 cDNA (in sterile water) was mixed (~300ng/ml) with this solution of permeabilised cells (4°C, 30min). The reaction mixture was then placed in a 42°C water bath for 3min after which time 1ml of LB was added. Cells were then maintained at 37°C for 45min with occasional gentle mixing.

Successful transformants were selected by their resistance to ampicilin, the gene for which is included in the bluescript plasmid. Cells treated as above were spread on selective media (LB containing 1.5%(w/v) agarose and 100μg/ml ampicilin) until absorbed into the agar, inverted and maintained at 37°C (12-16h). Plates were stored at 4°C. Competent cells, distinguishable by their red colour, were carefully removed from plates into ampicilin-containing LB (one colony per 3ml LB) and these colonies incubated overnight in a 37°C shaker.

3.2.5.2 Transformant nucleic acid viability

Cell lysis using alkali

Successful α7 gene transformants were lysed and subjected to nucleic acid digestion with restriction enzymes. Competent cells were harvested by centrifugation (4000g, 10min, 4°C) of 1ml samples from a selection of colonies. Pelleted cells were washed in 150μl ice-cold GTE (Glucose 50mM, TRIS 25mM (pH8), EDTA 10mM), and kept on ice for ~10min before lysis with 300μl of a mixture of SDS (1%(w/v)) and NaOH (0.2M). The mixed solution was kept on ice for 10min. Addition of 200μl of ice-cold 5M KAc (pH4.5 in 3M acetic acid) and thorough inversion precipitated the larger cell remnants (4°C, 10min).

Isolation of plasmid nucleic acid

Cellular DNA and bacterial debris was spun down at high speed (20,000rpm, 4°C, 20min) leaving the lighter plasmid DNA in the supernatant. Extraction of the latter was achieved using isopropanol (0.6 vols) which was gently mixed with the supernatant (15min, 4°C). Plasmid DNA was recovered from the solvent layer by precipitation with absolute ethanol (2 vols, 4°C), spun down (12000g, 30min, 20°C) and the pellet washed with 70% ethanol before eventually being dried (vacuum dessicator) and resuspended in ~50μl TE (Tris 10mM, EDTA 1mM, pH8) containing RNAse (1mg/ml).

Restriction enzyme digestion

The α7 sequence is flanked by a BamH1 and HindIII site in the bluescript plasmid. Digestion with these enzymes should yield two fragments of lengths 1830 and ~5000 bp corresponding to α7 and bluescript respectively. These enzymes require specific buffers in order to be maximally effective so digestion was two-step, requiring ethanol precipitation in between. For each of the colonies under scrutiny, 5μl of the corresponding DNA (in TE+RNAse) was mixed with either BamH1 or HindIII (1μl (1unit) stored at -20°C), the appropriate buffer (2μl, commercial preparation) and made up to 20μl with sterile water. The reaction was incubated at 37°C for 1h.

The reaction was stopped by the addition of 0.5M EDTA (pH7.5) to a final concentration of 10mM. Fragmented DNA was precipitated by the addition of 3M NaAc (1.1vol) and cold absolute ethanol (2.5vols), followed by cooling to -20°C for 30min. Precipitate was centrifuged (14,000rpm, 20min, 4 °C), and the pellet washed in 70% ethanol. Following recentrifugation the DNA was dried and cut with the second enzyme using the appropriate buffer, as before.

Digestion analysis on agarose gel

The double-digested DNA pellet was resuspended in 10μl Gel Loading Buffer (GLB; glycerol 30%(v/v), xylene cyanol 0.25%(v/v), bromophenol blue 0.25%(v/v)) and run on a 1% agarose gel along with λHindIII markers, at a P.D. of ~5V/cm for 30min. Gel running buffer, TBE (TRIS 89mM, borate 89mM, EDTA 2mM), included ethidium bromide (0.5μg/ml).

3.2.5.3 Increasing nucleic acid yield (Maxi-prep)

Essentially this involved scaling up the quantities in the method previously described (section 3.2.5.2). Transformants were chosen from the colonies identified in the 'mini-prep.' whose digestion products of the bluescript plasmid were of the correct size. Samples (500µl) were grown-up overnight at 37°C in sterile LB (800ml), containing ampicillin (100µg/ml). Cells were harvested by centrifugation (4000g, 15min, 4°C) and the pellet resuspended in GTE (10ml/500ml original culture). Cells were lysed by the addition of lysis buffer (2 vols: NaOH 0.2M, SDS 1%(w/v)) with frequent, gentle inversion on ice for ~15min, prior to the addition of KAc (0.5vol: 5M). This solution was thoroughly mixed and retained on ice for 10min. The pellet produced on centrifugation (Beckman SW27 20,000rpm, 10min, 4°C) was discarded and the plasmid DNA in the supernatant precipitated in ice-cold isopropanol (0.6vols, 15min, 4°C). Recentrifugation (10,000rpm, 30min, 4°C) following ethanol extraction produced the DNA pellet which was vacuum dried before being resuspended in sterile water (8ml/500ml original culture). RNA material was digested by addition of RNAse (5µg/ml) and incubation at 37°C for 20min.

Caesium chloride purification of plasmid DNA

Centrifugation to equilibrium was performed in gradient of CsCl (1g/ml of DNA solution) including ethidium bromide (600µg/ml). The thoroughly mixed CsCl/DNA solution was sealed into 5ml ultracentrifuge tubes (Beckman 50 rotor). Centrifugation was carried out in a fixed angle rotor at 55,000rpm at 20°C for 18h.

The plasmid DNA containing the α7 gene appeared as the lower band and was removed under UV light using a hypodermic syringe. DNA was pooled from all tubes. Ethidium bromide was extracted in isoamyl alcohol (1vol) following thorough mixing and centrifugation (1500g, 3min, 20°C). The aqueous phase containing plasmid DNA was removed and the extraction repeated until the pink colour disappeared. CsCl salt was removed following precipitation of DNA (-20°C in ethanol (4vols)) leaving CsCl in solution. Centrifugation (12,000rpm, 30min, 4°C) pelleted the DNA, which was vacuum dried, resuspended in sterile water and transferred to an eppendorf for reprecipitation in NaAc (0.1 vol, 3M) and ice-cold absolute ethanol (2 vol). Recentrifugation (12,000rpm, 10min, 4°C) pelleted the DNA which was dried, washed and precipitated as before to remove any remaining CsCl. The final pellet was washed with 70% ethanol, vacuum dried and resuspended in ~200µl sterile water.

Digestion products

As previously, in order to determine whether the plasmid DNA contained the α7 gene, samples (serially diluted) were subjected to restriction enzyme digestion with BamH1 and HindIII consecutively - see section 3.2.5.2.

3.2.6 Spectrophotometric assessment of nucleic acid purity

DNA purity and concentration was determined spectrophotometrically. The optical density at 260nm and 280nm was measured for dilutions of the plasmid DNA solution following standardisation

with sterile water - a complete sweep was made between λ240-320. The OD_{260}/OD_{280} ratio was used to determine the purity of the DNA product. Pure preparations of DNA have a ratio of 1.8, contaminants will significantly reduce this value. An OD of 1 at λ260 corresponds to approximately 50μg/ml for double-stranded DNA.

3.3 Results

3.3.1 Endogenous cholinergic receptors in the oocyte membrane

Healthy oocytes prepared as described in section 3.2.1 recorded resting membrane potentials of between -30mV to -80mV on microelectrode impalement - potentials did not seem to be substantially affected by nuclear injection of exogenous nucleic acid. Responses resulting from the activation of endogenous muscarinic receptors by ACh on denuded oocytes (Figure 3.4a) were generally small (≤100nA), and characterised by slow activation to a prolonged maximum response. The response persisted for the period of agonist application and deminished to basal levels upon removal of the stimulus. This reflects the observations of Kusano and co-workers (1977) who first reported cholinergic responses in the oocyte. Studies since then have revealed more complex response patterns associated with this G-protein coupled receptor, involving multiple depolarisation and/or hyperpolarisation phases (rev. Dascal 1987). Inclusion of 0.5μM atropine in the perfusion buffer abolished all responses to cholinergic ligands (Figure 3.4b), confirming the muscarinic nature of this endogenous receptor. No antagonism was observed with nicotinic antagonists (not shown).

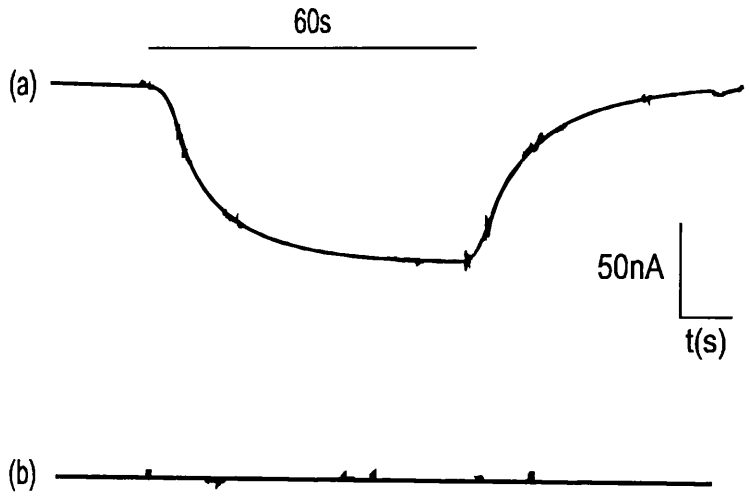

Figure 3.4: Endogenous muscarinic response of the oocyte. Representative trace demonstrating the inward current evoked on application of 10μM ACh (60s) to a denuded oocyte (a). The uninjected cell (stage V) was tested the day after dissection using dual electrode voltage clamp (see section 3.2.3.2). Inclusion of 0.5μM atropine in the perfusion buffer abolished all endogenous responses to cholinergic drugs on the same cell (b). Not all cells were assessed for muscarinic activity, though currents were detectable in the majority (8/13 cases) taken from various oocyte batches (3).

3.3.2 Characteristics of the reconstituted homomeric receptor

Digestion of the bluescript vector with BamH1 and HindIII was used to identify the presence of α7 cDNA transformants. Fragments corresponding to α7 (~1800) and bluescript (~5000) were detected on agarose gels. Figure 3.5a shows the digestion products from various bacterial colonies - λ/HindIII markers verified the presence of the α7 fragment in the majority of cases. In the case shown here the colony in lane six was used to perform a maxiprep, the digestion products of which are shown as serial dilutions in figure 3.5b. DNA yield was generally high (>10mg/ml) and showed little contamination (A_{260}/A_{280}>1.8) following spectrophotometric assessment (Figure 3.5c).

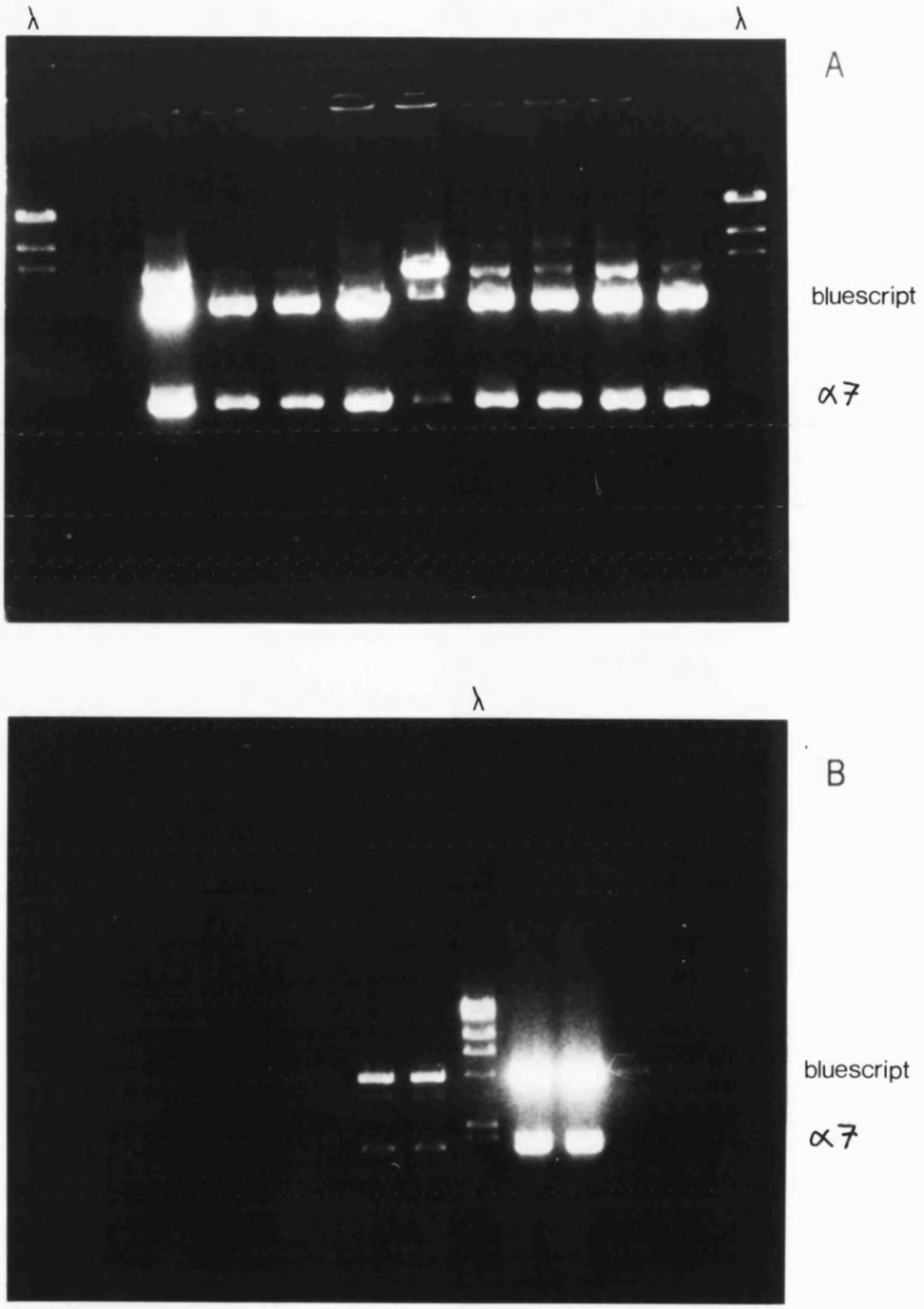

Figure 3.5: Transformation of bacterial cells with vector containing α7 cDNA. (a) DNA fragments produced following digestion of the isolated vector from transformed cells with BamH1 and HindIII restriction enzymes - the 9 central lanes (flanked by λ markers) each represent a separate bacterial colony prepared as described in section 3.2.5. Serial dilutions of the maxiprep products revealed the strong presence of the α7 gene (b) - in this case the yield was >10mg/ml and the 260nm:280nm ratio was 1.89 (c). Aliquots of the α7 cDNA were stored in sterile water at -20°C.

C

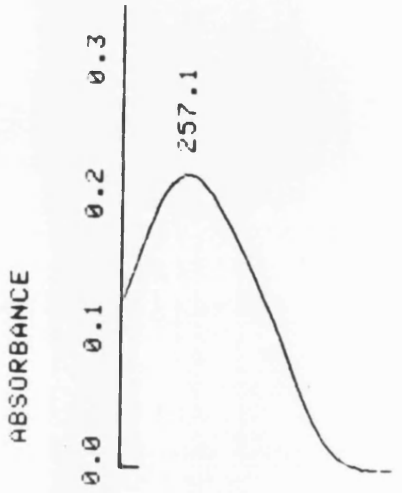

Following nuclear injection of α7 cDNA into *Xenopus* oocytes, responses to (-)nicotine could be recorded from >50% of eggs after 2 days. Large currents, typically 0.2-2.0μA, were recorded on application of saturating doses (high micromolar concentrations) of (-)nicotine to cells held at -70mV (Figure 3.6a). This holding potential was sufficiently far removed from the reversal potential to observe consistent, robust currents evoked by agonist stimulation, and ensured the physiological stability of the oocyte during prolonged periods of examination. Consequently -70mV became the standard holding potential of subsequent recordings. Cells injected with sterile water alone were insensitive to all ligands.

Receptor activation at low doses of (-)nicotine was slow with little or no desensitisation for agonist applications up to 10s duration (Figure 3.6b). At higher concentrations of (-)nicotine, activation rates were faster and displayed rapid desensitisation within the 3s application time, in keeping with published results for the same reconstituted homomer (Couturier *et al* 1990a). The importance of rapid application and removal of agonist is demonstrated in figure 3.7. An initial perfusion chamber with a volume of ~300μl (see section 3.2.3.1 and figure 3.3a) detected the two exponential components to the desensitisation phase of the α7 homomeric receptor (Figure 3.7a). Replacement of this chamber with one of smaller volume (~50μl), in addition identified a plateau representing incomplete desensitisation of the receptor population (Figure 3.7b), which generally occurred at levels below 10% of the peak response, and was further reduced at saturating agonist concentrations (Figure 3.7c). Basal current levels were recovered on removal of the agonist from the bath. The desensitisation plateau was observed for all agonists studied. Initial data was obtained with the larger chamber but subsequent experiments were performed with the smaller when its advantages had been realised.

3.3.3 Pharmacological properties of the reconstituted α7 protein complex

3.3.3.1 Antagonism of nicotine-induced responses

Currents evoked by (-)nicotine (40μM) were completely abolished following incubation (30min) of α7 injected oocytes with 10nM αcobratoxin (αCbt: Figure 3.8a) a toxin closely related to αbungarotoxin. Oocytes from 3 further animals were similarly sensitive to this toxin. The pseudo-irreversible nature of the inhibition was demonstrated by the inability of (-)nicotine, and other cholinergic agonists (not shown), to stimulate the receptor up to 45min after washing. Methyllycaconitine (MLA: 1nM) was also able to completely block nicotine-evoked currents (Figure 3.8b), following a 15min oocyte incubation period. Inhibition was reversible with full recovery of the response after ~30min washout. An inhibition-response curve for MLA was constructed (Figure 3.8c) by immediately measuring the extent to which the nicotine (25μM, 3s) induced response was depleted following incubation (15min) with increasing concentrations of MLA. Oocytes were washed (≥30min) following inhibition, prior to the application of consecutive standardising (-)nicotine pulses (40μM, 3s), another wash (10min), and subsequent incubation (15min) with a higher concentration MLA. Agonist application (3s, containing the same concentration of MLA as in the bath) was immediately after the incubation period. Peak heights were used to plot an inhibition curve of the 25μM (-)nicotine α7 response by MLA, with an IC_{50} value of 1.8±2.2pM.

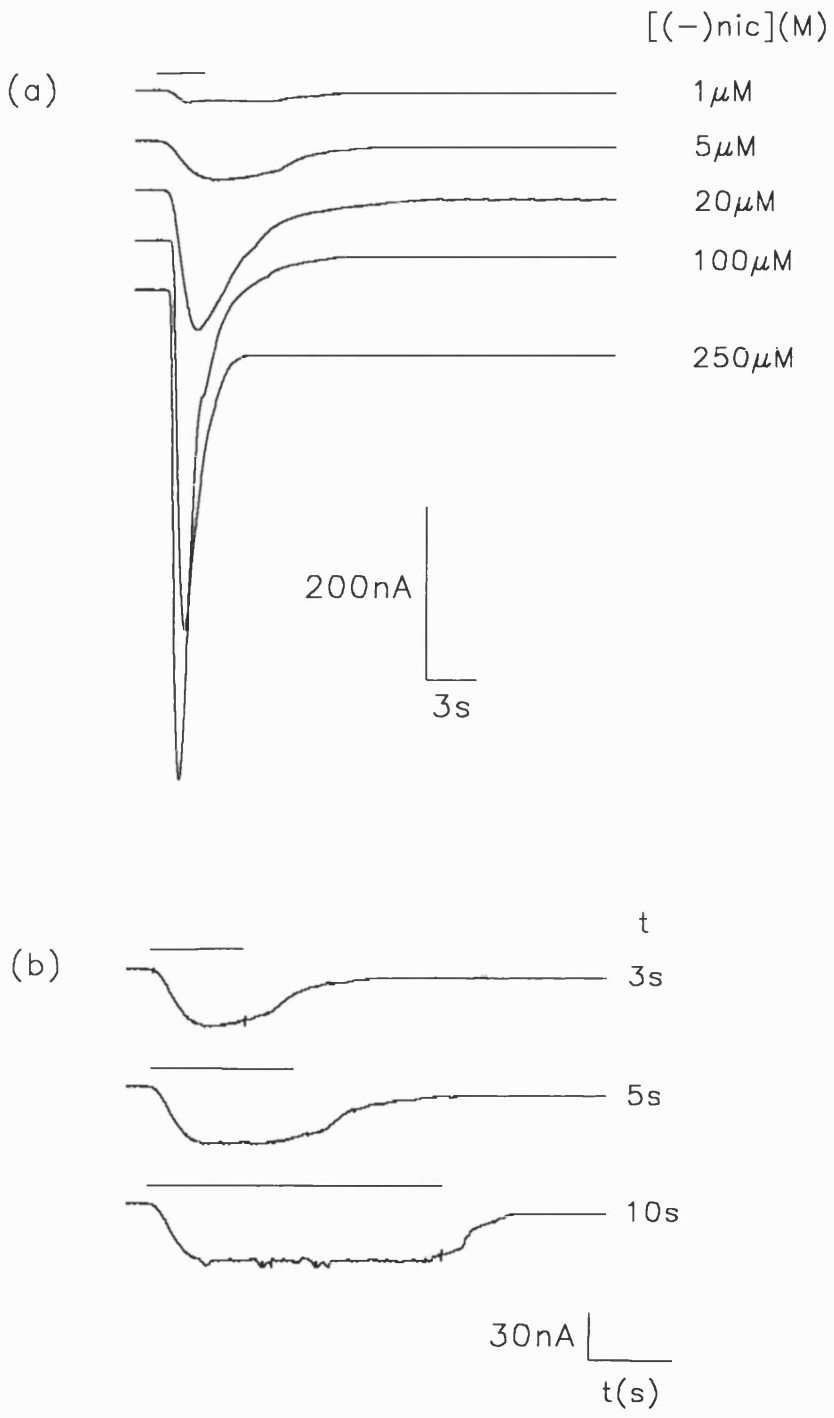

Figure 3.6: Cholinergic activation of the α7 receptor expressed in *Xenopus* oocytes. Superimposed traces of inward currents elicited by 3s pulses of increasing concentrations of (-) nicotine are indicated (a). Oocytes, injected with ~2.5ng of α7 cDNA four days previously, were rested for 10min between each agonist pulse to allow full recovery from desensitisation, V_H=-70mV. Little or no desensitisation was observed in response to low concentrations (3μM) of (-)nicotine applied to the same cell (b).

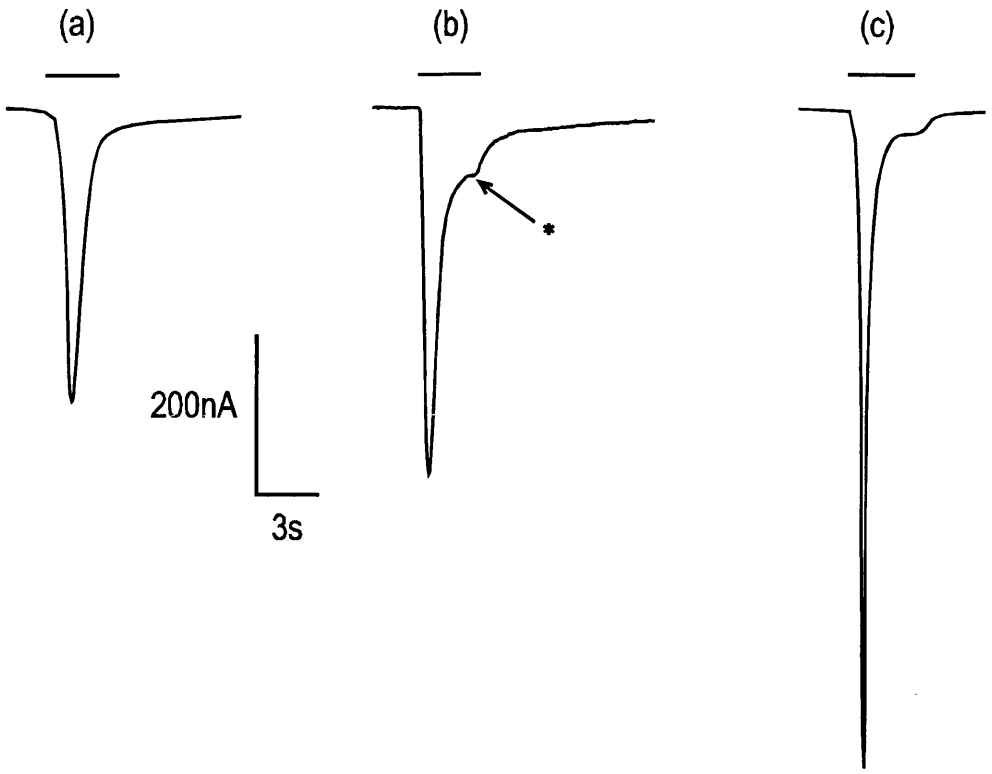

Figure 3.7: Desensitisation of the α7 response. Inward currents were recorded from oocytes perfused with 25μM (-)nicotine (3s), in a chamber (Figure 3.3a) of ~300μl volume (a). Agonist evoked currents constituted rapid activation and desensitisation phases, occurring within the 3s application time. A subsequent perfusion chamber (Figure 3.3b), 50μl volume, revealed a desensitisation plateau (b,*) which persisted until agonist (25μM (-)nicotine) was removed. The position of the plateau from basal level, relative to the current peak height, was reduced on application of saturating agonist doses (c).

3.3.3.2 Classical agonists

Several agonists were investigated for their ability to activate nicotinic currents in the oocyte resulting from the presence of the α7 homomer. In each case a range of agonist concentrations were tested on a single oocyte and dose-response curves of peak currents, normalised to (-)nicotine (25μM), were averaged from several such experiments on different batches of oocyte (Figure 3.9: Table 2.1). (-)Nicotine elicited half-maximal stimulation (EC_{50}) of the expressed α7 receptor at a concentration of 24μM. Nicotine stereoselectivity was not as pronounced in this functional system as in competition binding, in that the (+) enantiomer was only two times less potent (EC_{50}=45μM) than the (-) form. Experiments using (+) and (-) enantiomers on the same oocytes verified this.

(-)Cytisine was more than 4-fold more potent than (-)nicotine (EC_{50}=5.6μM), whereas ACh (EC_{50}=320μM) was the least potent of these agonists, giving a potency rank order of (-)cytisine>(-)nicotine>(+)nicotine>ACh at the α7 receptor. Normalisation of responses to 25μM (-)nicotine revealed that maximal responses resulting from application of cytisine were smaller than those of

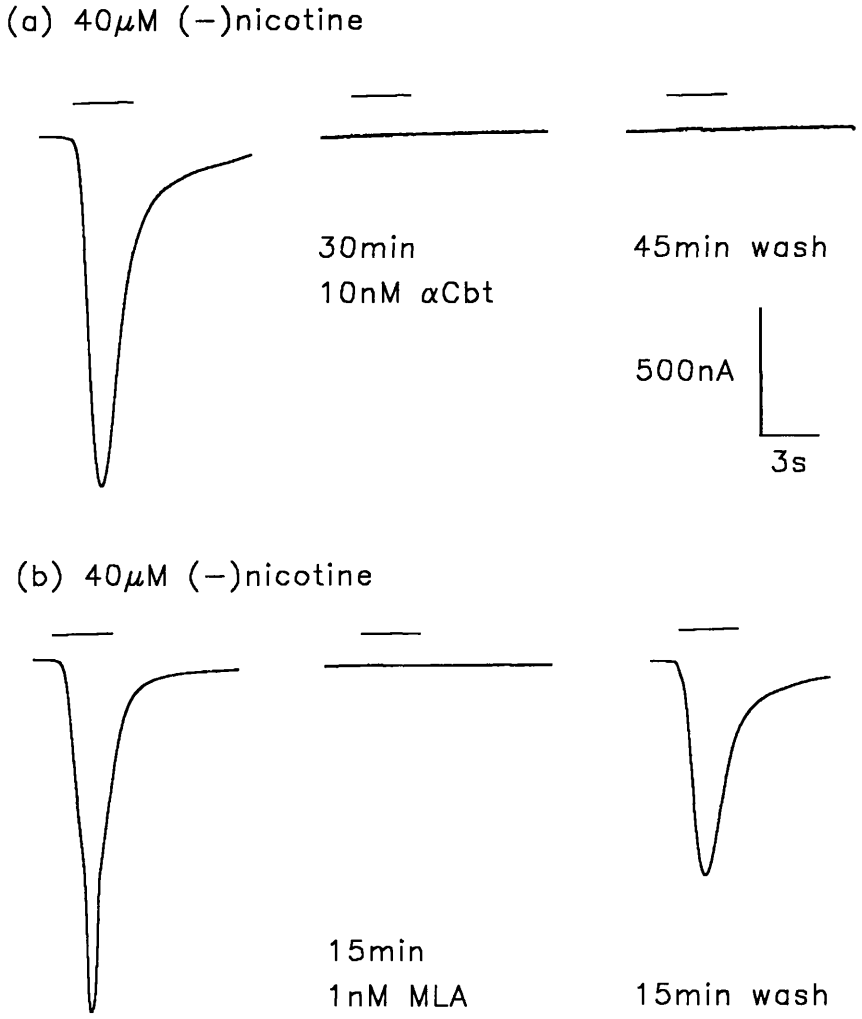

Figure 3.8: α7 channels are functionally blocked by αcobratoxin (αCbt) and methyllycaconitine (MLA). Responses of α7 injected oocytes to 40μM (-)nicotine were completely abolished after incubation (30min) with 10nM αCbt (a). No recovery was seen up to 45min after washing. Incubation (15min) of an independent oocyte with 1nM MLA also blocked currents evoked by 40μM (-) nicotine (b).

Roughly 60% recovery was observed after 15min washing, with full recovery after 30min. Inhibition of responses to 25μM (-)nicotine by various concentrations of MLA were assessed for several (n=6) oocytes from different batches. Data points (±SEM), representing the inhibition curve (c), were curve-fitted using the non-linear Hill equation (see section 3.2.4), producing an IC_{50} value of $1.8 \pm 2.2 \times 10^{-12}$M ($n_H$=0.51). V_H=-70mV for all experiments.

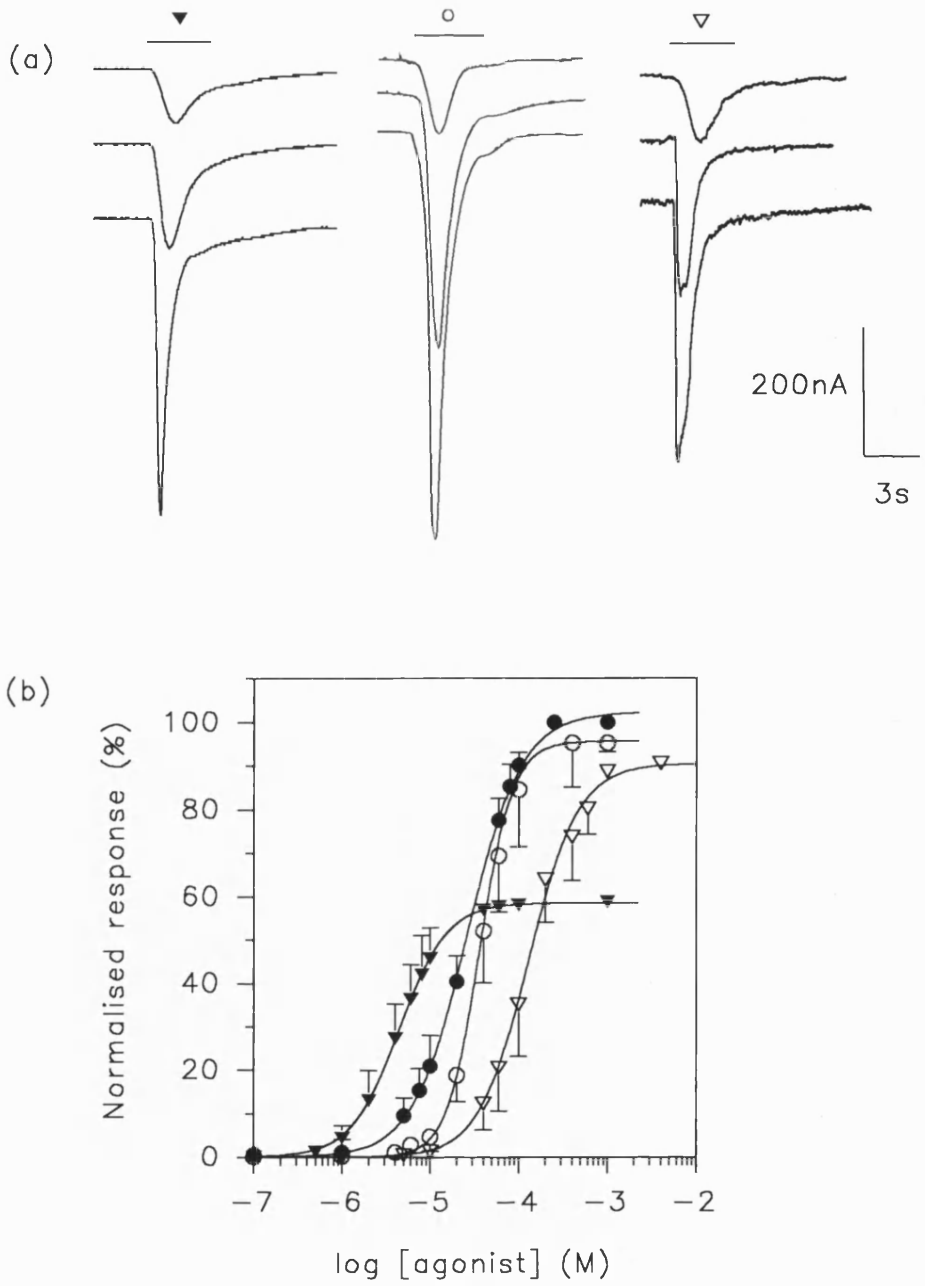

Figure 3.9: Dose response profiles for classical agonists activating the α7 receptor. Superimposed inward currents recorded from individual oocytes exposed to 3s pulses of increasing concentrations of agonist (a): (-) cytisine (▼), (+)nicotine(○) and ACh(∇) - see figure 3.6a for (-)nicotine(●) - ≥5min washing intervals between consecutive pulses were sufficient for full recovery from desensitisation, V_H=-70mV. Dose response curves (b) were calculated by normalisation of responses to the maximum peak height for data from at least three oocytes. Curves were subsequently normalised against (-)nicotine (25μM) applied to the same oocyte. (A more quantitative determination of agonist efficacies was later determined - see section 3.3.4). Symbols represent mean data points with SEM indicated by vertical bars. Lines represent the theoretical dose response curves fitted to the data points using the non-linear Hill equation (see section 3.2.4). EC_{50} values derived from the analysis are recorded in table 2.1.

Ligand	EC_{50} (M), α 7 (#)	n_H	Relative potency (EC_{50})	EC_{50}/K_i	Relative efficacy (%)
(-)nicotine	$2.4 \pm 0.7 \times 10^{-5}$ 4	1.4 ± 0.1	1	24	100
(+)nicotine	$4.5 \pm 1.0 \times 10^{-5}$ 3	2.5 ± 0.7	0.53	0.9*	95.2 ± 1.2
cytisine	$5.6 \pm 1.3 \times 10^{-6}$ 7	1.9 ± 0.2	4.3	2.2	58 ± 6.2
acetylcholine	$3.2 \pm 1.5 \times 10^{-4}$ 5	1.8 ± 0.3	0.08	29	91.5 ± 6.8
DMPP	$6.4 \pm 2.7 \times 10^{-5}$ 7	2.0 ± 0.2	0.37	16.8	20.9 ± 3.9
AMP.MeI	$1.7 \pm 0.3 \times 10^{-4}$ 5	1.3 ± 0.1	0.14	9.0	65.2 ± 5.1
AMP.HCl	$>10^{-3}$ 2	-	-	-	-
(+)anatoxin (AnTx)	$5.8 \pm 0.9 \times 10^{-7}$ 5	2.6 ± 0.3	41	1.1	111.2 ± 2.6
(±)HomoAnTx	$7.2 \pm 5.5 \times 10^{-7}$ 3	0.83 ± 0.1	33	2.1	102 ± 3.4
(±)IsopropylAnTx	$6.6 \pm 0.2 \times 10^{-7}$ 3	7.2 ± 0.3	36	5.5	95.4 ± 6.4

Table 2.1. Pharmacology of the reconstituted α7 homomeric receptor in *Xenopus* oocytes. EC_{50} values for various agonists activating the receptor were calculated using several oocytes (#) from independent animals more than 2 days after nuclear injection of α7 cDNA. Data were curve-fitted to the non-linear Hill equation (see section 3.2.4). Relative efficacies were determined following successive applications of the various agonists to the same oocyte (see section 3.3.4). EC_{50}/K_i ratios were calculated using K_i values from section 2.3.5, except *(Wonnacott 1986), at the [^{125}I] αBgt binding site.

nicotine and ACh - this discrepancy in efficacy was further investigated (see section 3.3.4). Hill slopes for all agonists were greater than one (Table 2.1), consistent with the binding of more than one agonist molecule for activation of the homomeric protein. (+)Nicotine produced a notably steeper activation curve (n_H=2.5±0.7).

3.3.3.3 Piperazine based compounds as agonists

The dose-response curve for DMPP (Figure 3.10), gave an EC_{50} of 64μM (Table 2.1), a potency intermediate to nicotine and ACh. Acetylated piperazines were less potent than DMPP, especially the monomethylated AMP.HCl which failed to elicit any response of the reconstituted protein up to 1mM concentration. The dimethylated analogue, AMP.MeI, produced an EC_{50} of 170μM, giving a potency rank order for these compounds in line with the competition binding data, namely: DMPP>AMP.MeI>>AMP.HCl. Limited availability and poor solubility of AMP.MeI precluded investigation above 1mM, therefore the curve fit may be underestimated. Significant differences were observed in the extent to which these ligands were able to activate α7 relative to nicotine, most noticeably DMPP, which was considerably less efficacious than nicotine - see also section 3.3.4. Hill numbers (Table 2.1) were greater than unity, indicative of more than one binding site.

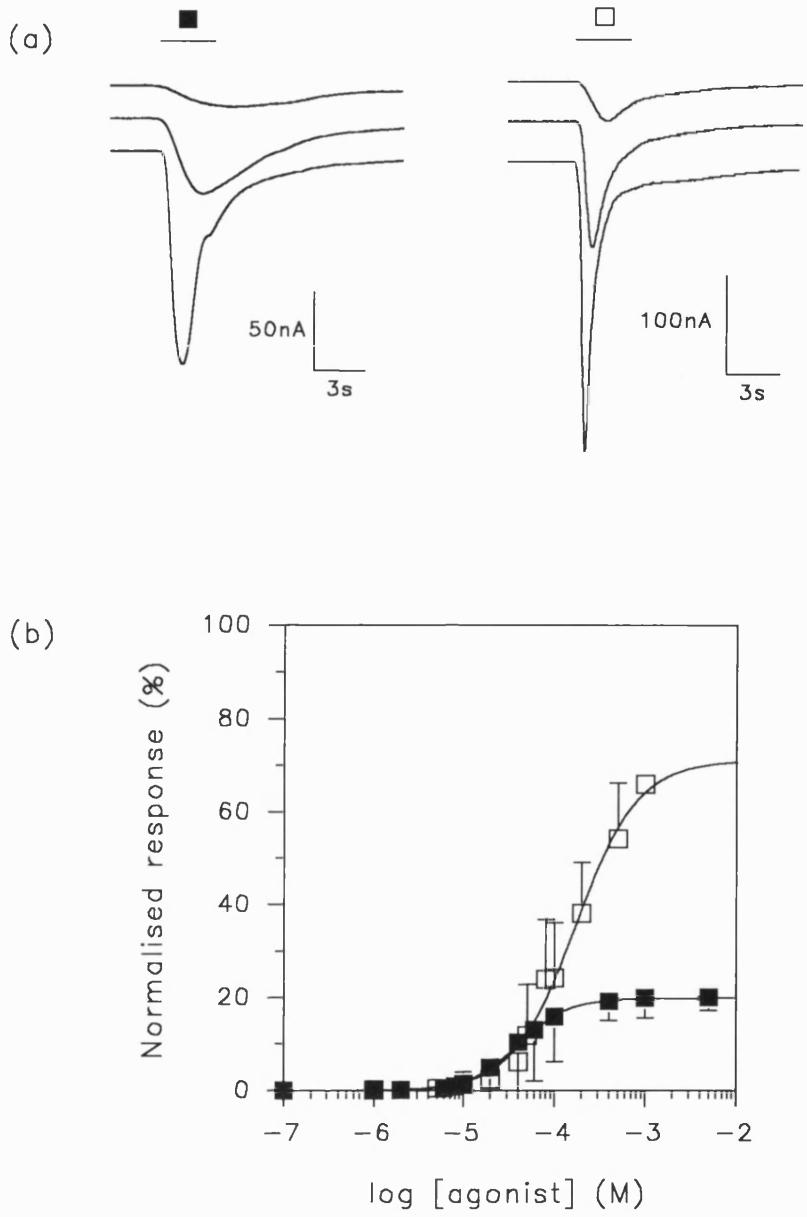

Figure 3.10: Activation of α7 nAChR by piperazine based compounds. Superimposed inward currents recorded from individual oocytes exposed to 3s pulses of increasing concentrations of agonist (a): DMPP(■) and AMP.Mel(□) - ≥5min washing intervals between consecutive pulses were sufficient for full recovery from desensitisation, V_H=-70mV. Dose response curves (b) were calculated by normalisation of responses to the maximum peak height for data from at least three oocytes. Curves were subsequently normalised against (-)nicotine (25μM) applied to the same oocyte. Symbols represent mean data points with SEM indicated by vertical bars. Lines represent the theoretical dose response curves fitted to the data points using the non-linear Hill equation (see section 3.2.4). EC_{50} values derived from the analysis are shown in table 2.1.

3.3.3.4 Anatoxin-a related compounds

(+)Anatoxin-a (AnTx) was clearly the most potent of the agonists tested at the α7 receptor with an EC_{50} value of 0.58μM (Table 2.1), some 550-fold more potent than ACh. Racemic preparations of the alkyl-modified side chain variants homoanatoxin-a (HomoAnTx) and Isopropylanatoxin-a (IsopropylAnTx) were equipotent agonists of the receptor (Figure 3.11), with EC_{50} values of 0.72 and 0.66μM, respectively. This reflects the competition binding data. (±)IsopropylAnTx, like (+)AnTx, consistently produced very rapid and full (relative to nicotine) activation of α7, with Hill coefficients in excess of 2 (Figure 3.11: Table 2.1). Higher concentrations (≥3μM) of IsopropylAnTx produced smaller currents resulting in a bell-shaped dose-response curve (Figure 3.11b). HomoAnTx, although equally efficacious (see section 3.3.4) produced a shallower dose response curve (n_H=0.7).

The overall potency rank order of all agonists at the functional homomeric α7 receptor was;

AnTx=HomoAnTx=IsopropylAnTx>>cytisine>(-)nicotine>(+)nicotine>DMPP>AMP.MeI>ACh>>AMP.HCl.

3.3.4 Apparent efficacies of the α7 agonists

Normalisation of piperazine dose-response data with respect to (-)nicotine (Figure 3.10), revealed the inability of DMPP to activate the α7 receptor to the same extent as (-)nicotine, despite their comparable potency (Table 2.1). Similarly poor activation of α7 channels was also noted for this drug by Bertrand and co-workers (1992). Lower efficacy was also evident for the structurally related compound AMP.MeI, though to a lesser extent. Similar observations were made with cytisine (Figure 3.9). In an attempt to establish the apparent efficacies of all agonists, relative to nicotine, a maximally effective dose of each agonist was applied consecutively to the same oocyte (Figure 3.12) - data for anatoxin-a analogues were obtained independently but also normalised to nicotine. These experiments corroborated the relative efficacies of agonists indicated by the mean dose-response curves. Agonists which showed reduced efficacy were cytisine (50% of (-)nicotine response), DMPP (20%) and AMP.MeI (60%). Limited availability and low solubility of AMP.MeI precluded investigations above 1mM, so 60% could be an underestimate (Amar *et al* 1993).

All other agonists, namely: AnTx, HomoAnTx, IsopropylAnTx, (+)nicotine and ACh, were able to activate the α7 receptor to comparable extents (Figure 3.12). Efficacy comparisons were also carried out at EC_{50} concentrations of the agonists. These experiments confirmed that AMP.MeI is at least three times more efficacious than DMPP, and verified the reduced efficacy of (-)cytisine.

3.3.5 Electrophysiological properties of the α7 receptor

The relationship between holding potential (V) and the extent of the agonist evoked current (I),was determined as described in section 3.2.3.2.1. Each of the agonists was applied at its approximate EC_{50} concentration as the membrane potential was stepped between -120mV and +40mV, in 10-20mV increments (Figure 3.13). The α7 receptor demonstrated the same relationship for all agonists, namely a strong linear dependence of current responses with membrane potential between -120mV and about -40mV. Strong inward rectification of the receptor was observed at more depolarised potentials, persisting up to +30mV, with no apparent reversal of current.

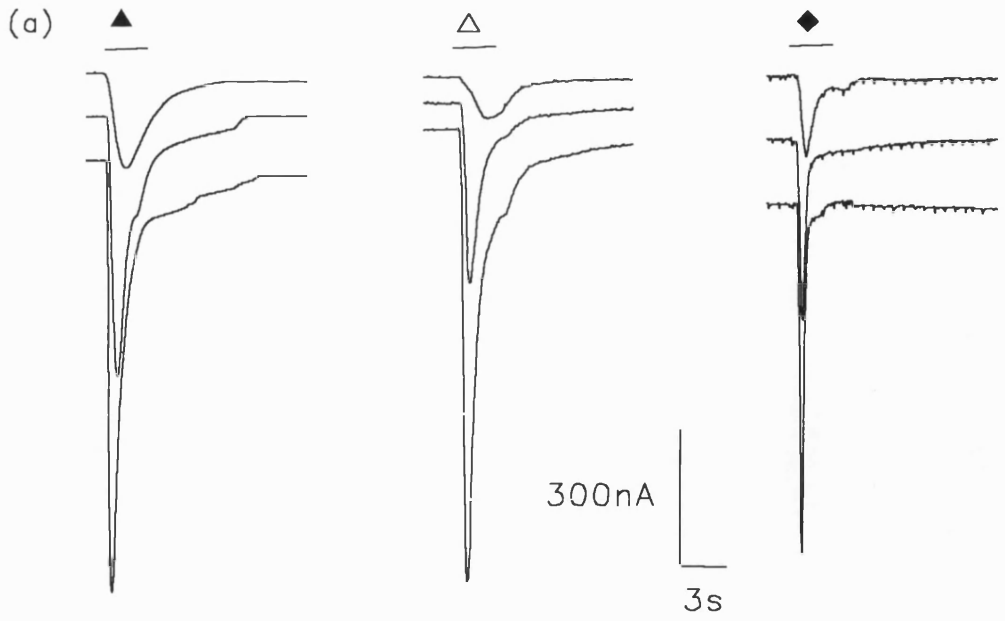

Figure 3.11: (+)Anatoxin-a and alkyl-modified side chain variants as agonists of the α7 receptor. Superimposed inward currents recorded from individual oocytes exposed to 3s pulses of increasing concentrations of agonist (a): (+)AnTx(▲), (±)HomoAnTx(Δ) and (±)IsopropylAnTx(◆) - ≥5min washing intervals between consecutive pulses were sufficient for full recovery from desensitisation, V_H=-70mV. Dose response curves (b) were calculated by normalisation of responses to the maximum peak height for data from at least three oocytes. Curves were subsequently normalised against (-)nicotine (25μM) applied to the same oocyte. Symbols represent mean data points with SEM indicated by vertical bars. Lines represent the theoretical dose response curves fitted to the data points using the non-linear Hill equation (see section 3.2.4). EC_{50} values derived from the analysis are shown in table 2.1.

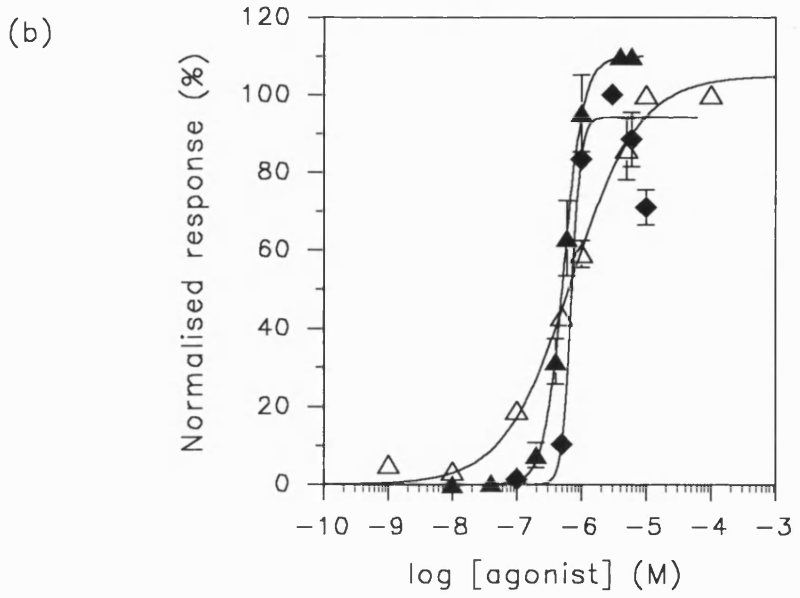

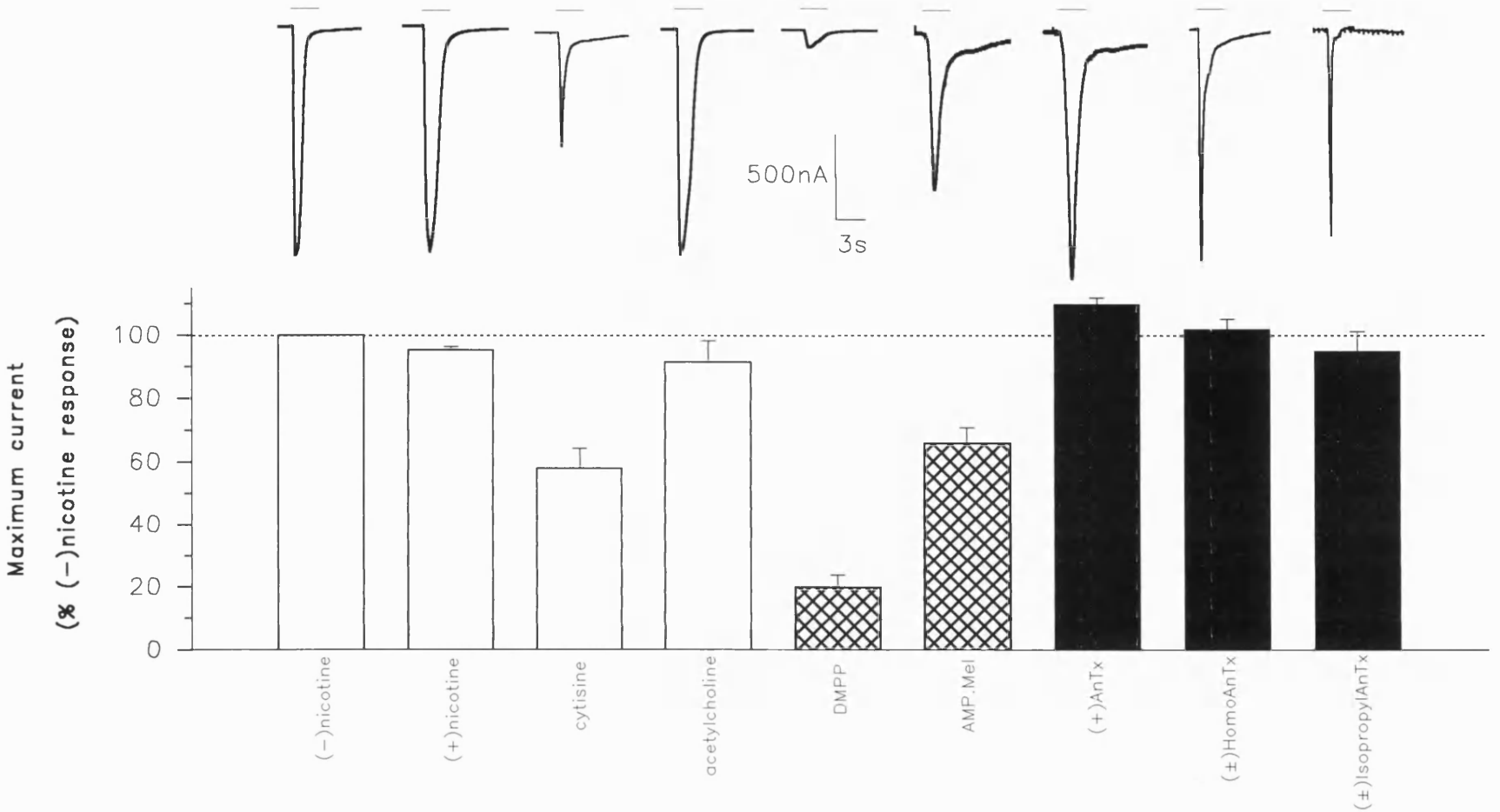

Figure 3.12: Relative efficacies of agonists at their maximally effective concentrations. Seven agonists were tested sequentially on the same oocyte for their ability to activate the α7 receptor. Agonists were applied at their maximally effective concentrations: (-)nicotine (250μM); (+)nicotine (300μM); cytisine (100μM); ACh (4mM); DMPP (1mM); AMP.MeI (1mM) and (+)AnTx (4μM). An independent oocyte was similarly exposed to maximally effective concentrations of (-)nicotine (250μM), (±)HomoAnTx (10μM) and (±)IsopropylAnTx (3μM). Current responses were normalised with respect to currents evoked by 250μM (-)nicotine. Oocytes were clamped at -70mV and ≥12 min intervals separated consecutive agonist applications. Bars (□ classical agonists, ⊠ piperazine and ■ anatoxin analogues) represent the mean (±SEM) from 5 (3 for the anatoxin analogues) individual oocytes. Representative current traces are shown above the mean values of the data.

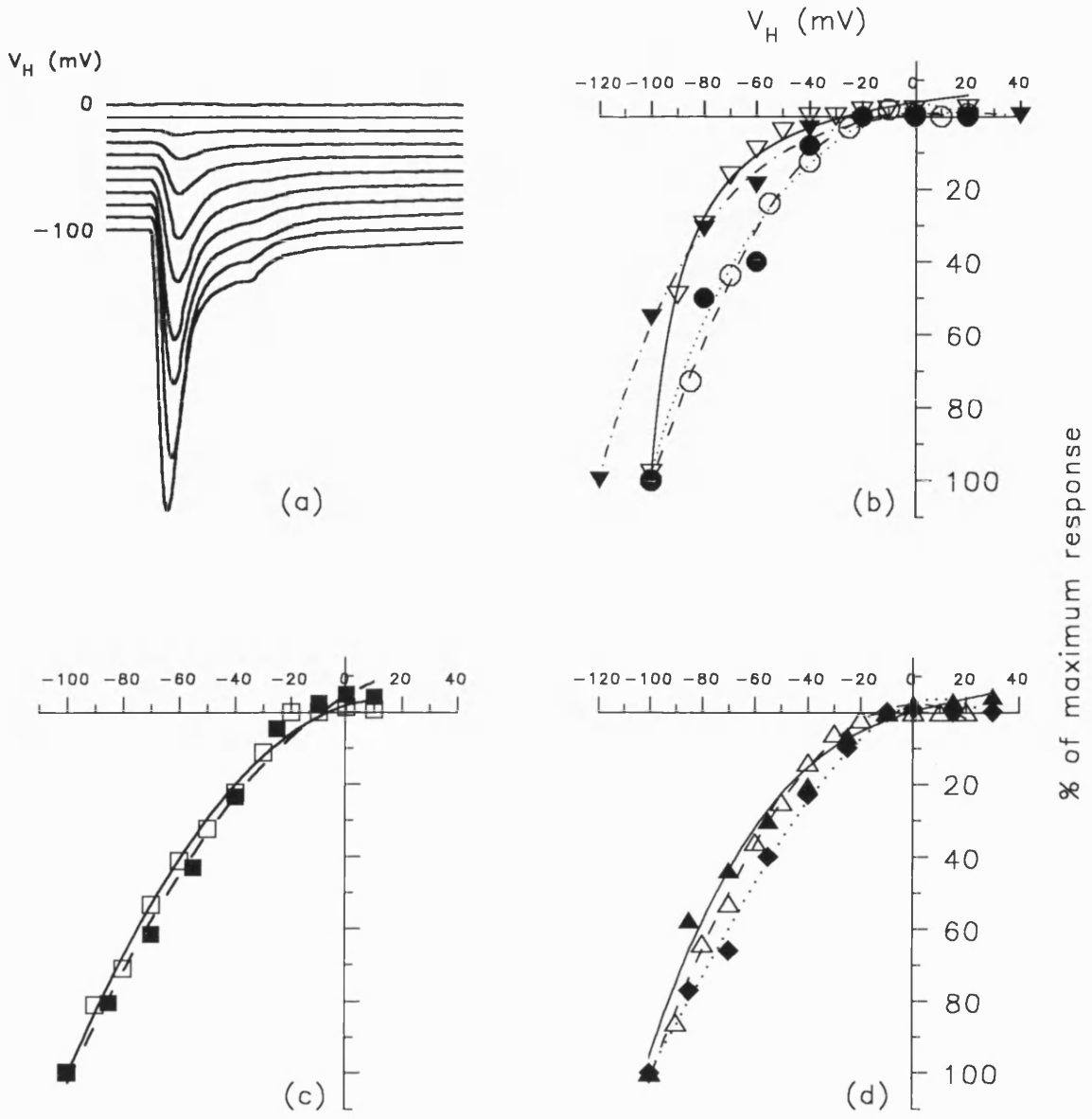

Figure 3.13: Current-voltage relationships of the α7 receptor. Each of the nine agonists were examined by successive application (3s) at ≥5min intervals while the membrane holding potential was stepped between -120mV and +40mV, as represented by HomoAnTx activated currents (a). Current responses were normalised with respect to the maximum response. Representative curves demonstrate the voltage dependence of currents induced by classical agonists (b), piperaziniums (c) and anatoxin-a analogues (d). Agonist concentrations approximated to their EC_{50} concentrations: (b), (-)nicotine 25μM(••●••); (+)nicotine 40μM (– ❍ –); (-)cytisine 5μM(• –▼• –); ACh 200μM (—∇—); (c), DMPP 60μM(– ■ –); AMP.MeI 100μM(—□—); (d), (+)AnTx 0.5μM(—▲—); (±)HomoAnTx 1μM(– Δ –); (±)IsopropylAnTx 1μM(••♦••). The strong linear IV relationship and rectification properties were evident with at least 4 independent oocytes for all agonists.

3.4 Discussion

3.4.1 Pharmacological properties of the α7 homomer

The chicken neuronal α7 subunit gene has been successfully expressed in *Xenopus* oocytes where it assembles as a functional homomeric ligand-gated cation channel which demonstrates a nicotinic pharmacology. Chicken α7 is clearly a member of the nicotinic ACh receptor gene family. Until very recently the α7 homomeric receptor was unique among the reconstituted neuronal receptor subtypes in its acute sensitivity to αBgt (Couturier *et al* 1990a). This observation has been corroborated in this study and is a property shared only by two other nicotinic AChRs, namely the α 8 homomer (Gerzanich *et al* 1994) and the muscle nicotinic receptor (Li *et al* 1993). Thus the myth surrounding non-functional αBgt-sensitive neuronal nAChRs seems now to have been dispelled.

Results described in this study generally corroborate and extend the quantitative agonist profile of the chicken homomeric α7 receptor. EC_{50} values for (-)nicotine and ACh agree well with those described previously (Bertrand *et al* 1992). These are also typical of rat and human α7 homomer responses (Segeula *et al* 1992: Peng *et al* 1994) and the α7-like responses of Type IA currents of hippocampal neurons (Zorumski *et al* 1992: Alkondon & Albuquerque 1993). (+)nicotine was two-fold weaker than the naturally occurring enantiomer, an observation that reflects the stereoselectivity exhibited by the fast channels of hippocampal neurons (Alkondon & Albuquerque 1993) and αBgt-sensitive binding sites in *Torpedo* and brain (Wonnacott *et al* 1986), yet is in marked contrast to α Bgt-insensitive Type II hippocampal nAChR and brain binding sites which show a 100-fold preference for (-)nicotine (Rapier *et al* 1988). A difference in steepness between (-)- and (+)-nicotine dose-response curves was apparent (n=1.4 and 2.5) and also occurs among the anatoxins (see section 3.4.6).

Cytisine was more potent than (-)nicotine in the present study. Conversely, this rigid agonist was found to be slightly less potent than (-)nicotine in the previous chicken α7 study (Bertrand *et al* 1992), and also other functional α7 homomers from rat and human (Segeula *et al* 1992: Peng *et al* 1994) and additionally fast channels in hippocampus (Alkondon & Albuquerque 1993). Interestingly, the relative potencies of (-)nicotine and cytisine for chicken α7 homomers as measured by their ability to inhibit the binding of 2nM αBgt (Anand *et al* 1993) are 0.55μM and 0.08μM respectively. The order is reversed for the immunopurified native brain α7 nAChRs (1.4μM and 3.9μM respectively). This near 50-fold difference in affinity exhibited by cytisine between these two α7-containing receptor sites was exceptional in this latter study and emphasises the acute sensitivity of this semi-rigid alkaloid with regard to the receptor constitution. A more obvious instance is apparent among the αBgt-insensitive heterologously expressed nAChRs in *Xenopus* oocytes which are most sensitive to cytisine when the β4 subunit is present, whereas β2-containing receptors are almost completely insensitive to cytisine (Luetje & Patrick 1991). This selectivity may reflect a situation whereby cytisine interacts with a more subunit interface oriented region of the binding site than most other agonists. Chimeras of β4.β2 expressed with α3 reveal two residues at positions 108 and 110 in the N-terminal region of the β subunit which account for much of the relative cytisine sensitivity (Figl *et al* 1992). This region does not evidently contribute to the binding site (see section 1.4.3.1) so

may be an important subunit contact region (Verall & Hall 1992), which if imprecise might alter the structural attributes of the N-terminal region and an interface binding site.

Anomalous post-translational modification of the α7 subunit seems unlikely to account for the slightly accentuated sensitivity to cytisine in the present study, as dose-response data were generated from 7 separate oocytes from independent donors (Table 2.1). Besides, *Torpedo* nAChRs reconstituted in *Xenopus* oocytes are pharmacologically and functionally indistinguishable from native *Torpedo* receptors (Sakmann *et al* 1985), despite the altered glycosylation pattern of expressed subunits (Buller & White 1990a). Although fairly stable, chemical modification of the cytisine stock may also have been contributory, given the consistency of the data.

Cytisine was only ~58% as effective as nicotine at stimulating the α7 homomer (Figure 3.12). This observation is also inconsistent with other α7 studies of different species (Bertrand *et al* 1992: Seguela *et al* 1992: Peng *et al* 1994). However, cytisine-stimulated rubidium efflux from a synaptosome preparation is only 20-30% as effective as (-)nicotine (Marks *et al* 1993). ACh-induced responses of β2-containing neuronal nAChR heterooligomers almost insensitive to cytisine (see above) are reduced upon coapplication with cytisine, an inhibition which is not voltage dependent but which is more likely to take place through direct competition with ACh at the agonist binding site (Papke & Heinemann 1993). Thus it seems for α3β2 and α4β2 receptors at least, cytisine is a true partial agonist in that it does not demonstrate local anaesthetic-like actions yet is intrinsically poor at opening the ion channel.

1,1-Dimethyl-4-phenylpiperazinium iodide (DMPP) was a relatively potent agonist at α7 nAChR though was only 20% effective as (-)nicotine at activating the receptor. Bertrand and co-workers (1992) observed no significant currents (<3%) with DMPP even at concentrations up to 600μM. Current responses were somewhat larger in the present study (on occasions mA currents were observed) which may have enabled the detection of DMPP-evoked responses. The recently cloned rat α7 subunit (Seguela *et al* 1992) also shows anomalous dose-dependency for DMPP (although it may be fully effective), raising the possibility of some channel blocking activity (Sine & Steinbach 1984), or occlusion by receptor desensitisation and slow solution changes associated with the large 300μl perfusion chamber used. However, no obvious differences are evident upon inspection of the current traces of this agonist in its rate of activation or desensitisation (Figure 3.10). A striking difference in efficacy is shown with human α7 homomers (Peng *et al* 1994) and αBgt-sensitive rat hippocampal nAChR (Type IA: Alkondon & Albuquerque 1993), where DMPP demonstrates comparable potency, yet crucially is as efficacious as ACh. Most oocyte studies with α7 homomers have been performed at holding voltages around -60mV, a voltage at which secondary Ca^{++}-dependent Cl^- currents (see section 3.4.4) appear to be proportional to the activation (Vijayaraghavan *et al* 1992: Gerzanich *et al* 1994). No such poor relative efficacy of DMPP is indicated by any other neuronal nAChR, but as with cytisine, DMPP seems to be extremely sensitive to the constitution of the receptor as regards the β subunits (Luetje & Patrick 1991).

An analogue of DMPP, dithiobis-DMAP (DT-DMAP), is both less potent and less efficacious than a comparable ACh analogue (DT-ACh) as an agonist of α3, α4, β2-containing nicotinic receptors in chick retina (Xie *et al* 1992). Although these compounds display equal potency in their oxidation of the reduced α192-193 disulphide bond of the receptor, the oxidation products (which are also agonists) of DT-DMAP are also less potent and less efficacious than DT-ACh. Besides demonstrating that oxidation is independent of receptor activation this confirms that a close analogue of DMPP also has reduced efficacy at other neuronal receptors.

The related compound AMP.MeI was only slightly less potent than DMPP but was at least three times more efficacious and may be a fully effective agonist - determination of this was only precluded by a lack of material. Absence of a methyl group in AMP.HCl reduced the potency such that no detectable currents were observed up to mM concentrations. It seems, therefore, that the benzene ring of DMPP confers properties consistent with poor efficacy to this piperazine-based compound. AMP.MeI is a potent activator of the frog rectus abdominus muscle (Spivak *et al* 1989a) where it is some 17-fold more potent than carbamylcholine. In behavioural experiments, AMP.MeI has also been shown to function as an agonist in the rat CNS as evinced by its ability to induce nicotine-like discriminative stimulus effects (Garcha *et al* 1993). However, differences in the behavioural profile relative to (-)nicotine, and the piperadine-based isoarecolone, may be attributable to action on more than one class of receptor, or to partial agonist properties at a single receptor type. Interestingly, arecolone only effects ~40% activation of the receptor (Alkondon & Albuquerque 1993) and is a weak agonist (EC_{50}~640μM).

(+)Anatoxin-a, ((+)AnTX), a highly selective nicotinic, not muscarinic, receptor toxin (Aronstam & Witkop 1981), was the most potent of the agonists tested at the reconstituted α7 nAChR, as is the case with other heterooligomeric neuronal nicotinic receptors (Thomas *et al* 1993). This conclusion is supported by studies with nAChRs of frog skeletal muscle and *Torpedo* electroplaque (Spivak *et al* 1980: Swanson *et al* 1986), where this semi-rigid neurotoxin is between 12-110 times more potent than ACh and 2-8 times more potent than carbamylcholine - AnTx (EC_{50}~4μM) is 33-fold more potent than ACh and 64-fold more potent than carbamylcholine in eliciting fast activating Type IA currents of the rat hippocampus (Alkondon & Albuquerque 1993). The (-) enantiomer is an agonist of the muscle nAChR only in the μM range (Swanson *et al* 1986).

Homoanatoxin-a (HomoAnTx) and Isopropylanatoxin-a (IsopropylAnTx), synthetic homologues of anatoxin-a differing only in the addition of one or two methylene units respectively to the acetyl side chain, were almost equipotent with the parent compound in their ability to activate the α7 receptor (Figure 3.11). This was despite their use as racemic compounds in which case the assays may underestimate nicotinic potency by a factor of two, given that anatoxin's potency resides predominantly, and probably exclusively, in the configuration represented by the (+) enantiomer (Spivak *et al* 1983). Although these are novel compounds to be assessed in the functional oocyte system, HomoAnTx has previously been demonstrated to elicit muscle contracture in frog muscle (Wonnacott *et al* 1992) where it has 4 times the potency of carbachol and only 1/10th the potency of

the parent compound. The presence of the inactive (-)racemate was thought to play a large part in the potency discrepancy perhaps through channel blocking activity (Kofuji *et al* 1990), the NCI site showing no stereoselectivity for AnTx. No direct evidence of this is apparent upon visual inspection of α7 currents, and both HomoAnTx and IsopropylAnTx were found to be maximally effective. At high concentrations of IsopropylAnTx however, the dose-response curve became hooked (Figure 3.11) suggestive of some rapid desensitisation or inactivation. It is therefore apparent that these alkyl-modified sidechain variants of anatoxin-a are at least able to retain the functional potency and efficacy associated with the parent compound active at the α7 nAChR. The agonist binding site for receptor activation can accommodate extension of the side chain which has implications for a model of the binding surface of AnTx and the orientation of residues in the binding pocket.

Nicotine (25μM)-induced currents through the α7 homomer were strongly blocked by subnanomolar concentrations of MLA (Figure 3.8). Inhibition was reversible and a full dose-response curve for this toxin gave an EC_{50}~2pM. Competitive and reversible inhibition of nicotinic responses by MLA is a finding common to most functional nicotinic receptors, though variation in potency is much evident. α Bgt-sensitive nAChRs of brain and ganglia (α3β2 and α4β2 reconstituted receptors), and muscle nAChR require μM concentrations of MLA for inhibition. Contrastingly, the αBgt-sensitive fast activating receptor in rat hippocampal neurons, and chick α7 in this study, define MLA as a unique probe for the discrimination between α7-containing and other nACh receptors. Functional characterisation of α7 receptors has relied on αBgt for its discrimination. Disadvantages such as poor accessibility and slow onset of inhibition of this large polypeptide should see supersedence by the equipotent (perhaps more potent) MLA which is more selective, having >1000-fold lower affinity for muscle nAChR. Perhaps surprisingly. MLA has similarly high potency at insect αBgt-sensitive nAChR. High sequence homology between the α7 gene product (Couturier *et al* 1990a) and the α L1 gene product (Marshall *et al* 1990) may underlie this unique sensitivity to MLA.

The spectrum of agonist sensitivities and efficacies recorded here for the chicken α7 homomeric nAChR reconstituted in *Xenopus* oocytes is quite specific and different from those displayed by other reconstituted neuronal nicotinic receptors (Couturier *et al* 1990b: Luetje & Patrick 1991). As regards comparison with the pharmacology of other α7-containing receptors, differences are apparent in potency and efficacy of some agonists both between species (chicken, rat and human) and for the native αBgt-sensitive receptors. This is exemplified by comparison of agonist rank orders of potency of the same agonists used in this study:

α7 chicken (this study)	(+)AnTx>cytisine>(-)nicotine>(+)nicotine>DMPP>ACh
α7 chicken (Bertrand *et al* 1992)	cytisine=(-)nicotine>ACh>>DMPP
α7 rat (Seguela *et al* 1992)	(-)nicotine)cytisine>DMPP>ACh
α7 human (Peng *et al* 1994)	DMPP>(-)nicotine>cytisine>ACh
α7-containing rat (Type IA) (Alkondon & Albuquerque 1993)	(+)AnTx>>DMPP>(-)nicotine>cytisine>ACh>(+)nicotine

Despite these indifferences the pharmacological and functional profile of the α7-containing nAChR is beginning to be defined.

3.4.2 Is the recombinant α7 homomer representative of a physiological receptor?

That the pharmacological observations made in this study are of the purely homomeric α7 receptor there is little doubt. In the initial instance when the subunit gene was cloned and expressed (Couturier *et al* 1990a) control for the possible interference of nAChR α-like subunits that might be endogenously produced in the oocytes (Buller & White 1990b: Hartman & Claudio 1990) was undertaken by injection of equimolar mixtures of β1, γ and δ cDNAs or β2, β3 or β4 cDNAs. All such cells failed to respond to 100μM ACh - conversely αβγδ and α4β2 combinations were responsive. Similarly, expression of the rat α7 gene co-injected with α3, α5, β2 or β4, did not lead to receptors pharmacologically distinct from α7 alone (Seguela *et al* 1992), and currents were proportional to the amount of α7 RNA or cDNA injected. More recently still, Anand and co-workers (1993) have used sucrose gradient sedimentation analysis to compare the chicken α7 protein expressed in *Xenopus* oocytes and native brain α7 nAChRs. The [^{125}I]αBgt labelled receptors co-sediment at ~10S implying a common size and shape. Interestingly [^{35}S]methionine labelling of the expressed α7 reveals association with a broad array of protein complexes of which only the ones similar in size to native nAChRs bind [^{125}I]αBgt. Furthermore, fractionation and SDS-PAGE of this latter band reveals it is only comprised of entities of the same size (~60kDa), thus unless endogenously expressed oocyte nAChR subunits have the same weight as α7 then these observations support the formation of a purely homomeric α7 nAChR in the oocyte membrane.

There is also little doubt that α7 homomers the size of native nAChRs exhibit the pentagonal symmetry common to other members of the neuronal nAChR gene family (Anand *et al* 1991: Cooper *et al* 1991). For instance the calculated protein molecular weight of the pentameric *Torpedo* α1βγδ nAChR monomer is 268kDa, compared to chicken α7 which is 272kDa (Anand *et al* 1993).

Two other cases of functional homomeric receptors forming following injection into *Xenopus* oocytes support the use of the α7 homomer as a valid pharmacological receptor. In the mammalian brain one of the two transcripts of the α4 subunit gene forms a functional nicotinic receptor, though responses in the presence of high concentrations (100μM) of ACh are not as robust as α7 (Boulter *et al* 1987). The invertebrate nervous system, the nicotinic receptors of which are largely blocked by αBgt (David & Sattelle 1984), has also manifested a nicotinic subunit able to form functional homomeric channels in the form of the locust gene αL1 which contains cysteines at positions 201 and 202, and shares 44% and 46% homology with the mouse α1 and rat α3 genes respectively (Marshall *et al* 1990). The magnitudes of the nicotine-induced depolarisations compare favourably with α7 and αβ combinations of mammalian neuronal subunits. Interestingly, the pharmacology of this locust homomeric nAChR closely resembles that of the *in vivo* insect receptor (Sattelle 1985) and an affinity purified receptor reconstituted in lipid bilayers (Hanke & Breer 1986), including block by both αBgt and nBgt. Thus this locust homomeric receptor may represent the nAChRs with similar pharmacology in invertebrate CNS. The formation of a functional channel following expression of a

single subunit gene in *Xenopus* oocytes is also observed for the $GABA_A$ (Blair *et al* 1988) and glycine receptors (Schmeiden *et al* 1989), though their resemblance to the more usual heterooligomers *in vivo* is weak.

3.4.3 Desensitisation kinetics and channel block

The agonist-induced whole cell α7 currents undergo very fast and thorough desensitisation which can be described by two exponentials represented by an initial fast phase followed by a slow decay plateau which persists until the agonist is removed. Even in the nAChR-expressing oocyte, which is obviously a large cell when compared to cultured foetal neurons for example, the activation phase and fast decay component of the agonist-evoked whole cell current generally occurred in under 2s and became shorter still at saturating agonist concentrations. The whole cell currents associated with the α7 expressing oocyte decline to a greater extent than in any other expressed neuronal nAChR (Couturier *et al* 1990b).

Using an improved perfusion system which better identified the slow decay phase, the ratio of current peak to plateau for the α7 homomer in this study was at least 16:1 at saturating agonist doses. Couturier and co-workers (1990a) obtained a ratio of 25:1 for (-)nicotine and ACh. These observations are reflected by the supposed α7-containing Type IA channels of hippocampal neurons (Alkondon & Albuquerque 1993), which exhibit a similar response profile to the chicken α7 homomer, rat and human α7 (Seguela *et al* 1992: Peng *et al* 1994) and the human α8 homomer (Gerzanich *et al* 1994), desensitising more fully than either Type II currents (~α4β2) or Type III currents (~α3β4) on the same neuron. The whole cell Type IA currents (~600pA at their peak) for these neurons are able to activate and undergo fast desensitisation in well under 0.5s. Indeed when the fast and slow desensitisation components are fitted to a double exponential Type IA currents exhibit decay rates of 27ms and 300ms respectively (Alkondon & Albuquerque 1993). A similar foetal hippocampal channel exhibits an 8ms fast component (Zorumski *et al* 1992), which has been resolved to 0.5ms for the single Type IA channel (Castro & Albuquerque 1993). Desensitising whole cell α7 nAChR currents in the present study have fast and slow components of 510$\pm$75ms (n=4) and 16.2$\pm$3.1s (n=4) respectively when maximally effective doses of (-)nicotine- and ACh-stimulated currents are fitted to a double exponential function using Sigmaplot 4.1. These values are comparable to values of 260ms and 13s respectively obtained for the same α7 homomer (Couturier *et al* 1990a). Consistent with either desensitisation or open channel block, the contribution of the fast decay component to the overall current was consistently seen to increase with increasing concentrations of agonist (Figure 3.7), concurrent with other studies - similarly at low concentrations the fast decay component reduced to the extent where desensitisation followed a single exponential.

Whether inactivation is a consequence of desensitisation because the receptor has greater access to the agonist, and/or open channel block is unclear. However, ACh, carbamylcholine and succinamide (Sine & Steinbach 1984: Ogden & Colquhoun 1985), (+)- and (-)-nicotine (Rozental *et al* 1989) and anatoxin (Kofuji *et al* 1990) all demonstrate open channel blockade of the nAChR. Presumably, depolarisation of the membrane would reduce the influence of open channel blockade,

particularly for the positively charged nicotinic agonists. Single exponential decay time constants of whole cell Type IA currents in hippocampal neurons were not voltage sensitive for any of the agonists tested (which included (-)- and (+)-nicotine, ACh, cytisine, DMPP and AnTx) (Alkondon & Albuquerque 1993), suggesting that the rapid decay phase is not influenced by open channel blockade but is more probably a consequence of stabilisation of the desensitised state. In contrast, Type II currents (~$\alpha4\beta2$) are clearly susceptible to open channel block. Interestingly, the $\alpha7$ channel in oocytes (Revah *et al* 1991) has a much longer open time (>10ms) than the Type IA current in hippocampal neurons (~0.1ms: Castro & Albuquerque 1993). Desensitisation rates of the latter channel were found to be independent of ACh concentration and only weakly voltage dependent supporting the insignificant role of channel block to the much reduced burst-time of this possible $\alpha7$-containing nAChR. The differences are more likely to be a consequence of structural anomalies between the native and expressed $\alpha7$ receptor.

Biphasic decay of the fast $\alpha7$ channels might be explained by the existence of the same nAChR subtype in different conductance states with different closing rates, one contributing to the fast and the other to the slow decay. Notably, the single channel conductance for $\alpha7$ nAChR is reported to be 45pS (Revah *et al* 1991) whereas Type IA channels have a conductance of 73pS (Castro & Albuquerque 1993). These two channels which are pharmacologically not dissimilar, may represent the same nAChR, the differences in observed conductances being a consequence of the nature of the preparation.

3.4.4 Current-voltage relationships, rectification and calcium permeability

Current responses to all the agonists assayed at the $\alpha7$ receptor exhibited a linear dependence with membrane potential up to approximately -25mV (Figure 3.13). At more depolarised potentials (up to +40mV) agonist responses became dramatically voltage sensitive and rectified to the extent that reversal currents were not detectable with any ligand. This data shadows that for homomers of chicken, rat and human $\alpha7$, and chicken $\alpha8$ (Couturier *et al* 1990a: Seguela *et al* 1992: Gerzanich *et al* 1994: Peng *et al* 1994). The $\alpha7$-like channel of hippocampal neurons have a slightly more positive reversal potential (7mV) and may (Alkondon & Albuquerque 1991: Zorumski *et al* 1992) or may not (Alkondon & Albuquerque 1993) show rectification. Most of the neuronal nAChR (with the exception of retinal ganglion cells (Lipton *et al* 1987)) reveal inward rectification of their macroscopic currents (Mathie *et al* 1990: Mulle & Changeux 1990: Zhang & Feltz 1990: Ifune & Steinbach 1992). Several mechanisms have been proposed for the observed inward rectification of neuronal channels which include Mg^{++} block of outward currents (in PC12 cells) and voltage-dependent gating kinetics of channels (Mathie *et al* 1990: Ifune & Steinbach 1992). The shape of the I-V curve for $\alpha7$-like hippocampal channels is unaffected by intracellular Mg^{++} (Zorumski *et al* 1992), and Cs^{+}, contrary to the claims of Hirando and co-workers (1987). Interestingly, nAChR rectification in cultured midbrain neurons is removed when atropine is applied suggesting that the muscarinic AChR masks the nicotinic component at positive membrane potentials (Bijak *et al* 1991), though nicotinic currents in the hippocampus are not likewise affected (Zorumski *et al* 1992).

The absence of current reversal up to potentials of 40mV suggests α7 currents are carried by non-selective cations. The positive reversal potential of the Type IA current is compatible with the high calcium permeability found in human α7 (Peng *et al* 1994), chicken α7 and α8 (Gerzanich *et al* 1994) and rat α7 (Segeula *et al* 1992) homomers in *Xenopus* oocytes, perhaps the highest among the known LGICs. A major proportion of the rat α7 currents result from the secondary activation of endogenous Ca^{++} dependent Cl^- channels which can represent up to 80% of the α7 current. Interestingly, the αBgt and MLA sensitive nAChR of chick ciliary ganglion mediate Ca^{++} influx without generating currents (Vijayaraghaven *et al* 1992). The α7-containing receptor therefore may possibly play an important role in neuronal physiology.

3.4.5 Nature of native neuronal nAChRs sensitive to [^{125}I]αbungarotoxin

Whether the α7 homomer expressed in *Xenopus* oocytes represents the native nAChR found *in situ* is unclear. αBgt affinity purification of αBgtBPs from mammalian brain yields fractions containing one to five bands on denaturing gels ranging from 48 to 72kDa in weight (Norman *et al* 1982: Conti-Tronconi *et al* 1985: Kemp *et al* 1985: Whiting & Lindstrom 1987a). The affinity labels [^{3}H]MBTA and [^{3}H]BAC, (instrumental identifiers of binding site residues of the α subunit), alkylate only the 55kDa protein presumed to be the α subunit (Kemp *et al* 1985: Norman *et al* 1982). The components that sometimes copurify with this subunit may represent other subunits of the native α BgtBP heterooligomer, or may be proteolytic breakdown products or associated peptides which are not integral to the αBgtBP.

Although largely ineffective, αBgt can antagonise a few agonist-mediated nicotinic effects in the CNS, such as in the inferior colliculus (Farley *et al* 1983), and the cerebellum (de la Garza *et al* 1987). It has not been until relatively recently that αBgt-sensitive, functional nAChR have been shown in the mammalian CNS by more direct approaches (see Zorumski *et al* 1992: Alkondon & Albuquerque 1993). Electrophysiological studies of these nicotinic receptors present on the neurons of rat hippocampus reveal the presence of multiple structural subtypes of the receptor, which differ in their sensitivity to not only αBgt, but also nBgt, MLA, DHβE and mecamylamine (Alkondon & Albuquerque 1991: Zorumski *et al* 1992). Consideration of decay characteristics, rectification profiles and agonist sensitivities has revealed four discrete subtypes. As we have already seen, the currents associated with the Type IA channel probably represent α7-containing receptor(s), being blocked by 10nM αBgt and are most prevalent appearing on ~83% of neurons. These channels closely resemble those of α7-containing receptors in terms of pharmacology, desensitisation etc, and presently represent the best characterised potentially α7-containing native nAChR.

In the avian brain the picture is a little clearer. Schoepfer and co-workers (1990) demonstrated that over 90% of the immunoprecipitated αBgtBPs contain the α7 gene, whereas α8 is only represented in about 15% of cases. Values of 68% and 8% respectively are obtained for the presence of α7 and α8 in αBgt-sensitive nAChRs for a similar tissue preparation (Keyser *et al* 1992). A mixed α7α8 AChR subtype occurred in 23% of the cases. Two αBgt-sensitive AChR subtypes have also been purified in the chick optic lobe (Gotti *et al* 1993). Polyclonal antibodies against synthetic peptides of

chick α7 and α8 subunits recognise a predominant subtype (α7-containing) representing 60% of α BgtBPs, and another subtype (α7α8-containing) present in 20% of the receptors. In addition to the α7 and/or α8 subunits (MW~57kDa), both subtypes are associated with other subunits (MW~52kDa). These two subtypes have the same affinity for antagonists, but α7α8 has higher affinity for agonists. Characterisation of these subunits was taken a step further with their reconstitution in lipid bilayer. Both are able to form cationic channels but the α7α8 receptor is less homogenous (channel conductance ranges between 10-50pS) than α7 which has conductance of 45pS (Gotti *et al* 1993).

3.4.6 Extrapolating the significance of the Hill coefficients observed for the α7 homomer in this study

Hill coefficients for most agonists interacting with α7 were typically greater than unity indicating the binding of more than one agonist molecule per homomer. Coefficients ~1.5-2 are the norm for heterooligomeric nicotinic AChRs, which are expected to interact with two ligand molecules for activation before lapsing into a desensitised state when affinity for the agonist is enhanced. This generally turned out to be the case for the α7 receptor in this study (Table 2.1), exceptions being (+)nicotine and anatoxin and its analogues. The significance of this is unclear but anomalies are perhaps unsurprising given that the α7 receptor in *Xenopus* oocytes is homomeric and therefore potentially provides five binding sites for activating ligands. HomoAnTx's Hill coefficient was less than one (0.83). Consistently low coefficients (0.83-0.91) are observed for Type II (~α4β2) currents in the hippocampus (Alkondon & Albuquerque 1993). Desensitisation and open channel blockade by the agonist was suggested to be the cause. Alternatively the binding of only one agonist molecule to a single α subunit might be sufficient to activate the receptor, which could also feasibly be imposed by an nAChR population of $\alpha_1\beta_4$ stoichiometry (Role 1992). This does not explain a Hill number of <1 for the α7 homomer though.

(+)Nicotine, (+)AnTx and (±)IsopropylAnTx exhibited Hill coefficients in excess of 2. This may be more consistent with the provision and occupation of ≥2 binding sites by agonists, possibly as many as 5 if a pentameric structure is supported. Increasing the concentration of ligand at the receptor may produce a commensurate increase in the number of sites occupied on each receptor (the extent of occupation might be ligand specific). This would create greater structural perturbations and mean that larger currents may be seen than if only 1 or 2 sites were occupied. Similarly, fast desensitisation might be more extensive which is possibly why IsopropylAnTx (η_H=7.2) produces a hooked dose-response curve - possibly all ligand binding sites are occupied on the receptor so currents are occluded by significant stabilisation of the desensitised state. This model would also argue against channel block as being the desensitisation mechanism, for higher affinity ligand binding sites would probably be fully occupied before the NCI site.

3.4.7 Sequence homology and the receptor structure

The chicken α7 subunit gene used in this study shares 92% identity with the human α7 gene (Peng *et al* 1994). The human gene sequence is 94% identical to rat α7 emphasising the high

degree of conservation of the mature α7 subunit peptide across the different species. Greatest diversity is apparent in the large intracellular loop between M3 and M4. Transmembrane regions M1, M2 and M3 are identical for all three species, therefore if M2 lines the channel (see Karlin 1993) then these α7 homomers should share identical cation channel properties. As we have seen the chicken, rat and human α7 receptor, and also α8, all exhibit the same rapid activation/desensitisation profile, inward rectification and Ca^{++} permeability (this study: Couturier *et al* 1990a: Seguela *et al* 1992: Vijayaraghavan *et al* 1992: Gerzanich *et al* 1994: Peng *et al* 1994).

Only limited sequence diversity (11 out of the 207 residues between chicken and human) occurs in the large N-terminal domain. The amino acids that do differ are not among those that participate in the binding site (Galzi *et al* 1990: Galzi *et al* 1991b) or sites for specific interactions between adjacent subunits (Verall & Hall 1992). Either these few residues are important in maintaining structural integrity of the regions adjacent to the binding site, or they are major participants in the transduction and/or allosteric mechanisms, or alternatively the large phosphorylatable intracellular loop is in some way responsible for modulating the receptor and manifesting the differences that are observed in pharmacologies between these α7 homomeric channels.

3.4.8 Functional role of αbungarotoxin-sensitive nAChRs

Now that functional αBgt-sensitive nAChRs are recognised and pharmacological correlations can be observed between reconstituted and native receptors, inferences about the physiological role of this receptor can be made. The endogenous ligand for this/these nAChR subtype(s) is unlikely to be ACh as it is nicotine which, when acutely administered, regulates [^{125}I]αBgtBPs (Marks *et al* 1985) and furthermore, anticholinesterase agents do not have the same effect. The fast desensitisation obviates ACh as the endogenous ligand as this precludes the need for ACh hydrolysis. Given that αBgtBPs are located predominantly in non-synaptic membranes in embryonic and adult neurons, it is unlikely that these possible α7-containing receptors contribute directly to synaptic transmission. A more plausible role for these αBgt-sensitive receptors would be a modulatory one, given the extensive calcium permeability of native (Vijayaraghavan *et al* 1992: Castro & Albuquerque 1995) and recombinant (Galzi *et al* 1992: Seguela *et al* 1993: Sands *et al* 1993) receptors, thus providing the potential for influencing a vast array of calcium related events in neurons. For instance, the nAChR of pseudodendrites that bind αBgt have been implicated to mediate neuronal morphology (Pugh & Berg 1994). Divalent cations are not thought to directly modulate αBgtBPs themselves (Sands *et al* 1993), as occurs with αBgt-insensitive neuronal nAChRs.

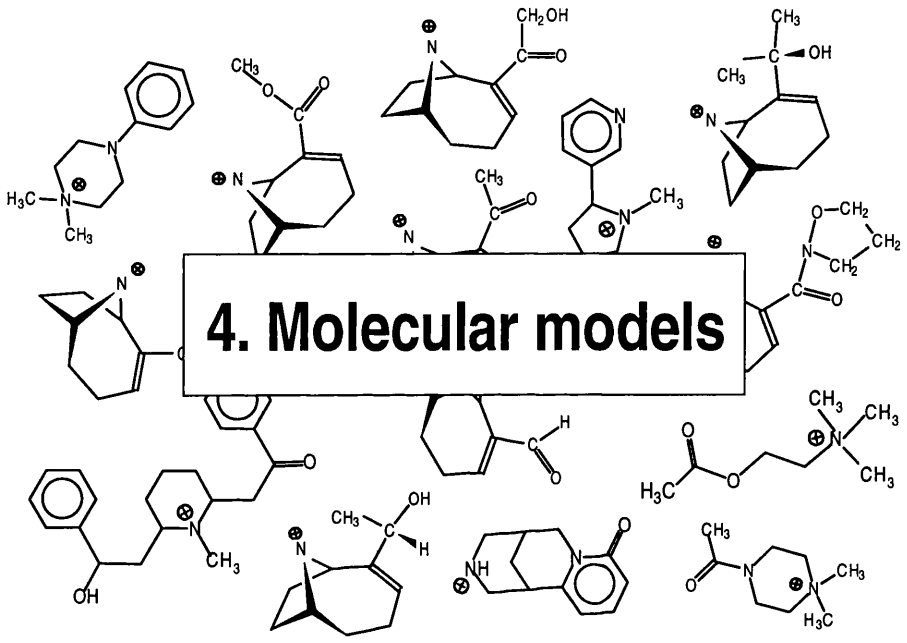

4. Molecular models

4.1 Introduction

4.1.1 Molecular modelling techniques and application

Molecular modelling is the term used to describe the theoretical aspects of chemistry which simulate the 3-dimensional structure and energetics of molecular systems. It encompasses techniques for the construction, manipulation and analysis of explicit atomic models which can be used to aid the understanding of the relationship between structure and physical/biological properties. It is a field that has recently seen increased development of commercial and academic molecular modelling packages as a result of the explosive growth in computer hardware.

In order that a new bioactive molecule may be rationally designed an assessment must be made of the structure-activity relationships of related molecules. Molecular features of molecules to be used for such purposes can be constructed through experiment or hypothetically. Interaction of small ligands with their particular macromolecular target is an important consideration in the formulation of hypotheses about the required features of an active molecule. For instance, ligand-receptor interaction involves specific intermolecular interactions based on geometry, size, shape, charge, polarity and so on. Such information may be available from experiment but equally may be derived from a catalogue of chemical structures and their biological potency, as is the case with the molecules studied in this project.

Before a computer graphic model of a molecular structure can be displayed and manipulated, and before structurally-dependent molecular properties can be calculated, the 3-dimensional co-ordinates of all atoms comprising the molecule must be provided. Co-ordinates for some compounds can be found from x-ray crystallographic data and other databases. Generally though, the 3-D structures of compounds of interest are not readily available so it is necessary to sketch crude representations for such compounds using molecular graphics facilities. This structure must then be refined (or optimised) prior to it being used for predictive purposes. Optimisation is accomplished through adjustments to the atomic co-ordinates to minimise the potential energy of the molecular system through the use of molecular mechanics (MM - see section 4.1.1.2) or molecular orbital (MO) methods.

4.1.1.1 Molecular graphics

Graphics permit the visual display of 3-dimensional aspects of molecular systems generated through a model builder. One of the molecular graphics packages used in this study was INSIGHT (Biosym Technologies Inc., San Diego, USA) run on a MicroVax II computer and displayed through an Evans and Sutherland PS-300 vector graphic interface. The system displays structures from small ligands to large proteins with colour, a variety of surface representations, depth-cueing and stereo images. Additionally, it provides the facilities required for the construction, analysis and storage of molecular systems.

Another useful facility of INSIGHT is its ability to give an assessment of the 'goodness' of fit between the atomic co-ordinates of two similar molecular structures. The 'by eye' method provides a qualitative method of the fit by manual rotation and translation of one structure over another. A more

quantitative method is provided when corresponding sets of atoms in the two structures are selected and a 'rigid body' movement performed such that the sum of the differences in the corresponding atom co-ordinates is a minimum - the root mean square (RMS) deviation calculated for the co-ordinates of the superpositioned molecules quantitates the goodness of fit (see section 4.2.3)

The molecular modelling program HYPERCHEM (Autodesk Inc., San Diego, USA) was also used extensively for building and conformational searching and was run on a 486DX/2-50 personal computer. This relatively new modelling package, which operates through a Microsoft Windows environment, includes functions for drawing molecules and conversion into 3-D models, graphical manipulation of structures, changing display conditions and performing chemical calculations. The ability of the program to interface with other Microsoft applications such as EXCEL allows for flexible manipulation of calculations and data.

4.1.1.2 Molecular mechanics

Molecular mechanics, as the name implies, is a method by which the principles of mechanics are used to calculate the structure of a molecule. Molecular mechanics calculations treat the molecular system as a related set of spheres (atoms) that are associated by springs (bonds) whose interaction is governed by classical-mechanical potential functions (force-fields). In general, molecular mechanics force fields describe the potential energy of a molecular system using terms which simulate bond stretching, bond angles, torsion angles and Van der Waals interactions, i.e.:

$$\Sigma E_{total}=\Sigma E_{stretch}+\Sigma E_{bend}+\Sigma E_{torsion}+\Sigma E_{VdW}$$

Force constants are applied to each of these terms to describe their distortion. There exist many such functions which may contain any number of extra terms to describe phenomena such as distortion from planarity, the coupling of movements, electrostatics and non-bond interactions. The combination of the form of the potential energy function and the numerical value of the force constants are important to the success of any system for modelling. Force constants are derived mainly from experimental data and the values are constantly being updated and improved. The chemical structure is thus calculated by minimising the potential energy function for a particular molecular structure by using one, or maybe more, of a number of minimisation methods. Electronic descriptors (charge), used in the calculation of electrostatic interactions, are usually generated by semi-empirical MO methods (see section 4.2.2)

Structure predictions using molecular mechanics are less appropriate for systems which have a high degree of conformational flexibility. Semi-empirical or *ab initio* MO methods are preferable in such situations. A popular approach for large flexible molecules such as membrane proteins is molecular dynamics, though the drawback to this and the former two methods is the cost in computer time.

4.1.1.3 Potential energy force-fields

Molecular mechanics calculations include a force-field which correlates the energy of molecular species and their internal co-ordinates. The force field contains adjustable parameters that are optimised to obtain the best fit of calculated and experimental values, and because of the intimate association between structure and energy a calculation will always involve parameters and force constants.

In this study the va09a force field of the program DISCOVER and MM+ force field of HYPERCHEM were used. Once all the correct parameters are defined it is possible to calculate the magnitude of the various interactions and their contributions to the total potential energy. The potential energy of a molecular system is described by an analytical function, the internal co-ordinates and the inter-atomic distances. The Biosym va09a and HYPERCHEM MM+ function comprise terms for; bond stretching, bond dipoles, angle bending, bond stretch and angle bending cross terms, out-of-plane bending, torsion angle rotation, and Van der Waals interactions. The MM+ function is an extended version of Allinger's MM2 force field. MM+ uses the latest MM2 (1991) parameters and atom types with the 1977 functional form modified to incorporate non-bonded cut-offs, periodic boundary conditions, and the bond stretch term switched from cubic to quadratic form at long range.

4.1.1.4 Energy minimisation

Potential energy minimisation uses molecular mechanics to alter the molecular geometry within the constraints of the force field. The explicit aim is to minimise the energy of the system thus yielding a stable conformation. As the iterative calculations of the minimisation progress, searches are made for a molecular conformation in which the energy does not change with infinitesimal changes in geometry - i.e. the derivative of the energy with respect to the cartesian co-ordinates (the gradient) is close to zero. This is known as the 'stationary point' on the potential energy surface.

Minimisation calculations cannot cross or penetrate potential energy barriers so the minimum energy will represent the potential energy closest to the starting structure of the molecule. If the energy of the molecule increases with small changes in geometric parameters then the conformation is relatively stable, and has reached a minimum. However, if the energy decreases in one or more dimensions, but not all, then the conformation is a saddle point. A molecular system can have many minima, the lowest energy being the 'global minimum' and the other(s) being 'local minima'.

4.1.2 Exploration of the conformations of ligands studied in the project

Despite the wealth of natural and synthetic compounds which have been demonstrated to bind to and/or activate the nicotinic receptor, the functional features and geometrical requirements of the pharmacophore for this receptor remain unclear. Since the actual structure of the receptor is unknown, indirect methods have been developed to gain insight into the structure, binding mechanism and geometry of the binding site, an insight that can be aided to a large extent by the definition of geometric and chemical descriptors of active molecules. The pharmacophore model proposed by Beers and Reich (see section 1.5.1) has essentially stood the test of time and remains

probably the most informative model for the nicotinic receptor. Development of this model has in part been compounded by the flexibility of many ligands, which has created difficulties in determining the exact nature of bioactive conformations, a task inexact enough even for rigid molecules. In an attempt to extrude more information with which to assimilate a more complete picture of the nicotinic pharmacophore, a conformational search was initiated for an extensive ensemble of agonists and related molecules. This search is outlined in this chapter.

Historical background

The conformations of acetylcholine and other cholinergic ligands have been studied experimentally and computationally by many workers. Many calculations have focused on the derivation of energy surfaces for discrete conformations of flexible molecules subjected to dihedral driver calculations. Early workers on both the nicotinic and muscarinic receptors have, for example, attempted to predict pharmacophore models based on experimental data for fixed conformations of agonists and antagonists bound to the receptor. Such models have proved insufficient to explain the full spectrum of pharmacological characteristics and have thus served to underlie the importance of deriving such models from flexible ligands and receptors. It is therefore apparent that the conformation of a bound ligand does not necessarily represent the conformation most pertinent to the initial receptor recognition event. Thus it has largely fallen to the predictive power of computer simulations of chemical structure, allied with methods such as QSAR (Quantitative Structure Activity Relationships), to generate theoretical molecular geometries which may represent bioactive conformations of pharmacologically active ligands. Comparison of the conformations of many such compounds should assist the building and development of the model of the pharmacophore for a particular receptor, a model which could provide the basis for predicting the interaction sites and geometrical constraints imposed in the receptor binding pocket itself.

Indeed the predictive power of computer simulation has been successful in the past on selective groups of nicotinic ligands. For example, the quantum mechanical calculations of the electronic properties of acetylcholine and nicotine (and muscarine) by Pullman and co-workers (1971), have demonstrated the excellent agreement that can be attained between theoretical and experimental data. Importantly, these workers also showed how the nitrogen of acetylcholine is almost neutral with the positive charge distributed among the three methyl groups forming a large positive area for interaction with the receptor. Pauling (1980) was able to determine which functional groups were necessary for pharmacological activity following calculations on anti-cholinergic compounds. He emphasised how the conformations represented in the crystal were not necessarily the global energy minimum for the structure.

The pharmacological activity and specificity of a molecule varies with its conformations and configurations, and since molecules are in a perpetual state of dynamic motion when in solution, the number of feasible geometrical varieties is almost limitless. The systematic computational study of the semi-rigid, and certain flexible, nicotinic receptor agonists detailed in this study, although by no means exhaustive, could assist in correlating the conformations of these molecules with their activity. Many of the ligands studied are conformationally restrained through the presence of cyclic

systems which remove the degrees of freedom and restrict the available geometries. Although such restrictions may alter the chemical reactivity of functional groups through alterations to strain energies or steric environment, some of the impositions must evidently have a role or the ligand(s) would not be biologically effective. Anatoxin-a (AnTx: see figure 2.1) is one such important semi-rigid nicotinic agonist which possess both a five- and seven-membered ring system with an unsaturated component. We have established this ligand to be the most potent agonist at certain neuronal nicotinic receptors (Thomas *et al* 1993), a property which when taken in conjunction with its rigidity makes it an excellent candidate for the exploration of structure activity relationships facilitated through molecular modelling. Indeed because AnTx is such an obvious candidate for exploring the nicotinic pharmacophore it has become the focus of much attention over recent years, and indeed prompted our probing of the structure through the synthesis of active analogues. Currently, the likely identity of the bioactive conformer of AnTx is controversial (Witkop & Brossi 1984: Koskinen & Rapoport 1985: Hacksell & Mellin 1989: Thompson *et al* 1992), though both boat, *cis* and chair, *cis* conformers of the azobicyclononene system meet the requirements of the Beers-Reich pharmacophore and may be likely candidates.

It is hoped that through the structural searches described in this chapter of some novel alkyl-modified side chain analogues of this molecule some light may be shed on this quandary, and that through collating geometrical information for a large number of active and inactive nicotinic agonists the opportunity might be presented to enhance the current model of the nicotinic pharmacophore.

4.2 Experimental procedures

4.2.1 Structure generation

This chapter describes molecular mechanical calculations performed on a variety of mainly semi-rigid agonists of the nicotinic receptor. The study has been extended to include families of structurally related ligands for which descriptors of biological potency have been established and recorded earlier (see Chapters 2 and 3), or have been reported in the literature. The basic molecular structures and core structures of all the compounds examined are represented in the relevant ensuing results sections.

Crystallographic data retrieval

Crystal structure information for a small number of the nicotinic ligands was obtained from the Cambridge Crystallographic Data Bank at Daresbury - the program permits structural identification through compound names, formulae, connectivity tables, crystal parameters, reference identifiers and query structures. Conversion of the compound's crystal co-ordinates to a usable format and removal of associated ions was required prior to manipulation.

Molecule construction

For those structures for which no x-ray data were available, or were not used, manual construction was required. Molecular sketches were generated either through the fragment libraries in INSIGHT, or drawn and converted into 3-D representations using HYPERCHEM. The stereochemistry of the molecules was examined carefully to obtain the correct starting structures prior to minimisation: i.e. (+) or (-), boat or chair, *cis* or *trans*, axial or equatorial, syn or anti forms. Potential function types, (i.e. the nature of the atom present and the form in which it appears, such as whether an oxygen is part of an hydroxyl, carbonyl etc. grouping), were also carefully checked.

4.2.2 Charge assignment

Partial charge assignment is important among the nicotinic receptor agonists as the nitrogen atom of the principal pharmacophore feature is highly protonated at physiological pH, and partial charge effects can contribute significantly to the energy of a molecule. The presence of oxygen and nitrogen atoms with negative partial charge in the nicotinic agonists create a non-uniform charge distribution. Partial charge on an atom is proportional to some extent on its electronegativity, the most electronegative atoms (oxygen, nitrogen, fluorine etc.) having more negative charge and the most electropositive atoms having the most positive charge. Partial charges were assigned so as to maintain localised electroneutrality of the molecule, which can be achieved through the freely variable partial charge of the carbon atom.

Partial charge interactions are not considered for bonded atoms since the forcefield is already parameterised for such effects. They are of greatest significance to non-bonded atoms where electrostatic through-space effects are important. Charge values were generally allocated using the experience gained in the molecular modelling facility at Bath, but were also calculated using Dewar's & Thiel's (1977) MNDO (Modified Neglect of Differential Overlap) method available in the HYPERCHEM program.

It should however be remembered that in reality charge is a smooth function of nuclei surrounded by electrons, thus in some ways the assignment of partial charges to atoms is somewhat artificial.

4.2.3 Energy minimisation

Following construction and partial charge assignment of the conformers, minimised energy conformations of every molecule were generated using one of the molecular mechanics force fields described in section 4.1.1.3. The minimising algorithm used in both the DISCOVER and HYPERCHEM program employed quasi Newton-Raphson molecular mechanics. This method calculates the gradient of the potential energy well occupied and also makes a numerical approximation of its curvature with respect to cartesian co-ordinates. This information dictates the direction and size of the iterative step making the equation increasingly accurate as convergence is reached. Unlike the full Newton-Raphson method, this algorithm calculates the second derivative matrix for one atom at a time. The minimiser in both packages was set to a maximum of 2000 iterations, and the criteria for the convergence limit set for an atomic co-ordinate energy derivative less than 0.01kcal/mol/Å.

It should be emphasised that all the calculations performed using both the DISCOVER and HYPERCHEM algorithm were on isolated molecules *in vacuo*.

Template forcing

A popular method for determining structural patterns of a particular receptor pharmacophore is to derive the possible conformations for similarly acting molecules and superimpose these structures to identify common features of active compounds. This approach is also useful for conformationally labile species in that comparison with more rigid analogues identifies the more pertinent conformations. Essentially the forcing method makes pair-wise comparisons of conformations, (the more rigid acting as a reference), and investigates the structural and geometric similarities or differences. Atoms incorporating important pharmacophore features were selected for superposition and initially a 'rigid body' comparison of the two molecules was performed - the RMS (root mean square) deviations between designated atoms in the two systems were minimised by an iterative non-linear least squares algorithm. Following this a minimising algorithm was used to locate the energetic balance between better superposition of the chosen atoms and the increasing potential energy of the flexible structure as it was forced toward this conformation (DISCOVER). This informative method of making structural comparisons was used only on a small number of the molecules examined.

4.2.4 Torsional energy barrier calculation

Ligands with rotatable bonds were subjected to dihedral driver calculations to explore other possible conformations relevant to the pharmacophore. Calculations, performed using HYPERCHEM and driven via a DDE (dynamic data exchange) link with EXCEL, involved applying an external torque about a specific dihedral angle during minimisation. Thus a specified torsion with a specified torsional forcing constant was imposed on a specific angle and held there while

minimisation of the remainder of the molecule was carried out. The angle to which the torsion was forced was increased iteratively (20° increments) and each corresponding conformation optimised. The variation in minimised energy was plotted for each angle and used as a measure of the torsional energy barrier to rotation.

4.2.5 Monitoring conformational changes

Changes that occurred to the geometry of molecules as the result of modification and subsequent minimisation were monitored by following torsional angle changes for the rotatable bonds (e.g. the enone function of anatoxin-a), or for angles defined by ring atoms. However, given the omnipresence of the electropositive centre associated with the protonated nitrogen and the hydrogen bond accepting moiety in all active molecules, and their importance in the present pharmacophore models (see section 1.5), it was decided that monitoring changes in this so-called 'Beers-Reich' distance would also be undertaken. Such measurements did not account for the Van der Waals extension of the hydrogen bond accepting atom but rather were simply atom-atom distance measurements (Å).

4.3 Results

4.3.1 Acetylcholine as a conformationally labile nicotinic agonist

Acetylcholine (ACh) shows considerable conformational flexibility and consequently a variety of crystal structures have been defined. The labile nature of the molecule results in significant differences in the conformations associated with bound and unbound states (Behling *et al* 1988). Sources which analyse the unbound molecule support a gauche conformation across the C5-C6 bond (see inset of figure 4.1) with the approximate torsion angles:

Φ1 N4-C5-C6-O7 = 75° (1)

Φ2 C5-C6-O7-C8 = 180°.

Minimisation of the crystal structure using the va09a algorithm in DISCOVER was undertaken and the conformation generated had the energy components described in table 4.1. The corresponding Beers-Reich distance (the measurement between carbonyl oxygen and quaternary ammonium ion) was only 4.35Å for this structure. Given the propensity of ACh to adopt numerous conformations, this structure was template forced onto the corresponding carbonyl group and nitrogen ion of the semi-rigid (+) *cis*, chair anatoxin (see 4.3.4), giving an RMS fit of 0.261. Distances of 0.31Å and 0.33Å respectively separated equivalent nitrogens and carbonyl carbons. This forced fit revealed a lower energy conformation than the original (E=78.263 kcal/mol) with an N-O distance of 4.99Å and the following torsion angles:

Phi	0.587
Bond	4.725
Theta	7.060
Non-bond	19.854
Coulomb	57.233
Total	79.267

Table 4.1

Φ1 N4-C5-C6-O7 = 294.6° (-65.4°) (2)

Φ2 C5-C6-O7-C8 = 168.3°.

In order to monitor other possible conformations of ACh that may best represent the bioactive state, the torsion angle Φ1 and Φ2, and additionally Φ3, of the original crystal structure were subjected to dihedral driver calculations. These HYPERCHEM calculations rotated the angles independently in 20° increments from the original co-ordinates. The energetic consequences to the conformation of the three rotated torsion angles are depicted in the figure 4.1. In general, rotation of the molecule around these points increased the energy of the system relative to the original structure - minimisation of the crystal structure using the HYPERCHEM algorithm generated a conformation with a potential energy 54.576 kcal/mol and N-O distance of 5.01Å). However, four important minima can be identified with an average potential energy of 50.829±0.358 kcal/mol. Generally, these conformations reveal that the carbonyl group prefers to be perpendicular to the plane of the ammonium head group. There is repulsion between the two ionic headgroups when Φ2=-100°, generating the most unstable state with the coulomb and torsion energy at their highest. A more planar conformation is preferred around Φ3 due to the conjugated carbonyl, with deviation from this creating instability through large increases in torsion energy (i.e. increases of up to 4.633 kcal/mol were observed).

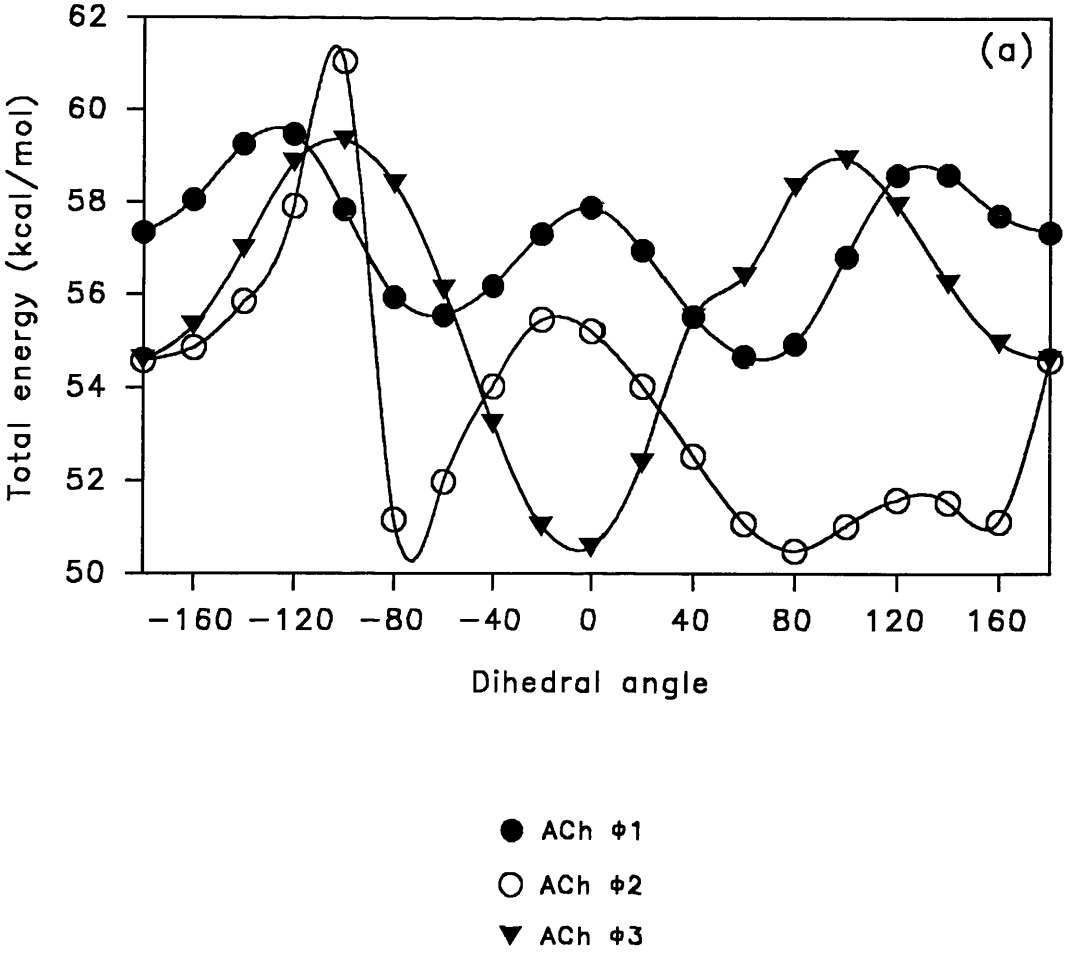

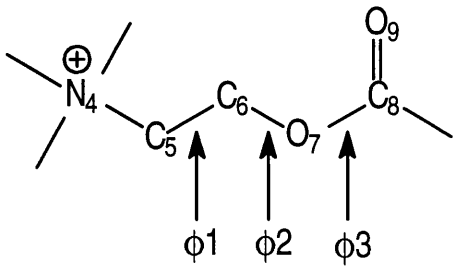

Figure 4.1: Comparison of acetylcholine conformations using computational chemistry. Intermediate conformations were explored by rotation of the indicated dihedral angles (Φ1, Φ2 and Φ3), involving the numbered atoms, in 20° increments, with minimisation at each step (see section 4.2.4). Changes to (a) the total energy (kcal/mol) were monitored. Graphs represent calculations performed on the initial minimised crystal conformation.

4.3.2 The conformers of the isoforms of nicotine

This bicyclic alkaloid, which through its activity lends its name to the nicotinic class of AChR, has a lone pair of electrons on the pyridine ring nitrogen as the hydrogen bond acceptor in place of the carbonyl group. Some of the nAChRs show selectivity in favour of the (-) isomer which is generally 20-70 times more potent an inhibitor of [^{3}H]nicotine binding to brain tissue than the (+) form (Wonnacott 1986), though little selectivity is evident for α7-containing receptors (see section 2.3.5.1). The structure exists mainly in the protonated state at physiological pH (Barlow *et al* 1986). The pyrrolidine ring nitrogen represents the cationic head, the pyrrolidine ring system itself preferentially adopts a perpendicular arrangement relative to the pyridine ring, though there is little preference for a syn or anti arrangement with respect to Hx and Hy (Inset 3: Whidby *et al* 1979). Methyl and pyridine groups favour a *trans* arrangement about the pyrrolidine ring (Pullman *et al* 1971), thus reducing conformational freedom.

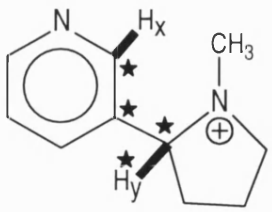

(3) ★ dihedral angle atoms
/ syn/anti hydrogens

Four (-)nicotine conformations and their mirror images were used to investigate the stereospecificity of the interactions between nAChR and this molecule. The initial crystal structure of the (-)*trans*, syn form of nicotine was minimised and used to generate the other conformers. Energy components and N-N distance values of the (-) isomers are given (Table 4.2) following minimisation.

Table 4.2

	(-) trans syn	*(-) trans anti*	*(-) cis syn*	*(-) cis anti*
N-N Dist (Å)	4.87	4.56	4.98	4.67
	Energies (kcal/mol)			
Phi	5.494	5.511	5.830	5.835
Bond	11.855	11.839	12.629	12.579
Theta	5.812	5.878	8.824	8.914
Non-bond	57.988	58.022	58.829	58.893
Coulomb	76.621	76.608	77.076	76.438
Total	128.063	128.054	132.263	131.641

Corresponding stereoisomers were essentially identical, the only difference being in the spatial arrangement of the atoms around the pharmacophore points. Preference for the *trans* arrangement, and the minor differences in the syn and anti forms, are corroborated by the models.

Rigid body comparisons with anatoxin were performed with the lowest energy *trans* form of the more active isomer (viz. (-) *trans*, anti) and the geometrically similar stereoisomer (viz. (+) *trans*, syn), both of which were deemed to show greatest structural correlation with the anatoxin pharmacophore. The syn/anti mode of the pyridine ring was chosen to achieve maximum correspondence to the pi bonding enone of anatoxin-a. Equivalent atoms in nicotine and anatoxin used for the fit are shown (inset 4) and the closest RMS fit was the (+) isomer with good overlap of the five-membered ring systems (inset 5).

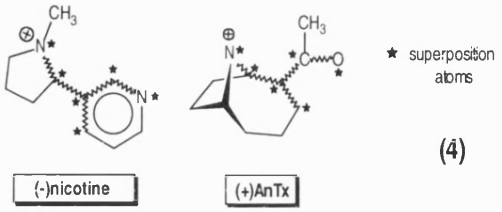

(4)

Nitrogens (secondary and pyridine)	(-)	0.242	
	(+)	0.397	(5)
All atoms	(-)	0.732	
	(+)	0.502	

Trans and *cis* conformations of (-) and (+) isomers were subjected to dihedral driver calculations (HYPERCHEM) through the syn and anti positions, in 20° steps (Figure 4.2a). The approximately symmetrical energy profiles of these isoforms indicate a slight preference for the syn form, with movement of the ring systems away from orthogonality creating energetically less favourable conformations by some 6.7±0.6 kcal/mol. Beers-Reich distances (Figure 4.2b) were 4.66±0.02Å for (-) and (+) isoforms in the absolute syn configuration (i.e. 0°), with the most favourable distances (i.e. 4.8±0.3Å) occurring between -20° to 160° for (-)nicotine (Figure 4.2b), though energy penalties are incurred. The reverse is true for the (+) isomer.

Nicotine monomethiodide - Minimised N-methylated (-)nicotine conformations (both *trans* and *cis*), constructed and analysed using HYPERCHEM, generated the total potential energy values and Beers-Reich distances represented in table 4.3.

Table 4.3

	(-) trans syn	*(-) trans anti*	*(-) cis syn*	*(-) cis anti*
N+/N- Dist (Å)	4.54	4.48	4.54	4.50
Disposition of rings (°)	-25.08	162.34	-25.47	163.41
Total Energy	58.735	58.846	57.788	57.918

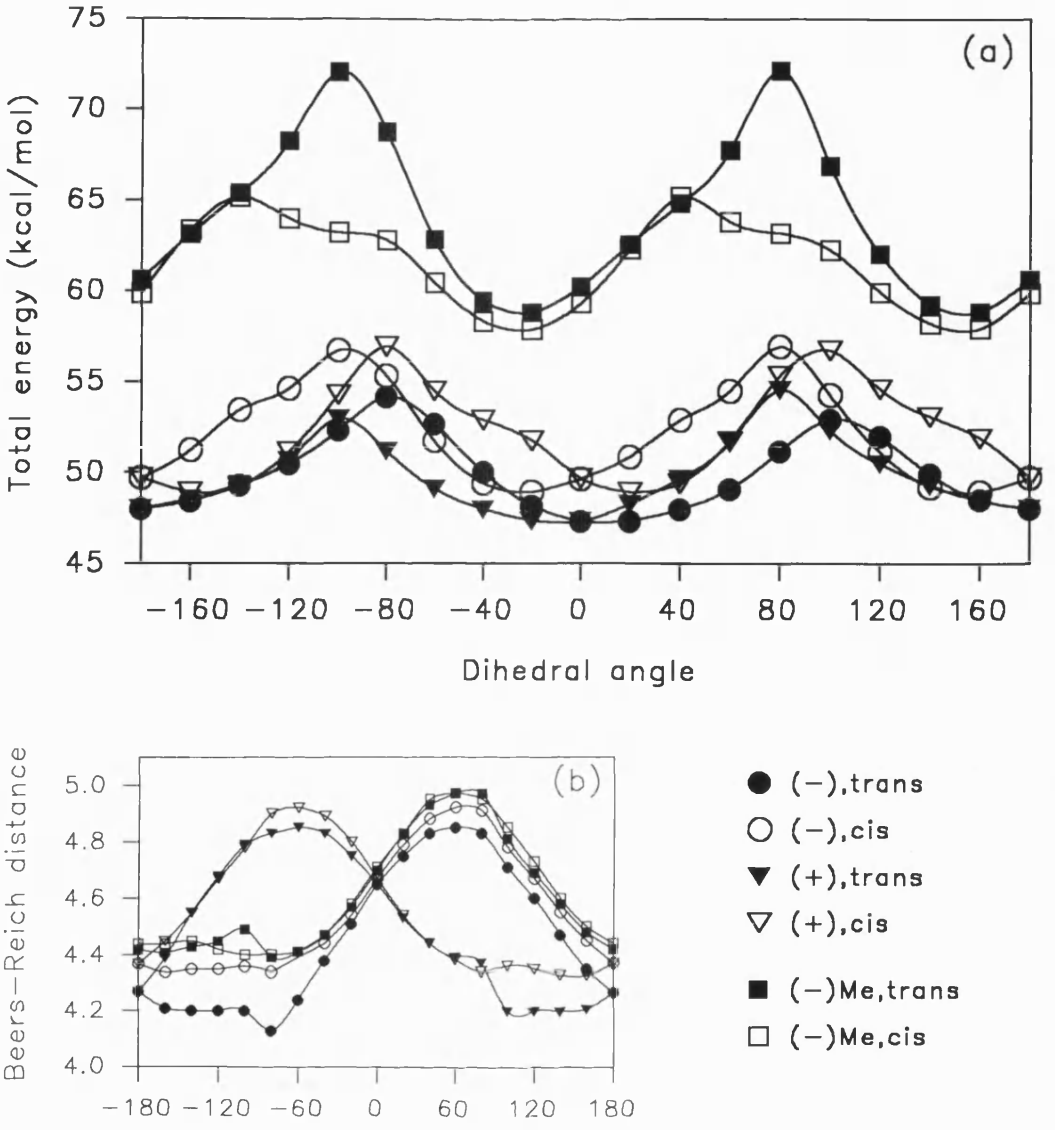

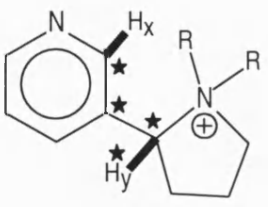

★ dihedral angle atoms

/ syn/anti hydrogens

Figure 4.2: Comparison of isomers of nicotine and nicotine mono-methiodide using computational chemistry. Intermediate conformations of trans and cis forms of each structure were explored by rotation of the dihedral angle associated with the two ring systems as indicated on the core structure (★), in 20° increments, with minimisation at each step (see section 4.2.4). Changes to (a) the total energy (kcal/mol), and (b) the Beers-Reich distance (Å) were monitored. In this case 0° implies a syn arrangement about the ring hydrogens indicated. Graphs represent calculations performed on the lowest energy conformers.

A *cis* arrangement of the same methyl carbon as used for (-)nicotine was energetically favoured over *trans*, with essentially no preference for the syn or anti forms. When (-)*trans*, anti was compared to (+)AnTx as previously, the following RMS fit of crucial pharmacophore points was observed (inset 6):

Nitrogens (secondary and pyridine)	(-)	0.261	(6)
All atoms	(-)	0.754	

This conformer best matched the conformation of (+)AnTx, though in order to attain the lowest RMS values a slight energy penalty was incurred. Rotation of the dihedral angle between the two ring systems from syn through anti to syn positions (Figure 4.2a) revealed a similar energy profile to nicotine, though the extra bulk of the methyl created pronounced clashes when the ring systems were moved away from orthogonal. This was more significant in the *trans* conformer ($\Delta E_{syn\text{-}anti}$=~14kcal/mol). Nitrogen-nitrogen distances were on average about 0.1Å greater than those for (-)nicotine though were more pronounced (up to 0.3Å) in the sweep between -180° to 0°, when the clash between methyls and pyridine ring force the nitrogens further apart as a result of electrostatic repulsion and the extra hydrophobic bulk (Figure 4.2b).

4.3.3 Conformers of substituted piperazine molecules

Piperazine is closely homologous to the cyclohexane ring which characteristically has multiple important minimum energy conformers which are accessed only by surmounting comparatively large energy barriers. The two basic low energy forms of this ring structure are the structurally rigid chair and the more flexible boat. In the former several of the C-C bonds are completely staggered, whereas the latter has C-C ring bonds which are eclipsed. Interconversion between the conformers requires around 10 kcal/mol making it possible at room temperature.

Simple substituted cyclohexanes will generally assume the chair conformation with substituents in equatorial and axial positions with respect to the ring plane - the equatorial position avoids the non-bond repulsive forces experienced by the axial substituent, so is consequently more stable. As substituent size increases, and therefore becomes sterically more demanding, so the equatorial conformer is increasingly favoured.

The tetrahedrally hybridised and trigonal nitrogen atoms, and the saturated 6-membered ring system of piperazine make for a structure which approximates to cyclohexane. Both chair and boat conformations of the three substituted piperazines (viz. DMPP, AMP.HCl and AMP.MeI - see structures with 2.3.5.3), were modelled, though AMP.MeI was too energetically unstable to adopt any form of boat conformation due to the presence of the two methyls. Chair arrangements generated using HYPERCHEM were preferentially adopted by both DMPP and AMP.MeI (Table 4.4) which are dimethylated at the tetrahedral nitrogen. N-O distance was monitored for these structures, as was the dihedral angle (★) depicted in the inset of figure 4.3

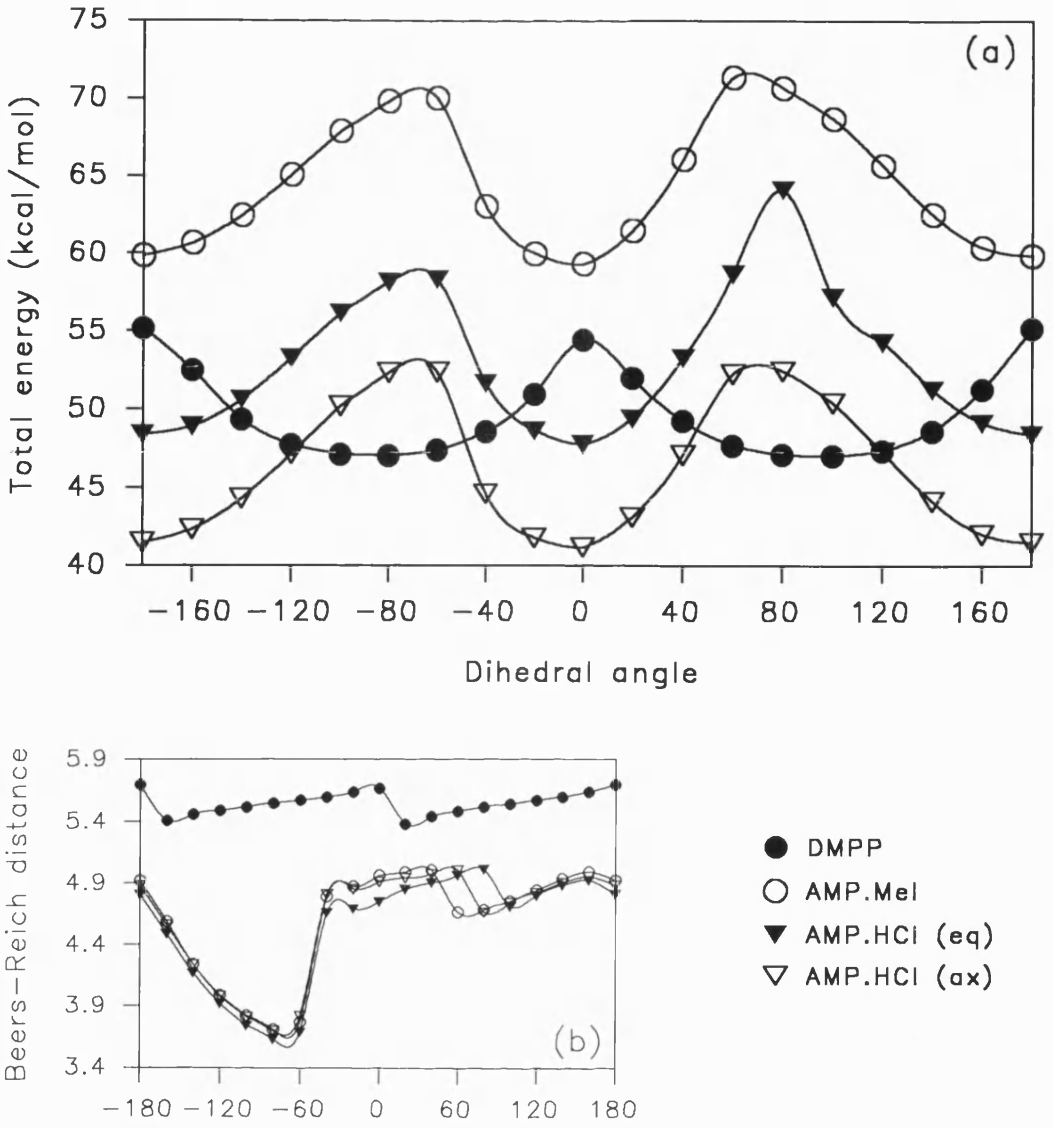

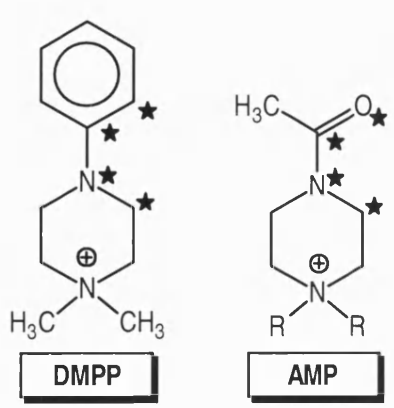

Figure 4.3: Comparison of piperazinium analogues using computational chemistry. Intermediate conformations of chair forms of each structure were explored by rotation of the dihedral angle indicated on the core structures (★) in 20° increments, with minimisation at each step (see section 4.2.4). Changes to (a) the total energy (kcal/mol), and (b) the Beers-Reich distance (Å) were monitored. Graphs represent calculations performed on the lowest energy chair conformers, and include both equatorial (eq) and axial (ax) forms of AMP.HCl.

Table 4.4

	E Chair (kcal/mol)	*N-O (Å)*	*Φ (°)*	*E Boat (kcal/mol)*	*N-O (Å)*	*Φ (°)*
DMPP	47.022	5.55	95.5	58.356	5.34	104.78
AMP.MeI	59.307	4.96	1.47	Too unstable to create		

The chair conformer of AMP.HCl, in which the methyl was in the axial position, was the lowest energy form of this structure though, notably, the chair, equatorial conformer was the most energetically unstable, even when compared to the boat (Table 4.5).

Table 4.5

	Total E (kcal/mol)	*N-O (Å)*	*Φ (°)*
Chair (ax)	41.078	4.90	-5.38
Chair (eq)	47.742	4.76	-3.23
Boat (ax)	43.689	4.97	2.05
Boat (eq)	44.478	4.69	-4.53

The benzene ring of DMPP lies orthogonal to the plane of the piperazine ring, optimising the overlap of ring hydrogens with little preference for syn or anti conformations. Deviations from this arrangement (Figure 4.3a) introduces non-bond repulsive interactions which in general increase the energy of the system by 7.045±0.351 kcal/mol. In the lowest energy form of the boat conformer, which is less stable than the chair by some 11.334 kcal/mol, the main contributions to this instability seem to originate from mainly unfavourable torsion, but also non-bonded and electrostatic (coulomb) interactions (Table 4.6).

Table 4.6

	E Chair (kcal/mol)	*E Boat (kcal/mol)*	*Δ E*
Torsion (phi)	-1.322	7.869	8.967
Non-bond	10.308	12.328	2.020
Coulomb	32.274	30.823	1.451

Because of the dispersed nature of the pi electron system associated with the benzene ring, which substitutes for the carbonyl pi system, the Beers-Reich distance has a certain amount of flexibility, though here it was taken to be the to the centre of the ring. As a result, distances from the cationic nitrogen to benzene carbon are consistently high (chair=5.54±0.09Å (Figure 4.3b), boat=5.32± 0.09Å) which are outside the acceptable limits for this distance (4.8±0.3Å), implying association with the complementary receptor point is possibly nearer C2 or C6 of the benzene ring, depending on the orientation.

Conversely, the acetyl group of AMP.MeI prefers to be coplanar with the piperazine ring as evinced by the dihedral angle C-N-C=O (Figure 4.3a and inset), being slightly more stable in the *cis* than *trans* configuration (ΔE=0.5kcal/mol). Deviations of up to 60° either side of *cis* increase the potential energy by a maximum of 11.068±0.997kcal/mol, the largest comparative differences being in the torsion energy (ΔE=12.037±0.776 kcal/mol). Beers-Reich distances are not satisfied between -160° and -50° (Figure 4.3b), though are in good agreement with the literature value for the two minima observed for *cis* and *trans*. Boat conformations of this dimethylated piperazinium were very unstable.

As mentioned above, AMP.HCl is also at its most stable in the chair form when the N-C(H_3) bond is axial. Again two minima are observed when the carbonyl is in either the *cis* or *trans* arrangement (bond C-N-C=O), with the potential energy rising by some 11kcal/mol in the orthogonal orientation relative to the ring position (Figure 4.3a). The chair, equatorial conformation incurs a 6.607 kcal/mol energy penalty in the *cis* configuration, largely due to steric clash of the methyl hydrogens with the C2 and C6 hydrogens which are forced to converge. In the boat configuration, there is little preference for the same methyl being axial or equatorial (ΔE=0.823 kcal/mol), but slightly larger energy penalties are incurred, relative to chair AMP.HCl, when the carbonyl is rotated out of planarity, due to the much closer proximity of the C=O and CH_3 of the acetyl side chain with the axial methyl of the tertiary nitrogen.

Significant differences (up to 1.55Å) are observed in the Beers-Reich distances for boat, axial and boat, equatorial conformations of AMP.HCl (not shown). Distances are smaller in the equatorial form as the carbonyl is rotated into the -90° position over the ring where steric clash is less pronounced, when compared to axial CH_3 forms. Consequently, the charged headgroups come close enough (within 2.83Å) to partially shield the electrostatic forces of the two species as the carbonyl oxygen moves over the ring. In terms of the pharmacophore and bioactive conformation, this configuration is unacceptable.

4.3.4 Anatoxin-a and its analogues

Anatoxin is now a well established probe for investigating the nAChRs of both muscle and brain. Among its many attributes are its stereospecificity, extreme agonist potency (see sections 2.3.5.4 and 3.3.3.4), semi-rigid structure and the amenability of its functional sidechain to chemical modification. As such the structural analogues of anatoxin are numerous and have made the structure the focus of extensive structure-activity relationships (SARs) at both muscle and brain nAChR sites. A series of eighteen analogues of anatoxin, assessed for their nicotinic pharmacology at peripheral (Swanson *et al* 1991) and neuronal (Wonnacott *et al* 1991) sites (Table 4.7), provided the opportunity to attempt to correlate observed affinities with possible conformations of these ligands. As such, these carbonyl, alcohol, amide and N-methylated derivatives were modelled and a summary of the pharmacological profiles of these derivatives is given in table 4.7. Also modelled were analogues (Thomas *et al* 1994), designed specifically to determine the absolute *cis* or *trans* configuration of the carbonyl group in the enone system and the effects on biological activity.

Analogue	Abbreviation	Sidechain structure R_1	R_2	[^{3}H]nicotine K_i (M)	[^{125}I]αBgt K_i (M)
Carbonyls					
(+)anatoxin-a	AnTx	-C=O	$-CH_3$	$3.5\pm1.1\times10^{-9}$	$3.8\pm2.1\times10^{-7}$
Dihydroanatoxin	H_2AnTx	-C=O	$-CH_3$	$2.7\pm1.0\times10^{-8}$	$1.2\pm0.5\times10^{-6}$
Anatoxinic acid methyl ester	AnTx-ME	-C=O	$-OCH_3$	$3.7\pm1.3\times10^{-8}$	$2.6\pm0.7\times10^{-6}$
Anatoxinal	AnTxal	-C=O	-H	$9.0\pm2.0\times10^{-7}$	$>2\times10^{-4}$
α-Hydroxyanatoxin	AnTxαOH	-C=O	$-CH_2OH$	$2.6\pm1.5\times10^{-6}$	$>2\times10^{-4}$
Alcohols					
Anatoxin(10S)alcohol	AnTx-(S)ol	-C-OH-H	$-CH_3$	$6.5\pm0.5\times10^{-7}$	$6.5\pm2.0\times10^{-5}$
Anatoxin(10R)alcohol	AnTx-(R)ol	-C-H	$-OH-CH_3$	$4.6\pm0.9\times10^{-6}$	$>2\times10^{-4}$
Noranatoxinol	AnTx-Norol	-C-OH-H	-H	$2.5\pm0.5\times10^{-5}$	$>2\times10^{-4}$
Anatoxin-10-methyl alcohol	AnTx-mol	-C-OH	$-(-CH_3)_2$	$1.5\pm2.8\times10^{-4}$	
Amides					
Anatoxinic acid isoxazolide	AnTx-isox	-C=O	$-NO(CH_2)_3$ cyclic	$3.6\pm1.0\times10^{-8}$	$4.0\pm0.2\times10^{-5}$
Anatoxinic acid methoxyamide	AnTx-NOMe	-C=O	$-NH-OCH_3$	$4.1\pm1.0\times10^{-8}$	$3.1\pm0.7\times10^{-5}$
Anatoxinic acid dimethylamide	AnTx-Me_2N	-C=O	$-N(CH_3)_2$	$1.9\pm1.0\times10^{-6}$	$1.3\pm0.5\times10^{-5}$
Anatoxinal-O-methyl oxime	AnTx-MeOX	$-C=NOCH_3$	-H	$1.8\pm0.9\times10^{-6}$	$7.5\pm3.0\times10^{-5}$
N-methylated					
N-methylanatoxin	Me-AnTx	-C=O	$-CH_3$	$2.6\pm0.5\times10^{-6}$	2×10^{-4}
N-dimethylanatoxin	Me_2-AnTx	-C=O	$-CH_3$	$2.0\pm0.3\times10^{-6}$	$7.5\pm3.5\times10^{-5}$
N-methylanatoxinic acid methyl ester	Me-AnTx-ME	-C=O	-OCH3	$1.2\pm0.3\times10^{-5}$	$>2\times10^{-4}$
(10S)-N-methylanatoxinol	Me-AnTx-(S)ol	-C-OH-H	$-CH_3$	$>2\times10^{-4}$	$>2\times10^{-4}$
(10R)-N-methylanatoxinol	Me-AnTx-(R)ol	-C-H-OH	$-CH_3$	$>2\times10^{-4}$	$>2\times10^{-4}$
N,1'-dimethylanatoxinol	Me-AnTx-mol	$-C-OH-CH_3$	$-CH_3$	$>2\times10^{-4}$	$>2\times10^{-4}$

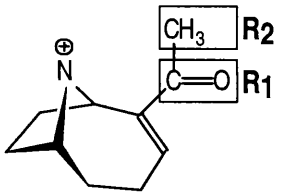

(+)AnTx

Table 4.7: Sidechain structure and inhibition binding parameters for anatoxin anologues. Values for the inhibition of ligand binding were taken from Wonnacott *et al* (1991), where anatoxin analogues were assessed in competition binding assays on rat P_2 membranes using [^{3}H](-)-nicotine and [^{125}I]αbungarotoxin according to the method of Rapier *et al* (1990). Ki values were calculated using the relationship $K_i=IC_{50}/(1+[L]/K_d)$. The synthesis of the analogues have been described elsewhere (Sardina *et al* 1989; Howard *et al* 1990).

4.3.4.1 Carbonyls - In the case of all these structures the accepted pharmacophore points suggested by Beers and Reich (1970), namely the quaternary nitrogen and carbonyl dipole, were retained (inset 7). AnTx is >99% protonated at physiological pH with a pKa=9.36. The likely bioactive

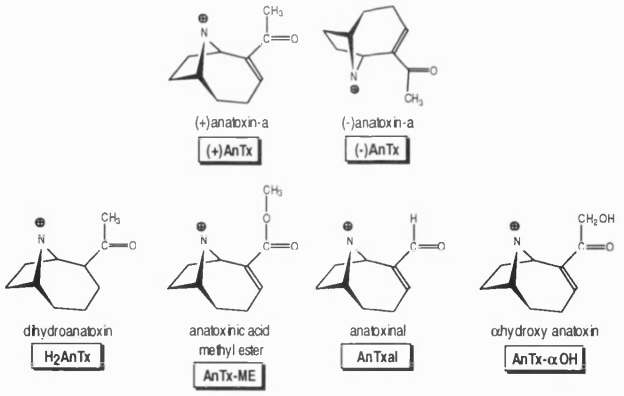

(7)

conformation for AnTx has been suggested to be where the carbonyl moiety of the enone system is either *cis* (chair or boat: Hacksell & Mellin 1989: Koskinen & Rapoport 1985: Witkop & Brossi 1984), or *trans* (chair: Hacksell & Mellin 1989). As activity resides in the (+) form of AnTx, all derivatives were built as the (+) isomer and manipulated to achieve boat and chair conformations, (which included (-)anatoxin) - total energy values for the minimum energy conformations are given in table 4.8. As can be seen chair forms are preferred, with the carbonyl in the *trans* position (Φ~180°) - the decreased stability of boat forms can be attributed to steric crowding.

Table 4.8

	Boat			Chair		
	E (kcal/mol)	*N-O (Å)*	*Φ (°)*	*E (kcal/mol)*	*N-O (Å)*	*Φ (°)*
(+)AnTx	49.399	4.06	178.84	48.405	3.75	-179.22
(-)AnTx	49.398	4.06	-178.86	48.406	3.75	179.25
H_2AnTx	41.746	4.21	-174.49	41.228	3.26	-156.63
AnTx-ME	37.121	4.06	178.87	36.333	3.74	-179.37
AnTxal	57.134	4.13	179.27	56.319	3.83	-179.37
AnTx-αOH	68.710	4.05	175.13	67.817	3.75	176.98

The relatively small distances between nitrogen and carbonyl oxygen, in both chair and boat low energy forms of the carbonyls, suggest the *cis* conformation might better fit these pharmacophore points. This was born out by subjecting the torsion angle defined by C=C-C=O (see inset of figure 4.4) in each analogue to dihedral driver calculations and monitoring the energy variation (Figure 4.4a) and the effects on the Beers-Reich distance (Figure 4.4b) introduced by these changes. Although energies were generally higher in the *cis* position, N-O distances were better fulfilled, being 4.57±0.05Å for the chair forms - the closest agreement with the Beers-Reich distance was

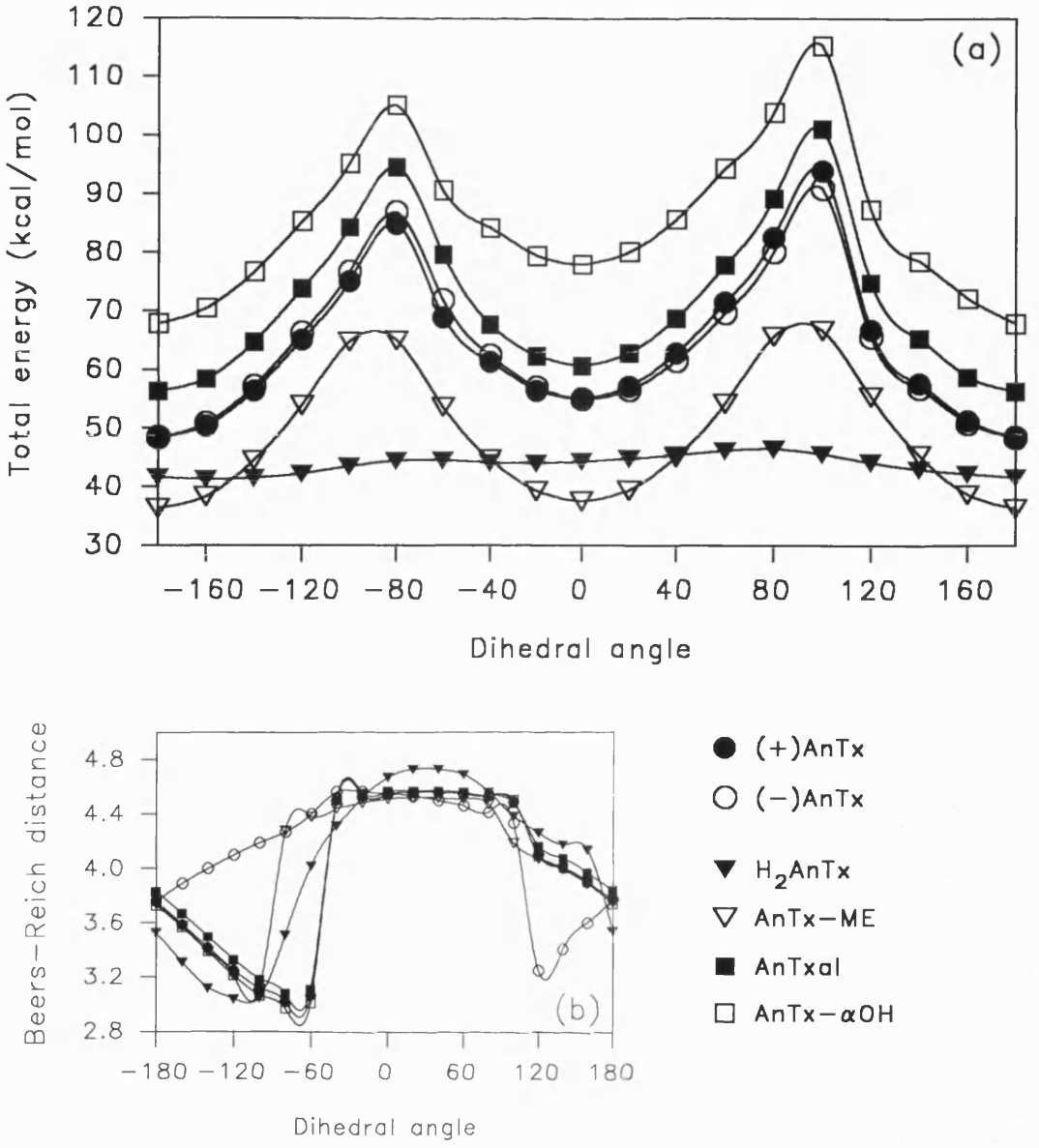

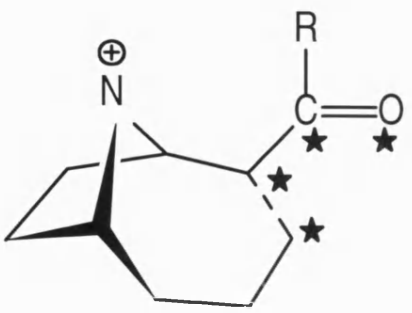

Figure 4.4: Comparison of carbonyl analogues of (+)anatoxin using computational chemistry. Intermediate conformations of chair forms of each structure, including (-)anatoxin, were explored by rotation of the dihedral angle, (C=C-C=O) indicated on the core structure (★), in 20° increments, with minimisation at each step (see section 4.2.4). Changes to (a) the total energy (kcal/mol), and (b) the Beers-Reich distance (Å) were monitored. Graphs represent calculations performed on the lowest energy twist, chair conformers.

achieved by boat conformations (4.72±0.02Å for all derivatives). As the cationic and hydrogen-bond acceptor moiety are prerequisites for the model of the pharmacophore interacting with the receptor, their spatial displacement (distance apart) is important and should fulfil the basic criteria laid down by other active ligands, even if there is some energetic cost. With this in mind, the bioactive conformations of AnTx and its carbonyl derivatives are probably (+) boat, *cis*, as the Beers-Reich pharmacophore distance is fulfilled, despite the energy penalty incurred - although the *cis* position is a local minimum in every case. Energy penalties incurred in achieving the distances are shown (Table 4.9) for boat and chair structures.

Table 4.9

	Boat (cis → trans)		Chair (cis → trans)	
	Δ E (kcal/mol)	Δ N-O (Å)	Δ E (kcal/mol)	Δ N-O (Å)
(+)AnTx	5.903	0.64	6.636	0.79
(-)AnTx	6.108	0.65	6.528	0.79
H_2AnTx	2.442	0.54	2.686	1.14
AnTx-ME	1.044	0.64	1.190	0.77
AnTxal	1.141	0.61	4.388	0.74
AnTx-αOH	4.063	0.66	10.123	0.82

Differences in N-O distance between *cis* and *trans* for (+) and (-) AnTx are similar in boat and chair forms but, as can be seen from figure 4.4b, in orientations where the enone carbonyl lies in between *cis* and *trans*, the distances are quite different (up to 1.4Å at -60°) which may partially contribute to the differences in activity (Table 4.7).

Removal of conjugation in the azabicyclononene ring (H_2AnTx) reduces the potential energy of the structure by some 6.782 kcal/mol (chair, *trans*), radically reducing the stresses imposed on the structure through the rotation of the carbonyl group which originate from large torsion energies (inset 8 - AnTx (●), H_2AnTx (○)).

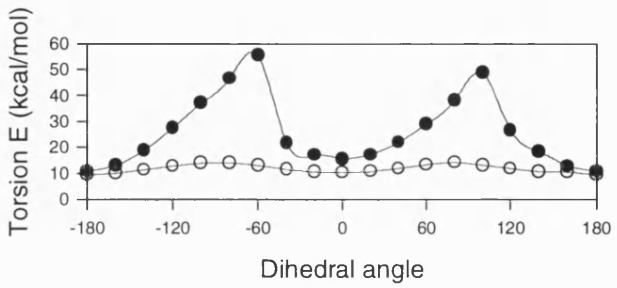

(8)

The lowest global minimum energy conformation among the carbonyls is seen in AnTx-ME which is 12.277 and 12.073 kcal/mol lower in energy than the respective (+)boat and (+)chair conformers of AnTx. The main differences occur in the electrostatic energy which is roughly 14.6 kcal/mol lower in AnTx-ME in which the pi system of C=O is more delocalised being associated with the additional oxygen.

4.3.4.2 Alcohols - Primary (AnTx-norol), secondary (AnTx-(S)ol and AnTx-(R)ol), and tertiary (AnTx-mol) alcohols (inset 9) exhibited lower global minimum energy conformations than the parent

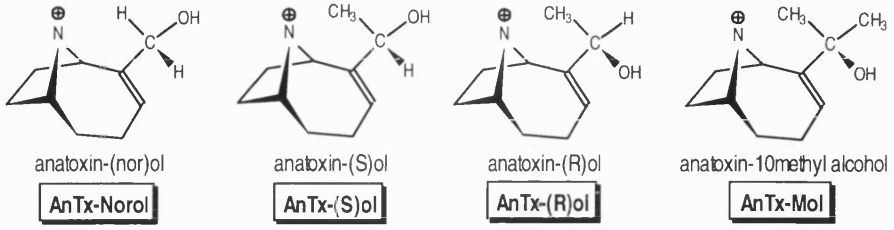

(9)

AnTx (Table 4.10). Chair conformations were slightly favoured. Rotation of the dihedral angle (which specified the OH group as the anionic centre - see inset of figure 4.5), revealed at least three local energy minima for each analogue (Figure 4.5a), but the torsional barriers between these were relatively small (Chair conformations: largest = 5.656 kcal/mol (AnTx-(R)-ol), smallest = 0.133 kcal/mol (AnTx-mol)), due largely to the absence of the conjugated carbonyl. Beers-Reich distances varied more widely among the alcohols than the carbonyls partly due to the longer O-H bond, and were better fulfilled in boat conformations (not shown) being 4.85±0.02Å in the *cis* position, though global minima of both chair and boat structures of all analogues had unsatisfactory N-O distances (Table 4.10).

Table 4.10

	Boat			*Chair*		
	E (kcal/mol)	*N-O (Å)*	*Φ (°)*	*E (kcal/mol)*	*N-O (Å)*	*Φ (°)*
AnTx-norol	48.277	4.03	-118.76	46.919	3.44	-120.72
AnTx-(S)-ol	48.038	4.24	142.85	46.842	3.37	-121.68
AnTx-(R)-ol	48.776	3.97	-123.50	47.564	3.53	-137.92
AnTx-mol	48.143	4.12	161.34	47.509	3.46	-138.23

Consequently bioactive conformations are likely to be those in the higher energy saddles where the OH group is approximately *cis* with respect to the C=C bond of the ring. Interestingly, the double methylated AnTx-mol appears not to sterically inhibit the rest of the structure to any significant extent, and the extra methyl bulks do not adversely alter the observed distances between nitrogen and oxygen atoms. Absence of the pi electrons associated with the carbonyl dipole create a weaker hydrogen bond acceptor which is likely to contribute significantly to the reduced activity associated

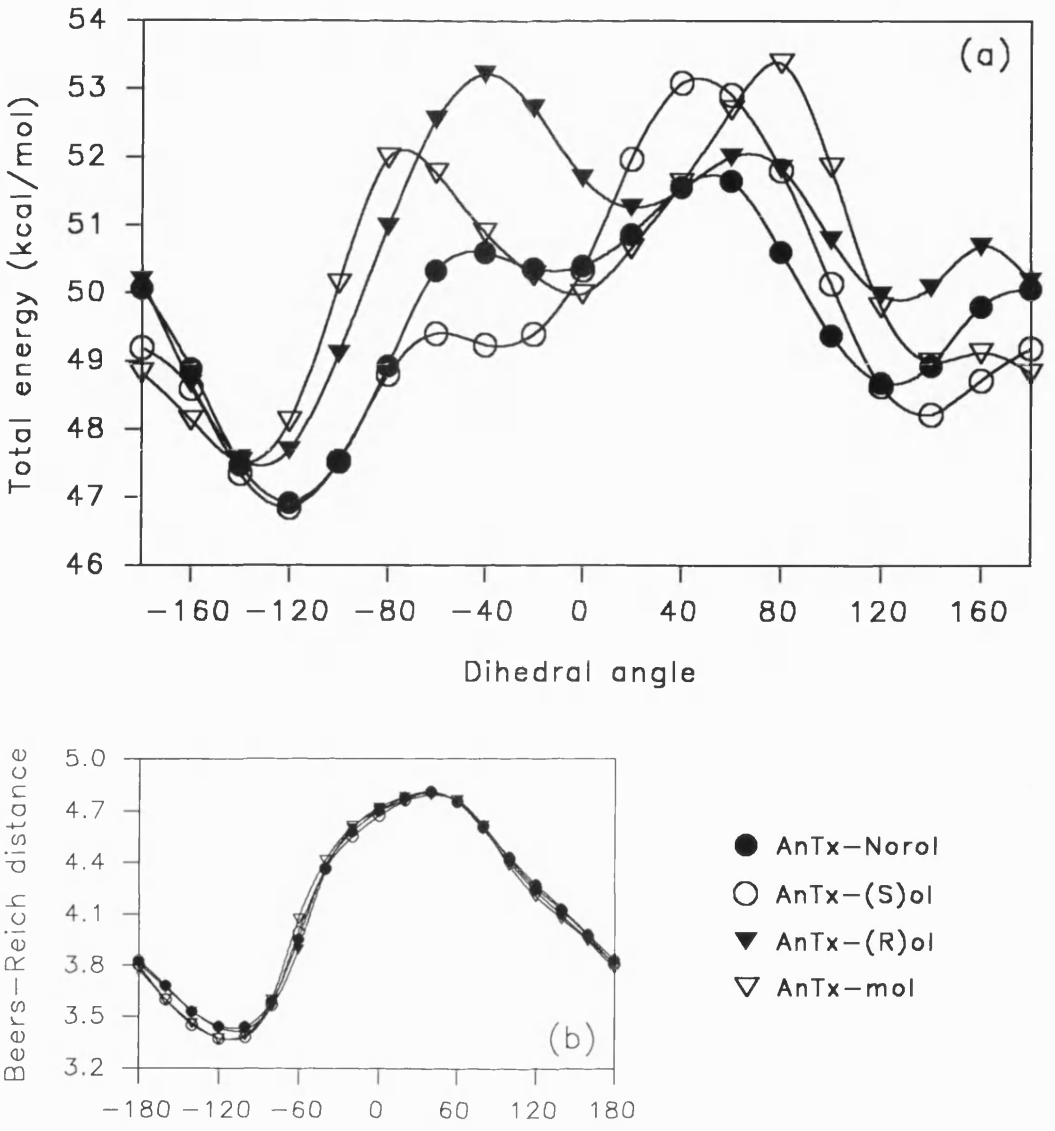

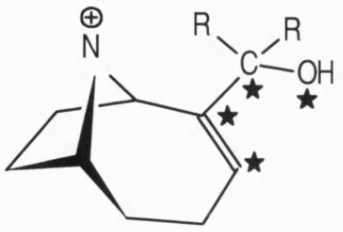

Figure 4.5: Comparison of alcohol analogues of (+)anatoxin using computational chemistry. Intermediate conformations of chair forms of each structure were explored by rotation of the dihedral angle (C=C-C-O) indicated on the core structure (★) in 20° increments, with minimisation at each step (see section 4.2.4). Changes to (a) the total energy (kcal/mol), and (b) the Beers-Reich distance (Å) were monitored. Graphs represent calculations performed on the lowest energy twist, chair conformers.

with these structures (Table 4.7). The hydrophobic nature of the substituent groups allied to the sidechain will also greatly influence the electronegative character of the hydroxyl.

4.3.4.3 Amides - Global minima were observed for all these analogues, (where a nitrogen is attached to the carbonyl - inset 10), in the chair conformers, except AnTx-MeOX which slightly favoured the boat configuration (Table 4.11).

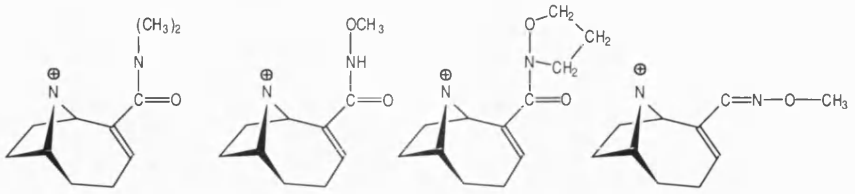

anatoxinic acid dimethylamide **AnTx-Me$_2$N** | anatoxinic acid methoxyamide **AnTx-NOMe** | anatoxinic acid isoxazolidide **AnTx-isox** | anatoxinic acid O-methyloxime **AnTx-MeOX**

(10)

Table 4.11

	Boat			Chair		
	E (kcal/mol)	*N-O (Å)*	*Φ (°)*	*E (kcal/mol)*	*N-O (Å)*	*Φ (°)*
AnTx-Me$_2$N	43.019	4.00	-160.37	41.562	3.52	-154.21
AnTx-NOMe	56.799	4.05	178.41	56.171	3.69	-175.70
AnTx-isox	52.255	4.08	169.04	51.434	3.81	170.28
AnTx-MeOX	53.372	4.24(N-N)	174.35	54.189	4.02(N-N)	173.57

In the case of AnTx-Me$_2$N, AnTx-NOMe and AnTx-isox the pi electrons associated with the carbonyl will be more delocalised due to the proximity of the nitrogen with its lone pair of electrons. AnTx-MeOX, which has the C=O substituted by a nitrogen juxtaposed with an oxygen atom, will have similarly well dispersed electronegative character. Each analogue introduces charged bulk around the hydrogen bond acceptor moiety, yet this does not seem to affect activity too adversely (Table 4.7), with AnTx-isox and AnTx-NOMe being only some 10 times less active than the parent (+)AnTx. In each of the analogues case, this bulk can be directed away from the nitrogen cationic head because of the flexibility of the amide-bonded side chain, including the cyclic AnTx-isox. The energy barriers to rotation between *cis* and *trans* forms (Figure 4.6a) are relatively small compared to the carbonyl analogues for example, the largest being for AnTx-MeOX in the chair form (22.5 kcal/mol). Several energy minima can be observed for the tricyclic AnTx-isox due to a number of chiral centres in the side chain and the saturated nature of the five membered ring system. A pseudo-chair arrangement of the amine ring is preferred. Beers-Reich distances for these species are acceptable for the pharmacophore model in chair, *cis* conformations (Figure 4.6b), though there are obviously significant attractive forces as the amide side chains pass over the azabicyclononene ring as distances reduce towards ~3Å in chair conformations in all but AnTx-MeOX. It is the boat forms which increase the ionic headgroup separation most probably forced by steric clash.

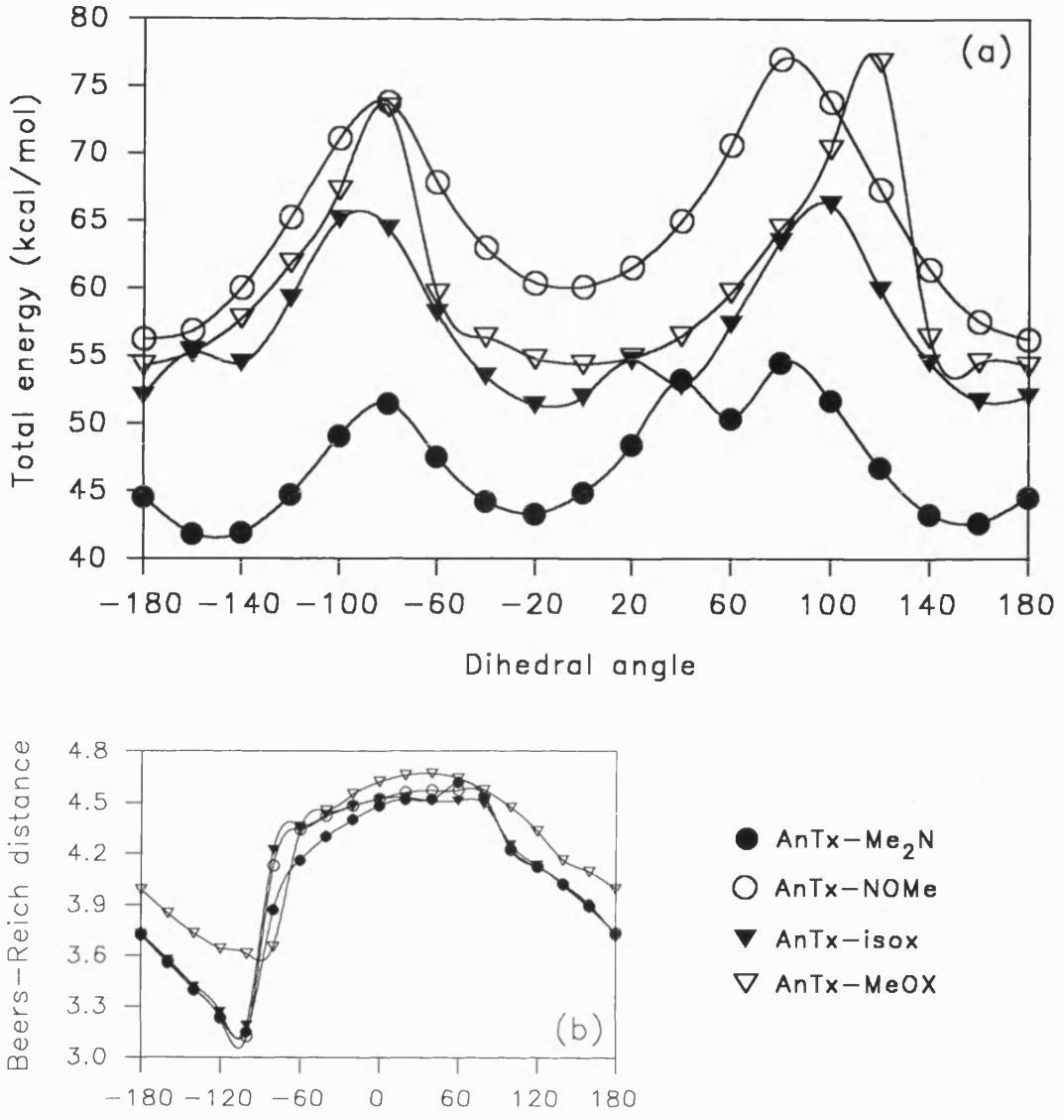

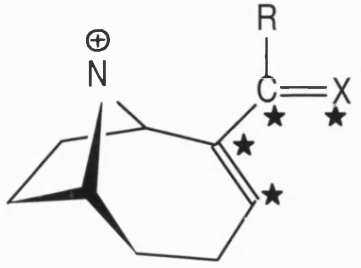

Figure 4.6: Comparison of amide analogues of (+)anatoxin using computational chemistry. Intermediate conformations of chair forms of each structure were explored by rotation of the dihedral angle (C=C-C=X) indicated on the core structure (★) in 20° increments, with minimisation at each step (see section 4.2.4). Changes to (a) the total energy (kcal/mol), and (b) the Beers-Reich distance (Å) were monitored. Graphs represent calculations performed on the lowest energy twist, chair conformers.

It is therefore difficult to assess bioactive conformation when so many electron-rich species are present in the sidechain, as the electronegative character is diffuse, unlike the directional dipole associated with the carbonyl group of other analogues. These analogues are useful in that they provide information regarding the extent and directionality of the electronegative character required for activity at one receptor subtype or another, and additionally probe the accessible volume of the binding pocket.

4.3.4.4 N-methylated anatoxins - Addition of one methyl unit to the nitrogen of (+)AnTx (inset 11) incurs an energy penalty of 13.901 kcal/mol in the global energy minimum conformer, and 22.661 kcal/mol in the dimethylated structure (Table 4.12). This energy increase was found to be similar for the methylation of other analogues.

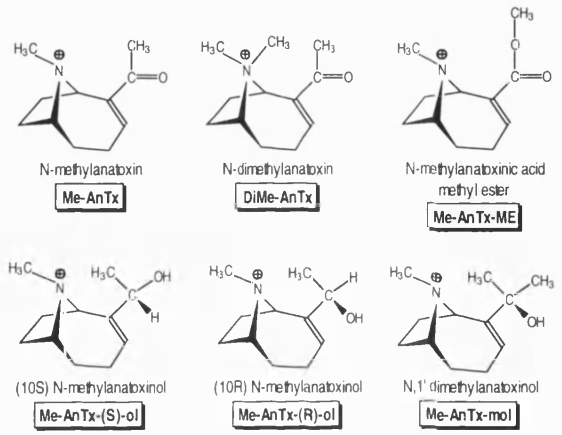

(11)

Table 4.12

	Chair, trans		
	E (kcal/mol) Me	*E (kcal/mol) Non-Me*	*Δ E (Me↔ NonMe)*
Me-AnTx	62.306 (R)	48.405	13.901
DiMe-AnTx	71.066	48.405	22.661
Me-AnTx-ME	50.323 (R)	36.333	13.999
Me-AnTx-(S)-ol	60.117 (R)	46.842	13.275
Me-AnTx-(R)-ol	60.877 (R)	47.442	13.435
Me-AnTx-mol	69.605 (R)	49.970	19.635

Commensurate with (+)AnTx, the mono- and di-methylated forms (inset 11) prefer a chair, *trans* conformation with the methyl preferably in an R configuration about the chiral nitrogen. The energy barriers to conversion between *trans* and *cis* forms (Figure 4.7a) are only as pronounced as in the non-methylated structures. There is obvious steric clash of the bulky methyls associated with Me-AnTx-mol which increases the energy of the system by about 8 kcal/mol above the comparative methylation of (S) and (R) forms of Me-AnTx-ol. Methylation does not make the Beers-Reich

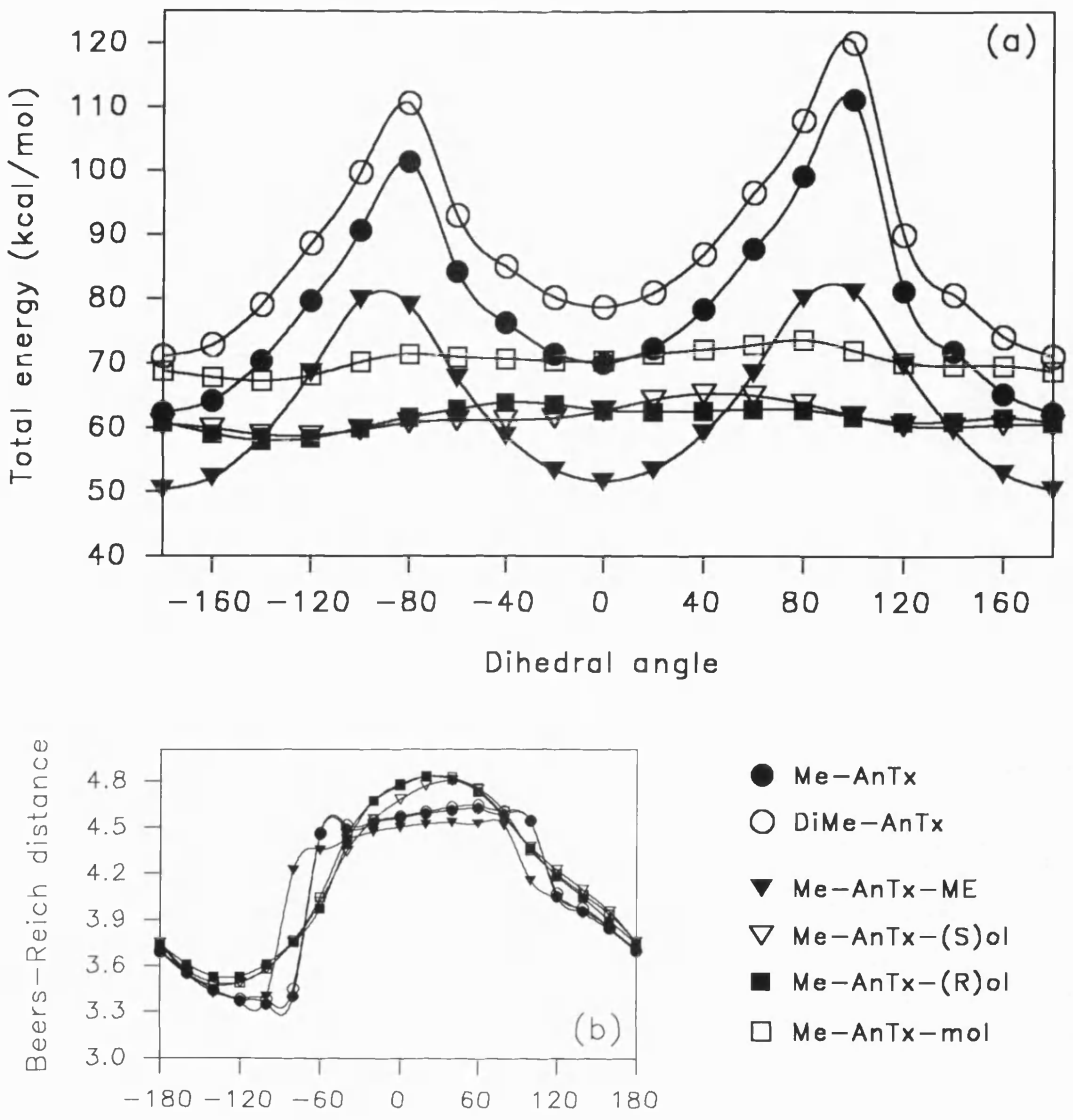

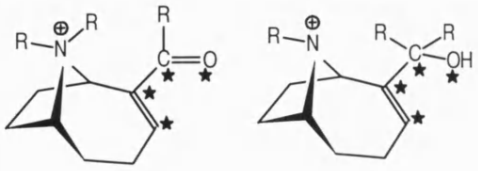

Figure 4.7: Comparison of N-methylated analogues of (+)anatoxin using computational chemistry. Intermediate conformations of chair forms of each structure were explored by rotation of the dihedral angle indicated on the core structures (★) in 20° increments, with minimisation at each step (see section 4.2.4). Changes to (a) the total energy (kcal/mol), and (b) the Beers-Reich distance (Å) were monitored. Graphs represent calculations performed on the lowest energy twist, chair conformers with the N-methyl monomethylated structures in the (R) form.

distance significantly more or less favourable in any case (Figure 4.7b). It therefore looks as though the principle results of N-methylation are an inevitable decrease in stability and added bulk around an important pharmacophore point. Otherwise, the conformations are essentially the same as for the non-methylated analogues implying that the bioactive forms will be the same. Biological activity of these same analogues (Table 4.7) is reduced by at least 100-fold in nearly every case. If the bioactive conformations are the same as the non-methylated molecules then this reduction in activity may be exclusively attributable to interference with the volume, and extent over which the positive charge is distributed around the nitrogen.

4.3.4.5 Alkyl-modified sidechain analogues - Approaches to determine the bioactive conformation of (+)AnTx, by restricting movement around the acetyl sidechain, were invoked through the addition of one or more methine or methylene units to the anatoxin sidechain (Thomas *et al* 1994). These

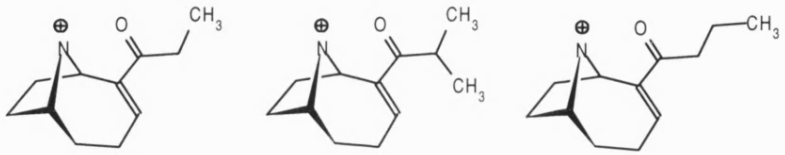

(12)

derivatives, designated HomoAnTx, PropylAnTx and IsopropylAnTx (inset 12), have been assessed for their biological potency (see sections 2.3.5.4 and 3.3.3.4) and the likely bioactive conformations modelled.

Chair conformations of all analogues were the most stable, and, as with the parent (+)AnTx, the *trans* configuration of the enone dihedral (see inset of figure 4.8) was favoured (Table 4.13).

Table 4.13

	Chair, trans		*Chair, cis*		*Boat, trans*		*Boat, cis*	
	E (kcal/mol)	*N-O (Å)*	*E (kcal/mol)*	*N-O (Å)*	*E (kcal/mol)*	*N-O (Å)*	*E (kcal/mol)*	*N-O (Å)*
HomoAnTx	48.067	3.74	53.482	4.53	48.786	4.05	53.510	4.69
PropylAnTx	50.167	3.74	55.825	4.55	50.900	4.05	55.799	4.71
IsopropylAnTx	51.887	3.71	57.099	4.55	52.395	4.02	56.528	4.71

The difference in energy between *trans* chair and boat forms was not significant (0.653±0.103 kcal/mol) so both forms should be well populated. *Trans* conformers were some 5.428±0.182 kcal/mol (chair) and 4.585±0.328 kcal/mol (boat) lower in energy than corresponding *cis* forms, which are roughly 1kcal/mol less than that observed for (+)AnTx (6.636 kcal/mol (chair), 5.903 kcal/mol (boat)), a difference attributable to the extra bulk of the additional methine/methylene units. The increased hydrophobic bulk α to the carbonyl carbon has no significant influence on the preference for *trans* as deviations from the mean energy are small. The enone moiety (C=C-C=O)

adopts a very planar arrangement in global minima of all analogues (-178.82±0.26°) - the crystal structure of AnTx.HCl (Koskinen and Rapoport 1985) is distorted by ~18°. All other conformations explored by dihedral driver calculations of the enone moiety (Figure 4.8a) increased the energy of each system.

Beers-Reich distances are best fulfilled by boat, *cis* structures (Table 4.13) whereas in *trans* configurations (especially chair), these pharmacophore points are in close proximity (Figure 4.8b), though with an obvious energetic advantage. Given the small energy barriers to overcome in converting from chair to boat, probably the most likely bioactive conformations exist as chair, *cis* and boat, *cis*.

4.3.4.6 Conformationally constrained analogues - A more radical attempt to ascertain the geometry of the enone system of anatoxin was addressed through a series of conformationally

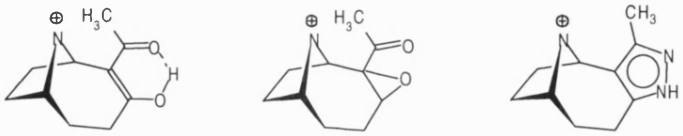

HydroxyAnTx EpoxyAnTx HeteroAnTx (13)

locked analogues of anatoxin. These structures include two *cis* analogues (HydroxyAnTx and HeteroAnTx), and an epoxide (EpoxyAnTx) - see inset 13 - also synthesised by Paul Brough.

The crystal structure of HydroxyAnTx reveals the *cis* configuration reinforced through the presence of a hydrogen bond (Brough *et al* 1992). Although this conformation exists as the crystal form, and as a local energy minimum, as revealed by bond breaking and dihedral driver calculations (Figure 4.8a), the energetically preferred conformer is *trans* - chair forms being the most stable (Table 4.14).

Table 4.14

	Chair, trans		*Chair, cis*		*Boat, trans*		*Boat, cis*	
	E (kcal/mol)	*N-O (Å)*	*E (kcal/mol)*	*N-O (Å)*	*E (kcal/mol)*	*N-O (Å)*	*E (kcal/mol)*	*N-O (Å)*
HydroxyAnTx	28.764	3.61	30.799	4.54	30.486	3.98	32.517	4.74
EpoxyAnTx	203.174	4.19	205.600	4.70	207.913	4.11	-	-
HeteroAnTx	-	-	43.255	4.49	-	-	44.668	4.56

HydroxyAnTx appears to be the most stable structure among AnTx and its analogues. The 19.639 kcal/mol lower potential energy of HydroxyAnTx relative to (+)AnTx can be explained by the 25.558 kcal/mol difference in electrostatic energy of the global energy minima forms of the two structures. Beers-Reich distances otherwise match those of AnTx and the alkyl-modified analogues (Figure 4.8b).

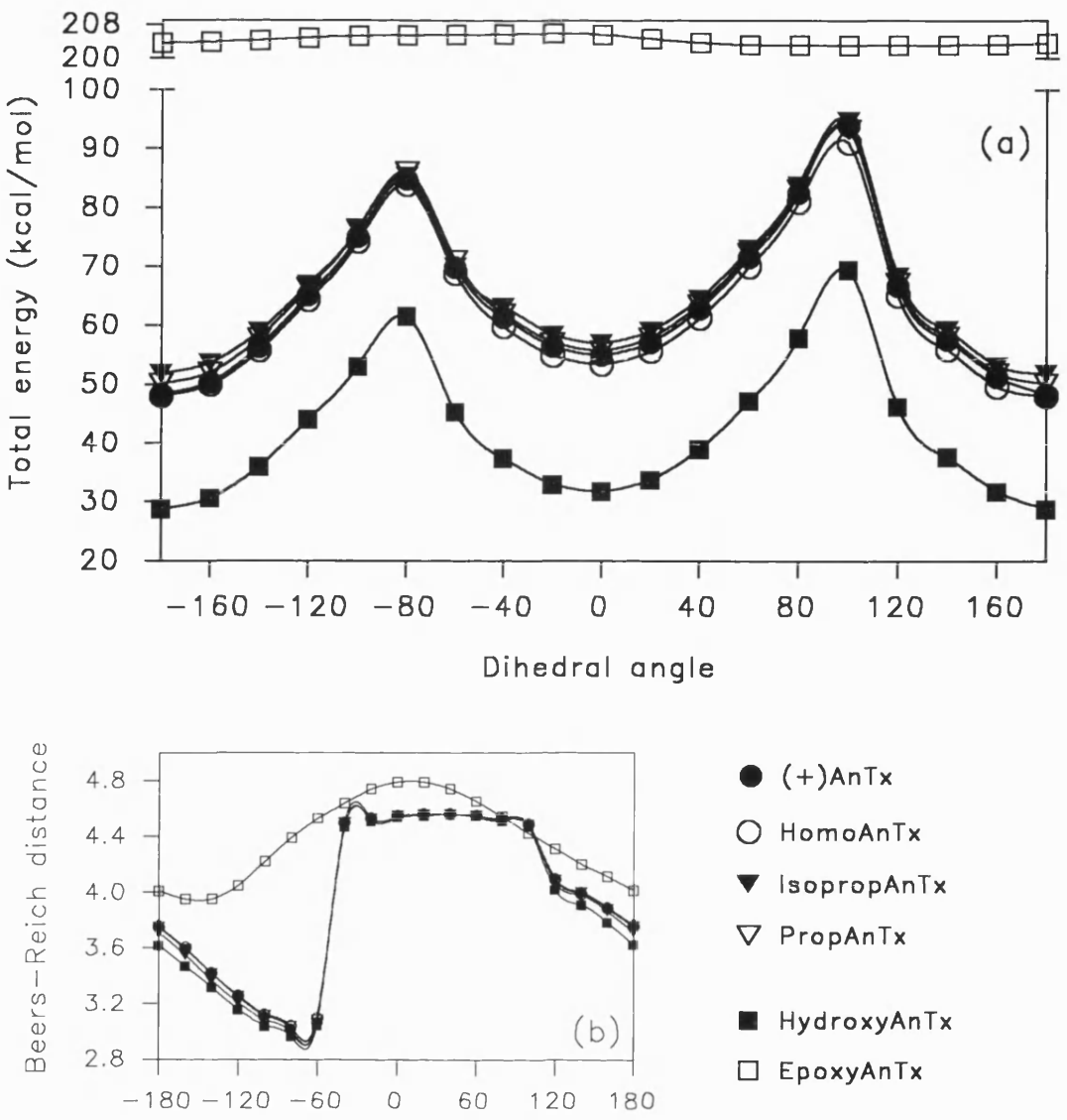

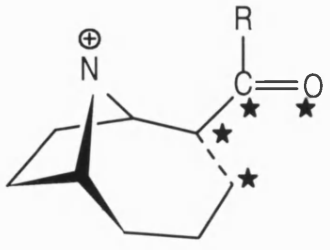

Figure 4.8: Comparison of alkyl-modified sidechain analogues and conformationally constrained analogues of (+)anatoxin using computational chemistry. Intermediate conformations of chair forms of each structure were explored by rotation of the dihedral angle (C=C-C=O) indicated on the core structure (★) in 20° increments, with minimisation at each step (see section 4.2.4). Changes to (a) the total energy (kcal/mol), and (b) the Beers-Reich distance (Å), were monitored. Graphs represent calculations performed on the lowest energy twist, chair conformers.

EpoxyAnTx is an extremely unstable structure induced by the proximity of the two electronegative centres. The lowest energy structure exists as a chair, *trans* form (Table 4.14) with significant contributions to the instability being due to high bend energies. Rotation of the carbonyl, and epoxide orientation, have little effect on stability, though the *cis* arrangement conforms best to the pharmacophore distance (Figure 4.8b).

HeteroAnTx is a tricyclic derivative of AnTx with little conformational freedom. The addition of the methylated pyrazole ring mimics the *cis* conformation of the enone carbonyl in AnTx with the electron-rich nitrogen substituting for the carbonyl oxygen. This extra ring makes for a structure which is more stable than AnTx, having an energy value of 43.255 kcal/mol and an N-N distance of 4.49Å in its lowest energy, chair form. Rigorous conformational restriction or the extra bulk may account for its poor activity (see section 2.3.5.4).

4.4 Discussion

In order to validate the correlation of structural conformation and biological activity, an assumption of this study has been that a search would be made for the optimal, static pharmacophore which is initially presented to the receptor. Although other conformations pertinent to the later stages of interaction between ligand and receptor might be relevant to functional activity and therefore should not to be ignored, for the purposes of simplifying the conformational searching the preceeding, static pharmacophore was assumed. The pharmacophore model proposed by Beers and Reich in 1970 seems to have stood the test of time. The model has more recently been corroborated using a *distance geometry* method (Sheridan *et al* 1986) and, given its indisputable integrity, though remaining largely unrefined, was used as a guide in this project to explore the effects of structural alterations and to aid the search for bioactive conformations.

Although the proposed pharmacophore models (see section 1.5) appear adequate to justify some of the 3-dimensional structural requirements of many nicotinic agonists, they are incomplete as they do not explain the activity of analogues of certain established nicotinic agonists. This is perhaps not surprising given the alterations to the ground state, electronic character and innumerable other physicochemical parameters associated with even very subtle structural modifications. Another contributory factor to this stagnation of the model may be the conflict that is often observed between the conformational preferences of the isolated and receptor bound ligand. For instance ^{1}H-NMR studies reveal that the conformation adopted by acetylcholine when bound to the receptor is quite distinct to that found in either the solid state or those predominant in solution (see below: Behling *et al* 1988). The bound conformation of a ligand represents a pharmacophore mode perhaps different to that the receptor must initially be confronted with and which determines whether interaction is going to take place. Although the flexibility of acetylcholine presents an exception to the rule among the otherwise semi-rigid nicotinic agonists, this observation highlights complications in the attempted derivation of a pharmacophore model from conformation searches in more than one environment. These observations do then bring into perspective the existence of several pharmacophore modes, each of which is associated with a particular receptor state, be it resting, activated, or one of the many desensitised states.

4.4.1 Acetylcholine

Following template forcing of the crystal structure of ACh onto the conformation assumed by *cis*, chair anatoxin-a, a lower energy structure was obtained which also overlaid very well with the more potent AnTx. The new conformation was not highly strained but was by no means the most stable conformer the structure can assume (see Figure 4.1). The distance between the nitrogen and oxygen centres was well within the limits defined for the Beers-Reich pharmacophore, and the torsion angles (see section 4.3.1, inset 2) agreed well with those quoted for the crystal and solution conformations of ACh (Behling *et al* 1988), which adopt a gauche arrangement about the N-C-C-O backbone. In order to attain a good fit with the AnTx template, the ACh molecule adopts an extended conformation, whereas it is reported that when bound to the nicotinic receptor of *Torpedo* the molecule is in a bent (*trans*, relative to the N-C-C-O backbone) conformation in which the oxygens are adjacent and the methyl groups form an uninterrupted hydrophobic surface over the rest of the

molecule (Behling *et al* 1988). This conformation also exists for the molecule when it is bound to lipid. Behling and co-workers speculated that the receptor bound conformation of ACh may be dictated by a generally hydrophobic environment in which there is also adequate provision for the interaction of the charged centres with complementary receptor points. Both the hydrophobic and hydrophilic 'surfaces' of the molecule must interact with regions of the receptor suggesting that the whole molecule is virtually 'consumed' when bound, which would require the provision of a substantial binding pocket to accommodate both the length of the molecule and its various interacting groups.

Directionality of the lone pair of the carbonyl oxygen was comparable to that of the template AnTx molecule. Little discrepancy was observed between the relative volumes occupied by ACh and AnTx, with only the methyl groups associated with the quaternary ammonium extending beyond the space occupied by AnTx - this space is however occupied by the methyls associated with the N-methylated forms of AnTx. Notably, N-methylated analogues of AnTx (both Me-AnTx and Me_2-AnTx - Table 4.7) are less potent than ACh (Table 2.3) which could indicate that in order for methylation around the nitrogen centre to be accommodated in the binding pocket there must be a certain degree of flexibility in the ligand structure. This flexibility is largely absent in AnTx but among the piperazines, for example, inversion of the cyclohexane-like ring may give sufficient flexibility.

Relative to many other nicotinic agonists, ACh has only moderate potency at the neuronal receptors studied here. This may be a consequence of a series of factors, though the increased flexibility of this structure must dictate its potency to a large extent. Energy barriers to interconversion between some conformers are relatively small (Figure 4.1) so isomerisation may occur readily at room temperature - conversely, in the analogous acyclic analogue of AMP.MeI (see below: McGroody *et al* 1994), energy barriers to interconversion are high (~19kcal/mol) restricting the number of conformers at room temperature. The more conformational states that are accessible at room temperature the less dominant the bioactive species becomes and consequently less opportunities arise for interaction of the bioactive conformer with the receptor.

4.4.2 Nicotine

Preferred orientations of the pyrolidine and pyridine ring systems of nicotine modelled in this study corroborated those reported from NMR and quantum mechanical data (Pullman *et al* 1971). The methyl and pyridine group favoured a *trans* arrangement. The *cis* isomer was susceptible to steric effects associated with the bulky N-methyl group creating energetic differences between the syn and anti forms, though these effects were not apparent in the *trans* isomer. It might be expected that given the small energetic difference between syn and anti forms of the *trans* isomer, and the relatively small energy barrier to rotation of the rings between syn and anti forms, then rotation of the rings may be promiscuous event and thus both forms might be equally populated.

Strangely, the stereoselectivity exhibited in favour of the (-) enantiomer by the [^{3}H]-(-)-nicotine labelled receptor is not explained by differences in the distance between the charged centres, for the separation of these atoms in both (+) and (-) isomers of nicotine are identical in the lower energy syn

and anti forms, although distances more acceptable to the pharmacophore model were evident for syn forms. Therefore, handedness of the molecule (i.e. volume displacement of the molecule relative to the functional groups) could be a more important determinant of potency at [^{3}H]-(-)-nicotine labelled, than [^{125}I]αBgt labelled, receptors. This stereoselectivity is not exhibited by the [^{125}I]αBgt-labelled (α7-containing) receptor indicative of geometrical differences in the binding sites of these two receptors. Overlap of the carbon skeletons of (+)nicotine and (+)AnTx was better than that seen for (-)nicotine, although the RMS fit for the nitrogen centres alone was better for (-)nicotine (see section 4.3.2, inset 5). Orientation of the N-methyl group relative to the rest of the carbon skeleton may determine the relative inactivity of the (+) isoform nicotine.

Addition of a methyl group to the pyrrolidine nitrogen of nicotine decreases the stability of the structure considerably, especially in the *trans* isomer. Besides dispersing the positive charge associated with the cationic headgroup, this introduction creates steric clash between the hydrogens of the respective ring systems making interconversion between isomers much more energetically expensive, although relatively insignificant changes occur to the N(+)-N(-) distance. Methylation of nornicotine to nicotine increases potency, and is tolerated in nicotine monomethiodide. The pyrrolidine and pyridine rings of the nicotine skeleton are given greater flexibility over, say AnTx, due to the rotatable bond which connects the ring systems. This greater degree of relative flexibility may contribute to toleration of N-methylation in nicotine, as is seen with acetylcholine.

The absence of a directional dipole in nicotine seems not to denigrate the potency of this ligand. Much like the benzene ring of DMPP, the electronic character of the pyridine ring is probably diffuse though with an electronegative hotspot. Nicotine and DMPP are structurally quite similar in that their ring systems do not lie in the same plane, and the presence of a large delocalised electron cloud associated with the unsaturated ring. The fact that the carbonyl of AMP.MeI can be substituted with an unsaturated ring system which bestows greater potency on DMPP, the presence of a similar ring in the potent nicotine structure, and the greater than 100-fold loss of potency following substitution of the carbonyl with hydroxyl groups in AnTx (Table 4.7), lends less credence to the requirement for the formation of a hydrogen bond in the interaction between receptor and ligand, and supports the importance of some form of hydrophobic interaction in the site. We have already seen that possible alterations to the extent of the dipole in the Homo-, Propyl- and Isopropyl-AnTx derivatives does not seem to effect biological affinity of activity, thus could conclude that the dipole is not a prerequisite of the pharmacophore, and much less so is the extent of the charge separation associated with it. This is consistent with the presence of many hydrophobic residues in or around the binding pocket and with the absence of hydrogen bonding candidates in the receptor.

4.4.3 Piperazine-based compounds

All conformations of boat and chair forms were surveyed by rotation of the sidechain (either acetyl or benzene group) hinged to the six-membered, piperazine ring. Global minima occur at angles that maximise orbital overlap (i.e. 0° and 180° for acetyl-containing AMP analogues, and 90° and 270° for DMPP). As mentioned above, DMPP may be fortunate in its possession of a benzene ring which provides a cloud of delocalised electrons in place of the discrete dipole of AMP. The

presence of this hydrophobic ring bestows greater potency upon this piperazine compound relative to its analogues which possess a hydrogen bond accepting group (see sections 2.3.5.3 and 3.3.3.3). The torsional energy barrier for rotation of the benzene ring is roughly 3kcal/mol less than for the acetyl (AMP) analogues, thus if the bioactive conformation, which maximises either the hydrophobic or possible hydrogen binding interaction, requires these sidechains to be other than in the local energy minimum, then the energy penalty incurred through rotation of the benzene ring will be less than a similar alteration to the acetyl sidechain. The hydrophobic interaction between the benzene ring and receptor binding residues is also likely to be more vague than that associated with the directional dipole, which forms a hydrogen bond with an orbital containing an unshared pair of electrons, (i.e. at ±60° from the plane defined by the carbonyl carbon and its substituents for the sp^2-hybridised orbitals of a carbonyl oxygen). Therefore, perhaps the bioactive conformer of DMPP is attained through a smaller deviation from its global minimum energy conformation, whereas the same may not be true of the acetyl analogues which would thus incur a larger energy penalty. A consequence of the absence of a discrete electronegative centre in DMPP permits some flexibility in the measurement of the Beers-Reich distance and indeed, although this distance is some 0.7Å longer on average than for the AMP analogues (Figure 4.3b), deviations are small indicating that in the majority of conformations explored a pi electron system is apparently appropriately placed for interaction with the receptor. Substitution of the benzene of DMPP with the acetyl-like sidechain in AMP.MeI increases the global minimum energy by some 12kcal/mol, the result of an increase in the electrostatic energy. It would appear this increase in electrostatic character, although in the form of a carbonyl, destabilises the structure enough to reduce potency.

Differences in the energetics of desolvation of ligands which interact with the nicotinic receptor could play a significant part in the observed potencies. Substitution of functional groups with those that increase the number of hydrogen bonds to water should, all other effects being constant, conceivably decrease the potency of a ligand as more energy is required to strip the hydration shell prior to binding. Such extrapolations cannot confidently be made as other intramolecular changes may also influence the binding reaction (see below). However, McGroddy and co-workers (1994) have performed molecular dynamics conformational searches of hydrated forms (i.e. in the presence of some 499 water molecules) of AMP.MeI and its less potent, acyclic derivative HTED (*N,N,N,N'*-tetramethyl-*N'*-acetylethylenediamine iodide). They demonstrate that AMP.MeI and HTED show relatively similar functions for the interaction between water molecules and their carbonyl oxygen and quaternary amine nitrogen. Flexibility of the HTED N-C-C-N(+) backbone tends to vary the extent of solvation, though conformers which are more compact shield the charged species (C=O(δ-) and N(+)) reducing the number of water molecules participating in the formation of the hydration shell - these more compact molecules do not however conform particularly well to the Beers-Reich distance, a finding consistent with the need for an extended conformation of acetylcholine. The solvation shell of AMP.MeI is less extensive than any of the HTED structures that conform to the Beers-Reich criteria, by some 3-5 water molecules on average - the differences are largely due to the replacement of the methyls of HTED by methylene groups in AMP.MeI. These differences in solvation energy suggest that more energy may be required to desolvate HTED compared to AMP.MeI, an observation that could be extended to other nicotinic ligands though, given the

relatively similar sizes of agonists, this contribution to differences in biological potency may not be as significant as variations in intramolecular interactions. Additionally, the more water molecules there are in the primary solvation shell of a particular conformation of a molecule the greater the entropic energy deficit incurred, which could influence the proportions of different conformers in solution and therefore available to interact with the receptor. The loss of entropic energy on binding would be a more important consideration for flexible molecules such as ACh, but may be less so for the majority of structurally rigid nicotinic agonists. The primary hydration shell of DMPP would feasibly contain a larger number of water molecules than would that of the AMP analogues. This should favour the binding of AMP over DMPP to the receptor though unfortunately this is not the case as electrostatic differences in these molecules must overshadow the desolvation issue.

In the same study involving AMP.MeI (McGroddy *et al* 1994) it has been demonstrated that although AMP.MeI maintains rigidity around the quaternary amine due to stable solvation, the ring undergoes significant dynamics at the acetyl end. The sp^2 hybridisation of the amide nitrogen favours a planar conformation with a bond angle of 120°. These authors observe that upon molecular dynamics simulations most of the trajectory is populated by approximate half-chair ring conformations in which this amide nitrogen at the acetyl end of the molecule is in the same plane as the methylene groups of the ring. Other deviations at the acetyl end of the ring produced chair and twist boat conformations. The comparatively rigid quaternary amine remains out of the plane of the methylene groups throughout the simulation. Ring structures of cyclohexane are not reported to favour these conformations adopted by AMP.MeI, thus the piperazines used in this study may populate unusual ring conformations due to quaternisation of one of the nitrogens and the planarity of the other. It is conceivable that AMP.HCl is less rigid around its quaternary amine and therefore less able to keep the quaternary amine out of the plane of the ring methylenes. This disposition of the electropositive centre out of the plane of the hydrogen bond accepting group may be responsible for the lower potency of AMP.HCl relative to AMP.MeI (and possibly DMPP). Additionally, although AMP.HCl is generally very stable and has comparable Beers-Reich distance to AMP.MeI, the volume around the quaternary nitrogen may be insufficient to occupy the binding pocket and the extra methyl may be required to disperse the electropositive charge.

Molecular dynamics calculations and experimental determinations of the conformation of HTED in solution (McGroddy *et al* 1993b & c), identify the *trans* conformer of the carbonyl as being most stable, with a *trans*/*cis* equilibrium constant of greater than 4. However, it has been suggested from ^{19}F NMR experiments that only the less stable *cis* conformer of the carbonyl of HTED is able to interact with the nAChR from *Torpedo* electroplaque (McGroddy *et al* 1993a). This reflects observations with bound and unbound conformations of acetylcholine. In this current study there was little or no preference for the *cis* or *trans* orientation of the acetyl sidechain in the semi-rigid cyclic equivalent AMP.MeI, or even AMP.HCl. It is likely that with more flexible molecules, such as HTED and acetylcholine, the receptor is able to recognise conformations which closely approximate to the ideal pharmacophore and once initiated in the binding reaction these ligands are forced to undergo conformational reorientations such that interactions with the complementary receptor points are maximised and the new conformer stabilised. This is probably the difference between the

observed conformations for solution and receptor bound states of flexible ligands. The extent of these reorientations determine the energy of binding and are reflected in the ligand's potency. More rigid molecules such as AnTx must be close to the optimum pharmacophore model, for its potency suggests little or no structural reorientation on binding, if large conformational changes were necessary then they would be energetically expensive for this rigid structure and therefore costly in terms of increase in binding energy. AnTx should therefore remain the principal line of attack in determining the requisite features of the nicotinic pharmacophore.

In a study conducted on a series of carbamyl analogues of potent nicotinic agonists containing piperadine and piperazine structures (Spivak *et al* 1989a), the effect of having an NH_2 or CH_3 group α to the carbonyl moiety was assessed. These structures, which are structurally highly homologous to the piperazines used in this study, included AMP.MeI and isoarecolone methiodide (a structure which resembles AMP.MeI except that the nitrogen at the acetyl end of the ring is replaced by an unsaturated carbon atom). Interestingly, substitution of the CH_3 group by NH_2 in the synthesis of carbamyl analogues, reduced their potency at the frog neuromuscular junction (Spivak *et al* 1989a). The presence of the NH_2 in these molecules, which may have the effect of donating hydrogen bonds to water thus raising the energy barrier for desolvation that precedes receptor binding (see above), was predicted to confer a constant reduction in potency of the carbamyl analogues relative to the acetyl. However, the effect of this replacement was not constant for these structures the discrepancy being more likely due to intramolecular changes. Carbamyl analogues demonstrate a less negative electrostatic potential about the carbonyl oxygen, most probably due to the introduction of the electronegative NH_2 group which disperses the negative character of this group. Thus these results tend to support a role for the acetyl-like methyl group of the piperazines in accentuating the dipole of the carbonyl, and also for providing essential hydrophobic bulk around the carbonyl carbon. Notably, if the acetyl-like methyl is removed from AnTx (AnTxal in table 4.7) there is a significant reduction in potency.

4.4.4 Anatoxin-a: a template ligand for the nicotinic pharmacophore

The recent nicotinic pharmacophore model of Hacksell and Mellin (1989) was derived by re-examination of an *Active Analogue Approach* to generate a model which derived from novel potent nicotinic agonists. These authors examined the features of agonist conformations that explain the stereoselective actions of the receptor, using (+)AnTx as the central focus of the investigation. While the bioactive conformation of AnTx remains controversial (Witkop & Brossi 1984: Koskinen & Rapoport 1985: Hacksell & Mellin 1989), both the *cis*, boat and *cis*, chair conformers meet the requirements of the Beers-Reich pharmacophore and have consequently been suggested to represent the bioactive state (Witkop & Brossi 1984: Koskinen & Rapoport 1985). The *cis* conformers do not comply with the pharmacophore model generated through the *active analogue approach* (Hacksell & Mellin 1989) and do not explain the activity profiles of other AnTx analogues. Therefore the *trans*, chair conformation has also been proposed by these latter authors to represent the bioactive state. We determined that such a fundamental discrepancy in determining the likely bioactive conformation of this important ligand could be addressed more directly through the synthesis of analogues which might stabilise either the *cis* or *trans* conformation, and/or the

conformation of the ring system. We have attempted to integrate the structural and biological relationships derived from these synthetic analogues with observations of other AnTx analogues.

Boat or chair conformation?

The conformational studies undertaken in this project reveal that anatoxin and many of its less radically modified analogues could feasibly flip easily between boat and chair conformations of the seven-membered ring, with the exception of the sterically crowded N-methylated derivatives (see below). Chair conformers were favoured by about 1kcal/mol over the corresponding boat conformers in the global minimum energy conformations of the carbonyls, though this varied depending on the complexity of the sidechain modification. In general, most of this energy difference is accounted for by the difference in torsion energy between the two forms. However, among the carbonyls, these conformations were insufficient to fulfil the Beers-Reich distance criteria. In order for the chair conformations to conform to this model an energy penalty is incurred creating instability among the structures. Thus it may be that although chair conformations are energetically preferable the boat conformation may be the dominant bioactive form for most of the anatoxin analogues. Koskinen & Rapoport (1985) have suggested that the solution conformation of AnTx.HCl in D_2O is in the energetically preferred twist-chair form, and indeed all other evidence from experimental (i.e. X-ray, U.V., I.R. and N.M.R.) and theoretical sources (see Thompson *et al* 1992) corroborate this.

The N-methylated forms of the anatoxin analogues expectedly prefer to assume the chair conformation due the steric crowding associated with the extra bulk. N-methylation profoundly decreases the potency of anatoxin and its analogues (Table 4.7: Wonnacott *et al* 1992). This decrease may be a consequence of greater charge distribution about the cationic headgroup, an unacceptable increase in volume in the same area, or due to the instability of the boat conformation (i.e. N,N-dimethyl AnTx is unable to adopt a boat conformation). The latter speculation would favour a bioactive conformation for anatoxin whereby the seven-membered ring would adopt the boat conformation. Variation in the electronic environment of the nitrogen centre may have a significant effect on overall conformation (Koskinen & Rapoport 1985), though this study found that methylation had little effect on the energetic profiles of analogues besides an expected relative increase in the energy of the structures.

Cis or trans orientation of the enone carbonyl?

The conformation of the enone system of AnTx is reported to adopt a *trans* orientation in the solid state (AnTx.HCl), a *cis* orientation in MO calculations, and is more freely rotating in solution (Koskinen & Rapoport 1985). In this project all global energy minimum conformations of anatoxin and its analogues were oriented with the dihedral close to 180° - the *trans* isomer was found to be favoured by around 6kcal/mol in both boat and chair conformations of anatoxin itself, and although the energy difference varied, this pattern was repeated for all of the analogues. The requirement for planar restriction of the enone system of AnTx through conjugation, is evident from the poorer activity of dihydroanatoxin. Koskinen & Rapoport (1985) determined the *cis* conformer to be 0.75kcal/mol lower in energy than its *trans* isomer. The energy difference observed between *cis* and *trans* conformers in this study were attributable to intramolecular coulombic effects. In the less stable

cis isomer of the anatoxin structure itself, non-bonded attractive interactions between the partial negative charge on the carbonyl oxygen and the positively charged hydrogen atoms associated with the nitrogen centre, most probably account for the increased instability - the same is probably true of the boat conformers. These nuclei are further apart in the *cis* conformer explaining the increase in coulombic energy. Support for the increased stability of the *trans* configuration is much evident from various other geometry optimisation methods, (i.e. molecular mechanical and molecular orbital methods: see Thompson *et al* 1992).

The difference in energy between *cis* and *trans* forms, although not considerable, may infer the predominance of the *trans* form in the population. An interesting result from studies of the I.R. spectrum of AnTx in $CHCl_3$ (Koskinen & Rapoport 1985) indicate the presence of both *cis* and *trans* populations of AnTx, although the proportions were not quantitatively determined. The N.O.e. difference spectrum of AnTx in $CDCl_3$ suggests that both *cis* and *trans* conformations are significantly populated (Koskinen & Rapoport 1985), though Spivak and co-workers (1980) infer that the *cis* conformation represents a 'considerable proportion' of the mixed population. It is probable that intramolecular electrostatic effects of the agonist molecule may be attenuated to some extent at the nicotinic receptor binding site, as the pharmacophore model implies that the nitrogen and carbonyl oxygen atoms interact with complementary receptor points which would thus smother the electrostatic effects of the ligand. Coulombic interactions may also be attenuated by polar solvents, thus the NMR data obtained for the AnTx conformations in $CDCl_3$ may mimic to a certain extent the situation at the level of receptor recognition/interaction. If the intramolecular electrostatic interactions are neglected from *in vacuo* calculations, then the energy difference between the *cis* and *trans* conformer, especially of the chair conformation, becomes almost insignificant. Thus, either the *cis* or *trans* orientation of the enone moiety may be the conceivable bioactive conformation.

Thompson and co-workers (1992) made a search of the crystallographic data base using the 1-acetyl-1-cyclohexene sub-structure as a geometrically equivalent structure to part of the ring system of AnTx in order to deduce the incidence of *cis* and *trans* orientations in energetically stable conformations. They discovered that six out of the seven extracted structures possessed a *trans* configuration, the seventh being locked in the *cis* orientation due to an internal hydrogen bond. The average dihedral angle for the enone function among these structures was 175.9°, planarity similar to that observed for our derived minimum energy conformations, and for the AnTx structures generated by Thompson and co-workers (1992), although generally more planar than the angle found in the AnTx.HCl crystal (-162.7°: Koskinen & Rapoport 1985). A *trans* configuration of the enone moiety (175.4°) in the crystal conformation of the N-acetyl derivative of AnTx is also reported (see Thompson *et al* 1992), the seven-membered ring being in the chair conformation. Although the enone function retained its conjugation using the torsional parameters described in the HYPERCHEM forcefield, it appears to have been insufficient to permit the slight twisting of this function, as would be expected from any steric interactions.

The conformational flexibility of the acetyl sidechain of AnTx and its analogues appears to depend on the extent of the electrostatic interaction between the partial negative charge of the oxygen and

the positively charged hydrogen atoms of the nitrogen centre. Thompson and co-workers (1992), using the semi-empirical MO program MOPAC, observed how the energy of each conformation of AnTx, where the acetyl group was subjected to dihedral driver calculations, was mirrored by the distance between the nitrogen and oxygen atoms (i.e. if the distance increases then so does the energy of the system).

Other observations of AnTx and its relatives

Pyridohomotropane (PHT: Figure 2.1), like the anatoxin analogues, loses affinity when methylated, though we have already seen that it seems the presence of methyl groups around the nitrogen centre is essential for conferring activity to agonists such as DMPP (see above and section 2.3.5.3), isoarecolone methiodide and ferruginine methiodide (Spivak *et al* 1983: Figure 2.1). The effect of N-methylation in AnTx may be due to a destabilisation of the AnTx skeleton, as was suggested by Kofuji and co-workers (1990), and consequent destabilisation of the *cis* conformation of AnTx. These observations have been used to support the view that the bioactive conformation of AnTx is represented by the *cis* and not the *trans* form (Kofuji *et al* 1990). Although PHT has poor activity even with the hydrogen bond accepting group confined to the *cis* orientation, this, like our synthetic HeteroAnTx (see below), does not imply that inactivity is a direct consequence of a *cis* orientation, as other factors may also be contributing to the poor biological activity of these molecules. For instance the *receptor essential volume* described by Hacksell and Mellin (1989) may be impinged upon by the likes of PHT and HeteroAnTx, and indeed the same exclusive volume may prevent the effective interaction of the N-methylated AnTx analogues. A modification of the relative position of the methyl groups was implicated in the decrease in nicotinic potency that resulted from the reduction of isoarecolone methiodide to DMPP (Spivak *et al* 1986). Spivak and Albuquerque (1982) proposed that the displacement of the charged centre out of the carbonyl hydrogen bonding plane might contribute to potency of the secondary amine of AnTx, a displacement that could be exceeded in N-methylated AnTx analogues.

AnTx has the unusual advantage of being a secondary amine, and it can therefore achieve a stronger coulombic bond with the receptor than can the bulkier quaternary amines - the energy of the electrostatic interaction between ligand and receptor depends inversely upon the distance between the cationic headgroup and anionic site of the receptor.

Although not formally overlaid, the (+) and (-) forms of anatoxin clearly demonstrated the quite different volumes they would occupy in the receptor binding site. No energetic difference, or difference in the distance between the pharmacophore points, was apparent for these two molecules. The reason for the inactivity of the (-) isomer must therefore lie solely with the geometric configuration of the remainder of the molecule. The handedness of the molecule must be incompatible with the receptor binding site, which may result from either the volume requirements not being satisfied, or from the placement of otherwise crucial groups for the binding reaction on the wrong side of the molecule. The same must be true, at least in part, for the stereoisomers of nicotine (see above)

Synthetic analogues and the cis/trans conformation of the enone

Conformational studies investigating the influence of methine or methylene units upon the conformation of the enone system proved to be inconclusive though the *trans* arrangement was the lowest energy configuration. Extension of the alkyl sidechain did not appear to distort the conformation of the anatoxin skeleton, and the energy barrier to rotation between *cis* and *trans* arrangement remains essentially unchanged relative to the parent. No preference was observed for the boat or chair conformation. These observations are consistent with the retention of biological activity by these analogues. Whether it is the hydrophobic nature of these sidechains, their weaker influence on the ground state conformation, or their greater flexibility over previous anatoxin analogues (Swanson *et al* 1991: Wonnacott *et al* 1991) which makes them tolerable is unclear.

The more conformationally constrained analogues (HydroxyAnTx, EpoxyAnTx and HeteroAnTx) all have very poor biological activity, a consequence which cannot be wholly attributed to the pseudo-*cis* orientation of the carbonyl in HydroxyAnTx, or its equivalent in HeteroAnTx, neither to conformation adopted in the Epoxide. Inactivity in these species is most likely due to several factors among them unfavourable intramolecular electrostatic interactions, (especially in the epoxide), the introduction of too much steric bulk in sensitive regions, and unreasonable constraints on the conformation of the molecules as a whole.

5 General discussion

The techniques applied in this study have been used to generate biological and structural descriptors for existing and novel ligands of the neuronal nicotinic receptors. Collation of this data has provided the opportunity to correlate the activity of these molecules with the differences and similarities between their structural attributes. As a result of these comparative studies we have made attempts, (using rationally designed synthetic analogues of a potent nicotinic agonist), to probe the model of the pharmacophore for the nicotinic receptor in order to ascertain the specific structural requirements of active ligands. It is hoped that this study has developed this structural model, and as a result will provide greater insight into the essential requirements of the receptor binding pocket of the nicotinic receptor in terms of volume constraints, the choice and relative orientation of potential charged centres partaking in the interaction (be they on the α subunit or those adjacent to it), and other information not available at present but which would provide pointers to refine the 3-dimensional structure of the neuronal nicotinic receptor.

5.1 Features of the pharmacophore of active nicotinic agonists

Before a model of an optimum active molecule can evolve, consistent, reliable data on the activity of a series of such ligands must be generated. In this study activity indicators were generated from two distinct biological systems (viz. the receptor binding assay and the functional oocyte expression system). Although these systems are both consistent and reliable within their experimental limitations, their output is representative of the biological situation unique to it. For instance, whereas the receptor binding assays may regard aspects of the pharmacophore model which are important in stabilising the desensitised state, the functional responses of the α7 homomer could be a result of additional features of active ligands which are perhaps less important in the initial recognition but are realised only in the proceeding activation, as well as desensitisation, events. Thus the determination of a truly complete pharmacophore model can only be derived through consideration of structural elements of the activating molecules which induce the complex sequence of interacting processes responsible for activity. However, in order for an agonist to be effective the recognition barrier must first be overcome, therefore all molecules which either bind to, activate or subsequently desensitise the receptor must possess common structural features which allow them to access the receptor. The way in which these features are presented determines whether one molecule is more potent than another.

Cationic head

A centre of positive charge is a prerequisite of all nicotinic agonists. It would appear, however, that this centre is very sensitive to the nature of the groups over which the charge is dispersed, even among homologous structures. We have seen that N-methylation of the cationic head in nicotine and anatoxin diminishes activity, most significantly in the latter case, whereas among piperazine ring based structures N-methylation is essential for activity. Activity as a function of successive methylation shows no consistent trend among bi- and tri-cyclic agonists - the ferruginines are structural analogues of anatoxin yet methylation among them defies simple order. These differential effects on potency of the juxtaposition of methyl groups and the sensitive nitrogen centre may be a

consequence of many effects: for example, N-methylation may redistribute and/or disperse the positive charge (consequently altering the separation distance of the charged centres), increase the bulk about this indispensable region, displace the charged head relative to the plane defined by the hydrogen bond accepting group, for example, alter the ground state of the carbon skeleton, stabilise particular conformations through increased solvation, besides inducing more subtle electrostatic effects. It is apparent that particular carbon skeletons are more suited to N-methylation. It may be that more flexible molecules, such as acetylcholine and the piperazines in this study, require to be N-methylated in order to be active and for this cationic head to be removed out of the plane defined by the hydrogen bond accepting group, or its substitute. More rigid systems such as anatoxin do not tolerate the effects due to N-methylation, though as little or no difference was observed in the conformations of methylated and non-methylated structures this is unlikely to be a consequence of reorientation of the basic carbon skeleton.

Structural similarity is not sufficient to explain potency. The electrostatic potential pattern of the interacting groups must also be considered. Anatoxin reveals a very high positive potential (140-160 kcal) about the ammonium head (Yao 1991). Binding of this region to the receptor is coulombic, therefore decreases in the positive potential should have the effect of weakening the interaction and reducing potency. This is clearly observable among the N-methyl and N-dimethyl anatoxin analogues which exhibit a dispersal, and therefore reduction, in the positive potential for the Van der Waals surfaces in this region (Yao 1991).

Hydrogen bond acceptor group

The function of the carbonyl oxygen as a hydrogen bond acceptor was incorporated as a critical element of the pharmacophore for nicotinic ligands by Beers and Reich (1970). This functional group is regarded to be of secondary importance in the recognition reaction given, a) that a hydrogen bond has not been proved to occur in the ligand-receptor interaction and, b) the incidence of auxiliary forms, (although it appears as a carbonyl oxygen in many agonists it is also represented by a phenolic or alcoholic OH, or an amine group (see Gund & Spivak 1991)). In more extreme cases this hydrogen bond accepting group appears to be present but irrelevant. For example in DMPP, although an amine group is present its near proximity to the cationic head (i.e. across the piperazine ring) probably excludes it as an important interacting species, it being overshadowed by the delocalised electron cloud of the benzene ring which may be an important hydrophobic interaction site.

Areas of high electron density, and lowest electrostatic potentials (0-40 kcal), are seen about the carbonyl group in anatoxin (Yao 1991). Although not ubiquitous among the nAChR agonists, if present, the more extreme the charge separation of the dipole the greater should be the hydrogen bonding strength and potency. However, it appears that the area of low potential requires to be consistent, and the greater the deviance from this value the lower the potency of the anatoxin analogue (Yao 1991). Thus possession of a permanent, directional dipole does not appear to be critical.

Hydrogen bonding is not the only determinant of potency in this region, the acetyl-like methyl present in many agonists must also play an important role in the binding. Its presence in the potent anatoxin structure suggests a role in determining the electrostatic character of the carbonyl oxygen, and/or its occupation of a specific hydrophobic niche in the receptor binding cavity. In many of the anatoxin analogues which have probed the character of this region of the molecule (Swanson *et al* 1991: Wonnacott *et al* 1991) substitution of this methyl with charged species had a detrimental effect on activity. For example, the CH_3O- and $(CH_3)_2N$- group, while donating electrons which may enhance the hydrogen bonding of the carbonyl, may be of an inappropriate size or charge to fit a hydrophobic niche occupied by the methyl. In our attempts to restrict the enone conformation of the anatoxin molecule methine or methylene units were added to this region. Affinity and activity of these structures at both of the nAChRs studied were comparable to the parent and may even have increased affinity. Such alterations to the structure in the synthesis of Homo- Propyl- and Isopropyl-anatoxin would probably have insignificant effects on the electrostatic potential of the carbonyl group relative to the parent structure, but quite obviously would impinge on the space and hydrophobic environment around the atom α to the carbonyl carbon. Additional to the coulombic interaction, (and possible hydrogen bonding), hydrophobic interactions may therefore also be an important feature of the pharmacophore and determinant of potency. The anatoxin structure may provide appropriate orientation of the acetyl-like methyl such that this interaction is effective and contributory to the binding reaction. However, given that some of the alkyl modified sidechain analogues of anatoxin retain and may enhance potency, it is feasible that this interaction has not been fully exploited in anatoxin and is realised only when the sidechain is extended in these analogues. However, it may be that this interaction has been overexploited in IsopropylAnTx which exhibits a hooked dose response curve. The perturbation of the receptor structure that occurs on activation in the case of this molecule may become exaggerated resulting in conversion to, or increased stabilisation of, a desensitised state.

Three dimensional structure

Nicotinic receptors, especially the [^{3}H]-(-)-nicotine labelled receptor in this study, demonstrate selectivity in favour of certain stereoisomers of particular ligands - most extremely nicotine and anatoxin. Although functional groups are identical for stereoisomers their relative orientations are important in their recognition by the receptor as a result of the configuration of the carbon skeleton. It appears the receptor is capable of recognising handedness in certain activating ligands suggesting that among the semi-rigid agonists at least possession of the basic functional groups is insufficient for activity. Thus the absolute configuration of carbon atoms that make up the rigid structural skeleton must be such that interacting groups are appropriately presented to the receptor to maximise the interaction. Flexible molecules overcome the problem of not presenting the correct rigid conformation of the carbon skeleton through their ability to more easily interconvert between different conformers, though their effective interaction with the receptor may mean a more induced fit forced by the functional groups of the receptor, which is energetically expensive and thus reflects the reduced potencies of the less rigid ligands.

5.2 Residues important in the formation of the receptor binding pocket

Potential complementary amino acid residues for the cationic headgroup of activating ligands are not forthcoming among those residues identified by photolabelling ligands directed at the region of the nAChR α subunit around cysteines 192 and 193 (see section 1.4.3.1), or the region crucial to the interaction of the potent αbungarotoxin molecule (see section 1.4.4). This suggests the area for such long-range charge-charge interactions may only be present at the interface between α and other subunits (see below). Affinity labelling and site-directed mutagenesis has identified, (besides the two adjacent disulphide-linked cysteines at α192 and α193), at least four aromatic residues in the α subunit sequence of the receptor which directly affect ligand binding and receptor function (see section 1.4.3.4). Three of these four residues are tyrosines (Tyr93, Tyr190 and Tyr198) and each stabilises the cationic headgroup of the agonist as determined by the binding of phenyltrimethylammonium (PTMA: Aylwin *et al* 1994) and tetramethylammonium (TMA: Sine *et al* 1994). Each also contributes equally to the binding energy (Sine *et al* 1994). The exact nature of these contributions are, however, not equivalent for while replacement of Tyr with Phe, Trp or Ser reduces the apparent affinity of ACh the severity of the reduction is dependent both on the position and chemical nature of the substitution. For Tyr93 and Tyr190 the hydroxyl is essential for activity, yet it is the aromatic facet of the Tyr198 sidechain which appears to be important (Aylwin *et al* 1994: Sine *et al* 1994). The significance of the hydroxyl groups may be their ability to form a salt bridge-type interaction with the ammonium group of the ligand - this would require that the pK_a of this group be reduced by the local environment around it so that a significant portion of the anionic tyrosinate form exists (Aylwin *et al* 1994). The covalent interaction of lophotoxin with Tyr190 (Abramson *et al* 1989) supports the nucleophilic state of this residue. Likewise the aromatic portion of Tyr198 could interact with the ligand cation, but could equally likely provide a region of hydrophobic interaction. This latter residue, and possibly the aromatic of Tyr190, have been suggested to maintain the disposition of the tyrosine triad either through direct interaction with the neighbouring tyrosines, or via local residues of the binding pocket (Sine *et al* 1994).

These aromatics (including Trp149) presently provide the only plausible sites in the receptor α subunits for interaction with nicotinic ligands. The strong presence of these aromatic groups is consistent with the provision of a hydrophobic environment in which interactions could occur between the cation of nicotinic ligands and the π electrons of the aromatic ring. Additionally, hydrophobic interactions would accommodate the conjugated systems which appear in so many nicotinic agonists, including the unsaturated ring systems which substitute for the discreet potential hydrogen bond accepting group in certain agonists (e.g. DMPP). It is likely that the cation-π electron interaction diminishes rapidly with distance, and that the hydrophobic effect would be still weaker given the requirement for close contact to displace water from the interacting surfaces. The ability of the alkyl-modified sidechain variants of anatoxin to interact with the receptor as effectively as the parent structure supports the provision of a relatively hydrophobic environment in the binding site, and indicates the space constraints associated with this region. The participation of aromatics in the binding of nicotinic ligands to the receptor is consistent with the affinity demonstrated by quaternary ammonium groups for aromatic rings of synthetic macrocycles (see section 1.4.3.4) and with the nature of the acetylcholinesterase binding site.

It must be stressed that the role of the residues identified on the α subunit in the binding reaction is likely to be a contributory one, in that they probably do not represent the complete picture of the binding site. Acidic residues also contribute to the binding of ACh and the fact that candidates are found in the δ and γ subunits supports the notion of a binding site formed at the interface of adjacent nicotinic subunits. For instance in the region δ164-224 there are some 6 aspartates and 5 glutamates. In this same region of the *Torpedo* ACh receptor the crosslinker S-(2-glycylaminoethyl)dithio-2-pyridine (GCP), attached by a disulphide bond to Cys192 or Cys193, forms an amide bond with aspartate or glutamate residues. Given the length of this crosslinker (0.9nm fully extended) this puts an important acidic residue within 0.9nm of the α subunit binding site disulphide, providing a possible site for coulombic charge-charge interaction with the cationic centre of nicotinic ligands. Of the 12 acidic residues in this region the most functionally important appears to be δ Asp180, which when neutralised, (by mutation to Asn of the homologous residue in mouse muscle), decreased affinity of the receptor for ACh by some 100-fold (Czajkowski *et al* 1993). Only mutation of one other acidic residue in this region, δGlu189, significantly affected function (a 10-fold reduction in affinity of ACh), whereas mutation of the ten other acidic residues in this δ164-224 segment did not have such profound effects. However, δAsp165 and δGlu182 of the *Torpedo* receptor, have been confirmed to be labelled by the same GCP crosslinker that reacts with δAsp180, but not δ Asp189 (Czajkowski & Karlin 1995). It is therefore probable that δAsp180 contributes directly to the binding of ACh, though the functional roles of δAsp165 and δGlu182, which also lie within 0.9nm of Cys192 and 193, remain unclear.

The holistic model of the binding site for interacting nicotinic ligands emerging from such crosslinking experiments appears to be consistent with the residues δAsp165, δAsp180 and δGlu182 facing α Cys192 and 193 across a water-filled cavity between α and δ subunits. The reduction in binding affinity observed on neutralisation of δAsp180 could quite feasibly result from the removal of the electrostatic interaction between the carboxylate of this residue and the cationic group of ACh, though structural perturbations can not be discounted - δAsp165 and δGlu182 are probably not in such close proximity to the ammonium group of the ligand. Of these three residues, only δAsp180 is identically conserved among aligned sequences of the δ, γ and ε subunits on muscle-type receptor (Czajkowski *et al* 1993).

The evidence that the ACh binding site contains both acidic and aromatic residues supports findings which indicate a negative electrostatic potential associated with the site in the *Torpedo* receptor (Stauffer & Karlin 1994). Assuming that the long-range attractive coulombic interaction between anionic and cationic centres, as might be present in the binding reaction between nicotinic ligand and receptor, would be sensitive to ionic strength, these authors assessed the reaction rates of charged methanethiosulphonates with the cysteine residues in the binding site. Analysis of rate constants provided evidence consistent with the ACh binding site containing either two or three negative charges which would account for the three acidic residues labelled by GPC (Czajkowski & Karlin 1995). An electrostatic potential of -80mV at the binding site, (which includes a contribution of -30mV from the Cys thiols), substantiates the existence of anionic residues in the binding cavity and

strengthens the involvement of some long-range electrostatic contribution to the binding of ligand to the receptor.

Our current understanding of the amino acid residues which contribute to the formation of the nicotinic receptor agonist binding site implicates the involvement of residues from different, adjacent subunits and thus supports an inter-subunit location for the site. It appears that ligands bind in some form of crevice in which there is provision for either charge-charge or cation-π electron interaction with the cationic headgroup of the nicotinic agonist, hydrophobic and other salt bridge-type interactions. An inter-subunit site may provide opportunity for more pronounced and/or less energetically expensive structural perturbation upon binding given that ligand accommodation will directly rearrange the tertiary structure of two protein chains at each binding site. The most likely reason for maintaining a cationic ammonium group in the structure of agonist molecules of the nAChR is likely to be for the fulfilment of a long-range coulombic interaction in the binding cavity, which probably represents the most significant reaction between ligand and receptor. The subsidiary interactions between the other functional groups of the ligand and residues present in the binding site could determine the intimacy of the association between ligand and surrounding receptor milieu, thus determining factors such as potency and efficacy. For instance, although many structural features may be common to many agonists which demonstrate disparate biological activities, these same features must alter in the way they are presented to the binding site residues, due to factors such as steric clash, volume displacement, extent of electrostatic potential, carbon skeleton and so on. It is the prioritisation of these factors which will generate a better understanding of the complex interactions that are involved between small agonist molecules and their very much larger protein receptors.

5.3 Future work

The determinations of the structural model of the nicotinic pharmacophore and receptor binding site are processes that are mutually exclusive, thus if further progress is to be made in the elucidation of the structure of these models then close, simultaneous attention must be paid to the results of structural modifications to both.

- As regards the nicotinic pharmacophore, the ligand that is potentially the most informative is anatoxin-a. Its rigidity restricts the number of possible conformations, thus the effects of structural modification should be more easily quantifiable, reducing the complications common to more flexible structures whose conformations are more readily influenced by even minor modifications to the skeleton. Perseverance with the type of sidechain modifications around the important carbonyl moiety carried in this project are essential if the bioactive conformation of this ligand is to be determined and used as a benchmark in the design of future ligands. It will be important to determine whether IsopropylAnTx is actually manifesting subtype selectivity - functional data for this ligand at the α7 receptor is required to extrapolate the competition binding observations. The series of extensively modified sidechain analogues of anatoxin studied previously (Swanson *et al* 1991: Wonnacott *et al* 1991) possibly introduced too many electrostatic modifications to the structure making interpretation difficult, besides which all had the effect of reducing potency considerably compared to the parent compound. Our slightly more rational, less complex approach should remain the angle of attack as further modification of the structure in this same region may produce an anatoxin-a analogue that has both selectivity for α 7-containing receptors, and the potential to be an affinity ligand. This would provide a selective receptor handle to facilitate probing receptor function especially in the complicated system of the brain. Such a tool is lacking at present in the nicotinic receptor field, although a recent report (De Fiebre *et al* 1995) that a derivative of anabasiene (a structure closely related to nicotine) exhibits selective agonist action at the neuronal nicotinic α7 receptor is encouraging. It also appears that α-conotoxin Imi is able to selectively antagonise the α7 and α9 homomeric receptors (Johnson *et al* 1995). Cytisine, a ligand not covered in this study, like anatoxin-a is a very potent and rigid nicotinic agonist, and given the extensive evidence regarding its sensitivity to the presence of different β subunits in the heterooligomeric nAChR complex, could prove to be an equally valuable tool in the determination of the pharmacophore and the binding site.

- The structural limitations and physicochemical nature of the interacting groups in the receptor binding pocket would complement the derivation of a pharmacophore model. Definition of a complementary receptor point to the cationic headgroup of interacting ligands remains unresolved - δAsp180 is a strong candidate, though α7 lacks an equivalent residue in this position (see section 1.4.3.5). Also, given the substitutable nature of the carbonyl group in many ligands speculation that the formation of a hydrogen bond is crucial for activity seems tenuous. The complementary receptor points for these interactions could be explored through mutagenesis of receptor residues that are either labelled by photosensitive probes or crosslinking agents, or are implicated to be in the vicinity of the bound ligand. Emphasis should be placed not only on the anionic residues but also the on the many aromatic amino acids

present in the potential binding site as observations with the piperazine structures and novel anatoxin-a analogues indicate the involvement of hydrophobic interactions in the binding of the ligand. The combination of site-directed mutagenesis and the analysis of functional consequences of the changes both through competition binding and receptor expression studies in the oocyte, would provide some insight into the interactions that may take place at the recognition and transduction levels.

- Although theoretical, the calculations of computational chemistry are becoming increasingly accurate and therefore no less emphasis should be placed on the use of such methods to derive structural models of both agonist conformations and possible receptor binding site models, and indeed the docking of the ligand to the receptor. Although the molecular modelling carried out in this project was informative, the more rigorous approaches of molecular dynamics calculations in the presence of water molecules would represent both a more physiologically accurate picture and reveal more subtle structural perturbations providing a picture of the predominant forms of the structure available for binding. Most importantly, there is a need to compare structural and physicochemical attributes through extensive superposition studies of many structurally and biologically diverse potential bioactive conformations of molecules. This would provide crucial information regarding the volume limitations about the basic pharmacophore points, flexibility of the Beers-Reich distance, handedness, physicochemical character of functional groups and many other attributes important to active ligands.

- It is increasingly evident that the $\alpha 7$ homomeric receptor does not represent native αBgt-sensitive receptors found *in situ*. It may therefore be prudent to continue expression studies but with the $\alpha 7$ subunit in the presence of other α or β subunits cloned. This would create an important extra dimension to this study for as well as representing a more physiological situation it would investigate the influence of heterologous neighbouring subunits on the formation of the binding site, an important issue given the lack of potential interacting amino acid residues from the α subunit.

5.4 Publications and communications resulting from this work

Thomas P, Brough PA, Gallagher T and Wonnacott S (1994). Alkyl-modified side chain variants of anatoxin-a: a series of potent nicotinic agonists. *Drug Develop. Res.* **31**, 147-156.

Thomas P, Stephens M, Wilkie G, Amar M, Lunt GG, Whiting P, Gallagher T, Pereira E, Alkondon M, Albuquerque EX and Wonnacott S (1993). (+)-Anatoxin-a is a potent agonist at neuronal nicotinic acetylcholine receptors. *J. Neurochem.* **60**, 2308-2311.

Amar M, Thomas P, Johnson C, Lunt GG and Wonnacott S (1993). Agonist pharmacology of the neuronal α7 nicotinic receptor expressed in *Xenopus* oocytes. *FEBS Lett.* **3**, 284-288.

Garcha HS, Thomas P, Spivak CE, Wonnacott S and Stolerman IP (1993). Behavioural and ligand binding studies in rats with 1-acetyl-4-methylpiperazine, a novel nicotinic agonist. *Psychopharmacol.* **110**, 347-354.

Brough PA, Gallagher T, Thomas P, Wonnacott S, Baker R, Abdul Malik KM and Hursthouse MB (1992). Synthesis and X-ray crystal structure of 2-acetyl-9-azabicyclo[4.2.1]nonan-3-one. A comformationally locked s-*cis* analogue of anatoxin-a. *J. Chem. Soc. Chem. Comm.* **15**, 1087-1089.

Thomas P, Amar M, Goosey M, Wonnacott S and Lunt GG (1992). Comparison of a vertebrate and invertebrate homo-oligomeric nicotinic acetylcholine receptor. *Soc. Neurosci. Abs.* **18**, 631.13.

Thomas P, Brough PA, Stephens MW, Gallagher T and Wonnacott S (1993). Anatoxin structure-activity studies: (II) Biological and computational evaluation. Poster communication presented at the *IVth International Symposium on Neurotoxins in Neurobiology* held at University of Bath, Bath, UK.

Thomas P, Wonnacott S and Lunt GG (1992). Characterisation of the pharmacophore of a neuronal nicotinic acetylcholine receptor. Poster communication presented at the *Regional postgraduate meeting of the Biochemical Society* held at University College of North Wales, Bangor, UK.

References

Abramson SN, Li Y, Culver P, Taylor P (1989): An analogue of lophotoxin reacts covalently with Tyr 190 in the α subunit of the nicotinic acetylcholine receptor. J. Biol. Chem. **264**: 12666-12672.

Akabas MH, Stauffer DA, Xu M, Karlin A (1992): Acetylcholine receptor channel structure probed in cysteine-substitution mutants. Science **258**, 307-310.

Albuquerque EX, Alkondon M, Lima-Landman MT, Deshpande SS, Ramoa AS (1988): Molecular targets on non-competitive blockers at the central and peripheral nicotinic and glutamatergic receptors. In '*Neuromuscular Junction*', eds. Sellin LS, Libelius R, Thesleff S, **13**, pp273-300. New York: Elsevier.

Alkondon M & Albuquerque EX (1991): Initial characterisation of the nicotinic acetylcholine receptors in rat hippocampal neurons. J. Receptor Res. **11**, 1001-1022

Alkondon M & Albuquerque EX (1993): Diversity of nicotinic acetylcholine receptors in rat hippocampal neurons. I, Pharmacological and functional evidence for distinct structural subtypes. J. Pharmacol. Exp. Ther. **265**, 1455-1473.

Amar M, Pichon Y, Inoue L (1991): Micromolar concentrations of veratridine activate sodium channels in embryonic cockroach neurones in culture. Pflugers Arch. Eur. J. Physiol. **417**, 500-508.

Amar M, Thomas P, Johnson C, Lunt GG, Wonnacott S (1993): Agonist pharmacology of the neuronal α7 nicotinic receptor expressed in *Xenopus* oocytes. FEBS Lett. **327**, 284-288.

Anand R, Conroy WG, Schoepfer R, Whiting P, Lindstrom J, (1991): Neuronal nicotinic acetylcholine receptors expressed in *Xenopus* oocytes have a pentameric quaternary structure. J. Biol. Chem. **266**, 11192-11198.

Anand R, Peng X, Ballesta JJ, Lindstrom J (1993): Pharmacological characterisation of α-bungarotoxin-sensitive acetylcholine receptors immunoisolated from chick retina: Contrasting properties of α7 and α8 subunit-containing subtypes. Mol. Pharmacol. **44**, 1046-1050.

Aronstam RS & Witkop B (1981): Anatoxin-a interactions with cholinergic synaptic molecules. Proc. Natl. Acad. Sci. (USA) **78**, 4639-4643.

Aylwin ML & White MM ((1994): Ligand-receptor interactions in the nicotinic acetylcholine receptor probed using multiple substituions at conserved tyrosines on the α subunit. FEBS Lett. **394**, 99-103.

Ballivet M, Nef P, Couturrier S,Rungger D, Bader CR, Bertrand D, Cooper E (1988): Electrophysiology of a chick neuronal nicotinic acetylcholine receptor expressed in *Xenopus* oocytes after cDNA injection. Neuron 1, 847-852.

Barlow RB & Mcloed LJ ((1969: Some studies on cytisine and its methylated derivatives. Br. J. Pharmacol. **35**, 161-174..

Barlow RB, Howard JAK, Johnson O (1986): Structures of nicotine monomethyl iodide and nicotine monohydrogen iodide.. Acta. Cryst. **C42**, 853-856.

Barlow RB & Johnson O (1989): Relations between structure and nicotine-like activity: X-ray crystal structure analysis of (-)-cytisine and (-)-lobeline hydrochloride and a comparison with (-)-nicotine and other nicotine-like compounds. Br. J. Pharmacol. **98**, 799-808.

Barnard EA, Miledi R, Sumikawa K (1982): Translation of exogenous messenger RNA coding for nicotinic acetylcholine receptors produces functional receptors in *Xenopus* oocytes. Proc. Royal Soc. Lon. - B. Biol. Sci. **215**, 241-246.

Beers WH & Reich E (1970): Structure and activity of acetylcholine. Nature **288**, 917-922.

Behling RW, Yamane T, Navon G, Jelinski LW (1988): Conformation of acetylcholine bound to the nicotinic acetylcholine receptor. Proc. Natl. Acad. Sci. (USA) **85**, 6721-6725.

Benwell MEM & Balfour DJK (1985): Nicotine binding to brain tissue from drug-naive and nicotine-treated rats. J. Pharm. & Pharmacol. **37**, 405-409.

Bertrand D, Ballivet M, Rungger D (1990): Activation and blocking of neuronal nicotinic acetylcholine receptor reconstituted in *Xenopus* oocytes. Proc. Natl. Acad. Sci. (USA) **87**, 1993-1997.

Bertrand D, Cooper E, Valera S, Rungger D, Ballivet M (1991): Electrophysiology of neuronal nicotinic acetylcholine receptors expressed in *Xenopus* oocytes following nuclear injection of genes or cDNAs. In '*Methods in Neuroscience*', ed. Conn M, **4**, pp174-193. New York: Academic press.

Bertrand D, Galzi J-L, Devillers-Thiery A, Bertrand S, Changeux J-P (1993): Stratification of the channel domain in neurotransmitter receptors. Curr. Op. Cell Biol. **5**, 688-693.

Betz H (1981): Characterisation of the αbungarotoxin receptor in chick embryo retina. Eur. J. Biochem. **117**, 131-139.

Bijak M, Jarolimek W, Misgeld U (1991): Effects of antagonists on quisqualate and nicotinic receptor-mediated currents of midbrain neurones in culture. Br. J. Pharmacol. **102**, 699-705.

Blair LAC, Levitan ES, Marshall J, Dionne VE, Barnard EA (1988): Single subunits of the $GABA_A$ receptor form ion channels with properties of the native receptor. Science **242**, 577-579.

Blount P & Merlie JP (1989): Molecular basis of the two non-equivalent ligand binding sites of the muscle nicotinic acetylcholine receptor. Neuron **3**, 349-357.

Bolger MB, Dionne V, Chrivia J, Johnson DA, Taylor P (1984): Interaction of a fluorescent acyldicholine with the nicotinic acetylcholine receptor and acetylcholinesterase. Mol. Pharmacol. **26**, 57-69.

Boulter J, Connolly JG, Deneris E, Goldman D, Heinemann S, Patrick J (1987): Functional expression of two neuronal nicotinic acetylcholine receptors from cDNA clones identifies a gene family. Proc. Natl. Acad. Sci. (USA) **84**, 7763-7767.

Boulter J, O'Shea-Greenfield A, Duvoisin RM, Connolly JG, Wada E, Jensen A, Gardner P, Ballivet M, Deneris E, McKinnon D, Heinemann S, Patrick J (1990): α3, α5 and β4: three members of the rat neuronal nicotinic acetylcholine receptor-related gene family form a gene cluster. J. Biol. Chem. **265**, 4472-4482.

Breer H, Kleene R, Hinz G (1985): Molecular forms and subunit structure of the acetylcholine receptor in the central nervous system of insects. J. Neurosci. **5**, 3386-3392.

Brough PA, Gallagher T, Thomas P, Wonnacott S, Baker R, Malik KMA, Hursthouse MB (1992): Synthesis and X-ray crystal structure of 2-acetyl-9-azabicyclo(4.2.1)nonan-3-one. A conformationally locked *s-cis* analogue of anatoxin-a. J. Chem. Soc. - Ser. Chem. Comm. **15**, 1087-1089.

Buller AL & White MM (1990a): Altered patterns of N-linked glycosylation of the *Torpedo* acetylcholine receptor expressed in *Xenopus* oocytes. J. Memb. Biol. **115**, 179-189.

Buller AL & White MM (1990b): Functional acetylcholine receptors expressed in *Xenopus* oocytes after injection of *Torpedo* β, γ, and δ subunit RNAs are a consequence of endogenous oocyte gene expression. Mol. Pharmacol. **37**, 423-428.

Camacho P, Liu Y, Mandel G, Brehm P (1993): The epsilon subunit confers fast channel gating on multiple classes of acetylcholine receptors. J. Neurosci. **13**, 605-613.

Carbonetto ST, Fambrough DM, Muller KJ (1978): Non-equivalence of αbungarotoxin receptors and acetylcholine receptors in chick sympathetic neurons. Proc. Natl. Acad. Sci. (USA) **75**, 1016-1020.

Castro NG & Albuquerque EX (1993): Brief-lifetime, fast inactivating ion channels account for the α bungarotoxin-sensitive nicotinic response in hippocampal neurons. Neurosci. Lett. **164**, 137-140.

Castro NG & Albuquerque EX (1995): α-Bungarotoxin sensitive hippocampal nicotinic receptor channel has a high calcium permeability. Biophys. J. **68**, 516-524.

Changeux J-P (1990): Functional architecture and dynamics of the nicotinic acetylcholine receptor: an allosteric ligand-gated ion channel. Fidia Res. Found. Neurosci. Found. Lect. **4**, 21-168, New York: Raven.

Charnet P, Labarca C, Cohen BN, Davidson N, Lester HA, Pilar G (1992a): Pharmacological and kinetic properties of α4β2 neuronal nicotinic acetylcholine receptors expressed in *Xenopus* oocytes. J. Physiol. **450**, 375-394.

Charnet P, Labarca C, Lester H (1992b): Structure of the γ-less nicotinic acetylcholine receptor: learning from omission. Mol. Pharmacol. **41**, 708-717.

Cheng YC & Prusoff WH (1973): Relationships between the inhibition constant (K_i) and the concentration of inhibitor which causes 50 per cent inhibition (IC_{50}) of an enzymatic reaction. Biochem. Pharmacol. **22**, 3099-3108.

Chiappinelli VA (1983): Kappa-bungarotoxin: A probe for the neuronal nicotinic receptor in the avian ciliary ganglion. Brain Research **277**, 9-21.

Clarke PBS, Schwartz RD, Paul SM, Pert CB, Pert A (1985): Nicotinic binding in rat brain: autoradiographic comparison of [^{3}H]acetylcholine, [^{3}H]nicotine and [^{125}I]αbungarotoxin. J. Neurosci. **5**, 1307-1315.

Clarke PBS (1992): The fall and rise of neuronal αbungarotoxin binding proteins. Trends Pharmacol. Sci. **13**, 407-413.

Cockcroft VB, Osguthorpe DJ, Barnard EA, Lunt GG (1990): Modelling of agonist binding to the ligand-gated ion channel superfamily of receptors. Proteins **8**, 386-397.

Cohen JB, Sharp SD, Liu WS (1991): Structure of the agonist binding site of the nicotinic acetylcholine receptor: [^{3}H]acetylcholine mustard identifies residues in the cation binding subsite. J. Biol. Chem. **266**, 23354-23364.

Cohen BN, Labarca C, Davidson N, Lester HA (1992): Mutations in M2 alter the selectivity of the mouse nicotinic acetylcholine receptor for organic and alkali metal cations. J. Gen. Physiol. **100**, 373-400.

Cole KS (1949): Dynamic electrical characteristics of the squid giant axon membrane. Arch. Sci. Physiol. **3**, 253-258.

Colman A & Drummond (1986): The stability and movement of mRNA in *Xenopus* oocytes and embryos. J. Embryol. Exp. Morphol. **97** suppl. 197-209.

Conroy WG, Vernallis AB & Berg DK (1992): The α5 gene product assembles with multiple acetylcholine receptor subunits to form distinctive receptor subtypes in the brain. Neuron **9**, 679-691.

Conti-Tronconi BM & Raftery MA (1982): The nicotinic cholinergic receptor: Correlation of molecular structure with functional properties. Annu. Rev.Biochem. **51**, 491-530.

Conti-Tronconi BM, Dunn SMJ, Barnard EA, Dolly JO, Lai FA, Ray N, Raftery M (1985): Brain and muscle nicotinic acetylcholine receptors are different but homologous proteins. Proc. Natl. Acad. Sci. (USA) **82**, 5208-5212.

Conti-Tronconi BM, Tang F, Diethelm BM, Spencer SR, Reinhardt-Maelicke S, Maelicke A (1990): Mapping of a cholinergic binding site by means of synthetic peptides, monoclonal antibodies and α-bungarotoxin. Biochem. **29**, 6221-6230.

Conti-Tronconi BM, Diethelm BD, Wu X, Tang F, Bertazzon T, Schroder B, Reinhardt-Maelicke S, Maelicke A (1991): α-Bungarotoxin and the competing antibody WF6 interact with different amino acids within the same cholinergic subsite. Biochem. **30**, 2575-2584

Cooper E, Couturier S, Ballivet M (1991): Pentameric structure and subunit stoichiometry of a neuronal acetylcholine receptor. Nature **350**, 235-238.

Copeland JR, Adem A, Jacob P (III), Nordberg A (1991): A comparison of the binding of nicotine and nornicotine stereoisomers to nicotinic binding sites in rat brain cortex. Naunyn-Schmiedeberg's Arch. Pharmacol. **343**, 123-127.

Corringer P-J, Galzi J-L, Eisele J-L, Bertrand S, Changeux J-P & Bertrand D (1995): Identification of a new component of the agonist binding site of the nicotinic α7 homooligomeric receptor. J. Biol. Chem. **270** (20), 11749-11752.

Couturier S, Bertrand D, Matter J-M, Hernandez M-C, Bertrand S, Millar N, Valera S, Barkas T, Ballivet M (1990a): A neuronal nicotinic acetylcholine receptor subunit (α7) is developmentally regulated and forms a homo-oligomeric channel blocked by αBTX. Neuron **5**, 847-856.

Couturier S, Erkman L, Valera S, Rungger D, Bertrand S, Boulter J, Ballivet M, Bertrand D (1990b): α5, α3 and non-α3: three clustered avian genes encoding neuronal nicotinic acetylcholine receptor-related subunits. J. Biol. Chem. **265**, 17560-17567.

Czajkowski C & Karlin A (1991): Agonist binding site of *Torpedo* electric tissue nicotinic acetylcholine receptor: a negatively charged region of the δ subunit within 0.9nm of the α subunit binding site disulphide. J. Biol. Chem. **266**, 22603-22612.

Czajkowski C & Karlin A (1995): Structure of the nicotinic receptor acetylcholine-binding site. J. Biol. Chem. **270**, 3160-3164.

Czajkowski C, Kaufmann C & Karlin A (1993): Negatively charged amino acid residues in the nicotinic receptor δ subunit that contribute to the binding of acetylcholine. Proc. Natl. Acad. Sci. (USA) **90**, 6285-6289.

Dani JA & Eisenmann G (1987): Monovalent and divalent cation permeation in acetylcholine receptor channels: ion transport related to transport. J. Gen. Physiol. **89**, 959-983.

Dascal N, Yekuel R, Oron Y (1985): Cholinergic modulation of progesterone-induced maturation of *Xenopus* oocytes *in vitro*. Gamete Res. **12**, 171-181.

Dascal N (1987): The use of *Xenopus* oocytes for the study of ion channels. CRC Crit. Rev. Biochem. **22**, 317-387.

David JA & Satelle DB (1984): Actions of cholinergic pharmacological agents on the cell body membrane of the fast coaxial depressor motor neurone of the cockroach (*Periplaneta americana*). J. Exp. Biol. **108**, 119-136.

De Fiebre CM, Meyer EM, Henry JC, Muraskin SI, Kem WR, Papke RL (1995): Characterisation of a series of anabaseine-derived compounds reveals that the 3-(4)-dimethylaminocinnamylidine derivative is a selective agonist at neuronal nicotinic α7/[^{125}I]αbungarotoxin receptor subtypes. Mol. Pharmacol. **47**, 164-171.

De la Garza R, Bickford-Wimer PC, Hoffer BJ, Freedman R (1987): Heterogeneity of nicotine actions in the rat cerebellum: An *in vivo* electrophysiologic study. J. Pharmacol. Exp. Ther. **240**, 689-695.

Deneris ES, Connolly JG, Boulter J, Wada E, Wada K, Swanson LW, Patrick J, Heineman SF (1988): Primary structure and expression of β2: a novel subunit of neuronal nicotinic acetylcholine receptors. Neuron **1**, 45-54.

Deneris ES, Boulter J, Swanson LW, Patrick J, Heinemann S (1989): β3: a new member of nicotinic acetylcholine receptor gene family is expressed in brain. J. Biol. Chem. **264**, 6268-6272.

Deneris ES, Connolly J, Rogers SW, Duvoisin R (1991): Pharmacological and functional diversity of neuronal nicotinic acetylcholine receptors. Trends Pharmacol. Sci. **12**, 34-40.

Dennis M, Giraudat J, Kotzyba-Hibert F, Goeldner M, Hirth C, Chang J-Y, Changeux J-P (1986): A photoaffinity ligand of the acetylcholine binding site predominantly labels the region 179-207 of the α subunit on native acetylcholine receptor from *Torpedo mamorata*. FEBS Lett. **207**, 243-249.

Dennis M, Giraudat J, Kotzyba-Hibert F, Goeldner M, Hirth C, Chang J-Y, Lazure C, Chretien M, Changeux J-P (1988): Amino acids of the *Torpedo mamorata* acetylcholine receptor α subunit labelled by a photoaffinity ligand for the acetylcholine binding site. Biochem. **27**, 2346-2357.

Devillers-Theiry A, Galzi J-L, Bertrand S, Bertrand D, Changeux J-P (1993): Functional architecture of the nicotinic acetylcholine receptor: a prototype of ligand-gated ion channel. J. Memb. Biol. **136**, 97-112.

Dewar MJS & Thiel W (1977): Ground states of molecules. 38. The MNDO method. Approximations and parameters. J. Am. Chem. Soc. **99**, 4899-4907.

DiPaola M, Czajkowski C, Karlin A (1989): The sidedness of the COOH terminus of the acetylcholine receptor δ subunit. J. Biol. Chem. **264**, 1-7.

Dougherty DA & Stauffer DA (1990): Acetylcholine binding by a synthetic receptor: implications for biological recognition. Science **250**, 1558-1560.

Drasdo A, Caulfield M, Bertrand D, Bertrand S, Wonnacott S (1992): Methyllycaconitine: A novel nicotinic antagonist. Mol. Cell Neurosci. **3**, 237-243.

Dufton MJ & Harvey AL (1989): The long and the short of snake toxins. Trends Pharmacol. Sci. **10**, 258-259.

Dunn SMJ, Conti-Tronconi BM, Raftery MA (1986): Acetylcholine receptor dimers are stabilised by extracellular disulphide bonding. Biochem. Biophys. Res. Comm. **139**, 830-837.

Duvoisin RM, Deneris ES, Patrick J, Heinemann S (1989): The functional diversity of neuronal nicotinic acetylcholine receptors is increased by a novel subunit: β4. Neuron **3**, 487-496.

Elgoyhen AB, Johnson DS, Boulter J, Vetter DE & Heinemann S (1994): α9: An acetylcholine receptor with novel pharmacological properties expressed in rat cochlear hair cells. Cell **79**, 705-715.

Farley JM & Narahashi T (1983): Effects of drugs on acetylcholine-activated ionic channels of internally perfused chick myoballs. J. Physiol. **337**, 753-768.

Figl A, Cohen BN, Quick MW, Davidson N, Lester HA (1992): Regions of β4*mDβ2 subunit chimeras that contribute to the agonist selectivity of neuronal nicotinic receptors. FEBS Lett. **308**, 245-248.

Finer-Moore J & Stroud R (1984): Amphipathic analysis and possible formation of the ion channel in an acetylcholine receptor. Proc. Natl. Acad. Sci. (USA) **81**, 155-159.

Flores CM, Rogers SW, Pabreza LA, Wolfe BB, Kellar KJ (1992): A subtype of nicotinic cholinergic receptor in rat brain is composed of α4 and β2 subunits and is upregulated by chronic nicotine treatment. Mol. Pharmacol. **41**, 31-37.

Fraenkel Y, Gershoni JM, Navon G (1991): Acetylcholine interacts with Tryptophan-184 of the α subunit of the nicotinic acetylcholine receptor revealed by transferred nuclear overhauser effect. FEBS Lett. **291**, 225-228.

Galzi J-L, Revah F, Black D, Goeldner M, Hirth C, Changeux J-P (1990): Identification of a novel amino acid αTyr93 within the active site of the acetylcholine receptor by photoaffinity labelling: additional evidence for a three-loop model of the acetylcholine binding site. J. Biol. Chem. **265**, 10430-10437.

Galzi J-L, Revah F, Bessis A, Changeux J-P (1991a): Functional architecture of the nicotinic acetylcholine receptor: from electric organ to brain. Annu. Rev. Pharmacol. Toxicol. **31**, 37-72.

Galzi J-L, Bertrand D, Devillers-Thiery A, Revah F, Bertrand S, Changeux J-P (1991b): Functional significance of aromatic amino acids from three peptide loops of the α7 neuronal nicotinic receptor site investigated by site directed mutagenesis. FEBS Lett. **294**, 198-202.

Garcha HS, Thomas P, Spivak CE, Wonnacott S, Stolerman IP (1993): Behavioural and ligand-binding studies in rats with 1-acetyl-4-methylpiperazine, a novel nicotinic agonist. Psychopharmacol. **110**, 347-354.

Gerzanich V, Anand R, Lindstrom J (1994): Homomers of α8 and α7 subunits of nicotinic receptors exhibit similar channel but contrasting binding site properties. Mol. Pharmacol. **45**, 212-220.

Giraudat J, Dennis M, Heidmann T, Chang JY, Changeux J-P (1986): Structure of the high affinity binding site for non-competitive blockers of the acetylcholine receptor: Serine-262 of the δ subunit is labelled by [^{3}H]chlorpromazine. Proc. Natl. Acad. Sci. (USA) **83**, 2719-2723.

Giraudat J, Dennis M, Heidmann T, Haumont P, Lederer F, Changeux J-P (1987): Structure of the high affinity binding site for non-competitive blockers of the acetylcholine receptor: [^{3}H]chlorpromazine labels homologous residues in the β and δ chains. Biochem. **26**, 2410-2418.

Giraudat J, Galzi J-L, Revah F, Changeux J-P, Haumont P, Lederer F (1989): The non-competitive blocker [^{3}H]chlorpromazine labels segment M2 but not segment M1 of the nicotinic acetylcholine receptor α subunit. FEBS Lett. **253**, 190-198.

Golino MD & Hamill OP (1992): Subunit requirements for *Torpedo* ACh receptor channel expression: a specific role for the δ subunit in voltage dependent gating. J. Memb. Biol. **129**, 297-309.

Gotti C, Moretti M, Longhi R, Briscini L, Manera E, Clementi F (1993): Anti-peptide specific antibodies for the characterisation of different α subunits of α-bungarotoxin binding acetylcholine receptors present in chick optic lobe. J. Recept. Res **13**, 453-465.

Gross A, Ballivet M, Rungger D, Bertrand D (1991): Neuronal nicotinic acetylcholine receptors expressed in *Xenopus* oocytes: role of the α subunit in agonist sensitivity and desensitisation. Pflugers Arch. **419**, 545-551.

Gund TM, & Spivak CE (1991): Pharmacophore for nicotinic agonists. Meth. Enzymol. **203**, 677-693.

Gurdon JB, Lane CD, Woodland HR, Marbaix G (1971): Use of frog eggs and oocytes for the study of messenger RNA and its translation in living cells. Nature **233**, 177-182.

Gurdon JB & Wickens MP (1983): The use of *Xenopus* oocytes for the expression of cloned genes. Meth. Enzymol. **101**, 370-386.

Guy HR (1984): Structural model of the acetylcholine receptor channel based on partition energy and helix packing calculations. Biophys. J. **45**, 249-261.

Haggerty JG & Froehner SC (1981): Restoration of [^{125}I]αbungarotoxin binding activity to the α subunit of *Torpedo* acetylcholine receptor isolated by gel electrophoresis in sodium dodecyl sulfate. J. Biol. Chem. **256**, 8294-8297.

Hacksell U & Mellin C (1989): Stereoselectivity of nicotinic receptors. In '*Nicotinic receptors in the CNS*', eds. Nordberg A, Fuxe K, Holmstedt B, Sundwall A, Prog. Brain Res. **79**, pp95-100. Amsterdam: Elsevier.

Halvorsen SW & Berg DK (1986): Identification of a nicotinic acetylcholine receptor on neurons using an αneurotoxin that blocks receptor function. J. Neurosci. **6**, 3405-3412.

Hanke W & Breer H (1986): Channel properties of an insect neuronal acetylcholine receptor protein reconstituted in planar lipid bilayers. Nature **321**, 171-174.

Hartman DS & Claudio T (1990): Coexpression of two distinct muscle acetylcholine receptor α-subunits during development. Nature **343**, 372-375.

Heidman T, Oswald RE, Changeux J-P (1983): Multiple sites of action for non-competitive blockers on acetylcholine receptor-rich membrane fragment from *Torpedo mamorata*. Biochem. **22**, 3112-3127.

Heidman T & Changeux J-P (1984): Time-resolved photolabelling by the non-competitive blocker chlorpromazine of the acetylcholine receptor in its transiently open and closed ion channel conformations. Proc. Natl. Acad. Sci. (USA) **81**, 1897-1901.

Henley JM & Oswald RE (1987): Two distinct (-)nicotine binding sites in goldfish brain. J. Biol. Chem. **262**, 6691-6698.

Herz JM, Johnson DA, Taylor P (1989): Distance between the agonist and non-competitive inhibitor sites on the nicotinic acetylcholine receptor. J. Biol. Chem. **264**, 12439-12448.

Higgins LS & Berg DK (1988): A desensitised form of neuronal acetylcholine receptor detected by [^{3}H]-nicotine binding on bovine adrenal chromaffin cells. J. Neurosci. **8** (4), 1436-1446.

Hirano T, Kidokoro Y, Ohmori H (1987): Acetylcholine dose-response relation and the effect of caesium ions in the rat adrenal chromaffin cell under voltage clamp. Pflugers Arch. **408**, 401-407.

Hodgkin AL & Huxley AF (1952): A quantitative description of membrane current and its application to conduction and excitation in nerve. J. Physiol. **117**, 500-554.

Howard MH, Sardina FJ, Rapoport H (1990): Chirospecific synthesis of nitrogen and side chain modified anatoxin analogues. Synthesis of (1R)-anatoxinal and (1R)-anatoxinic acid derivatives. J. Org. Chem. **55**, 2829-2838.

Huganir RL & Greengard P (1990): Regulation of neurotransmitter receptor desensitisation by protein phosphorylation. Neuron **5**, 555-567.

Huby NJS, Thompsom P, Wonnacott S, Gallager T (1991): Structural modification of anatoxin-a. Synthesis of model affinity ligands for the nicotinic acetylcholine receptor. J. Chem. Soc. Chem. Comm. **4**, 243-245.

Hucho F (1986): The nicotinic acetylcholine receptor and its ion channel. Eur. J. Biochem. **158**, 211-226

Ifune CK & Steinbach JH (1992): Inward rectification of acetylcholine-elicited currents in rat phaeochromocytoma cells. J. Physiol. **457**, 143-165.

Isenberg KE & Meyer GE (1989): Cloning of a putative neuronal nicotinic acetylcholine receptor subunit. J. Neurochem. **52**, 988-991.

Jacob NH & Berg DK (1983): The ultrastructural localisation of αbungarotoxin binding sites in relation to synapses on chick ciliary ganglion neurons. J. Neurosci. **3**, 260-270.

Johnson DS, Martinez J, Elgoyhen AB, Heinemann SF & McIntosh JM (1995): α-Conotoxin Imi exhibits subtype-specific nicotinic acetylcholine receptor blockade: preferential inhibition of homomeric α7 and α9 receptors. Mol. Pharmacol. **48**, 194-199.

Kane DB & Abood LG (1988): Synthesis and biological characterisation of pyridohomotropanes. Structure-activity relationships of conformationally restricted nicotinoids. J. Med. Chem. **31**, 506-509.

Kao P, Dwork A, Kaldany R (1984): Identification of the α subunit half cysteine specifically labelled by an affinity reagent for the acetylcholine receptor binding site. J. Biol. Chem. **259**, 11662-11665.

Kao PN & Karlin A (1986): Acetylcholine receptor binding site contains a disulphide crosslink between adjacent half-cystinyl residues. J. Biol. Chem. **261**, 8085-8088.

Karlin A (1991): Explorations of the nicotinic acetylcholine receptor. Harvey Lect. **71**, 71-107.

Karlin A (1993): Structure of nicotinic acetylcholine receptors. Current Op. Neurobiol. **3**, 299-309.

Kellar KJ & Wonnacott S (1990): Nicotinic cholinergic receptors in Alzheimer's disease. In '*Nicotine psycopharmacology*', eds. Wonnacott S, Russell AH, Stolerman IP, pp341-373: Oxford, Oxford Univ. press.

Kemp G, Bentley L, McNamee MG, Morley BJ (1985): Purification and characterisation of the α bungarotoxin binding protein from rat brain. Brain Res. **347**, 274-283.

Keyser KT, Britto LRG, Schoepfer R, Whiting P, Cooper J, Conroy W, BrozozowskaPrechtl A, Karten HJ, Lindstrom J (1993): Three subtypes of α-bungarotoxin-sensitive nicotinic acetylcholine receptors are expressed in chick retina. J. Neurosci. **13**, 442-454.

Klarsfeld A, Devillers-Thiery A, Giraudat J, Changeux J-P (1984): A single gene codes for the nicotinic acetylcholine receptor α subunit in *Torpedo mamorata*: Structural and developmental implications. EMBO J. **3**, 35-41.

Kofuji P, Aracava Y, Swanson KL, Aronstam RS, Rapoport H, Albuquerque EX (1990): Activation and blockade of the acetylcholine receptor-ion channel by the agonists (+)-anatoxin-a, the N-methyl derivative and the enantiomer. J. Pharmacol. Exp. Ther. **252**, 517-525.

Koskinen AMP & Rapoport HJ (1985): Synthetic, conformational and pharmacological studies of anatoxin-a, a potent toxic acetylcholine agonist. J. Med. Chem. **28**, 1301-1309.

Krnjevic K (1974): Chemical nature of synaptic transmission in vertebrates. Physiol. Rev. **54**, 418-540.

Kubalek E, Ralston S, Lindstrom J (1987): Location of subunits within the acetylcholine receptor: analysis of tubular crystals from *Torpedo mamorata*. J. Cell Biol. **105**, 9-18.

Kusano K, Miledi R, Stinnakre J (1977): Acetylcholine receptors in the oocyte membrane. Nature **270**, 739-741.

Kusano K, Miledi R, Stinnakre J (1982): Cholinergic and catecholinergic receptors in the *Xenopus* oocyte membrane. J. Physiol. **328**, 143-170.

Langenbuch-Cachet J, Bon C, Goeldner M, Hirth C, Changeux J-P (1988): Photoaffinity labelling by aryldiazonium derivatives of *Torpedo mamorata* acetylcholine receptor. Biochem. **27**, 2337-2345.

Langley JN (1905): On the reaction of cells and of nerve-endings to certain poisons, chiefly as regards the reaction of striated muscle to nicotine and to curare. J. Physiol. **33**, 374-413.

Larsson C & Nordberg A (1985): Comparative analysis of nicotine-like receptor-ligand interactions in rodent brain homogenate. J. Neurochem. **45**, 24-31.

Li Y, Gerzanich V, Anand R, Lindstrom J (1993): Functional properties of neuronal $\alpha 7$ acetylcholine receptor expressed in *Xenopus* oocytes: a comparison with neuronal $\alpha 4\beta 2$ and electric organ $\alpha 1\beta 1 \gamma\delta$ acetylcholine receptors. Biophys J. **64**, A322.

Lindstrom J, Merlie J, Yogeeswaran G (1979): Biochemical properties of acetylcholine receptor subunits From *Torpedo californica*. Biochem. **18**, 4465-4470.

Lindstrom J, Schoepfer R, Whiting P (1987): Molecular studies of the neuronal nicotinic acetylcholine receptor family. Mol. Neurobiol. **1**, 281-337.

Lippiello PM, Sears SB, Fernandes KG (1987): Kinetics and mechanism of [^{3}H]-(-)-nicotine binding to putative high affinity receptor sites in rat brain. Mol. Pharmacol. **31**, 392-400.

Lipton SA, Aizenman E, Loring RH (1987): Neural nicotinic acetylcholine responses in solitary mammalian retinal ganglion cells. Pflugers Arch. Eur. J. Physiol. **410**, 37-43.

Listerud M, Brussard AB, Devay P, Colman DR & Role LW (1991): Functional contribution of neuronal AChR subunits revealed by antisense oligonucleotides. Science **254**, 1518-1521.

Loring RH, Chiappinelli VA, Zigmond RE, Cohen JB (1984): Characterization of a snake venom neurotoxin which blocks nicotinic transmission in the avian ciliary ganglion. Neurosci **11**, 989-999.

Loring RH & Zigmond RE (1988): Characterisation of neuronal nicotinic receptors by snake venom neurotoxins. Trends Neurosci. **11**, 73-78.

Lowry OH, Rosebrough NJ, Farr AL, Randall RJ (1951): Protein measurement with the Folin phenol reagent. J. Biol. Chem. **193**, 165-175.

Luetje CW, Wada K, Rogers S, Abramson SN, Tsuji K, Heinemann S, Patrick J (1990): Neurotoxins distinguish different neuronal nicotinic acetylcholine receptor subunit combinations. J. Neurochem. **55**, 632-640.

Luetje CW & Patrick J (1991): Both α and β subunits contribute to the agonist sensitivity of neuronal nicotinic acetylcholine receptors. J. Neurosci. **11**, 837-845.

Lukas RJ & Bennett EL (1979): Effects of local anaesthetics on cholinergic agonist binding affinity of central nervous system α-bungarotoxin receptors. FEBS Lett. **108**, 356-358.

Lukas RJ & Bennett EL (1980): Interaction of nicotinic receptor affinity reagents with central nervous system α-bungarotoxin-binding entities. Mol. Pharmacol. **17**, 149-155.

Lukas RJ (1986): Immunochemical and pharmacological distinctions between curaremimetic neurotoxin binding sites of central, autonomic and peripheral origin. Proc. Natl. Acad. Sci. (USA) **83**, 5741-5745.

MacAllen DRE, Lunt GG, Wonnacott S, Swanson KL, Rapoport H, Albuquerque EX (1988): Methyllycaconitine and (+)anatoxin-a differentiate between nicotinic receptors in vertebrate and invertebrate nervous systems. FEBS Lett. **226**, 357-363.

Margiotta JF, Berg DF, Dionne VE (1987): The properties and regulation of functional acetylcholine receptors on chick ciliary ganglion neurons. J. Neurochem. **7**, 3612-3622.

Marks MJ & Collins AC (1982): Characterisation of nicotine binding in mouse brain and comparison with the binding of αbungarotoxin and quinuclidinyl benzilate. Mol. Pharmacol. **22**, 554-564.

Marks MJ, Stitzel JA, Collins AC (1985): Time course study of the effects of chronic nicotine infusion on drug response and brain receptors. J. Pharmacol. Exp. Ther. **235**, 619-628.

Marks MJ, Stitzel JA, Romm E, Wehner JM, Collins AC (1986): Nicotinic binding sites in rat and mouse brain: comparison of acetylcholine, nicotine and αbungarotoxin. Mol. Pharmacol. **30**, 427-436.

Marks MJ, Farnham DA, Grady SR, Collins AC (1993): Nicotinic receptor function determined by stimulation of rubidium efflux from mouse brain synaptosomes. J. Pharmacol. Exp. Ther. **264**, 542-552.

Marshall J, Buckingham SD, Shingai R, Lunt GG, Goosey MW, Darlison MG, Sattelle DB, Barnard EA (1990): Sequence and functional expression of a single α subunit of an insect nicotinic acetylcholine receptor. EMBO J. **9**, 4391-4398.

Martino-Barrows AM & Kellar KJ (1987): [^{3}H]Acetylcholine and [^{3}H]-(-)-nicotine label the same recognition site in rat brain. Mol. Pharmacol. **31**, 169-174.

Mathie A, Colquhoun D, Cull-Candy SG (1990): Rectification of currents activated by nicotinic acetylcholine receptors in rat sympathetic ganglion neurones. J. Physiol. **427**, 625-655.

Mathie A, Cull-Candy SG, Colquhoun D (1991): Conductance and kinetic properties of single nicotinic acetylcholine receptor channels in rat sympathetic neurones. J. Physiol. **439**, 717-750.

McCormick DJ & Atassi MZ (1984): Localisation and synthesis of the acetylcholine binding site in the α chain of the *Torpedo californica* acetylcholine receptor. Biochem. J. **224**, 995-1000.

McGehee DS, Heath MJS, Gelber S, Devay P & Role LW (1995): Nicotine enhancement of fast excitatory synaptic transmission in CNS by presynaptic receptors. Science **269**, 1692-1696.

McGroddy KA, Carter AA, Tubbert MM, Oswald RE (1993a): Analysis of cyclic and acyclic nicotinic cholinergic agonists using radioligand binding, single channel recording, and nuclear magnetic resonance spectroscopy. Biophys. J. **64**, 325-338.

McGroddy KA, Oswald RE (1993b): Solution structure and dynamics of cyclic and acyclic cholinergic agonists. Biophys. J. **64**, 314-324.

McGroddy KA, Brady JW, Oswald RE (1994): Computer simulations of cyclic and acyclic cholinergic agonists: Conformational search and molecular dynamics simulations. Biophys. J. **66**, 314-324.

McLane KE, Wu X, Conti-Tronconi BM (1991a): Structural determinants within residues 180-199 of the rodent α5 nicotinic acetylcholine receptor subunit involved in αbungarotoxin binding. Biochem **30**, 10730-10738.

McLane KE, Wu X, Diethelm BM, Conti-Tronconi BM (1991b): Structural determinants of α-bungarotoxin binding to the sequence segment 181-200 of the muscle nicotinic acetylcholine receptor α subunit: effects of cysteine/cystine modification and species-specific amino acid substitutions. Biochem. **30**, 4925-4934.

McLane KE, Wu X, Schoepfer R, Lindstrom JM, Conti-Tronconi BM (1991c): Identification of sequence segments forming the αbungarotoxin binding sites on two nicotinic acetylcholine receptor α subunits from the avian brain. J. Biol. Chem. **266**, 15230-15239.

McLane KE, Wu X, Conti-Tronconi (1994): An αbungarotoxin binding sequence on the *Torpedo* nicotinic acetylcholine receptor α subunit: conservative amino acid substitutions reveal side-chain specific interactions. Biochem. **33**, 2576-2585.

Merlie J, Sebbane R, Gardner S, Olsen E, Lindstrom J (1983): Regulation of acetylcholine receptor gene expression: molecular cloning of a cDNA specific for α subunit of the receptor from the mouse muscle cell line BC3H1. Proc. Natl. Acad. Sci. (USA) **80**, 3845-3849.

Messing A & Kim SU (1981): Development of αbungarotoxin receptors in cultured chick ciliary ganglion neurons. Brain Res. **208**, 479-486.

Mills A & Wonnacott S (1984): Antibodies to nicotinic acetylcholine receptors used to probe the structural and functional relationships between brain αbungarotoxin binding sites and nicotinic receptors. Neurochem. Intl. **6**, 249-257.

Mishina M, Tobimatsu T, Imoto K, Tanaka K, Fujita Y, Fukuda K, Kurasaki M, Takahashi H, Morimoto Y, Hirose T, Inayama S, Takahashi T, Kuon M, Numa S (1985): Location of functional regions of acetylcholine receptor α subunit by site-directed mutagenesis. Nature **313**, 364-369.

Morley BJ, Dwyer DS, Strang-Brown PF, Bradley RJ, Kemp GE (1983): Evidence that certain peripheral anti-acetylcholine receptor antibodies do not interact with brain αBgt binding sites. Brain Res. **262**, 109-116.

Morris BJ, Hicks AA, Wisden W, Darlison MG, Hunt SP, Barnard EA (1990): Distinct regional expression of nicotinic acetylcholine receptor genes in chick brain. Mol. Brain Res. **7**, 305-315.

Mulac-Jericevic B & Atassi MZ (1987): αNeurotoxin binding to acetylcholine receptor: localisation of the full profile of the cobratoxin-binding regions on the α-chain of *Torpedo californica* acetylcholine receptor by a comprehensive synthetic strategy. J. Prot. Chem. **6**, 365-373.
Mulle C & Changeux J-P (1990): A novel type of nicotinic receptor in the rat central nervous system characterised by patch-clamp techniques. J. Neurosci. **10**, 169-175.

Mulle C, Vidal C, Beniot P, Changeux J-P (1991): Existence of different subtypes of nicotinic acetylcholine receptors in the rat habenulo-interpeduncular system. J. Neurosci. **11**, 2588-2597.

Nef P, Oneyser C, Alloid C, Couturier S, Ballivet M (1988): Genes expressed in the brain define three distinct neuronal nicotinic acetylcholine receptors. EMBO J. **7**, 595-601.

Neher E & Steinbach JH (1978): Local anaesthetics transiently block currents through single acetylcholine receptor channels. J. Physiol. **277**, 153-176.

Noda M, Takahashi H, Tanabe T, Toyosato M, Kikyotani S, Furutani Y, Hirose T, Takashima H, Inayama S, Miyata T, Numa S (1983): Structural homology of *Torpedo californica* acetylcholine receptor subunits. Nature **302**, 528-532.

Norman RI, Mehraben F, Barnard EA, Dolly JD (1982): Nicotinic acetylcholine receptor from chick optic lobe. Proc. Natl. Acad. Sci. (USA) **79**, 1321-1325.

Numa S, Noda M, Takahashi H, Tanabe T, Toyosato M, Furutani Y, Kikyotani S (1983): Molecular structure of the nicotinic acetylcholine receptor. Cold Spr. Hbr. Symp. Quant. Biol. **48**, 57-84.

Ogden DC & Colquhoun D (1985): Ion channel block by acetylcholine, carbachol and suberyldicholine at the frog neuromuscular junction. Proc. Royal Soc. Lon. - B. Biol. Sci. **225**, 329-355.

O'leary ME & White MM (1992): Mutation analysis of ligand-induced activation of the *Torpedo* acetylcholine receptor. J. Biol. Chem. **267**, 8360-8365.

Oswald RE & Changeux J-P (1982): Crosslinking of α-bungarotoxin to the acetylcholine receptor from *Torpedo mamorata* by ultraviolet light irradiation. FEBS Lett. **139**, 225-229.

Pabreza LA, Dhawan S, Kellar KJ (1991): [^{3}H]cytisine binding to nicotinic cholinergic receptors in brain. Mol. Pharmacol. **39**, 9-12.

Papke RL, Boulter J, Patrick J, Heinemann S (1989): Single channel currents of rat neuronal nicotinic acetylcholine receptor expressed in *Xenopus* oocytes. Neuron **3**, 589-596.

Papke RL & Heinemann SF (1991): The role of the β4 subunit in determining the kinetic properties of rat neuronal acetylcholine receptors expressed in *Xenopus laevis* oocytes. Neuron **3**, 589-596.

Papke RL & Heinemann SF (1993): Partial agonist properties of cytisine on neuronal nicotinic receptors containing the β2 subunit. Mol. Pharmacol. **45**, 142-149.

Pauling P (1980): Structural differences between typical anticholinergic substances and those used for Parkinson's syndrome. Brit. J. Pharmacol. **69**, 333P.

Pederson SE & Cohen JB (1990): d-Tubocurarine binding sites are located at α-γ and α-δ subunit interfaces of the nicotinic acetylcholine receptor. Proc. Natl. Acad. Sci. (USA) **87**, 2785-2789.

Peng X, Katz M, Gerzanich V, Anand R, Lindstrom J (1994): Human α7 acetylcholine receptor: Cloning of the α7 subunit from the SH- SY5Y cell line and determination of pharmacological properties of native receptors and functional α7 homomers expressed in *Xenopus* oocytes. Mol. Pharmacol. **45**, 546-554.

Pugh PC & Berg DK (1994): Neuronal acetylcholine receptors that bind α-bungarotoxin mediate neurite retraction in a calcium-dependent manner. J. Neurosci. **14** (2), 889-896.

Pullman B, Courriere P, Coubeils JP (1971): Investigations into the conformations of nicotine. Mol. Pharmacol. **7**, 397-405.

Ramoa AS, Alkondon M, Aracava Y, Irons J, Lunt GG, Desphande SS, Wonnacott S, Aronstam RS, Albuquerque EX (1990): The anticonvulsant MK-801 interacts with the peripheral and central nicotinic acetylcholine receptor ion channels. J. Pharmacol. Exp. Ther. **254**, 71-82.

Rapier C, Harrison R, Lunt GG, Wonnacott S (1985): Neosurugatoxin blocks nicotinic acetylcholine receptors in the brain. Neurochem. Int. **7**, 389-396.

Rapier C, Wonnacott S, Lunt GG, Albuquerque EX (1987): The neurotoxin histrionicotoxin interacts with the putative ion channel of the nicotinic acetylcholine receptors in the central nervous system. FEBS Lett. **212** (2), 292-296.

Rapier C, Lunt GG, Wonnacott S (1988): Stereoselective nicotine-induced release of dopamine from striatal synaptosomes: Concentration dependence and repetitive stimulation. J. Neurochem. **50**, 1123-1130.

Ratnam M, Gullick W, Speiss J, Wan K, Criado M, Lindstrom J (1986): Structural heterogeneity of the α subunits of the nicotinic acetylcholine receptor in relation to agonist affinity alkylation and antagonist binding. Biochem. **25**, 4268-4275.

Ravdin PM & Berg DK (1979): Inhibition of neuronal ACh sensitivity by αtoxins from *Bungarus multicinctus* venom. Proc. Natl. Acad. Sci. (USA) **76**, 2072-2076.

Reavill C, Spivak CE, Stolerman IP, Waters JA (1987): Isoarecolone can inhibit nicotine binding and produce nicotine-like discriminative stimulus effects in rats. Neuropharmacol. **26**, 789-792.

Reavill C, Jenner P, Kumar R, Stolerman IP (1988): High affinity binding of [^{3}H] (-)-nicotine to rat brain membranes and its inhibition by analogues of nicotine. Neuropharmacol. **27**, 235-241

Revah F, Galzi J-L, Giraudat J, Haumont PY, Lederer F, Changeux J-P (1990): The non-competitive blocker [^{3}H]chlorpromazine labels three amino acids of the acetylcholine receptor γ subunit: implications for the α helical organisation of the MII segments and the structure of the ion channel. Proc. Natl. Acad. Sci. (USA) **87** (12), 4675-4679.

Revah F, Bertrand D, Galzi J-L, Devillers-Thiery A, Mulle C, Hussy N, Bertrand S, Ballivet M, Changeux J-P (1991): Mutations in the channel domain alter desensitisation of a neuronal nicotinic receptor. Nature **353**, 846-849.

Reynolds JA & Karlin A (1978): Molecular weight in detergent solution of acetylcholine receptor from *Torpedo californica*. Biochem. **17**, 2035-2038.

Role LW (1992): Diversity in primary structure and function of neuronal nicotinic acetylcholine receptor channels. Curr. Op. Neurobiol. **2**, 254-262.

Romano C & Goldstein A (1980): Stereospecific nicotine receptors in rat brain membranes. Science **210**, 647-649.

Romm E, Lippiello PM, Marks MJ, Collins AC (1990): Purification of L-[^{3}H]nicotine eliminates low affinity binding. Life Sci. **46**, 935-943.

Rozental R, Aracava Y, Scoble GT, Swanson KL, Wonnacott S, Albuquerque EX (1989): Agonist recognition site of the peripheral acetylcholine receptor ion channel complex differentiates the enantiomers of nicotine. J. Pharmacol. Exp. Ther. **251**, 395-404.

Ruan K-H, Spurlino J, Quiocho FA, Atassi MZ (1990): Acetylcholine receptor-αbungarotoxin interactions: determination of the region-to-region contacts by peptide-peptide interactions and molecular modelling of the receptor cavity. Proc. Natl. Acad. Sci. (USA) **87**, 6156-6160.

Ruan K-H, Stiles BG, Atassi MZ (1991): The short-neurotoxin-binding regions of the α-chain of human and *Torpedo californica* acetylcholine receptors. Biochem. J. **274**, 849-854.

Sakmann B, Methfessel C, Mishina M, Takahashi T, Takai T, Kuraski M, Fukuda K, Numa S (1985): Role of acetylcholine receptor subunits in gating of the channel. Nature **318**, 538-543.

Sands SB & Barish ME (1991): Calcium permeability of neuronal nicotinic acetylcholine receptor channels in PC12 cells. Brain Res. **560**, 38-42.

Sands SB, Costa ACS & Patrick JW (1993): Barium permeability of neuronal nicotinic receptor α7 expressed in *Xenopus* oocytes. Biophys. J. **65**, 2614-2621.

Sardina FJ, Howard MH, Koshkinen AMP, Rapoport H (1989): Chirospecific synthesis of nitrogen and side chain modified analogues of (+)anatoxin. J. Org. Chem. **54**, 4654-4660.

Sargent PB (1993): The diversity of neuronal nicotinic acetylcholine receptors. Annu. Rev. Neurosci. **16**, 403-443.

Sattelle DB (1985) In *'Comprehensive insect physiology, biochemistry and pharmacology'*, eds. KerkutGA, Gilbert LI, **11**, pp395-434. Oxford: Pergamon press.

Schleiffer LS & Eldefrawi ME (1974): Identification of the nicotinic and muscarinic acetylcholine receptors in subcellular fractions of mouse brains. Neuropharmacol. **13**, 53-63.

Schmieden V, Grenningloh G, Schofield PR, Betz H (1989): Functional expression in *Xenopus* oocytes of the strychnine binding 48kD subunit of the glycine receptor. EMBO J. **8**, 695-700.

Schmidt J & Raftery MA (1973): A simple assay for the study of solubilised acetylcholine receptors. Anal. Biochem. **52**, 349-354.

Schmidt J, Hunt S, Polz-Tejera G (1980): Nicotinic receptors of the central and autonomic nervous system. In '*Neurotransmitters, receptors and drug action*', pp1-45. Spectrum.

Schneider M, Adee C, Betz H, Schmidt J (1985): Biochemical characterisation of two nicotinic receptors from the chick optic lobe. J. Biol. Chem. **260**, 14505-14512.

Schoepfer R, Conroy WG, Whiting P, Gore M, Lindstrom J (1990): Brain αbungarotoxin binding protein cDNAs and MAbs reveal subtypes of this branch of the ligand-gated ion channel gene superfamily. Neuron **5**, 35-48.

Schwartz RD, McGee R, Kellar KJ (1982): Nicotinic cholinergic receptors labelled by [^{3}H]acetylcholine in rat brain. Mol. Pharmacol. **22**, 56-62.

Seguela P, Waduche J, Dineley-Miller K, Dani JA, Patrick JW (1992): Molecular cloning, functional properties and distribution of rat brain α7: a nicotinic cation channel highly permeable to calcium. J. Neurosci. **13**, 596-604.

Sheridan RP, Nilakantan R, Dixon JS, Venkataraghaven R (1986): The ensemble approach to distance geometry: application to the nicotinic pharmacophore. J. Med. Chem. **29**, 899-906.

Sine SM & Steinbach JH (1984): Agonists block currents through acetylcholine receptor channels. Biophys. J. **46**, 277-284.

Sine SM & Claudio T (1991): γ and δ subunits regulate the affinity and the cooperativity of ligand binding to the acetylcholine receptor. J. Biol. Chem. **266**, 19369-19377.

Sine SM, Quiram P, Papanikolaou F, Kreienkamp H-J, Taylor P (1994): Conserved tyrosines in the α subunit of the nicotinic acetylcholine receptor stabilise quaternary ammonium groups of agonists and curariform antagonists. J. Biol. Chem. **269**, 8808-8816.

Smith MA, Margiotta JF, Franco A, Lindstrom J, Berg DK (1986): Cholinergic modulation of an acetylcholine receptor-like antigen on the surface of chick ciliary ganglion neurons in cell culture. J. Neurosci. **6**, 946-953.

Snutch TP (1988): The use of *Xenopus* oocytes to probe synaptic communication. Trends Pharmacol. Sci. **11**, 250-256.

Spivak CE, Witkop B, Albuquerque EX (1980): Anatoxin-a: A novel, potent agonist at the nicotinic receptor. Mol. Pharmacol. **18**, 384-394.

Spivak CE & Albuquerque EX (1982): Dynamic properties of the nicotinic acetylcholine receptor ionic channel complex: Activation and blockade. In '*Progress in cholinergic biology: Model cholinergic synapses*', eds. Hanin I, Goldberg AM, pp323-357. New York: Raven press.

Spivak CE, Waters J, Witkop B, Albuquerque EX (1983): Potencies and channel properties induced by semirigid agonists at frog nicotinic acetylcholine receptors. Mol. Pharmacol. **23**, 337-343.

Spivak CE, Gund TM, Liang RF, Waters JA (1986): Structural and electronic requirements for potent agonists at a nicotinic receptor. Eur. J. Pharmacol. **120**, 127-131.

Spivak CE, Yadav JS, Shang W-C, Hermsmeier M, Gund TM (1989a): Carbamyl analogues of potent nicotinic agonist: pharmacology and computer-assisted molecular modelling study. J. Med. Chem. **32** (2), 305-309.

Spivak CE, Waters JA, Aronstam RS (1989b): Binding of semirigid nicotinic agonists to nicotinic and muscarinic receptors. Mol. Pharmacol. **36**, 177-184.

Stauffer DA & Karlin A (1994): Electrostatic potential of the acetylcholine binding sites in the nicotinic receptor probed by reactions of binding site cysteines with charged methanethiosulfonates. Biochemistry **33**, 6840-6849.

Stroud RM, McCarthy MP, Shuster M (1990): Nicotinic acetylcholine receptor superfamily of ligand-gated channels. Biochem. **29**, 11009-11023.

Sumikawa K, Houghton M, Emtage JS, Richards BM, Barnard EA (1981): Active multi-subunit ACh receptor assembled by translation of heterologous mRNA in *Xenopus* oocytes. Nature **292**, 862-864.

Sussman JL, Harel M, Frolow F, Oefner C, Goldman A, Toker L, Silman I (1991): Atomic structure of Acetylcholinesterase from *Torpedo californica*: a prototypic acetylcholine-binding protein. Science **253**, 872-878.

Swanson KL, Allen CN, Aronstam RS, Rapoport H, Albuquerque EX (1986): Molecular mechanisms of the potent and stereospecific nicotinic receptor agonist (+)-anatoxin-a. Mol. Pharmacol. **29**, 250-257.

Swanson LW, Simmons DM, Whiting P, Lindstrom J (1987): Immunohistochemical localisation of neuronal nicotinic receptors in rodent central nervous system. J. Neurosci. **7**, 3334-3342.

Swanson KL, Aronstam RS, Wonnacott S, Rapoport H, Albuquerque EX (1991): Nicotinic pharmacology of anatoxin analogues: I. Side chain structure-activity relationships at peripheral agonist and non-competitive antagonist sites. J. Pharmacol. Exp. Ther. **259**, 377-386.

Swanson KL & Albuquerque (1992): Nicotinic acetylcholine receptors and low molecular weight toxins. In '*Selective neurotoxicity*', eds. Herken H, Hucho F. Berlin: Springer-Verlag.

Thomas P, Stephens M, Wilkie G, Amar M, Lunt GG, Whiting P, Gallagher T, Pereira E, Alkondon M, Albuquerque EX, Wonnacott S (1993): (+)-Anatoxin-a is a potent agonist at neuronal nicotinic acetylcholine receptors. J. Neurochem. **60**, 2308-2311.

Thomas P, Brough PA, Gallagher T, Wonnacott S (1994): Alkyl-modified side chain variants of anatoxin-a: A series of potent nicotinic agonists. Drug Devel. Res. **31**, 147-156.

Thompson PE, Manallack DT, Blaney FE, Gallagher T (1992): Conformational studies on (+)anatoxin-a and derivatives. J. Computer-Aided Mol. Design **6**, 287-298.

Toyoshima C & Unwin N (1990): Three-dimensional structure of the acetylcholine receptor by cryoelectron microscopy and helical image reconstitution. J. Cell Biol. **111**, 2623-2635.

Unwin N (1993): The nicotinic acetylcholine receptor at 9Å resolution. J. Mol. Biol. **229**, 1101-1124.

Verrall S & Hall ZW (1992): The N-terminal domains of acetylcholine receptor subunits contain recognition signals for the initial steps of receptor assembly. Cell **68**, 23-31.

Vijayaraghavan S, Pugh PC, Zhang Z-W, Rathuoz MM, Berg DK (1992): Nicotinic receptors that bind αbungarotoxin on neurons raise intracellular free Ca^{++}. Neuron **8**, 353-362.

Wada K, Ballivet M, Boulter J, Connolly J, Wada E, Deneris ES, Swanson LW, Heinemann SF, Patrick J (1988): Functional expression of a new pharmacological subtype of brain nicotinic acetylcholine receptor. Science **240**, 330-334.

Wada E, Wada K, Boulter J, Deneris E, Heinemann S, Patrick J, Swanson LW (1989): Distribution of α2, α3, α4, and β2 neuronal nicotinic receptor subunit mRNAs in the central nervous system: a hybridisation histochemical study in the rat. J. Compar. Neurol. **284**, 314-335.

Waksman G, Changeux J-P, Roques B (1980): Structural requirements for agonist and non-competitive blocking action of acylcholine derivatives on *Electrophorus electricus* electroplaque. Mol. Pharmacol. **18**, 20-27.

Wasserman NH, Bartels E, Erlanger BF (1979): Conformational properties of the acetylcholine receptor as revealed by studies with constrained depolarising ligands. Proc. Natl. Acad. Sci. (USA) **76**, 256-259.

Whiting P, Esch F, Shimasaki S, Lindstrom J (1987): Neuronal nicotinic acetylcholine receptor β subunit is coded for by the cDNA clone α4. FEBS Lett. **219**, 459-463.

Whiting P, Schoepfer R, Lindstrom J, Priestley T (1991): Structural and pharmacological characterisation of the major brain nicotinic acetylcholine receptor subtype stably expressed in mouse fibroblasts. Mol. Pharmacol. **40**, 463-472.

Witkop B & Brossi A (1984): In '*Natural products and drug development*', eds. Krogsgaard-Larsen P, Christensen SB, Kofod H, pp282-298. Alfred Benzon Symp. 20, Munksgaard, Copenhagen.

Wong GK & Schmidt J (1976): Receptors for αbungarotoxin in the developing visual system of the chick. Brain Res. **114**, 524-529.

Wonnacott S (1986): αBungarotoxin binds to low affinity binding sites in rat brain. J. Neurochem. **47**, 1706-1712.

Wonnacott S (1987a): Brain nicotine binding sites. Human Toxicol. **6**, 343-353.

Wonnacott S (1987b): Neurotoxin probes for neuronal nicotinic receptors. In '*Neurotoxins and their pharmacological implications*', ed. Jenner P, pp209-231: New York, Raven.

Wonnacott S (1990): Characterisation of nicotine receptor sites in the brain. In '*Nicotine Psycopharmacology: molecular, cellular and behavioural aspects*', ed. Wonnacott S, Russel MAH, Stolerman IP, pp226-277. Oxford: Oxford Univ. press.

Wonnacott S, Jackman S, Swanson KL, Rapoport H, Albuquerque EX (1991): Nicotinic pharmacology of anatoxin analogues: II. Side chain structure-activity relationships at neuronal nicotinic ligand binding sites. J. Pharmacol. Exp. Ther. **259**, 387-391.

Wonnacott S, Swanson KL, Albuquerque EX, Huby NJS, Thompson P, Gallagher T (1992): Homoanatoxin: A potent analogue of anatoxin-a. Biochem. Pharmacol. **43**, 419-423.

Xie Y, Jones SJ, Loring RH (1992): Effects of oxidising and reducing analogues of acetylcholine on neuronal nicotinic receptors. Mol. Pharmacol. **42**, 356-363.

Yamada S, Isogai M, Kagawa Y, Tokayanagi N, Hayashi E, Tsujiki K, Kosuge T (1985): Brain nicotinic acetylcholine receptors: biochemical characterisation by neosurugatoxin. Mol. Pharmacol. **28**, 120-127.

Yao Q (1991): Molecular modelling studies of anatoxin analogues. Masters thesis, New Jersey Int. Tech.

Zhang ZW & Feltz P (1990): Nicotinic acetylcholine receptors in porcine hypophyseal intermediate lobe cells. J. Physiol. **422**, 83-101.

Zhang X & Nordberg A (1993): The competition of [^{3}H]-(-)-nicotine binding by the enantiomers of nicotine, nornicotine and anatoxin-a in membranes and solubilised preparations of different brain regions of rat. Naunyn-Schmiedeberg's Arch. Pharmacol. **348**, 28-34.

Zhang ZW, Vijayaraghavan S & Berg DK (1994): Neuronal acetylcholine receptors that bind α-bungarotoxin with high affinity function as Ligand-Gated Ion Channels. Neuron **12**, 167-177.

Zorumski CF, Thio LL, Isenberg KE, Clifford DB (1992): Nicotinic acetylcholine currents in cultured postnatal rat hippocampal neurons. Mol. Pharmacol. **41**, 931-936.

Arsenicals have been used to explore the role of vicinal cysteines in enzymes, such as dihydrolipoamide dehydrogenase [Stevenson et al., 1978; Danson et al. 1986; Danson et al. 1987]. Arsenical reagents are attractive because bifunctional reagents can be generated to study residues in the vicinity of the vicinal cysteines. As a prerequisite to adopting such an approach to studying the agonist binding site of nAChR, it is necessary to establish that the monofunctional arsenical interacts with the receptor. Pike & Loring [1992] and Rossant et al [1994] have shown that this is the case for immunoisolated nAChR from chicken brain labelled with [^{3}H]agonists. Here we report that [^{3}H]cytisine binding to rat brain membranes is prevented by reduction and reaction with *p*-aminophenyldichloroarsine (APA; for structure see insert, Fig. 2) in a manner consistent with a specific modification of the pair of vicinal cysteines in the α subunit.

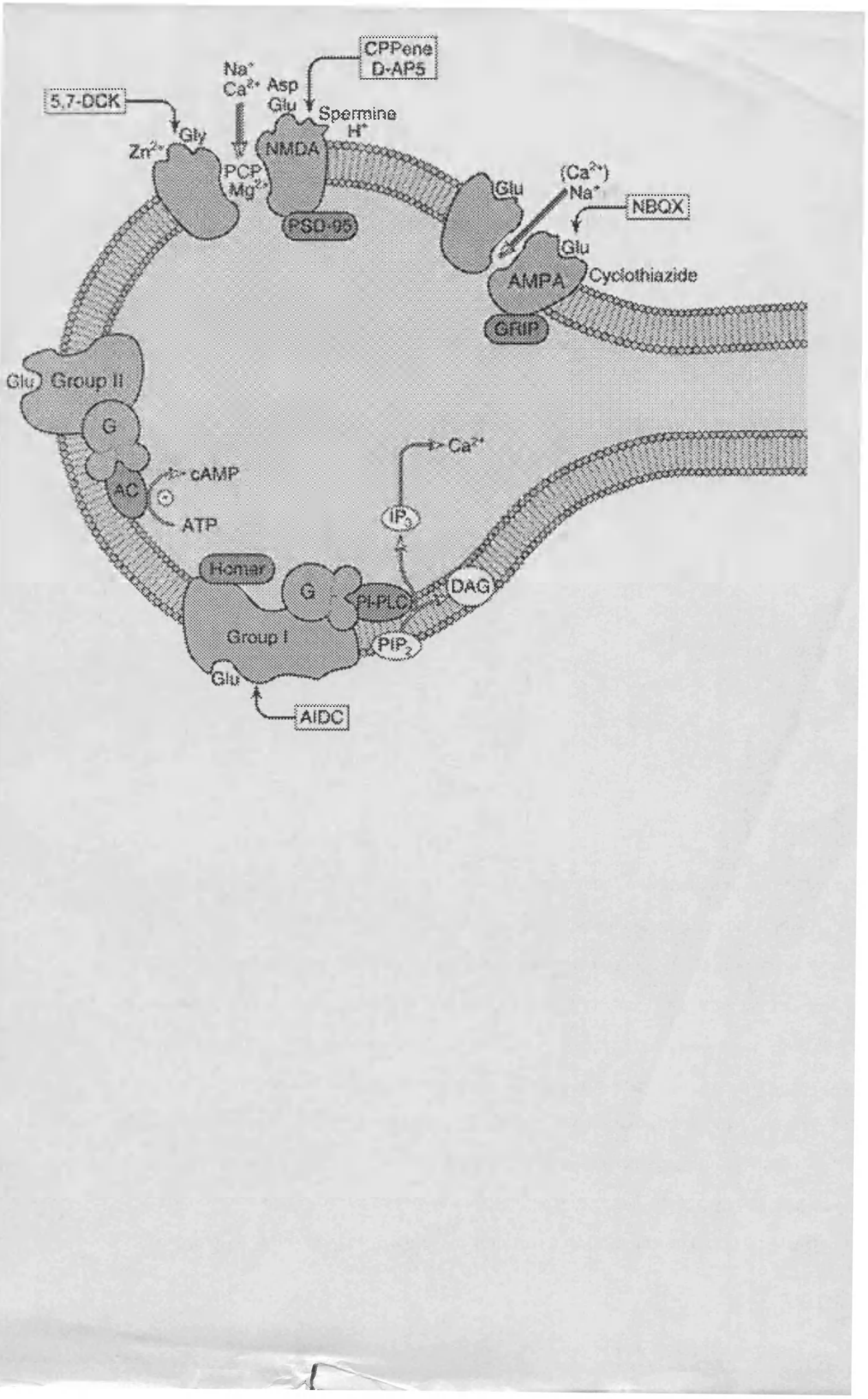
CPPene
D-AP5
Na+
Ca2+
Asp
Glu
5,7-DCK
Spermine
H+
Gly
Zn2+
NMDA
PCP
Mg2+
PSD-95
Glu
(Ca2+)
Na+
NBQX
Glu
AMPA
Cyclothiazide
GRIP
Glu
Group II
G
AC
cAMP
ATP
Ca2+
IP3
Homer
G
PI-PLC
DAG
Group I
PIP2
Glu
AIDC